The slow oscillation as an intrinsic and emergent property of the neocortex

Thèse

Maxime Lemieux

Doctorat en neurobiologie
Philosophiæ Doctor(Ph.D.)

Québec, Canada

Résumé

Le sommeil est présent chez pratiquement tous les animaux mais a atteint le plus haut niveau d'organisation chez les mammifères et les oiseaux avec le sommeil à ondes lentes et le sommeil paradoxal. De nombreuses études ont suggéré que le sommeil est généré par le cerveau pour ses propres besoins. L'oscillation lente est une caractéristique électroencéphalographique du sommeil à ondes lentes se traduisant par une alternance entre des états actif et silencieux du réseau thalamocortical. Elle a attiré le focus de plusieurs études étant donné son implication dans la plasticité synaptique et la consolidation de la mémoire. Plusieurs questions restent néanmoins en suspens. Quel est le rôle du thalamus dans l'oscillation lente? Quelles conditions mènent à l'état silencieux? Y a-t-il une variabilité entre espèces dans la synchronisation des ondes lentes? Dans la première étude de cette thèse, nous montrons que le thalamus est crucial à la genèse et à la propagation de l'oscillation lente alors que le cortex a la propriété intrinsèque de la restaurer en absence d'afférence fonctionnelle. Dans la seconde étude, nous nous intéressons aux conditions qui mènent à l'initiation des états silencieux dans le néocortex. Nous avons trouvé que l'inhibition dépendante du chlore est impliquée dans la terminaison des états actifs et que les afférences thalamocorticales jouent un rôle dans la synchronisation des états silencieux. Dans la troisième étude, nous comparons le niveau de synchronisation de l'oscillation lente dans les régions somatosensorielle et associative du néocortex chez le chat et le lapin. Nous rapportons que la synchronisation de l'oscillation lente corrèle avec le niveau de gyrification du cortex cérébral et le niveau hiérarchique dans le traitement de l'information d'une région néocorticale. Nous concluons que l'oscillation lente est une propriété intrinsèque du néocortex qui émerge du dialogue entre le néocortex et le thalamus, de la balance entre l'inhibition et l'excitation dans le réseau néocortical et dont la synchronisation a évolué avec le développement du cortex cérébral.

Abstract

Sleep is a defining feature of animals that achieved the highest degree of organization in mammals with two distinct types of sleep: the slow wave sleep (SWS) and the rapid eye movements sleep. A large body of evidences suggests that the sleep is generated by the brain to fulfill its own need. Among the electroencephalographic signatures of SWS and anesthesia, the slow oscillation (<1 Hz), a rhythmic alternation of active and silent states of the thalamocortical network, has attracted a lot of attention owing to its implication in synaptic plasticity and memory consolidation. Several questions remain unanswered on the mechanisms underlying the slow oscillation. For instance, what is the role of the thalamus in the slow oscillation? Which conditions lead to the onset of the silent state? Is there inter-species variability in the synchronization? In the first study of this thesis, we have investigated the respective contribution of the neocortex and the thalamus in the generation of the slow oscillation. We report that the thalamus is crucial to the generation and propagation of the active states of the slow oscillation while the neocortex has the intrinsic ability to recover the slow oscillation in absence of afferents. In the second study, we address the question regarding the conditions that lead to the onset of the silent state in the neocortex. We have found that chloride-mediated inhibition and functional thalamocortical afferents are involved in terminating the active states. In the third study, we compare the synchronization of the slow oscillation in the somatosensory and associative cortices of cats and rabbits. We have found that the synchronization of the slow waves correlates with the level of gyrification of the cerebral cortex and the hierarchical level of information processing of a neocortical region. We conclude that the slow oscillation is an intrinsic property of the neocortex that emerges from the dialogue between the neocortex and thalamus, the balance of inhibition and excitation in the neocortical network and that the synchronization of the slow oscillation evolved with the development of the cerebral cortex.

Table of Contents

Résumé iii
Abstract v
Table of Contents vii
List of Tables xiii
List of Figures xv
List of Abbreviations xvii
Acknowledgment xxi
Foreword xxiii
Chapter 1 General introduction 1
1.1 A brief introduction to sleep 1
1.2 Thalamocortical network 2
1.2.1 General organization 2
1.2.2 Neocortical pyramidal neurons 4
1.2.3 Neocortical spiny stellate cells 5
1.2.4 Neocortical interneurons (aspiny and sparsely spiny non-pyramidal neurons) 6
1.2.6 Thalamic neurons 7
1.2.7 Intrinsic properties of neurons 8
1.2.8 Electrophysiological types of neurons 9
1.3 Connectivity in the thalamocortical network 10
1.3.1 Thalamic connectivity 11
1.3.2 Thalamocortical afferents 12
1.3.3 Neocortical excitatory connectivity 14
1.3.4 Neocortical inhibitory connectivity 15
1.3.5 Neocortical efferents 17
1.3.6 Recurrent activity and the balance of excitation and inhibition 18
1.3.7 Synaptic and homeostatic plasticity 19
1.4 Brain rhythms in the states of vigilance 22
1.4.1 States of vigilance 22
1.4.2 Fast rhythms 22
1.4.3 Slow rhythms 23
1.4.4 Prolonged wakefulness and ascending activating systems 26

1.4.5 Slow oscillation during anesthesia 29
1.4.6 Why studying the slow oscillation? 30
1.5 Mechanisms of states transition during the slow oscillation 32
1.5.1 Slow rhythm in the isolated neocortical network 32
1.5.2 Cortical contribution to the initiation the active state 35
1.5.3 Thalamic contribution to the initiation of the active state 37
1.5.4 Synchronization in the thalamocortical network 39
1.5.5 Terminating the active state (or initiating the silent state) 40
1.6 Goals of the thesis 43
1.6.1 Thalamic and neocortical contribution to the slow oscillation 43
1.6.2 Inhibition in the transition to the silent state 44
1.6.3 A comparative electrophysiological study of the slow oscillation 44
Chapter 2 The impact of cortical deafferentation on the neocortical slow oscillation 47
2.1 Résumé 48
2.2 Abstract 49
2.3 Introduction 50
2.4 Materials and methods 51
2.4.1 Surgery 51
2.4.2 Electrophysiology 52
2.4.3 Data analysis 52
2.4.4 Computational models 53
2.5 Results 57
2.5.1 Thalamic inactivation disrupts cortical slow and fast activities 57
2.5.2 Time-dependent recovery of slow oscillation 59
2.5.3 Mechanisms of synchronization of slow oscillation and its recovery after thalamic inactivation 61
2.6 Discussion 64
2.6.1 Thalamic and neocortical contribution to the slow oscillation 64
2.6.2 The slow oscillation as the intrinsic property of the neocortex 66
2.7 References 68
2.8 Figure Legends 72
2.9 Table 84

Chapter 3: Neocortical inhibitory activities and thalamocortical afferents contribute to the onset of silent states of the neocortical slow oscillation 87
3.1 Résumé 88
3.2 Abstract 89
3.3 Introduction 90
3.4 Materials and methods 91
3.4.1 Surgery 91
3.4.2 Electrophysiological recordings 92
3.4.3 Thalamic inactivation and neocortical slabs 93
3.4.4 Electrical laminar stimulations 93
3.4.5 Data analysis and statistical tests 93
3.5 Results 95
3.5.1 Level of synchrony of the transition to the silent state 95
3.5.2 Disfacilitation and inhibition prior to the onset of the silent state 97
3.5.3 Laminar profile of stimulation efficacy to induce a silent state 99
3.5.4 Thalamic firing before the silent state 101
3.6 Discussion 101
3.6.1 Balance of excitation and inhibition 102
3.6.2 Synchronization of the cortical inhibition 104
3.6.3 Electrical stimulation 104
3.6.4 Sleep architecture, cortex and thalamus 105
3.6.5 Functional implications 105
3.7 References 106
3.8 Figures 110
Chapter 4 The slow oscillation in the somatosensory and associative cortices of rabbits and cats: a comparative study of recurrent activity in the mammalian neocortex. 127
4.1 Résumé 128
4.2 Abstract 129
4.3 Introduction 130
4.4 Methodology 130
4.4.1 Surgery 130
4.4.2 Electrophysiological recordings 131

4.4.3 Data analysis 131
4.4.4 Statistical tests 133
4.5 Results 133
4.5.1 Composition of the power spectra 133
4.5.2 Properties of the slow oscillation 134
4.5.3 Coherence and synchronization of the slow oscillation 135
4.5.4 Propagation of the slow oscillation 136
4.5.5 Isolated neocortical slabs 137
4.6 Discussion 138
4.6.1 Methodological consideration 138
4.6.2 Power spectral compositon in the different species-regions 139
4.6.3 Associative vs. somatosensory 139
4.6.4 Rabbit vs. cat 141
4.6.5 Concluding remarks 141
4.7 Literature cited 142
4.8 Figures 146
4.9 Table 158
Chapter 5 General discussion 159
5.0 Summary of the thesis 159
5.1 The roles of the thalamus 160
5.1.1 The rightful place of the thalamus 160
5.1.2 Technical limitations 161
5.1.3 Future studies 162
5.2 Is the slow oscillation the default state of the neocortex 162
5.2.1 Recovery of the slow oscillation 162
5.2.2 Limitations and future works 163
5.3 The silent state as a synchronous phenomenon 164
5.4 The fragile balance of excitation and inhibition 165
5.4.1 Chloride-mediated inhibition 165
5.4.2 Laminar stimulation 166
5.4.3 Future works 166
5.5 The evolution of the slow oscillation 167

5.5.1 Implications of the slow oscillation concordance 167
5.5.2 Emergence of the slow oscillation 167
5.5.3 Technical limitations 168
5.5.4 Future works 168
5.6 Concluding remarks 169
Bibliography 170

List of Tables

Table 2.1 Detailed geometry of thalamocortical network..... 84

Table 4.1 Properties of the slow oscillation in different species-regions 158

List of Figures

Figure 1.1 Schematic representation of a typical neocortical pyramidal neuron 5
Figure 1.2 Electrophysiological identification of neocortical neurons 10
Figure 1.3 Types of thalamic nuclei based on their projections to the neocortex 11
Figure 1.4 Summary of intracortical excitatory connectivity mediating the recurrent activity 15
Figure 1.5 Brain rhythms during wake and sleep 25
Figure 1.6 Spontaneous active states in the isolated neocortical slab 33
Figure 1.7 The thalamus is not necessary to generate the slow oscillation 38

Figure 2.1 Effects of partial thalamic inactivation on the cortical slow oscillation 72
Figure 2.2 LFP power distribution in intact vs. affected by thalamic inactivation cortical regions 73
Figure 2.3 Intracellular activity in intact and partially deafferented cortical areas after inactivation of thalamic LP nucleus. 74
Figure 2.4 Alternating involvement in active states of closely located cortical neurons in the cortical area affected by thalamic inactivation. 76
Figure 2.5 LFP activities in acute and chronically isolated neocortical slabs. 77
Figure 2.6 Upregulation of synaptic activites following thalamic inactivation. 78
Figure 2.7 The geometry of thalamocortical network model. 79
Figure 2.8 Modeling study of the effect of thalamic deafferentation on the neocortical slow oscillation. 80
Figure 2.9 Impact of thalamocortical diffuse (matrix) vs. specific (core) projections and the target radii on the synchronization of the slow oscillation. 81
Figure 2.10 Modeling study of scaling the intracortical connectivity on the recovery of the neocortical slow oscillation. 82
Figure 2.11 Role of different biophysical features inthe recovery of the slow oscillation 83

Figure 3.1 Removing inputs to the neocortex decreases the synchrony of the silent state onset. 110
Figure 3.2 Synchrony of silent state onset at the cellular level. 112
Figure 3.3 Disfacilitation prior to the silent state onset 114
Figure 3.4 Decreased cortical firing prior to the onset of silent states. 116
Figure 3.5 Chloride inhibition at the transition to the silent state. 118
Figure 3.6 Long duration inhibition prior to the onset of the silent state under ketamine-xylazine anesthesia. 120
Figure 3.7 Long duration inhibition prior to the onset of silent state during natural sleep. 121
Figure 3.8 Depth profile of the efficacy to trigger a silent state. 122
Figure 3.9 Depth profile of neuronal response to electrical stimuli. 123
Figure 3.10 Thalamic firing in relation to cortical onset of the silent state. 124

Figure 4.1 Defining state in the LFP recording. 146
Figure 4.2 Proportion of frequency bands characteristic of ketamine-xylazine anesthesia. 148
Figure 4.3 Spatiotemporal coincidence of the slow oscillation 150
Figure 4.4 Cross-correlation of the slow oscillation 152
Figure 4.5 Propagation of states transitions. 154

Figure 4.6 Active state duration in LFP recordings in the isolated neocortical slab. 156
Figure 4.7 Active state duration in intracellular recordings in slabs 157

Figure 5.1 Summary of the thalamic contribution to the neocortical slow oscillation 169

List of Abbreviations

AC	Alternative current
DC	Direct current
EEG	Electroencephalography
EMG	Electromyography
EOG	Electrooculography
EPSP	Excitatory postsynaptic potential
FRB	Fast rhythmically bursting
FS	Fast spiking
GABA	Gamma-aminobutyric acid
GAD	Glutamic acid decarboxylase
GFP	Green fluorescent protein
HSP	Homeostatic plasticity
HVA	High voltage activated (calcium channels)
I_A	Transient potassium current
I_H	Hyperpolarization activated cationic current
I_K	Fast delayed rectifying potassium current
$I_{K,Ca}$	Calcium-activated potassium current
I_{Nap}	Persistent sodium current
I_T	Transient calcium current
IB	Intrinsically bursting
i.m.	Intra-muscular
i.v.	Intra-venous
IPSP	Inhibitory postsynaptic potential
KAc	Potassium acetate
KCl	Potassium chloride
LDT	Lateral dorsal tegmentum
LFP	Local field potential
LGN	Lateral geniculate nucleus
LP	Lateral posterior (nucleus of the thalamus)
LTD	Long-term depression
LTP	Long-term potentiation
LTS	Low threshold spike
LVA	Low voltage activated (calcium channels)
MD	Medial dorsal (nucleus of the thalamus)
MEG	Magnetoencephalography
MGN	Medial geniculate nucleus
MUA	Multi-unit activity
NaCl	Potassium chloride
NBQX	2,3-dihydroxy-6-nitro-7-sulfamoyl-benzo[f]quinoxaline-2,3-dione
NMDA	N-methyl-D-aspartate
NREM	Non rapid eye movements
PB	Phosphate buffer

PBS	Phosphate buffer saline
PFA	Paraformaldehyde
PGO	Ponto-geniculo-occipital (waves)
PPT	Pedunculopontine tegmentum
QX-314	*N*-(2,6-Dimethylphenylcarbamoylmethyl)triethylammonium bromide
REM	Rapid eye movements
RS	Regular spiking
SD	Standard deviation
STD	Short-term depression
STDP	Spike-timing dependent plasticity
STF	Short-term facilitation
SWA	Slow wave activity
SWS	Slow wave sleep
TC	Thalamocortical
Trans-ACPD	Trans-(2R, 4R)-4-aminopyrrolidine-2,4-dicarboxylate
TTX	Tetrodotoxin
V_m	Membrane potential
VB	Ventrobasal complex of the thalamus
VLPO	Ventral lateral preoptic nucleus

.

Comment ne pourrais-je pas dédier cette thèse à ma compagne, Geneviève, qui malgré son refus de poursuivre des études graduées a quand même du les endurer?

Je dédie également cette these à la mémoire de mon père, Pierre, qui est l'une de mes inspirations à suivre une vie dédiée à la recherche et qui aurait tant voulu être présent pour ce jour.

"Life is what happens to you
When you're busy making other plans"
-John Lennon

Acknowledgment

I'm above all grateful to my thesis supervisor, Igor Timofeev, who welcomed me in his lab five years ago. Over the years, I've learned under his supervision the fine art of *in vivo* electrophysiology. Throughout our discussions, I've learned to develop a keener sense of criticism, never to believe but always to understand.

I would also like to thank colleagues and friends without whom this project would not have been the same. Foremost, I have in mind Sylvain Chauvette from whom I've learned so much and Josée Seigneur who's always so helpful, even when you don't ask for it. I'm also grateful to Sergiu Ftomov who helped me get out of the Bermuda Triangle of electrical noise quite a few times. For all our discussions, sometimes extending in the late night, I want to thank my former partner in crime, Francis Lajeunesse, and for their kind support, Reza Zomorrodi and Courtney Pinard. Many thanks also to Soumaïa Boubou, Mathieu Blais-D'Amours, Magda Kusmierczak and Laszlo Grand for their help during this thesis. For their friendship over the last years, a special thank to Farida El-Gaamouch and Bruce Mesnage.

I want to thank my family for their support over the years, and especially my mother, Christine, who always believed in me and encouraged me through the years. And of course, I thank my beloved companion, Geneviève, who has been so supportive and understanding over the last four years

Foreword

This thesis is a collection of three research articles (chapters 2-4). The first chapter is an introduction on the organization and rhythms generated by the thalamocortical network. The fifth chapter is a general discussion of the three studies. A special attention is given to the slow oscillation which is the scope of the three studies completed during the course of this thesis.

The first manuscript, "*The impact of cortical deafferentation on the neocortical slow oscillation"*, is published in the Journal of Neuroscience. This study was initially designed by me and my supervisor, Prof. Igor Timofeev, to investigate the role of the thalamus in the synchronization of the slow oscillation. To our surprise, we found that the inactivation of a restricted portion of the thalamus (lateral posterior nucleus) led to a dramatic decrease of the slow oscillation in the LFP recordings of a region of the suprasylvian gyrus. We further investigated with intracellular recordings this phenomenon in long experiments (36h) and we uncovered a partial restoration of the slow oscillation. In chronic experiments, we found a complete recovery in isolated neocortical slabs over a period of 2-3 weeks. These findings were supported by modeling experiments of the homeostatic plasticity in the thalamocortical network performed by the laboratory of Prof. Maxim Bazhenov. Both experimental and modeling studies were separately presented at SfN meeting in 2010 and were received with much excitement by our peers. We believed that the homeostatic nature of our results would have an impact not only on the thalamocortical field of research but also on neurosciences at large. We thus combined both experimental and modeling parts and submitted a manuscript in 2011 to *Science* and upon rejection, to *Nature Neuroscience* where the study was peer-reviewed for two months. Due to the controversial nature of our work (homeostatic issue), our work could not be published in its current form by the Nature Neuroscience. After several rounds of reviews, it was accepted in the Journal of Neuroscience

The second manuscript, "*Neocortical inhibitory activities and thalamocortical afferents contribute to the onset of silent states of the neocortical slow oscillation"*, has been reviewed twice in the Journal of Neurophysiology and we were invited to resubmit. I designed this study with my supervisor to address the question regarding the conditions that lead to onset of the silent state of the slow oscillation. This study combined LFP recordings in the intact and deafferented (thalamic inactivation, isolated neocortical slabs) neocortex, dual intracellular recordings (potassium chloride and potassium

acetate), recording of multi-unit activity in the thalamus and laminar electrical stimulation in the slab. Due to the similarity to my results on the laminar stimulation in the neocortical slabs, we included in this study results from Dr. Sylvain Chauvette on intracellular response to laminar stimulations and an analysis of the reduction in firing in the cortical depth prior the onset of the silent state.. To provide control data on the synchronization of the silent states onset in paired intracellular recordings, I also used recordings made by Dr. Chauvette.

The third manuscript, "*The slow oscillation in the somatosensory and associative cortices of rabbits and cats: a comparative study of recurrent activity in the mammalian neocortex"*, is in preparation for submission to the Journal of Comparative Neurology. This study uses multisite LFP recordings to compare the synchronization of the slow oscillation in the neocortex of rabbits and cats. Experiments were conducted in the intact and isolated neocortical slabs of the somatosensory and parietal associative cortex. This study was performed to evaluate the possibility of replacing cats by rabbits as an *in vivo* model of the thalamocortical processes in the laboratory of Prof. Timofeev. A weakness of this study is by consequence the small sample of rabbits used. We consider adding to this study data from experiments on mice conducted of Dr. Maxim Sheroziya. The inclusion of those analyses will delay the submission of the manuscript.

In the course my PhD, I have also had the opportunity to contribute to a modeling study by Dr. Maxime Bonjean on the role of the neocortex in terminating the thalamic spindles. I performed and analyzed juxtacellular recordings in the cat motor cortex under barbiturate anesthesia to confirm the model *in vivo*. The reference to this publication : Bonjean M, Baker T, **Lemieux** M, Timofeev I, Sejnowski T, Bazhenov M (2011) Corticothalamic feedback controls sleep spindle duration in vivo. J Neurosci 31:9124-9134.

I have also co-supervised with Prof. Timofeev the preparation of a stereotaxic atlas of the ferret brain. Brains were collected during the *in vivo* experiments of Francis Lajeunesse in the course of his Ph.D. training. I thank Francis who stayed with me late in the night after his experiments to make stereotaxic measurements and perfusion. I'm also grateful to Marie-Josée Wallman who did all the histology and preliminary scanning for the atlas. However, after exploring several possibilities, we could not find a suitable avenue for high-resolution scanning of the sections intended for both the hard copy and web-based versions of the atlas. I have hope that we will eventually find a convenient

solution in the future and fulfill the project we settled for in 2011. As of today, there is still no published atlas of the ferret which is a model of neuroscience research. We believe the publication of our anatomical data will profit the scientific community working or planning to work on the ferret brain.

Here is the list of manuscripts presented in this thesis

1- **Lemieux** M, Chen JY, Lonjers P, Bazhenov M, Timofeev I (2014) The impact of cortical deafferentation on the neocortical slow oscillation. J Neurosci 34:5689-5703.

2- **Lemieux** M., Chauvette S., Timofeev I. (in review in the Journal of Neurophysiology) Neocortical inhibitory activities and thalamocortical afferents contribute to the onset of silent states of the neocortical slow oscillation

3- **Lemieux** M., Timofeev I. (in preparation) *The slow oscillation in the somatosensory and associative cortices of rabbits and cats: a comparative study of recurrent activity in the mammalian neocortex*

Chapter 1 General introduction

1.1 A brief introduction to sleep

We experience everyday periods of wakefulness and sleep. Wakefulness is a state which we can easily relate to because it is in this state of vigilance that we consciously experience life, interpreting various sensorial inputs from our environment or from our own body and executing a rich repertoire of motor tasks. Sleep escapes to our conscious experience or at the very least our recollection of it. Our cerebral cortex, the alleged siege of consciousness, is disconnected during sleep from the external world during this state of vigilance. The disconnection of the cerebral cortex from the external world is attributed to the thalamic gating (Munglani and Jones, 1992; McCormick and Bal, 1994; Timofeev et al., 1996; Del Felice et al., 2012).

A large body of evidences has suggested that the sleep is controlled by the brain to fulfill some of its need (Hobson, 2005). However, the nature of those needs is still uncertain to this date although the most accepted theory is that sleep is necessary to memory consolidation (Maquet, 2001; Steriade and Timofeev, 2003; Diekelmann and Born, 2010; Wang et al., 2011). One thing is sure, sleep is a neural feature shared by almost all animals. Throughout the animal kingdom, sleep is defined as a quickly reversible period of inactivity (in comparison to coma or hibernation) associated with a reduced responsiveness to external inputs (Zimmerman et al., 2008). Sleep is driven by a circadian process (process C) and by a homeostatic one (process S) depending on the duration of wakefulness and dissipating exponentially during sleep (Borbely, 1982).

Sleep is defined as a state of inactivity from primitive cnidarians like jellyfish (Kavanau, 2006) up to the much more evolved arthropods like the fruitfly (Shaw et al., 2000). This definition of sleep as a period of inactivity remains for basal vertebrates like the zebrafish (Yokogawa et al., 2007). The complexity of sleep has reached its climax in mammals and birds with the generation of the slow wave activity (SWA) probably due to the highly developed connectivity within their cerebral cortex (Rattenborg, 2006). Even among these two classes of vertebrate, the extent of sleep varies with the ecological niche (migrating birds or cetaceans) or the position in the food chain (predators sleep more than herbivores). In other words, it is a state of adaptive inactivity (Siegel, 2009).

We have attempted in this thesis to shed light on some mechanisms in the generation by the thalamocortical network of a key feature of sleep, the SWA or slow oscillation. We have studied the

contribution of the neocortex and the thalamus in generating the normal pattern of the slow oscillation and more specifically, in the transition between the active and the silent states of this slow rhythm. The slow oscillation is a phenomenon of recurrent activity occurring globally in the cerebral cortex and as such, we hypothesized that the extent of its synchronization may vary across neocortical regions. We also tested the hypothesis that the level of synchronization within a homologous cortical region may vary across species. Before we address these questions, we will describe in the following introduction the organization of the thalamocortical network in terms of its cellular components and connectivity among them to understand how brain rhythms (including the SWA) are generated.

1.2 Thalamocortical network

1.2.1 General organization

The thalamocortical network is made of the cerebral cortex and the thalamus, as its name implies. The cerebral cortex is a structure on the outer surface of the forebrain. Histologically, it is characterized by an external gray matter and an inner white matter that is formed by myelinated fibers arriving or leaving the cortex. The gray matter contains generally six layers (neocortex or isocortex) but can be made of four or five layers (paleocortex). Layer I, located at the surface of the cerebral cortex, contains mainly fibers. Layer II and III form the supragranular layers, layer IV is called the granular layers V and VI, the infragranular layers. The thalamus is located anteriorly to the midbrain, ventrally to the cerebral cortex and dorsally to the hypothalamus. It can be divided into a ventral and a dorsal part. The dorsal thalamus is formed by sensorial relay (or first order) and non-specific (higher order) nuclei. The ventral thalamus surrounds the exterior part of the dorsal thalamus and is formed by the reticular nucleus and the zona incerta.

The thalamocortical network can be divided into subsystems relating to a general function (sensorial processing, motor tasks, associative tasks and cognition). Based on clustering analysis of connectivity between the cortex and the thalamus, four major systems can be defined (Scannell et al., 1999). The first one is the visual system that contains the lateral geniculate nucleus (the primary recipient of retinal inputs to the thalamocortical network) and up to 32 neocortical areas in the macaque and 16 in the cat similarly organized in hierarchical levels of processing. The visual system is distributed in the occipital (containing the primary visual cortex), parietal, temporal and frontal lobe (the frontal eye field) and occupies half of the macaque cerebral cortex (Felleman and Van Essen, 1991). The second system is the auditory system formed by primary and second auditory cortex as

well as anterior and posterior auditory fields in the cortex (Rouiller et al., 1991). The cortical auditory regions are interconnected with medial geniculate nuclei and the posterior nucleus (Andersen et al., 1980).

The third system is the somato-motor system containing the somatosensory and the motor cortical areas and the ventrobasal complex of the thalamus (VB). The VB nucleus receives somesthetic inputs from the medial lemniscus, the spinothalamic tract (both transmitting information from the body) and the trigeminal tracts (related to the face). It transmits this information to the primary somatosensory areas (Brodmann areas 1, 2 and 3). High-order processing occurs in the posterior parietal cortex (Brodmann areas 5 and 7) which also integrates visual and auditory information (Hendry and Hsiao, 2003). The cortical areas are concerned with motor functions are the primary motor, the premotor and the supplementary motor area. These motor regions receive inputs from the somatosensory and associative areas (Schieber and Baker, 2003).

The fourth system is the fronto-limbic containing the prefrontal areas, the limbic areas and the anterior, midline and intralaminar nuclei of the thalamus (Scannell et al., 1999). The prefrontal cortex is a set of cortical areas connected with all sensory and motor systems and is involved in decision making, planning and guidance in social behaviors (Niedermeyer, 1998; Miller, 2000). The limbic areas were defined according to their anatomical features of cortical organization rather than on their functions and refer to the cingulate, retrosplenial, prelimbic, infralimbic, perirhinal, entorhinal and subicular regions of the cerebral cortex. These regions receive inputs from sensory cortical areas and are in close association with the hippocampus, the amygdala and the septum (Lopes da Silva et al., 1990).

Within each cortical areas, neurons form mini-columns vertically arranged (approximately 50 μm in diameter) and columns (300-600 μm in diameter) via their horizontal connections (Mountcastle, 1997). Depending on the cortical area, a column is associated with a specific function and is present in primary sensory areas (as well as those involved in higher level of processing), motor areas and even prefrontal areas.

In the following sections (1.2.2-1.2.8), we will describe the morphology and properties of neurons of the neocortex and the thalamus. These neurons were described in various mammalian species and

because these neurons are ubiquitous to the mammalian neocortex, we will not mention the studied species.

In summary, the cerebral cortex is organized in different levels of information processing and its basic unit is the radial column of cortical neurons. One of the questions we will address is whether the extent of synchrony of the slow oscillation within an area correlates with the hierarchical level of information processing.

1.2.2 Neocortical pyramidal neurons

Spiny pyramidal neurons are the principal cellular element of the neocortex as they account for 70-85% of the neurons in this brain region (DeFelipe and Farinas, 1992). A typical pyramidal neuron, as illustrated in figure 1.1can be distinguish by the pyramidal or ovoid shape of its soma from which arises a prominent apical dendrite reaching layer I (except for layer VI pyramidal neurons) and several basal dendrites. The dendrites contain spines which receive mostly asymmetrical synapses (Colonnier, 1968), commonly accepted as excitatory synaptic contacts. Spines accounts for roughly a third of the surface of a pyramidal neuron while the soma makes up only 2-4% (Mungai, 1967). Present in every layer, spines are more abundant in the layer where is located the cell body (Larkman, 1991), suggesting that the majority of excitatory inputs to a neuron comes from its respective layer. The axon of pyramidal cells points downward and leaves collateral extending horizontally, dorsally or ventrally. These cells use glutamate as neurotransmitter, which makes these neurons excitatory ones.

The pyramidal neurons are present throughout the cortical column except in layer I (DeFelipe and Farinas, 1992). The pyramidal neurons located in the supragranular layers (layers II and III) are smaller than those in infragranular layers (V and VI). Although layer IV contains mainly stellate cells, it also contains pyramidal neurons. The layer V contains the pyramidal neurons with the largest dendritic arborization, extending up to layer I just below the pia mater. Layer VI pyramidal neurons are of a size similar to those in layer V but their apical dendrites do not extend further than layer IV.

Due to the abundance and the large size of pyramidal neurons, intracellular recordings *in vivo* are often biased toward this cellular type. In the course of our experiments, we will also stimulate the neocortical layers under the hypothesis that they have different impact on the neocortical recurrent activity.

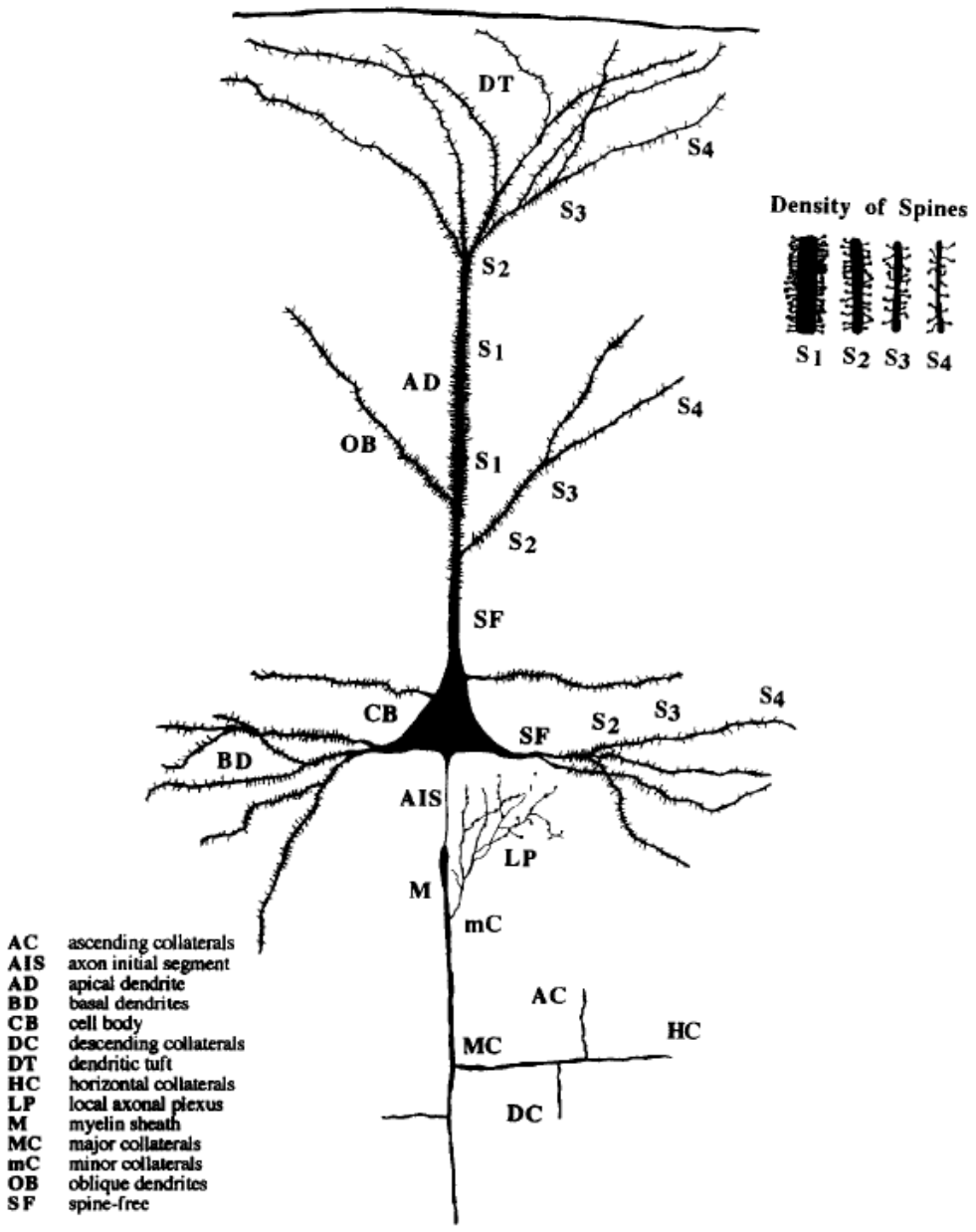

Figure 1.1 Schematic representation of a typical neocortical pyramidal neuron

Adapted from DeFelipe and Farinas (1992).

1.2.3 Neocortical spiny stellate cells

The spiny stellate cells are non-pyramidal neurons found only in layer IV. Their soma is round and 5-6 dendrites originate from it and radiate in all directions, branching once or twice. The axon emerges from the deeper surface, descends shortly and divides in 2-3 branches that turn sharply to ascend in

layer II/III and sometimes even in layer I. One descending branch reaches layer V or layer VI in some cases. The major characteristic that distinguishes the spiny stellate cell from other non-pyramidal neurons is the presence of spines on dendrites (Jones, 1975).

1.2.4 Neocortical interneurons (aspiny and sparsely spiny non-pyramidal neurons)

The absence of spine (aspiny) or the low presence of it (sparsely spiny) on these non-pyramidal neurons gives them a smooth aspect. They form a heterogenous population of neurons accounting for 15-30% of the neocortical neuronal population (DeFelipe and Farinas, 1992). These cells are immunoreactive for the glutamic acid decarboxylase (GAD), the synthesizing enzyme of the inhibitory neurotransmitter GABA, which makes these cells inhibitory interneurons (Ribak, 1978; Houser et al., 1983). There is a great diversity of interneurons in the neocortex that can be identified by their morphology and patterns of innervations (DeFelipe et al., 2013) as well as by their neurochemistry (Kawaguchi and Kubota, 1997). Although the classification varies depending on the authors, these cells can be broadly split in two groups based on their dendritic arborization: bitufted and multipolar. Furthermore, some classes of inhibitory neurons can be recognized based on the pattern of their axons.

The double bouquet is a typical example of bitufted cell. It is characterized by a vertical axonal bundle crossing radially layers II-V and with terminals making synapses on the soma, the dendritic shaft and the spines of non-pyramidal cells (Somogyi and Cowey, 1981). Double-bouquet cells can also be identified by their immunoreactivity for the vasoactive intestinal polypeptide (Kawaguchi and Kubota, 1996). The chandelier cell was named after the peculiar shape formed by its axon that descends from the lower pole of the soma and emits collaterals curving back to ascend. The axonal plexuses are located mostly beneath the soma of pyramidal neurons and form synapses on the initial segment of the axon (Somogyi, 1977; Fairén and Valverde, 1980; Peters et al., 1982). The dendritic arbor is bitufted with primary slender and sparse dendrites arising from the lower and upper poles of the fusiform soma.

The most commonly recognized type of multipolar interneuron is the basket cells. The ovoid soma of this cell emits long dendrites in every direction which branch once or twice. The term “basket” refers to the pattern made by their axon terminals around the soma and proximal dendrites of pyramidal neurons (Marin-Padilla, 1969; Jones, 1975; Kisvarday et al., 1987). The extent of their axonal

arborization is very large; it is even larger than any known dendritic arborization in the cortex (Somogyi et al., 1983). Another type of multipolar stellate cell is the Martinotti cell that sends its main axon and several collaterals to layer I. This type of interneurons is distinguishable by the expression of the somatostatin peptide (Kawaguchi and Kubota, 1996). The neurogliaform cell (also named spiderweb cell by Ramon y Cajal) is the smallest interneuron of the cortex and is frequently encountered in Golgi staining. It has several short dendrites radiating in every direction and branching once or twice; the axon emits several collaterals in a dichotomous manner and frequently changes course (Jones, 1975; Kisvarday et al., 1990).

This great diversity of inhibitory interneurons shapes the activity within the neocortical network, whether in response to a sensory stimulus or during spontaneous activity (Markram et al., 2004). Unfortunately, the lower proportion and smaller somatic size of these neurons have for consequence that they are difficult to record intracellularly *in vivo*. Alternative approaches (for example, pharmacological, genetic or alteration of ionic concentrations), are required to study their contribution to the network activity.

1.2.6 Thalamic neurons

In contrast to the diversity of cortical neurons, the morphology of the main cellular type of the thalamus, the relay cell or thalamocortical (TC) neuron, is much more homogenous among the nuclei of the dorsal thalamus, with some exception in the LGN (Jones, 2002) that is outside the scope of this thesis. These relay neurons come in different sizes and have a bushy appearance shaped by a variable number of radiating and dichotomously ramifying dendrites of up to 250 µm in length and bearing spines. Most of these cells project away from the thalamus although some cells in specific nuclei (but not in non-specific ones) were observed to have short local axons (Guillery, 1966; Scheibel and Scheibel, 1967). TC neurons are glutamatergic but there are also GABAergic cells in the dorsal thalamus. Accounting for approximately 30% of neurons in all nuclei of cats and monkeys, but restricted in the LGN in rodents, these local interneurons have a few thin dendrites with bulbous dilatations that look like axonal boutons [reviewed in (Jones, 2002)].

Neurons from the thalamic reticular nucleus have a round, ovoid or elongated soma. There have generally 3-6 elongated dendrites arising from the soma either from all around (multipolar) or from both poles (bitufted) of the soma and branching into second and third order dendrites. The dendrites

run parallel to the border of the nucleus. Spine-like varicosities are not present on first order dendrites but are on higher order ones. The axon of a thalamic reticular neuron leaves one or two collaterals in the thalamic reticular nucleus and curves toward the dorsal thalamus (Lübke, 1993). These cells are GABAergic and thus exclusively inhibitory neurons (Jones, 2002).

1.2.7 Intrinsic properties of neurons

The membrane potential of neurons is set by the distribution of potassium, sodium, calcium and chloride ions on each side of this membrane (Hille, 2001). Neurons are also rich in intrinsic voltage-gated channels for sodium, calcium and potassium ions that regulate the firing of neurons as well as allowing these cells to act as pacemaker and resonate with the network activity (Llinas, 1988). Sodium currents can be transient or persistent due to a different form of gating of the sodium channels. The transient opening of voltage-gated sodium channels generates the action potential which is the output the neuron (Hille, 2001). The persistent sodium current (I_{Nap}) may amplify distal dendritic excitation and be involved in subthreshold oscillating activity (Crill, 1996). I_{Nap} is activated during rhythmic firing (Stafstrom et al., 1984).

Voltage-dependent calcium currents also regulate the firing pattern of neurons. There are calcium channels activated at high voltage (HVA) and those activated at low voltage (LVA) (Llinas and Yarom, 1981). Another classification is based on the size of conductances and the rate of inactivation. Two types of HVA can be recognized based on the conductance size and kinetic of inactivation: the L-type with large conductance and slow rate of inactivation and the N-type with a lower conductance and a faster rate of inactivation. The LVA-type correspond to the transient calcium current (I_T) which carries the smallest conductance and the faster rate of inactivation (Tsien et al., 1988). The channels responsible of the I_T are inactivated at depolarized level, de-inactivated at hyperpolarized ones and activated at membrane potential more hyperpolarized by 15 mV than the firing threshold, making I_T ideal for oscillatory activity (Huguenard, 1996).

Another voltage-dependent current, the hyperpolarization activated cationic current (I_H), is responsible for slowly depolarizing the membrane potential of hyperpolarized neurons (activated between -90 to -60 mV depending on the cell). This current plays an important role in shaping the oscillating behavior of neurons (McCormick and Pape, 1990). The I_H and the voltage-dependent sodium and calcium currents are responsible for depolarizing neurons but there are also intrinsic

hyperpolarizing currents relying on the efflux of potassium ions. There is a rich diversity of potassium currents with different properties: the fast delayed rectifier (I_k), the slow delayed rectifier activated via muscarinic receptor (M current), the transient potassium current which is de-inactivated by hyperpolarization (I_A) and calcium-activated potassium currents ($I_{K,Ca}$) (Hille, 2001). Although some of the channels carrying these currents can leak at the rest, there is a different family of channels not gated by voltage and dedicated to the potassium leak current (Goldstein et al., 2001).

The interplay of these intrinsic currents plays a major role in shaping oscillatory behavior. For instance, they underlie the dual mode of firing in TC neurons, that is tonic and bursting firing (Jahnsen and Llinas, 1984). The currents responsible for the bursting behavior (I_H and the I_T) are also involved in an intrinsic pacemaker activity at 1-2 Hz present during SWS (McCormick and Pape, 1990). In this study, we will interfere with the bursting behavior of TC cells by blocking the I_T with QX-314 (Connors and Prince, 1982) to assess its impact on the neocortical activity.

1.2.8 Electrophysiological types of neurons

The morphology of a neuron also confers neurons a certain pattern in the firing. In the neocortex, there are four major types of firing pattern (or electrophysiological types) associated with a given morphology (McCormick et al., 1985; Connors and Gutnick, 1990) and more precisely with the dendritic structure and its electrotonic coupling with the soma (Mainen and Sejnowski, 1996). The most common type is the regular spiking (RS) neurons. In the original description of the RS type by Mountcastle and colleagues, the RS was said to present an adaptation in its firing rate (Mountcastle et al., 1969). The duration at half-amplitude of a RS action potential is generally 1-1.5 ms. The great majority of pyramidal neurons are RS. Fast spiking (FS) neurons increases steadily their firing rate with injected current. The action potential of FS neurons lasts in average less than 0.5 ms at half-amplitude. They are less frequently encountered than RS cells (Simons, 1978) and functionally correspond to inhibitory neurons (McCormick et al., 1985). However, not all inhibitory neurons are FS. For instance, Martinotti cells and most VIP-positive doublet bouquet cells are RS (Kawaguchi and Kubota, 1996). The intrinsically bursting (IB) neurons fire 3-5 action potentials at short intervals and each successive spike decreases in amplitude. About 15-20% of pyramidal neurons are IB cells and are generally found in layer V (McCormick et al., 1985; Timofeev et al., 2000a). Originally described as chattering cells in the supragranular layers of the visual cortex (Gray and McCormick, 1996), the fast rhythmically bursting (FRB) neurons fires thin spikes (0.3-0.4 ms at half-amplitude) at high

frequency (300-600 Hz) recurring rhythmically at 20-50 Hz. Although present in supragranular layers in cortical regions other than visual, FRB neurons are more numerous in infragranular layers (Timofeev et al., 2000a; Steriade et al., 2001). In our studies, most cells recorded intracellularly were of the RS type and to a lesser extent of the IB and FRB types. As no attempt was made to find differences between these cell types, data were pooled together.

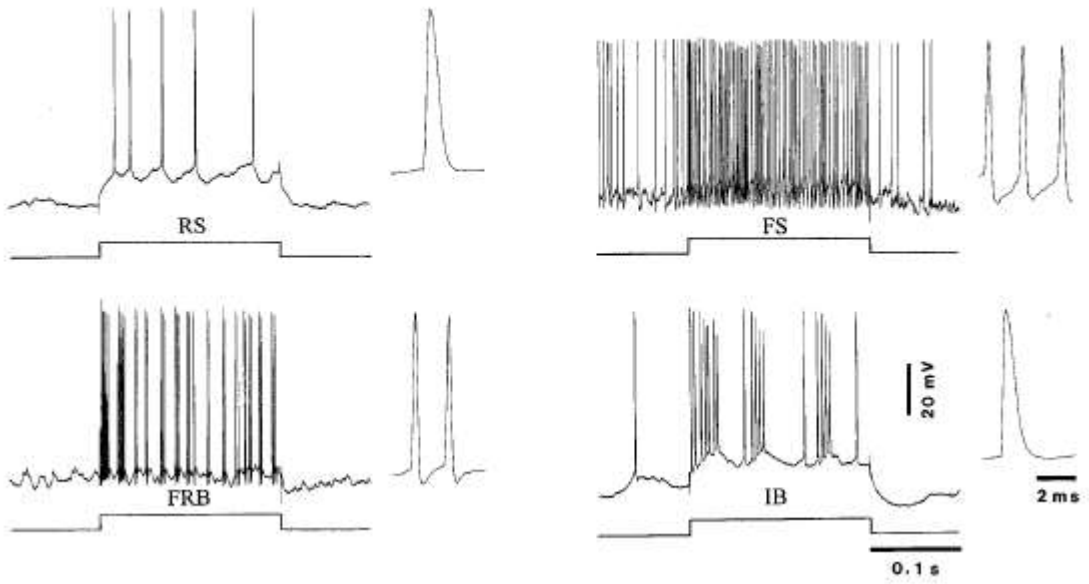

Figure 1.2 Electrophysiological identification of neocortical neurons

Intracellular responses to depolarizing current pulse: regular spiking (RS), fast spiking (FS), fast rhythmically bursting (FRB) and intrinsically bursting (IB). Modified from Steriade et al. (2001).

1.3 Connectivity in the thalamocortical network

We have introduced in the preceding section the general organization of the thalamocortical network. We also mentioned that neurons are equipped with intrinsic conductances that permit certain oscillatory behavior. However, the full expression of oscillations observed *in vivo* requires synaptic activity. In our study, we were particularly interested in how the connectivity between the thalamus and the cortex as well as the intracortical connectivity could generate the slow oscillation. In this section, we will discuss the connectivity between the different elements of the thalamocortical network.

1.3.1 Thalamic connectivity

Two classes of dorsal thalamic nuclei are recognized based on their projections to the neocortex: specific or relay (VB, LGN, MGN) and non-specific or associative (intralaminar, midline and posterior) nuclei (Fig. 1.3). TC neurons of relay nuclei project in a topographic and specific manner to the neocortex while those of the associative nuclei send diffuse projections to the neocortex (Jones, 1998; Sherman and Guillery, 2002). Relay TC neurons are also considered as thalamic core neurons and non-specific TC neurons as thalamic matrix neurons (Jones, 1998).

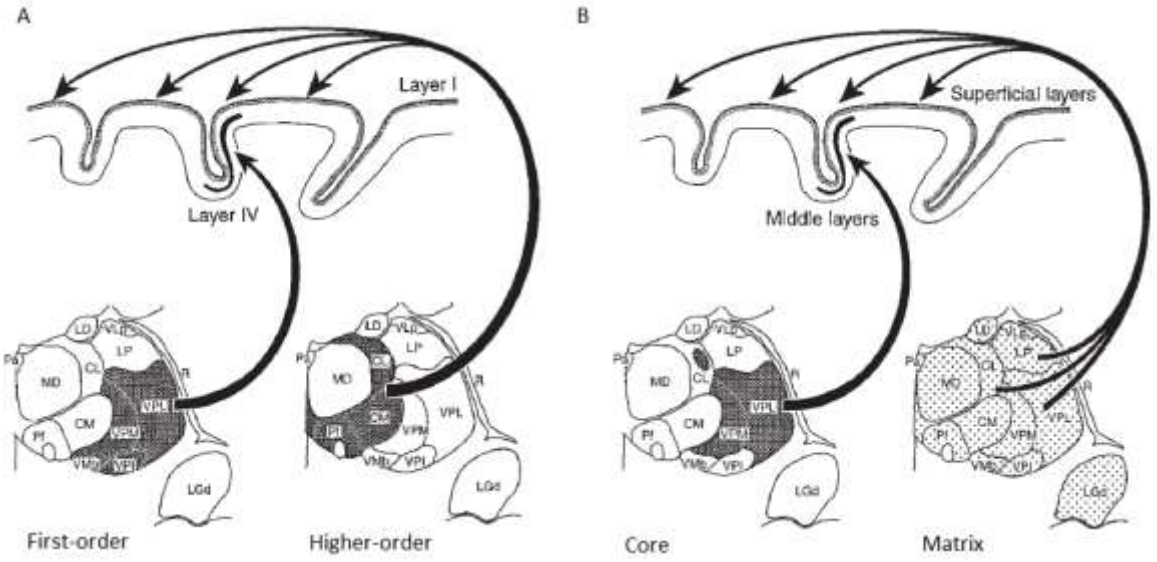

Figure 1.3 Types of thalamic nuclei based on their projections to the neocortex

(A) Traditional view of the first- and higher-order nuclei. (B) Recent view of the core vs. matrix TC projections. Modified from Jones (1998).

TC relay neurons are excited by thick axons from sensory afferents and by thin axons from corticothalamic afferents. These afferents are organized in a topographic manner. The GABAergic inhibition is provided by thalamic reticular neurons and, although less well characterized, by local interneurons (Sherman and Guillery, 1996; Jones, 2002). There are also non-specific modulatory afferents: acetylcholine, noradrenaline and serotonine from the brainstem and histamine from the tuberomamillary nucleus (Sherman and Guillery, 1996). In VB, sensory afferents from the medial lemniscus and the spinothalamic tract accounts for 15% of the synapses on TC relay cells, corticothalamic for approximately half of those synapses and inhibitory synapses (GABAergic

terminals) for the remaining third of synapses. Sensory afferents are mainly located on proximal dendrites and corticothalamic preferentially on distal dendrites. Inhibitory synapses are located on all compartments (Liu et al., 1995).

As for relay nuclei, TC neurons from associative nuclei receive dense and complexly ramifying afferents from the spinal cord, the brainstem, the tectum, the basal forebrain and the cerebral cortex. An important difference between relay and associative nuclei is the origin of corticothalamic afferents. In the case of relay nuclei (such as LGN), corticothalamic axons originate from layer VI pyramidal neurons, are thin and form small terminals in the distal dendrites. These axons are also present in associative nuclei (for example, the pulvinar) and, in addition, layer V pyramidal neurons send thick axons forming large terminals located more proximally than those formed by layer VI afferents. Functionally, layer V inputs acts as a driver on the thalamus whereas layer VI ones are modulating (Sherman and Guillery, 1996, 2002), suggesting a greater influence of the neocortex on associative than on relay thalamic nuclei.

Neurons from the thalamic reticular nucleus and zona incerta are innervated by the axonal collaterals from both layer VI corticothalamic and thalamocortical neurons (Jones, 2002), which makes these cells at the center of the dialogue between the cortex and the thalamus. Although layer V axons cross the reticular nucleus, they do not leave collaterals (Sherman and Guillery, 1996; Jones, 2002). The contribution of thalamic reticular neuron is the inhibition of thalamic relay cells and as we will see later, is essential in shaping oscillatory behavior in the thalamocortical network.

1.3.2 Thalamocortical afferents

The thalamus is the gateway to the cerebral cortex for the sensorial inputs (except for the olfaction). Furthermore, it transmits information from one cortical region to another one (Sherman and Guillery, 1996, 2002). The primary excitatory cortical recipient of TC inputs is the spiny stellate cells in layer IV (Gilbert and Wiesel, 1979). Some pyramidal neurons in layer VI also receive direct TC inputs and they project onto layer IV stellate cells (Gilbert and Wiesel, 1979; White and Hersch, 1982; Burkhalter, 1989; Ahmed et al., 1994; Hirsch et al., 1998a; Lee and Sherman, 2009; Thomson, 2010). TC synapses can also be found on the basal dendrites of layer III and apical dendrites of layer V pyramidal neurons (Hornung and Garey, 1981; Ichikawa et al., 1985). Although TC synapses on

stellate cells have nothing outstanding in comparison to intracortical synapses in terms of position in the dendritic trees or size of the their postsynaptic targets (da Costa and Martin, 2011), these afferents are associated with the highest amplitude of postsynaptic response in spiny stellate cells (Stratford et al., 1996). As spiny stellate cells have a high probability of transmitter release at synapses of layer II/III pyramidal neurons (Silver et al., 2003), thalamic afferents thus have a strong excitatory influence on the neocortical network.

TC inputs also recruit inhibition in the neocortex. Synaptic contacts are found on sparsely spiny and aspiny non-pyramidal neurons in layer IV (Hornung and Garey, 1981), which are inhibitory interneurons as described above. Several classes of interneurons having their soma in layer IV or at the border of layer IV and V receive inputs from the thalamus and their likelihood of firing is even higher than excitatory cells (Porter et al., 2001; Cruikshank et al., 2007; Hull et al., 2009). An increase in thalamic firing in response to stimulation of several whiskers in the somatosensory system, for example, is accompanied by a higher firing of FS units and a decrease of firing of RS units in the cortex (Brumberg et al., 1996). This phenomenon, believed to generate the surround inhibition in the cortex, also shows how inhibition in the neocortical network can be efficiently recruited by TC inputs. Furthermore, disynaptic inhibition in the neocortex caused by thalamic stimulation has been evidenced in layer V pyramidal neuron and its threshold was lower than for intracortical stimulation (Gil and Amitai, 1996).

In other words, TC neurons are a major source of excitation to the neocortex and they also influence, perhaps even control, the level of inhibition in the neocortical network. Most importantly, thalamocortical neurons are involved in the communication between cortical areas. In that sense, the thalamus is much more than a relay for sensory information to the neocortex, it is potentially a hub for the intracortical communication.

In this thesis, we have evaluated the contribution of an associative thalamic nucleus in propagating and synchronizing activity across different neocortical sites by pharmacologically inactivating the functional thalamocortical afferents. We chose as a model the associative cortex of the cat (area 5 and 7 located in the suprasylvian gyrus). We have targeted the lateral posterior (LP) nucleus of thalamus which provides most of the afferents to area 5 and 7 (Graybiel, 1972).

1.3.3 Neocortical excitatory connectivity

The activation of an excitatory synapse causes an excitatory postsynaptic potential cell (EPSP) that brings the postsynaptic cell closer to its firing threshold. The excitation in the neocortex is provided by pyramidal neurons and spiny stellate cells that make contacts on other pyramidal and stellate cells as well as on inhibitory interneurons. Most excitatory connections on pyramidal neurons are located on the dendritic spines (Colonnier, 1968) whereas those on interneurons (which are generally aspiny) are located mainly on the dendritic shaft (Winfield et al., 1981).

Within a cortical column, excitatory cells can communicate via intralaminar or interlaminar connections. Intralaminar connectivity refers to the communication between neurons located in the same layer. The probability of finding such connectivity between excitatory cells of layers II-III and layer V was evaluated to about 10-25%(Markram et al., 1997b; Gibson et al., 1999; Thomson et al., 2002). Interlaminar connectivity refers to a neuron making a connection with neurons of a different layer. It is very important as it forms the canonical flow of information starting in layer IV stellate cells relaying a signal to layer II/III pyramidal neurons which pass the input to layer V /VI pyramidal neurons (Gilbert and Wiesel, 1979). It is also involved in feedback excitation, that is deep layer neurons exciting back upper layer neurons. For instance, layer VI pyramidal neuron make excitatory and facilitating connections on layer IV neurons (Tarczy-Hornoch et al., 1999). There are several axonal processes of neurons in layer V and VI that are ascending to layers II/III (Burkhalter, 1989; Hirsch et al., 1998a). As summarized in figure 1.4, this ascending translaminar feedback excitation may be an essential substrate of recurrent (or sustained) activity within the neocortex.

Although we will not investigate directly the intracortical connectivity in this study, we will compare the duration of recurrent activity between different sites of a given neocortical area, different areas (associative vs. somatosensory) and different species (cat vs. rabbit).

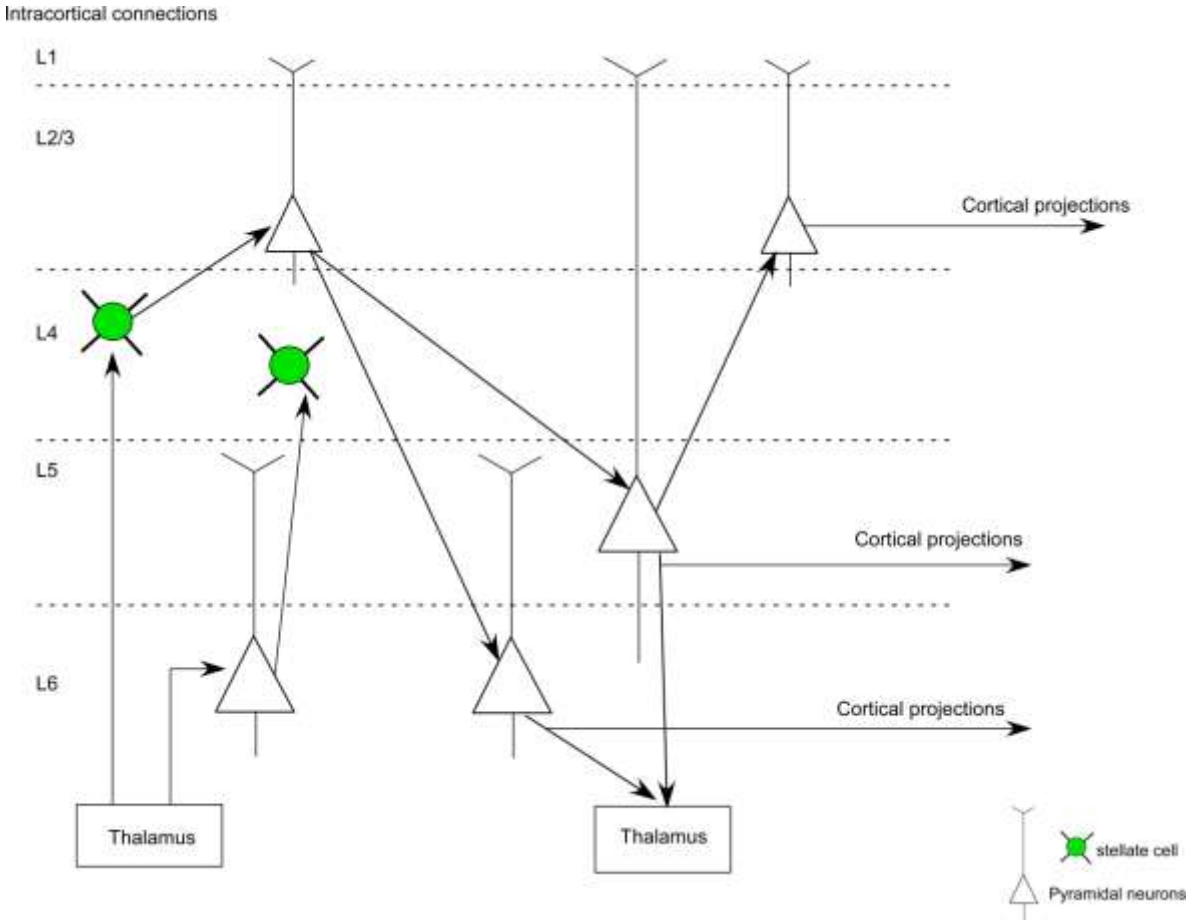

Figure 1.4 Summary of intracortical excitatory connectivity mediating the recurrent activity

Schematic representation of translaminar excitatory connectivity in the neocortex. Afferents from the thalamus andcortico-cortical and cortico-thalamic efferents from a neocortical columnare also shown.

1.3.4 Neocortical inhibitory connectivity

The synaptic response of a neuron to the firing of presynaptic interneurons is the inhibitory postsynaptic potential (IPSP). There are two types of IPSP (Connors et al., 1988). The first one reverses at -75 mV, has a short duration (10-20 ms) and is associated with a 70-90 nS conductance. The second one reverses at -90mV, lasts much longer than the first type but has a lower conductance (10-20 nS), that is a lower current and by extension, a response of smaller amplitude. The first type is attributable to currents activated by $GABA_A$ receptors while the second is characteristic of $GABA_B$ receptors activation. The activation of $GABA_A$ and glycine receptors is associated with an influx of chloride ions via a pore containing the receptor itself. $GABA_B$ receptors

are metabotropic; they activate a second messenger (a G-protein) that increases the conductance for potassium ions (Bormann, 1988). Most IPSPs recorded at the soma are identified by their reversal potential as the result of $GABA_A$ activation. The IPSPs elicited by FS and RS interneurons have comparable amplitude (0.2-2.2 mV) and reversal potential suggestive of $GABA_A$ activation, but the latter lasts longer (25-32 ms) than the former (10-20 ms) (Thomson et al., 1996).

Interneurons innervate all the compartments (soma, initial segment of the axon, dendritic shaft and spines) of pyramidal neurons and other interneurons (Hendry et al., 1983; Somogyi et al., 1983; Somogyi et al., 1998). Immunhistochemistry against GABA receptors at the electron microscopy level revealed that most (58%) GABA synapses are located on the dendritic shaft, a large portion (26.4%) on the spines and the balance on the soma (13.1%) and the axonal initial segments (2.5%) (Beaulieu and Somogyi, 1990). Considering that the soma accounts for 2-4 % of the surface of a pyramidal neuron (Mungai, 1967), it is fair to acknowledge that there is a lot of GABAergic synapses on the soma of pyramidal neurons (Freund et al., 1983). These inhibitory synapses on the soma are made by $GABA_A$ synapses as shown by a very strong immunoreactivity on the soma and proximal dendrites of pyramidal as well as non-pyramidal neurons of all layers, except in layer I where it is fainter (Gu et al., 1993).

Although the largest inhibition comes from their respective layer, there is interlaminar inhibition. Reconstruction of layer III interneurons showed that their axons descend in layer V (Somogyi et al., 1983; Thomson and Morris, 2002), pointing out that interneurons from upper layers can inhibit neurons in deeper layer. The occurrence of EPSC in layer V FS and RS interneurons after stimulation of layer II/III by glutamate puff (Otsuka and Kawaguchi, 2009), showing that monosynaptic translaminar connection indeed exists. The other way around is also true as pyramidal neurons located in layer II-III are contacted by interneurons of layers V and VI (Kisvarday et al., 1987; Thomson and Morris, 2002; Katzel et al., 2011). However, a study in which channelrhodopsine-2 was transfected in GAD67 neurons (interneurons) of mice has suggested that the monosynaptic inhibition on layer V and VI pyramidal neurons comes almost exclusively from their layer (Katzel et al., 2011). Even though monosynaptic inhibition appears to be mainly intralaminar, the translaminar inhibition could also pass through disynaptic inhibition.

The cortical inhibition is mainly a local phenomenon (i.e., at the columnar level) as interneurons create a powerful zone of inhibition within 350 μm of their soma (Salin and Prince, 1996a). However, retrograde labeling revealed that a small proportion of inhibitory neurons (0.5-5%) in layers II/III as well as layers V and VI have been observed to project farther than 0.5-1 mm in the rat visual cortex (McDonald and Burkhalter, 1993) and somatosensory cortex (Fabri and Manzoni, 1996).In both cases, the proportion of long-range projecting interneurons was larger in layers V and VI than in layer II/III. Similar observations were made in the cat visual cortex (Albus and Wahle, 1994) as well as in the motor, somatosensory and visual cortices of GAD67-GFP knock-in mice (Tomioka et al., 2005). Aside from monosynaptic connectivity, long-range inhibition can also be disynaptic as long-range excitatory projections can recruit inhibition in distant cortical sites in a supralinear manner (Tucker and Katz, 2003).

Retrograde labeling after injection in the contralateral cortex and subsequent intracellular injections in slice to reveal the cellular morphology showed that approximately 5% of the labeled neurons were aspiny non-pyramidal neurons and thus presumably inhibitory neurons. These inhibitory neurons projecting to the contralateral hemisphere were identified as basket and chandelier cells located in layer II-V and there was also a some neurons in layer I (Martínez-García et al., 1994). This suggested that, in addition to a strong local inhibition and a smaller proportion from distant sites in the ipsilateral cortex, inhibition could also come from the contralateral cortex.

In this thesis, we have investigated with intracellular recordings the contribution of chloride-mediated inhibition ($GABA_A$) in terminating the recurrent activity during the slow oscillation. We will also use electrical stimulation to test whether there are differences among cortical layers regarding the contribution of inhibition in terminating the recurrent activity.

1.3.5 Neocortical efferents

A neocortical column receives and integrates information, but it also transmits it to other neural structures. One of the targets of a neocortical column is neighboring neocortical area and its contralateral equivalent. Neurons in layer II/III are mainly responsible for these projections to neighboring cortical areas (Gilbert and Kelly, 1975) and to the contralateral cortex via the the corpus callosum. The latter, called callosal or commissural neurons, were found to be most numerous in

layer III but also in layer V in several sensorial and associative cortical regions of the rats, cats and monkeys (Jacobson and Trojanowski, 1974; Wise and Jones, 1976). Layer V also contains neurons projecting to neighboring cortical areas (Lund, 1973), indicating that neurons in both supra- and infragranular layers project to other cortical areas, including those on the contralateral side.

Layer V pyramidal neurons are considered as the main subcortical projecting neurons. Among their targets are the thalamus (Sherman and Guillery, 1996), the superior colliculus (Holländer, 1974; Gilbert and Kelly, 1975), the pontine nuclei (Abdel-Kader, 1968) and the spinal cord (Schieber and Baker, 2003). Layer VI is also a projection layer and contains three classes of pyramidal neurons according to their projection: other pyramidal neurons, the thalamus (both the dorsal and reticular ones) and the claustrum (Thomson, 2010).

In this thesis, we have focused mainly on the suprasylvian gyrus of the cat which is divided into area 5 and 7. Area 5 receives cortical inputs from somatosensory regions (Avendaño et al., 1988) and area 7 from visual ones (Olson and Lawler, 1987). These associative regions project to the LP nucleus of the thalamus. Area 5 also projects to the ventral lateral group and to the medial division of the posterior group and area 7 to the pulvinar. In addition, both sends axons to the thalamic reticular nucleus and to the central lateral and the paracentral (intralaminar) nuclei (Robertson and Cunningham, 1981).

1.3.6 Recurrent activity and the balance of excitation and inhibition

As we have discussed in the preceding sections, there are intralaminar and interlaminar connections in the neocortex, both excitatory and inhibitory. Of particular significance, the axon layer V pyramidal neurons leave several collaterals in the granular and infragranular layers (Burkhalter, 1989). These collaterals have boutons making synaptic contact onto the spines and shafts of both apical and basal dendrites of other infragranular layers pyramidal neurons (Gabbott et al., 1987). It is reasonable to assume that these intracortical connections made by the efferent neurons of the neocortex can generate recurrent activity within the neocortex.

However, too much excitation within a network could lead to paroxysmal activity typical of seizures. There are mechanisms that prevent such over-excitation. Firstly, there is frequency-dependent depression of synaptic transmission (Galarreta and Hestrin, 1998). Secondly, there is the GABAergic inhibition. Inhibition keeps on a leash neurons by preventing them from firing too much. Inhibitory

conductances are dominant in a majority of neurons (Rudolph et al., 2007; Haider et al., 2012) and it is when it decreases that an action potential is likely to happen (Rudolph et al., 2007). Instead of hyperpolarizing the membrane potential, the shunting inhibition decreases the amplitude of excitatory responses due to a large increase in the membrane conductance. This increase in membrane conductance was attributed to the activation of $GABA_A$ receptors based on the reversal potential, the large conductance and the short latency of response of cortical cells following a visual stimulus (Borg-Graham et al., 1998; Hirsch et al., 1998b). If the balance between excitation and inhibition is broken in favor of excitation, paroxysmal activity in the network is likely to follow. This has been observed for recurrent activity in neocortical slices (Sanchez-Vives and McCormick, 2000; Mann et al., 2009; Sanchez-Vives et al., 2010)

It is difficult to separate the cortical and thalamic contribution to the recurrent activity within the neocortex. As was mentioned previously, the thalamus receives input from the periphery but also from the cortex itself. Because they project widely to the cortex, thalamocortical neurons might also be involved in the recurrent activity in the neocortex. Modeling experiments have indeed shown that a thalamic drive on cortical pyramidal cells can reduce the duration of the silent state (Bazhenov et al., 2002). It remains to be demonstrated *in vivo*, but it would demonstrate that the recurrent activity is a property of the thalamocortical network as a whole.

We have tested in this study the impact of thalamocortical afferents on maintaining the recurrent activity in the neocortical network. We will also address the question about the balance of excitation and inhibition in terminating the recurrent activity.

1.3.7 Synaptic and homeostatic plasticity

The strength of synaptic connections between neurons is not fixed as it can be modified in an activity-dependent manner. This process is referred to as synaptic plasticity and translates in the potentiation or the depression of the amplitude of the postsynaptic response. The changes in amplitude can last on the timescale of milliseconds up to a second (short-term facilitation, STF, or short-term depression, STD) or for hours and days (long-term potentiation, LTP, or long-term depression, LTD) [reviewed in (Zucker, 1989; Byrne, 2003)]. There is also the medium-term plasticity which lasts from seconds to minutes (Timofeev et al., 2002).

LTP and LTD are dependent on the calcium entry in the postsynaptic cells. Low level, associated with a low frequency of stimulation (<15 Hz), leads to LTD while higher level caused by a higher stimulation frequency induces LTP (Artola and Singer, 1993). This form of synaptic plasticity depends largely, but not exclusively, on the highly calcium-permeable NMDA receptors (Malenka and Nicoll, 1993). Furthermore, the plasticity depending on the NMDA receptors is sensitive on the timing of the postsynaptic cell firing, a phenomenon called the spike-timing dependent plasticity (STDP) and depends on the postsynaptic firing (Markram et al., 1997a; Bi and Poo, 1998; Sjostrom et al., 2001). Within a narrow time window (approximately ±20ms), LTD is induced if the postsynaptic firing precedes the presynaptic action potential whereas LTP occurs if it follows.

The frequency-dependence of synaptic plasticity suggests that the intensity and direction of synaptic plasticity depend on the level of background activity in a network. In the presence of low level of background activity (for example, under barbiturate or in an isolated neocortical slab anesthesia), there is a lot of plasticity and it is dominated by depression. During higher level of background activity (ketamine-xylazine anesthesia), there is less plasticity but when there are changes, they are dominated by potentiation (Crochet et al., 2006). Wakefulness, a state of vigilance during which the cortex is bombarded by sensorial inputs, was associated with an increase in GluR1-containing AMPA receptors and was interpreted as a correlate of synaptic potentiation (Vyazovskiy et al., 2008).

LTP is linked to learning (Byrne, 2003). When learning occurs, it potentiates synapses related to that new memory formed. The first step of memory formation is the STF as it marks a synapse for potential LTP, and by extension, to become a persistent memory (Redondo and Morris, 2011). To do so, there must be mechanisms linking the functional changes in a synapse undergoing STF to the structural changes associated with LTP. The most likely candidate is the influx of calcium ions via cationic-permeable channels during the synaptic transmission that can activate various molecular pathways leading to protein synthesis involved, for example, in synaptic functions (Lamprecht and LeDoux, 2004; Ho et al., 2011; Bading, 2013).

Another form of plasticity is the homeostatic plasticity that is about the regulation of cells excitability. Blocking the activity in a primary culture of cortical neurons with TTX increases the frequency and amplitude of spike-independent miniature postsynaptic potentials, simply referred to as minis (Turrigiano et al., 1998). First discovered at the neuromuscular junction (Fatt and Katz, 1952), minis

are present in the central nervous system, including the cerebral cortex (Salin and Prince, 1996b; Pare et al., 1997). It appears that minis maintain a basal level of synaptic activation to ultimately prevent the loss of dendritic spines in absence of action potentials (McKinney et al., 1999). Aside from the upscaling of minis frequency, homeostatic plasticity also acts on the excitability of primary neurons in culture treated with TTX (Desai et al., 1999). A reduction in activity caused by a partial deafferentation of the cortex leads after weeks to an increase in connection probability and excitability (Prince and Tseng, 1993; Avramescu and Timofeev, 2008) and is accompanied by an increase in minis frequency (Li and Prince, 2002), supporting the role of minis in mediating the effect of homeostatic plasticity following a decrease in activity. On the other end, too much activity (by blocking inhibition with bicuculline) leads to a reduction of minis amplitude and frequency and decreases the excitability of neurons (Turrigiano et al., 1998).

Homeostatic synaptic plasticity modulates cellular excitability both on the presynaptic (Lazarevic et al., 2013) and the postsynaptic side (Vitureira and Goda, 2013). On the presynaptic side, homeostatic plasticity could increase excitability by increasing the release probability following a period of blocked activity (Murthy et al., 2001). The modulation of vesicular filling on the presynaptic side could also modify the strength of the postsynaptic response by changing the amount of neurotransmitter released in the synaptic cleft (De Gois et al., 2005). On the other hand, the synaptic strength could be reduced during elevated network activity via altering vesicle priming that decreases the size of the readily releasable pool at individual active zone (Moulder et al., 2006). Regarding the scaling of the postsynaptic response, rapid and local homeostatic changes would translate into the exocytosis (during reduced activity) or endocytosis (elevated activity) of AMPA receptors [reviewed in (Vitureira and Goda, 2013)]. There is also an intrinsic component to the homeostatic regulation of neuronal excitability (Turrigiano et al., 1994; Turrigiano et al., 1995; Desai et al., 1999; Lambo and Turrigiano, 2013)

In this thesis, we present data involving compensatory mechanisms for the recurrent activity following the partial or complete deafferentation of a neocortical region. Although peripheral denervation might have caused a decrease in recurrent activity in the neocortex during wakefulness, we opted to work directly at the level of the thalamocortical network under anesthesia or during natural sleep. The compensatory mechanisms following a period of deafferentation presumably reflect the presence of homeostatic plasticity in the neocortical network.

1.4 Brain rhythms in the states of vigilance

1.4.1 States of vigilance

In mammals, we formally define the states of vigilance by using the field potentials generated by the cerebral cortex recorded by electroencephalography (EEG) along with the muscle tone measured by electromyography (EMG) and the eye movements by electroculography (EOG). Wake appears as a state where the EEG is dominated by fast rhythms of low amplitude and is accompanied by a pronounced muscle tone (Hobson and Pace-Schott, 2003). With these three parameters, sleep can be segregated in two states of vigilance: the slow wave sleep (SWS) and the rapid eye movements (REM) sleep. Depending on the authors, SWS may also be referred to as non-rapid eye movements (NREM) sleep and REM sleep as paradoxical sleep. REM sleep is defined mainly by the EOG (as implied by the name) but also by a muscle atonia with some transient muscles activities. During REM, the EEG is composed of fast rhythms of low amplitude like in wakefulness. There is also a phasic activity in the EEG known as the ponto-geniculo-occipital waves (PGO waves) that often precedes eyes movements (Jouvet, 1967). SWS is further divided into 3 stages (N1-3). During N1, low amplitude waves of 4-7 Hz replace the 8-13 Hz present in the EEG during wakefulness with eyes closed. K-complexes and spindles dominate during N2; during deep sleep (N3), spindles persist but the EEG is dominated by a slow rhythm (0.5-2 Hz in humans) of high amplitude (Iber et al., 2007).

Some of the data we will present in this thesis was recorded during SWS.

1.4.2 Fast rhythms

Fast rhythms refer to beta (12-30 Hz), gamma rhythms (30-100 Hz) and ripples (>100 Hz). Beta and gamma rhythms are strong, for example, during a visual task (Gray and Singer, 1989) and somatomotor task (Murthy and Fetz, 1992). Although they are enhanced during attention, beta-gamma rhythms are also part of the background activity within the thalamocortical network during wake when it has the highest power. It is also present during slow wave sleep and even under ketamine-xylazine anesthestia. Following electrical stimulation of the cholinergic ascending activating reticular system, that is the pedunculopontine tegmentum (PPT) and the lateral dorsal tegmentum (LDT), the power of fast rhythms increases in the neocortex (Steriade et al., 1996a), suggesting it is promoted by higher level of acetylcholine in the thalamocortical network (Steriade et al., 1996a; Steriade et al., 1996b).

In the studies aforementioned, the good coherence between neuronal firing and the fast rhythms in the LFP suggested that fast rhythms are generated by a synchronous neuronal activity in recorded cortical location. Some line of evidences even suggested that inhibition might have a larger influence than excitation in shaping fast rhythms. Blocking $GABA_A$-mediated transmission *in vitro* with picrotoxin reduces the power of fast rhythms (Hasenstaub et al., 2005). Furthermore, the decay time constant of IPSP was shown to be essential in shaping fast rhythms. Barbiturates, which prolong the opening of GABAergic channels, increase this decay time constant and cause a decrease in the frequency peak of fast rhythms (Compte et al., 2008).

Ripples consist in fast (>100 Hz) rhythmic occurrence of small amplitude events generated either by peripheral stimulation (Jones and Barth, 1999) or during spontaneous activity in the neocortical network (Grenier et al., 2001). In-phase synchronous fast firing (100-400Hz) would generate ripples with a single peak in power spectrum whereas out-of-phase firing would account for broader frequency bands of fast ripples. These high-frequency oscillations may be generated by different factors including intrinsic membrane properties, synaptic interactions, spike timing and gap junctional as well as ephaptic coupling (Jefferys et al., 2012). Reduced by myelination, an ephaptic coupling is independent of synapses and refers to the excitatory field effect of an axon on an adjacent one that can affect synchronization of neuronal subthreshold activities (Arvanitaki, 1942).

In this thesis, we will use fast rhythms in LFP recordings as a measure of recurrent activity in the neocortical network.

1.4.3 Slow rhythms

Whereas fast rhythms appear as a local phenomenon, slow rhythms of the thalamocortical network emerge from the interaction and the intrinsic currents of cortical, TC and thalamic reticular neurons (Steriade et al., 1993c). Slow rhythms refer to the sigma (7-15 Hz), theta (4-7 Hz), delta (1-4 Hz) and slow (<1 Hz) oscillations. The infra-slow activity denotes oscillations with a period of seconds to minutes. The amplitude of such activity can be enhanced by metabolic disturbances, prolonged irritation of subcortical structures or prolonged stimulation of sensory afferents (Aladjalova, 1957).

Slow rhythms in the thalamocortical network are characteristic of sleep although they can be found during wakefulness. For instance, the alpha rhythm (8-13 Hz) is present in the EEG when a subject is

awake but with his eyes closed (Iber et al., 2007) but is also related to cognition and to some extent in sensory processing (Basar, 2012). The theta rhythm is mainly a hippocampal rhythm correlating with arousal, more specifically with readiness, and is quite obvious in rodents, less in cats and almost imperceptible in monkeys (Klemm, 1976). Because of their association with wakefulness, we will not further discuss the alpha and theta rhythms.

Spindles are a characteristic component of the stage 2 of SWS and persist in stage 3 (Molle et al., 2002; Iber et al., 2007). In EEG and cortical LFP recordings, a spindle sequence is characterized by a waxing and waning pattern in the amplitude of waves. Spindles are initiated by spikes bursting of neurons in the thalamic reticular nucleus (or perigeniculate nucleus for the LGN) that leads to IPSPs and rebound low threshold spike (LTS) in TC neurons (Steriade et al., 1993c; Bal et al., 1995; Timofeev and Steriade, 1996). When hyperpolarized, an IPSP has a depolarizing effect on thalamic reticular neurons and leads to an LTS in these cells (Bazhenov et al., 1999; Sun et al., 2012). Because thalamic reticular neurons are interconnected via gap junctions (Landisman et al., 2002), these cells can thus recruit neighboring neurons and causes a propagation of the spindle sequence (Bazhenov et al., 1999; Bazhenov et al., 2000). The ensuing LTS bursting in thalamocortical cells recruits at its turn an augmenting response in the neocortex. The neocortex cannot generate on its own an augmenting response characteristic of the spindle oscillation (Bazhenov et al., 1998). However, the cortex seems to have a part to play in the spindle oscillation as experimental data and models suggest it is involved in terminating the spindle activity (Timofeev et al., 2001b; Bonjean et al., 2011).

The delta rhythm (1-4 Hz) is most evident *in vivo* in TC neurons when they are sufficiently hyperpolarized (Dossi et al., 1992) and persists in thalamic slices (McCormick and Pape, 1990; Leresche et al., 1991). TC neurons generate this clocklike rhythm in absence of synaptic inputs (in presence of TTX) because it depends on their intrinsic conductances, the I_H and the I_T (McCormick and Pape, 1990). The involvement of these currents explains why the delta rhythm is favored by hyperpolarization. This thalamic clocklike rhythm, however, is largely occluded in the neocortex by the slow oscillation (Amzica and Steriade, 1998). The slow oscillation is the defining characteristic of the deepest level of SWS, the stage N3 (Iber et al., 2007).

The first description of the slow oscillation during sleep was first described by (Blake and Gerard, 1937). As the responsiveness of subjects was decreasing until it vanished, faster rhythms observed in the EEG were replaced by slow waves occurring every 0.5-3 sec (0.33-2Hz) (Fig. 1.5). In local field potential recordings, the slow oscillation appears as a depth-negativity interspaced by depth-positivity of shorter duration and recurring more or less every second. The depth-negativity groups fast rhythms and spindles whereas the depth-positivity is rather quiescent. This rhythm correlates with an alternation between hyperpolarized and depolarized levels of the membrane potentials in neocortical, TC and reticular thalamic neurons during anesthesia (Steriade et al., 1993d; Steriade et al., 1993b; Contreras and Steriade, 1995) and SWS (Steriade et al., 2001; Timofeev et al., 2001a).

The network is relatively quiescent during the hyperpolarized phase because the membrane potential of neurons is well below the firing threshold. Hence the name “silent state” for this period of long-duration hyperpolarization. When the network is depolarized, neurons are close to the firing threshold and may discharge in response to incoming EPSP. This results in an intense synaptic bombardment of neurons. It is why we refer to this depolarized phase as the active state of the slow oscillation. Fast rhythms and spindles are grouped by the slow oscillation; there are present during the active state and suppressed during the silent state in both cortical and thalamic neurons.

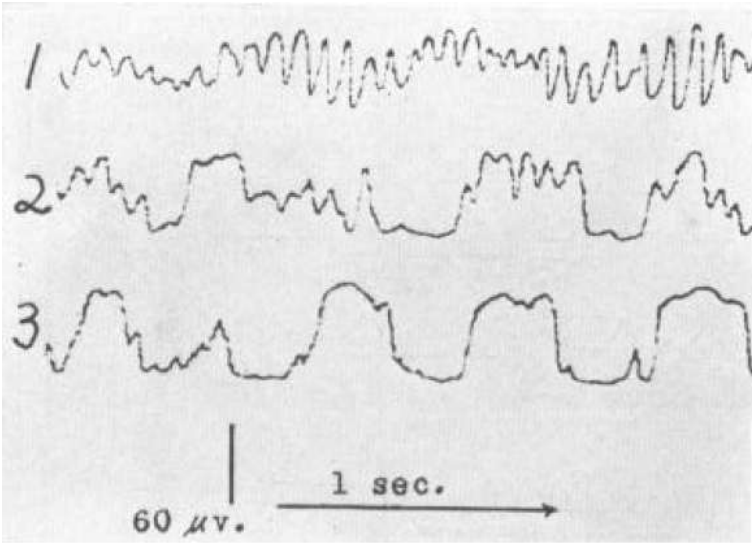

Figure 1.5 Brain rhythms during wake and sleep

Fast rhythms (10-80 Hz) during wakefulness (1) are replaced by slower rhythms (1-10 Hz) rhythm during moderate sleep (2) and by a slow oscillation during deep sleep (3). Adapted from Blake and Gerard (1937).

Some cycles of the slow oscillation, the slow waves, appears as a traveling wave. The use of 256 EEG in humans showed that the slow waves originate mainly (but not solely) from the prefrontal cortex and propagate to other regions of the cerebral cortex (Massimini et al., 2005). In other words, the slow oscillation is partly a global phenomenon where a cycle starts at a given spot and "invades" the neighboring sites. However, some studies have shown that most slow waves (up to 70%) are local, that is in given region of the cerebral cortex (Nir et al., 2011; Vyazovskiy et al., 2011). This finding raises an interesting question about the mechanisms and conditions to generate the slow oscillation. With this in mind, we will describe in the next two sections how prolonged wakefulness and anesthesia (with a focus on ketamine-xylazine) promote the slow oscillation.

In this thesis, all our studies were focused on the slow oscillation. As such, the rest of the introduction is dedicated to this brain rhythm.

1.4.4 Prolonged wakefulness and ascending activating systems

Sleep deprivation causes an increase in the slow wave activity (SWA), a measure for the homeostatic needs for sleep. The intensity of the SWA decreases as a function of time spent sleeping (Borbely, 1982; Franken et al., 1991). Aside from increasing SWA, sleep deprivation increases the number of "off" periods in the multi-units activity (MUA) that also decreases as a function of sleeping time (Vyazovskiy et al., 2011). Why does prolonged wakefulness (sustained synaptic drive) increase the sleep pressure and the need for the slow oscillation? As we will develop later in the introduction as well as in chapter 2, a reduction in connectivity (which mainly reduces the excitatory drive in a thalamocortical network) causes a depression of the neuronal activity. Given a certain period of time, the slow oscillation can recover up to a certain extent. The response of the thalamocortical network to both an increase and a decrease of the excitatory drive in the thalamocortical suggests that the slow oscillation may be the default state of the neocortex.

The sleep pressure following sleep deprivation seems to be linked to the accumulation of adenosine coming from the degradation of ATP, the energy molecule of all living cell, which can inhibits wake

promoting regions via the adenosine A1 receptor (Basheer et al., 2004). The hypnogenic effect of adenosine requires the gliotransmission (Halassa et al., 2009a). The gliotransmission acting via the A1 receptors reduces the limits of LTP (Pascual et al., 2005; Halassa et al., 2009b), suggesting that the effect of prolonged wakefulness reduce the ability to make new learnings. This topic regarding the slow oscillation is very important and we will discuss it further in section 1.4.6.

How can we remain awake in conditions of sleep deprivation? Are there external influences to keep the thalamocortical network awake to continue monitoring the environment? In other words, are there structures preventing the emergence of the slow oscillation even when the homeostatic need for it is strong? The neuromodulation by the reticular ascending activating systems controls the excitability and firing mode (tonic vs. bursting) of neurons of the thalamocortical system (Steriade et al., 1993c; McCormick and Bal, 1994) and is the most likely influence that keeps the thalamocortical network "awake". Most importantly, these ascending projections are themselves modulated by the circadian component of sleep, the ventral lateral preoptic (VLPO) nucleus. VLPO is sufficient and necessary to induce SWS (Fort et al., 2009) and is itself controlled by the suprachiasmatic nucleus (SCN) that keeps track of light/dark cycles (Reppert and Weaver, 2001). The reticular ascending activating system is also innervated by orexin/hypocretin neurons located in the posterior lateral nucleus of the hypothalamus. Orexin neurons stabilize wakefulness and their dysfunction is associated with narcolepsy (Sutcliffe and de Lecea, 2000; Saper et al., 2001). Of particular interest in controlling the states of the thalamocortical network are the acetylcholine, the noradrenaline and the serotonine.

The liberation of acetylcholine is minimal during SWS and is higher during wake and REM sleep (Williams et al., 1994), suggesting that acetylcholine prevents the occurrence of slow waves. Acetylcholine to the cortex comes mainly from the PPT, the LDT and the nucleus basalis. Acetylcholine activates thalamocortical neurons through nicotinic and muscarinic (M1) receptors (Sherman and Guillery, 1996). It antagonizes potassium currents, including the leak current, via the muscarinic receptors which depolarize the targeted neuron and promotes a tonic firing (Krnjevic et al., 1971; Cole and Nicoll, 1984; Williams et al., 1994).The acetylcholine is a promoter of wakefulness and in its absence, the leak current would be stronger and might favor the bursting behavior in the thalamus and the occurrence of slow waves.

However, the application of muscarinic and nicotinic blockers directly in the cortex did not affect the depolarization of the membrane potential characteristic of the waking state (Constantinople and Bruno, 2011). On the other hand, the destruction of the locus coeruleus, the source of noradrenaline in the neocortex, greatly affected the membrane potential of neocortical neurons. In rats anesthetized with halothane, the pharmacological activation of locus coeruleus abolished the slow waves in the EEG and led to the activation of the cortex and the hippocampus (Berridge and Foote, 1991). The discharge of noradrenergic neurons is maximal during wake (around 2 Hz), decreases by tenfold during SWS and is virtually silent (0.02 Hz) during REM (Aston-Jones and Bloom, 1981). During SWS, the firing of half of the locus coeruleus neurons is phase-locked with the transition from the silent to the active states of the slow oscillation in the prefrontal cortex (Eschenko et al., 2012). As acetylcholine, it promotes a tonic firing in thalamocortical neurons (Sherman and Guillery, 1996). All these findings suggest that noradrenaline is a promoter of wakefulness and contribute during SWS to the active state of the slow oscillation.

Sertonin has also been implicated in the neuromodulation across the states of vigilance. Extracellular recordings in freely behaving cats have shown a correlation between the firing in the dorsal raphe, the source of serotonin to the basal forebrain, and the states of vigilance. The highest firing was during wakefulness, decreased as SWS deepened and was lowest during REM sleep (Trulson and Jacobs, 1979). Levels of serotonin measured by microdialysis in the prefrontal cortex and the dorsal raphe of rats revealed a similar picture (Portas et al., 1998). The prefrontal cortex is enriched in serotonin receptors 5HT1A (inhibitory) and 5HT2A (excitatory). Both these receptors are co-expressed in a large proportion of cortical neurons which explains the complex effect of serotonin on the prefrontal cortical network (Puig and Gulledge, 2011). Nevertheless, low frequency (1 Hz) electrical stimulations of the dorsal raphe nucleus under anesthesia suggested that serotonin may play a role in promoting the active state of the slow oscillation in the prefrontal cortex (Puig et al., 2010). Serotonin might be involved in stabilizing the thalamocortical network in SWS as suggested by the effect of tryptophan side chain oxidase I, an enzyme that degrades serotonin. When injected intraperitoneally in rats, the degradation of serotonin increased the number of transition between wake and SWS (Nakamaru-Ogiso et al., 2012).

The combined effect of acetylcholine, noradrenaline and serotonine are promoters of wakefulness. Furthermore, they all inhibit potassium leak current (Goldstein et al., 2001), suggesting that the leak

current may play a critical role in shaping the slow oscillation during sleep. Another way of seeing this is that these modulating afferents keep the thalamocortical network in a responsive mode and prevent its building blocks (cortical columns, cortico-thalamo-cortical loops) from engaging into a slow oscillatory behavior.

1.4.5 Slow oscillation during anesthesia

Sleep in humans is associated with a reduction in connectivity between cortical areas (Massimini et al., 2005; Boly et al., 2012). A modeling experiment has suggested that this reduced connectivity was due to a cortical gate caused by a bias toward inhibition during SWS (Esser et al., 2009). This model did not take into consideration the possible implication of cortico-thalamo-cortical loops in the interareal propagation of activity (Sherman and Guillery, 1996, 2002). The disconnection of the cerebral cortex from the external world during anesthesia and SWS has been attributed to the thalamic gating of sensory information (Munglani and Jones, 1992; McCormick and Bal, 1994; Timofeev et al., 1996; Del Felice et al., 2012). As the reticular ascending activating systems promote wakefulness by reducing the thalamic gate, anesthesia increases the thalamic gating, and perhaps also a cortical gate.

There are indeed parallels between sleep and anesthesia as both lead to a reversible loss of consciousness and decrease the processing of sensory information by increasing the thalamic gating (Munglani and Jones, 1992; Timofeev et al., 1996). Indeed, a sleep-like slow oscillation can be reproduced by several anesthetics: urethane (Steriade et al., 1993b), isoflurane (Constantinople and Bruno, 2011) and ketamine-xylazine (Steriade et al., 1993b; Contreras and Steriade, 1995). Barbiturates promote spindle oscillations in the thalamocortical system (Andersen et al., 1967a, b) but they do not reproduce the bimodality of the membrane potentials characteristic of the slow oscillation (Dossi et al., 1992). All these anesthetics have in common that they antagonize excitation either by depressing excitatory ligand-gated ionic channels, potentiating inhibitory ones or enhancing potassium channels (Rudolph and Antkowiak, 2004; Alkire et al., 2008), suggesting that the removal of excitatory drive cause the emergence of the slow oscillation.

Ketamine-xylazine is an anesthesia that reproduces well the slow oscillation (Steriade et al., 1993b; Contreras and Steriade, 1995). Compared to the slow oscillation during natural sleep, the one

induced by ketamine-xylazine increases coherence, fast rhythms and the proportion of silent state (Chauvette et al., 2011). Ketamine is mainly a blocker of NMDA receptors (Anis et al., 1983) that acts in use-dependent manner (MacDonald et al., 1987). Aside from its main effect on voltage-depedent glutamatergic transmission, ketamine has also an effect on neuromodulation. Ketamine impairs in a concentration-dependent manner the muscarinic current by acting on M1 receptor (Durieux, 1995) and acetylcholine, as we know, is a promoter of wakefulness. When injected systemically, ketamine increases the liberation of serotonine in the prefrontal cortex (Amargos-Bosch et al., 2006) as it affects the recapture of both serotonine and norepinephrin (Zhao and Sun, 2008). By blocking NMDA receptors, excitatory drive is removed from the thalamocortical network and entrains a slow oscillation.

1.4.6 Why studying the slow oscillation?

The major role attributed to sleep is memory consolidation. The first study that showed a positive effect on memory was in reported in the 20's and concluded that sleep was protecting memories from decay (Jenkins and Dallenbach, 1924). In other words, we forget less during sleep than during wakefulness. More recent reports have shown with a sleep deprivation protocol that it is the first night of sleep after a new learning that is crucial to consolidate the newly formed memories. The subsequent nights of sleep further consolidate learning only if the subject slept the first night (Stickgold et al., 2000).

There are two models that could explain the consolidation of memories during sleep. The first model is a dual process where SWS consolidates declarative memory traces (explicit memory, a fact consciously recalled) while REM sleep is involved in consolidating procedural memory traces (implicit memory, unconscious knowledge). This model is not as well supported by many studies as is the second model which is a double-step (or sequential) process where memories (both implicit and explicit) are first consolidates during SWS and then during REM sleep (Maquet, 2001; Rasch and Born, 2013). For example, in a texture discrimination task (procedural memory), the subject performs better after the first part of the night which is dominated by SWS. By contrast, if the subjects learn the task in-between the first and the second part of the night (rich in REM sleep), the subject does not perform better in the morning. However, if the subject learns the task and is allowed to sleep all night, the performance is increased by a factor of three (Gais et al., 2000). This argued in favor a double-

process model and for the importance of SWS in consolidating memories. There is a third model, the active system consolidation hypothesis, which integrates elements from both the dual process and the double-step models. This model proposes that declarative memories temporarily stored in the hippocampus are reactivated during SWS and integrated in the neocortical network for long-term storage. Those newly integrated memories would then be stabilized during REM sleep (Rasch and Born, 2013).

What component(s) of SWS could mediate the consolidation of memories? The most obvious candidate was the slow oscillation. However, demonstrating that the slow oscillation is directly related to consolidating memories is not an obvious task. The first correlation of SWA was shown in human after a motor learning task (procedural memory). For test subjects, there was an increase in SWA in cortical regions related to motor learning in comparison to control subject. There was also a correlation between SWA and enhancement in performance (Huber et al., 2004). Although motor learning depends ultimately on REM, this study showed that slow waves were involved in consolidating this type of memories, arguing for the double-step process or the active system consolidation models.

The question whether the slow oscillation was an epiphenomenon or a truly active process was shown by transcranial stimulations (Marshall et al., 2006). Stimulations were delivered a frequency of 0.75 Hz in the prefrontal cortex of humans during sleep and enhanced the performance in a declarative task (memorization tasks of associated words). Stimulations at 0.75 Hz had no effect on a procedural task (finger- sequence tapping tasks), supporting the dual process instead of the double-step process model. Furthermore, stimulation at 5 Hz (at the frequency of hippocampal theta waves, not involved in a declarative task) had no effect on the enhancement of performance. This study showed that the frequency (slow oscillation) and the location where it occurred was specific and suggested that the slow oscillation was not an epiphenomenon but an actual process.

What is the cellular correlate of the slow oscillation effect on memory consolidation? There are two main hypotheses regarding this question. The first one, more intuitive, is that the slow oscillation potentiates the synapses underlying a given learning (that is, a newly formed memory). The second one, the synaptic homeostasis, proposes that wakefulness is associated with synaptic potentiation and that sleep depotentiates all synapses to avoid an over-growth of synapses while increasing the

signal-to-noise ratio (Tononi and Cirelli, 2006). Some evidences have indeed suggested that LTP is brought to saturation during learning and would paradoxically pave the way to the LTD (Rioult-Pedotti et al., 2000). The net effect would be the elimination of useless synapses while maintaining at a low metabolic cost those related to useful information. The reality is probably a combination of both hypotheses as there are evidences during sleep of synaptic potentiation (Chauvette et al., 2012) as well as depression (Vyazovskiy et al., 2008). So in the end, sleep and the associated slow oscillation is definitely important in forming new memories but the exact mechanisms remain elusive.

What is fundamental nature of the slow oscillation? An attractive hypothesis is that the need for the slow oscillation is a property of neuronal assemblies (such as a cortical column) following prolonged activity and that it gradually becomes a global phenomenon (Krueger et al., 2008). As such, the slow oscillation would be an intrinsic property of the neocortical assemblies that propagates in neocortical network and recruits the thalamus with which it is interconnected. Furthermore, intracortical stimulation in sleeping rats (Vyazovskiy et al., 2009) and transcranial magnetic stimulation (TMS) in humans during wake (Massimini et al., 2009) showed that an excitatory drive can switch the state of the network, which suggests the existence of active mechanisms for the transition of states during the slow oscillation.

In this thesis, we have investigated to which extent the normal expression of the slow oscillation is generated by the neocortex and what is the thalamic contribution in cats. We have also tested the hypothesis that active inhibition is involved in inducing silent states. Finally, we have explored the extent of the synchronization of the slow oscillation among neocortical sites of different areas and in different species (cats and rabbits).

1.5 Mechanisms of states transition during the slow oscillation

1.5.1 Slow rhythm in the isolated neocortical network

An isolated neocortical slab is a preparation where all afferents to a cortical region are removed but that is still irrigated by blood vessels on the pial surface (Kristiansen and Courtois, 1949). Under barbiturate anesthesia, the network of an isolated neocortical slab can generate rare burst of rhythmic activity in the alpha band. Electrical stimulations or acetylcholine application were efficient in

triggering this rhythmic activity. Under ketamine-xylazine, the network within the slab is also quiescent most of the time but once every 2-6 minutes in average, an active state occurs spontaneously (Fig. 1.6) and propagates slowly (10-100 mm/s). In an isolated gyrus, the occurrence of active states is similar to the intact cortex and suggests that the probability to trigger an active state depends on the number of neurons forming the network (Timofeev et al., 2000b). Even when isolated from the rest of the brain, a neocortical network displays a certain form of synchronous activity reminiscent of the slow oscillation.

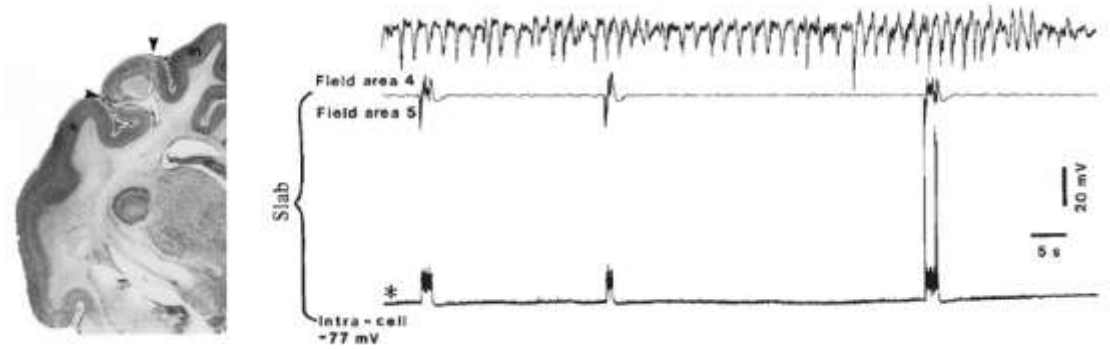

Figure 1.6 Spontaneous active states in the isolated neocortical slab

Left, photography of a forebrain section. Arrows indicate the mediolateral boundaries of the slab. Right, simultaneous LFP recordings from the intact cortex (top) and the slab (middle) and intracellular recording from the slab. Adapted from Timofeev et al. (2000b).

Cortical neurons within a slice can also display some form of synchronous activity. However, such activity has no periodicity and involves a relatively restrained percentage (~2%) of coactive neurons. Activity builds up gradually within different cellular arrangements (clusters, layers, columns or dispersed) and decreases also gradually (Cossart et al., 2003). Furthermore, neurons of a cortical network in a slice can generate repeated patterns of neuronal activation from simple to complex ("cortical songs") ones. These chains of synchronized neurons (the "synfire chain") were preferentially associated with periods defined as an active state (Ikegaya et al., 2004) and showed that even though they are stochastic in nature, cortical synapses could reliably produce some stereotypical dynamic in an isolated cortical network.

When the ionic concentrations in the bathing solution were adjusted to match physiological values (calcium 1.0-1.2 mM, magnesium 2 mM and potassium 3.5 mM), a slow oscillation-like rhythm at a

frequency comparable to halothane (0.1-0.5 Hz) could be generated by the network of a cortical slice (Sanchez-Vives and McCormick, 2000). The active ("up") states generated in these conditions group fast rhythms like in *in vivo* conditions, but the activity among neurons lacks the level of synchrony observed in an intact neocortical network. For instance, there are firing in layer V during the silent states (Sanchez-Vives and McCormick, 2000; Compte et al., 2008), which is not observed *in vivo*. Although some recurrent activity can still be generated in slices, it lacks the organization underlying the slow oscillation observed in the intact brain or even in the isolated neocortical slab.

Homeostatic plasticity mechanisms can upscale the network activity of neocortical organotypic slices. Initially absent in the first week, the frequency, duration and area of depolarization of active states progressively increased over time during the next three weeks even though the excitability of neurons was decreasing. If the slice was electrically stimulated, however, the increase in the frequency and the depolarization area of subthreshold postsynaptic events was reduced (Johnson and Buonomano, 2007). This suggested that the absence of inputs could trigger homeostatic processes in a neocortical network to upscale recurrent activity and, ultimately, to favor the generation of active states. However, a sleep-like slow oscillation could not be recovered and further suggests that a certain amount of connectivity is necessary to maintain such rhythm.

Neurons within a dissociated monolayer cortical culture are spontaneously active and calcium imaging of multiple neurons showed that calcium transients can occur synchronously in adjacent neurons (Murphy et al., 1992). A more recent study measured the firing in various location of the culture with a microelectrode array (60 electrodes organized in a grid) and pointed out that the activity of cultured neurons appeared as propagating bursts reminiscent of the sleep slow oscillation. At low frequency (0.05 Hz), electrical stimulations induced a bursting behavior which progressively decreased with increasing frequencies of stimulation until it completely disappeared above 1 Hz (Wagenaar et al., 2005), suggesting that it is the absence of inputs that induces synchronized bursts of activity. With a cocktail of agonists for glutamatergic receptors and neuromodulators (norepinephrin, serotonin, dopamine, histamine and orexin), it was even possible to switch the bursting behavior of cultured cortical neurons that is reminiscent of sleep rhythm into tonic firing, a wake-like rhythm (Hinard et al., 2012). Furthermore, the induction of this tonic firing induced the expression of genes (mainly associated with metabolism) that mirrors those expressed during sleep deprivation *in vivo*. These findings suggests that the bursting behavior and the sleep-like slow rhythm

is a consequence of removing a certain portion of inputs to a cortical system and that wake-like rhythm induces a metabolic load that is relieved during sleep.

In the developing cerebral cortex of premature and full-term infants, the sleep slow oscillation has not reach its normal pattern. In the extreme case of premature infants (24-25 weeks of gestation), the cortical activities are dominated by silent states interrupted by short and isolated sequences of slow waves. The occurrence of slow waves increases over the following weeks and the fast rhythms crowning these slow waves emerge after 30-31gestational weeks (André et al., 2010). Intracellular recordings in slices of the human fetal (20-21 gestational weeks) occipital cortex revealed that early cortical neurons generate spontaneous activity ranging from depolarizing events of low-amplitude to large depolarization plateau of long duration (mean of 0.9 s) resembling the slow oscillation. The membrane potential of these neurons was still dominated by the silent state due to the scarce connectivity within this developing network (Moore et al., 2011).

Data obtained from the isolated neocortical slabs, slices, primary cortical cultures and developing human neocortex all points to the ability of these cortical preparations to generate recurrent activity. But they also suggests that the rhythmicity of the slow oscillation and the grouping of the recurrent activity into the active state, as observed *in vivo,* depend on the integrity of the thalamocortical connectivity. In this thesis, we will directly address this question by disrupting this connectivity either by the removal of the thalamocortical afferents or by the complete deafferentation of a neocortical island. We will further explore that topic in an evolutionary perspective by comparing the propensity of the neocortical network of two mammalian species to generate and synchronize the recurrent activity forming the slow oscillation.

1.5.2 Cortical contribution to the initiation the active state

During the silent state, disfacilitation dominates and prevents cortical and thalamic neurons from firing (Timofeev et al., 2001a). How can the thalamocortical network escape this inertia then? Inputs could arise from a prethalamic source but this scenario seems unlikely (Timofeev and Steriade, 1996). Several lines of evidence have suggested that the neocortical network can escape the silent state on its own. The generation of active states persists after thalamic inactivation (Steriade et al., 1993a), in

the isolated neocortical slab (Timofeev et al., 2000b) and even in neocortical slices when ionic concentration are adjusted to physiological levels (Sanchez-Vives and McCormick, 2000).

The neocortex may escape the silent state on its own, but how? Is there a subset of pacemaker neurons responsible to trigger the active state? Layer V pyramidal neurons have been identified as the best candidate for this task. In neocortical slices, multiunit activity starts in layer V, propagates to layer VI and subsequently to layer II/III (Sanchez-Vives and McCormick, 2000). Similar results were obtained *in vivo* with multiunit activity (MUA) in the rat auditory cortex under urethane anesthesia (Sakata and Harris, 2009) and in cat suprasylvian gyrus using local field potential (LFP), MUA and intracellular recordings during both natural sleep and during ketamine-xylazine anesthesia (Chauvette et al., 2010). Furthermore, multiple intracellular recordings in vivo have revealed that IB neurons enter the active state earlier than RS neurons (Volgushev et al., 2006). The scenario proposed for the active state onset was that layer V pyramidal neurons (and mainly bursting ones) are the first active cells and recruit a sufficient number of cells for the network to enter the active state. The role of layer V over layers II/III in triggering an active state was supported by the findings of recent optogenetic studies in mice (Beltramo et al., 2013; Stroh et al., 2013).

Unfortunately this scenario was not confirmed in humans. Current source density (CSD), MUA and power spectral analysis obtained from epileptic patients prior to surgery have suggested that neurons from the supragranular layers (layer II/III) might be responsible to generate the active state (Csercsa et al., 2010). This could represent a difference in the evolution of the neocortex in humans and in carnivores or could be attributed to the epileptic focus.

Whether layer V cells are the first active or not, it is still uncertain how these neurons can reach the firing threshold with a quiescent synaptic background. Modeling experiments have been useful to explore the mechanisms of the active state onset b(Bazhenov et al., 2002; Compte et al., 2003; Hill and Tononi, 2005) from which emerged three main hypotheses not necessarily mutually exclusive. The first one is that the first active cells in layer V are pacemaker cells. This was predicted by a modeling experiment where some layer V neurons where still firing after the blockade of AMPA and NMDA synaptic transmission (Compte et al., 2003). The second one is based on the intrinsic conductance and suggested that the I_{Nap} was necessary for the onset of the active state. Upon activation by I_H, I_{Nap} would depolarize neurons until they reach the firing threshold and would stabilize

the active state by maintaining the membrane potential of neurons depolarized (Hill and Tononi, 2005). The third one hypothesized that the stochastic depolarization of neurons is caused by the summation of minis. According to this hypothesis, minis in a subset of neurons could depolarize their membrane sufficiently to activate the persistent sodium current and reach the firing threshold (Timofeev et al., 2000b; Bazhenov et al., 2002; Chauvette et al., 2010).

Minis are ubiquitously found in both supragranular and infragranular layers of the neocortex. Excitatory minis depend on the AMPA receptors (blocked by NBQX) and can occur at a frequency of up to 20-30 Hz in the intact cortex of the cat (Pare et al., 1997). Channels coupled to NMDA receptors can also contribute up to 20% of the miniature charge (Espinosa and Kavalali, 2009). Inhibitory minis are $GABA_A$-dependent (blocked by bicucculine) and occur at a frequency of ~9Hz in cortical slices (Salin and Prince, 1996b). There are evidences that vesicles spontaneously released belong to the same pool of vesicles used during network activity (Groemer and Klingauf, 2007), implying that it could happen at any synapse. The ubiquitous nature of minis combined with the large dendritic arbor of layer V pyramidal neurons (so more excitatory synapses) make the third hypothesis more likely to explain the deep layer origin of spontaneous active states in isolated cortical network (slab and slices).

In one of our studies, we used a computational model of the thalamocortical network in which the initiation of the active states was driven by minis.

1.5.3 Thalamic contribution to the initiation of the active state

The absence of the slow oscillation in the thalamus of decorticated cat (Timofeev and Steriade, 1996) and the persistence of the slow oscillation after extensive thalamic lesions (Steriade et al., 1993a) led to the conclusion that the thalamus was not necessary to generate the slow oscillation (Fig. 1.7). However, the thalamus is tightly interconnected with the cortex and it seems rather unlikely that it does not play a part in the normal pattern of the slow oscillation. In the intact thalamocortical network, the slow oscillation is indeed present in TC and thalamic reticular neurons (Steriade et al., 1993d; Contreras and Steriade, 1995; Timofeev and Steriade, 1996).

Thalamocortical neurons are naturally oscillating cells in the slow and delta frequency range (McCormick and Pape, 1990). After decortication, TC neurons display an intrinsic delta rhythm (0.5-4

Hz) when hyperpolarized (Dossi et al., 1992; Timofeev and Steriade, 1996). TC neurons in slices also express the slow and delta oscillation with low magnesium (unblocking NMDA channels) and high calcium in the bathing solution (Leresche et al., 1991). These oscillatory behaviors are possible because TC neurons are rich in intrinsic conductances (I_H, I_T and I_{CAN}) that allow a bistability of the membrane potential (that is an alternance between a depolarized level near the firing threshold and a hyperpolarized one away from the firing threshold) during the slow oscillation (Hughes et al., 2002; Crunelli et al., 2006).

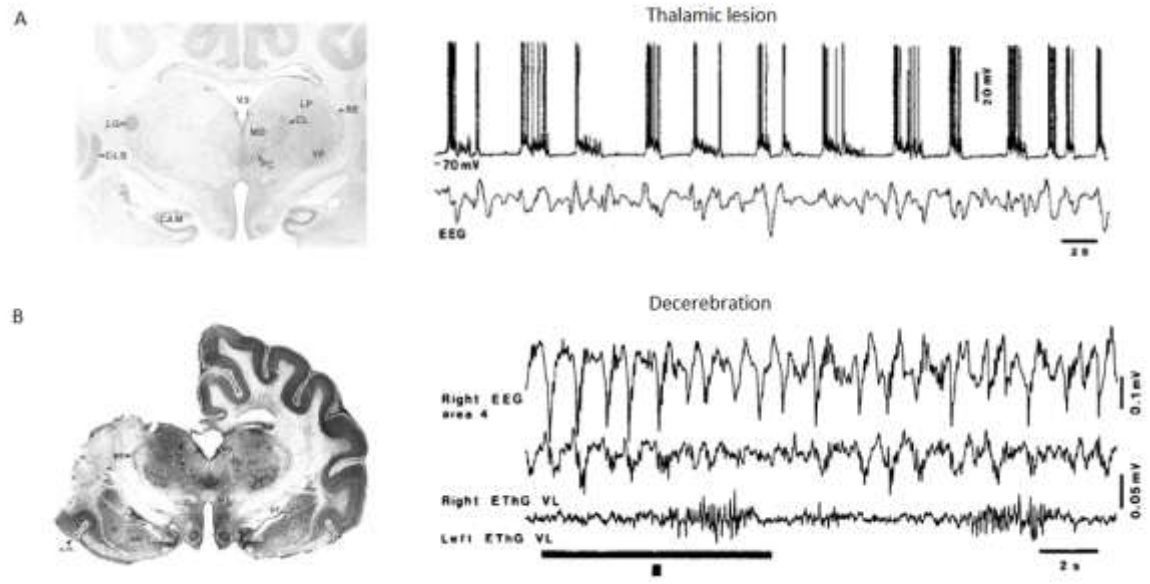

Figure 1.7 The thalamus is not necessary to generate the slow oscillation

A) The slow oscillation persists in the neocortex two days after thalamectomy. Adapted from Steriade et al. (1993a). B) The slow oscillation is absent from the thalamus ipsilateral to a decerebration. Adapted from Timofeev and Steriade (1996).

Thalamic cells can oscillate at the frequency of the slow oscillation but they require the activation of their corticothalamic synapses. *In vitro*, the exogenous activation of mGluR1a (associated with corticothalamic synapses) with a high concentration of the agonist trans-ACPD or the stimulation of corticothalamic fibers can induce a slow oscillation and vigorous firing during the active state in thalamic neurons from the cat LGN (Hughes et al., 2002) and the reticular thalamic nucleus (Blethyn

et al., 2006). In other thalamic nuclei (VB, MGB and VL), the great majority of neurons fired at the beginning of the active state (due to low-threshold calcium current) and were quiescent afterwards (Zhu et al., 2006). These studies showed that the effect of mGluR1a was to reduce the leak current. This leak current is strong in the reduced presence of acetylcholine, as during SWS for instance, and corticothalamic could release TC and thalamic reticular neurons from this disfacilitation, opening a temporal window where these cells could burst. This scenario requires that some corticothalamic neurons (in layer V and VI) must be active first.

Some evidences pointed to the contribution of TC neurons in the propagation of the slow oscillation. First, severing VB afferents in thalamocortical slices reduce the number the active states (Rigas and Castro-Alamancos, 2007). Second, the inhibition of the thalamic VB nucleus *in vivo* by muscimol (a $GABA_A$ agonist) greatly reduced the frequency of the slow oscillation in the somatosensory cortex (Doi et al., 2007). Third, stimulation of thalamic intralaminar nuclei could trigger burst in both cerebral hemisphere by activating NMDA receptors in the neocortex (Fox and Armstrong-James, 1986).

Once an active state is generated, the thalamus might also contribute in maintaining the neocortical network in that state. Electrical stimulation or glutamate application in the thalamus can lead to longer cortical active states (Rigas and Castro-Alamancos, 2007). TC neurons can trigger an augmenting response in the neocortex and it is stronger in layer V (and more specifically in burting neurons) than in superficial layers (Castro-Alamancos and Connors, 1996; Steriade et al., 1998). This augmenting response surely helps in maintaining the cortical active state.

One of our study is largely dedicated to investigating the contribution of functional thalamocortical afferents to the propagation of active states in the neocortex.

1.5.4 Synchronization in the thalamocortical network

Once generated in a given cortical location, the active states propagate throughout the cortex (Massimini et al., 2004; Volgushev et al., 2006). Although the active states propagate at a fine timescale for a network (tens of milliseconds), it appears synchronized at a lower temporal resolution (hundreds of milliseconds to seconds). This fine scale synchronization of the slow oscillation in distant sites of the same gyrus requires intracortical long-range projections (Amzica and Steriade, 1995).

The thalamic contribution to the cortical synchronization of the slow oscillation cannot be ruled out. The thalamic afferents to the cortex are both convergent and divergent. Following a peripheral nerve transection (Merzenich et al., 1983) or amputation of one or two digits (Merzenich et al., 1984), new receptive fields relaying inputs from the intact neighboring skin were formed in the deafferented somatosensory cortical regions. Although these experiments cannot distinguish between the intracortical and the thalamocortical contribution, there are anatomical evidences of the convergence/divergence of thalamocortical afferents coming from studies using dual injections of anterograde tracers in the VB complex of monkeys (Rausell et al., 1998) and multiple injections of retrograde tracers in the premotor cortex and supplementary motor area of monkeys (Morel et al., 2005). Even in the motor cortex of cats, about 40% of TC neurons from the VB complex were shown to have an axon with a wide cortical arborization (Shinoda et al., 1985). Despite these anatomical data to support a potential role in the cortical synchronization, the functional contribution of the thalamus remains uncertain.

The cortex, on the other hand, has a definitely a synchronizing influence on the thalamus. For instance, the removal of the neocortex desynchronizes spindle activity across the thalamus (Contreras et al., 1996b). The cortical influence on the thalamic synchronization may very well pass via the activation of the reticular nucleus which triggers at its turn bursting in TC neurons (Destexhe et al., 1998). Because TC neurons project back to the cortex, their synchronization by the cortex may very well further synchronize cortical neurons.

In this thesis, we will present results on the coincidence, synchronization and propagation of the slow oscillation across neocortical sites of different areas and species.

1.5.5 Terminating the active state (or initiating the silent state)

The idea that inhibitory and/or disfacilitatory mechanisms were involved in the transition to the silent state was proposed in the mid 90's to account for the relative synchrony of the slow oscillation within the thalamocortical network (Contreras and Steriade, 1995; Contreras et al., 1996a). Combined with the low calcium concentration in the extracellular space (Massimini and Amzica, 2001) that reduces the efficacy of the synaptic transmission (Crochet et al., 2005), the disfacilitation would create an inertia impossible for the network to escape, that is the silent state. Only after calcium has sufficiently

accumulated in the extracellular space would the conditions be in place for the network to return into the active state.

Is disfacilitation sufficient to initiate the silent state? It was proposed for neostriatal neurons expressing the slow oscillation that the membrane potential during the active state was maintained by synaptic inputs and kept in check by potassium conductances (Wilson and Kawaguchi, 1996). In neocortical neurons, Haider and McCormick evaluated that to maintain a depolarization of 20 mV in cortical neurons, 50-100 EPSP with a mean amplitude of 0.5 mV would be required every 10 ms. With 3000-10000 synapses on a pyramidal neuron, each synapse would need to be activated at every 0.1-1 second to maintain the observed depolarization (Haider and McCormick, 2009). In other words, a certain number of firing neurons would be required to maintain an active state. A recent optogenetic study showed that inhibiting 15% of neurons in layer V is more than sufficient to terminate the active state (Beltramo et al., 2013), suggesting that if the activity would fall below a certain threshold, the network would switch to the silent state.

An alternate hypothesis of the silent state onset revolves around the intrinsic currents of neurons, more specifically I_{KCa}, that may builds up during network activity and leads to the termination of the active states by hyperpolarizing neurons away from the firing threshold (Sanchez-Vives and McCormick, 2000; Compte et al., 2003). However, this hypothesis depends on a passive phenomenon that cannot explain the synchronous onset of the silent state in distant sites within the same cortical area (Volgushev et al., 2006). An active mechanism is required to explain such synchronization.

But what is synchronized exactly at the silent state onset? Because it controls the discharge of neurons (Hasenstaub et al., 2007; Rudolph et al., 2007), inhibition is probably the key to initiate a period of disfacilitation and, ultimately, to trigger a silent state. Inhibition can appear under many forms. It could be the entry of chloride ions at the soma after $GABA_A$ activation causing a hyperpolarization of the membrane potential that takes the neuron farther away from the firing threshold. It could be chloride- mediated ($GABA_A$) or potassium-mediated ($GABA_B$) inhibition of excitatory inputs in the dendrites. It could also be due to neuromodulation that hyperpolarizes neurons via G_i pathway. Whatever the forms of inhibition, the outcome would be the same. For a

given pyramidal neurons involved in maintaining recurrent activity, inhibition would prevent this neuron from firing and this excitatory neuron would be withdrawn from the active pool of neurons.

Several properties of inhibitory connections make it possible for inhibition to be biased towards the end of the active state. First, the connections of pyramidal neurons on interneurons undergo short-term facilitation whereas those between pyramidal neurons are subject to short-term depression (Thomson, 1997). Second, the frequency-dependent depression is higher for excitatory than inhibitory synapses on pyramidal neurons (Galarreta and Hestrin, 1998). Third, inhibition is a supralinear phenomenon. It appears when intracortical stimulation intensity is increased and coincides with a higher firing by interneurons (Hirsch and Gilbert, 1991). Due to the facilitatory nature of their inputs from pyramidal cells (Kapfer et al., 2007; Silberberg and Markram, 2007), somatostatin neurons could support the supralinearity of inhibition in the neocortical network. Fourth, FS interneurons are coupled through electrical synapses (Galarreta and Hestrin, 1999) and 52-66% of GABAergic neurons express connexin-36 (Atallah et al., 2012). Connexin-36 is the main constituent of electrical synapses (Condorelli et al., 1998; Sohl et al., 1998) and is involved in the synchronizing interneurons (Deans et al., 2001; Hormuzdi et al., 2001). Finally, another type of GABAergic interneurons expressing nitric oxide synthase (NOS) are sleep-active neurons (Kilduff et al., 2011) may also be involved in promoting the onset of the silent state.

In any case, if inhibition is involved in the transition to the silent state, an increase in firing of inhibitory interneurons prior to this transition should be observed. Two populations of FS interneurons have been reported *in vivo* based on their firing: one was biased toward the onset of the active state and the other was firing at the end of the active state (Puig et al., 2008). Electrical stimulation in slices can cause a silent state and intracellular recording of FS neurons have shown that this transition is associated with an increased firing of these cells (Shu et al., 2003). However, in neocortical slices with physiological ionic concentrations (spontaneously active), no increase in the firing of FS toward the end of the active states has been reported (Fanselow and Connors, 2010). To this day, the question of the inhibition in the transition from the active to the silent state remains attractive but unanswered.

Whisker stimulation can induce a transition to the silent state (Hasenstaub et al., 2007). According to the hypothesis we proposed about the role of inhibition in the silent state onset, TC neurons may

recruit neocortical inhibitory cells at the termination of the active states. FS units tend to scale with the thalamic firing while the firing of RS units decrease (Brumberg et al., 1996). In layer IV, FS cells are more responsive to thalamocortical inputs than RS cells (Porter et al., 2001; Cruikshank et al., 2007). Because of a high convergence of TC cells on a given interneuron and a high divergence of a single TC cells on several interneurons in the neocortex (Swadlow, 1995; Inoue and Imoto, 2006), the influence of the thalamus on inhibition can be widespread, a condition for long-range synchronization of the silent state onset in the neocortex.

In this thesis, we have investigated the role of chloride-mediated inhibition and of thalamocortical afferents in the transition from the active to the silent state onset in the neocortical network.

1.6 Goals of the thesis

In this thesis, we pursue three goals. The first one is to assess the extent of the neocortical and thalamic contribution to the full expression of the slow oscillation in the cat under ketamine-xylazine anesthesia. The second one is to evaluate the possible implication of chloride-mediated inhibition in the transition of the silent state and thus, in patterning the slow oscillation. The third and final goal is to investigate the extent of the synchronization of the slow oscillation in two different functional regions of the neocortex in two different species (cats and rabbits).

1.6.1 Thalamic and neocortical contribution to the slow oscillation

Despite its reciprocal connectivity with the neocortex, the role of thalamus in the slow oscillation remains controversial. To evaluate the contribution of the thalamus in the slow oscillation, we have inactivated the functional thalamocortical afferents with QX-314, a use-dependent blocker of sodium and low threshold calcium channels (Connors and Prince, 1982). We found in these experiments that the thalamus was critical for the normal expression of the slow oscillation but that the cortical slow oscillation started to recover within the investigated period (36 h). This suggested the involvement of homeostatic plasticity in maintaining the cortical slow oscillation. We extended the investigation of this cortical recovery of the slow oscillation in isolated neocortical slabs over 3 weeks and with a model of the thalamocortical network.

1.6.2 Inhibition in the transition to the silent state

Among different sites of a neocortical region, silent states are initiated with greater synchrony than active states. This suggests the contribution of an extracortical brain structure (such as the thalamus) in synchronizing a mechanism promoting the onset of the silent state. Among the different scenario that could initiate a silent state, the inhibition mediated by chloride ions (following $GABA_A$ activation) is the most likely candidate (discussed in section 1.5.5). We tested the hypothesis that chloride-mediated inhibition was involved in the transition to the silent state with dual intracellular recordings of closely located neurons. To do this, we filled one of the pipette with potassium chloride (KCl) 2M to reverse the concentration gradient of chloride and transform the hyperpolarizing effect of $GABA_A$ receptors activation into a depolarizing effect. Control cells were simultaneously recorded with a pipette filled with potassium acetate (KAc). We also used intracortical stimulation in the neocortical slab to test whether an excitatory input could trigger a silent state (presumably via disynaptic inhibition) and we investigated the depth profile of electrical stimulation efficacy to trigger a silent state. With extracellular recordings in the thalamus, we identified a subset of thalamic units that increased their firing prior to the onset of the silent state.

1.6.3 A comparative electrophysiological study of the slow oscillation

Studies reviewed in section 1.5.1 suggest that the slow oscillation emerges from the level of connectivity within a neocortical and thalamocortical network. In the third study, we hypothesized that the level of concordance of the slow oscillation correlates with the degree of evolution of the neocortex. To test this hypothesis, we evaluated the level of coincidence, synchronization and propagation of the slow oscillation in two mammalian species, the rabbit and the cat. The investigation was conducted in two cortical regions, a primary sensory region (somatosensory cortex) and a multimodal (associative) one. Because the level of gyrification of the cerebral cortex may reflect the amount of long-range intracortical projections (Zilles et al., 2013), we followed the hypothesis that a lower gyrification in rabbits would be associated with a lower synchrony of the slow oscillation in comparison to cats that possess a cerebral cortex with more gyrification. Furthermore, we hypothesized that due to the hierarchical level of the information (primary recipient vs. higher

integrative nature), the sensory region would show a lower coincidence, synchrony and time of propagation than associative ones.

Chapter 2 The impact of cortical deafferentation on the neocortical slow oscillation

Maxime Lemieux[1], Jen-Yung Chen[2], Peter Lonjers[2], Maxim Bazhenov[2] and Igor Timofeev[1,3†]

[1] The Centre de recherche de l'Institut Universitaire en Santé Mentale de Québec (CRIUSMQ), Laval University, Québec, G1J 2G3, Canada
[2] Department of Cell Biology and Neuroscience, University of California, Riverside, 92521, USA
[3] Department of Psychiatry and Neuroscience, Laval University, Québec G1V 0A6 Canada

Modified from : Lemieux M, Chen JY, Lonjers P, Bazhenov M, Timofeev I (2014) The impact of cortical deafferentation on the neocortical slow oscillation. J Neurosci 34:5689-5703.

Titre en français:
L'impact de la déafférentation sur l'oscillation lente nécorticale

2.1 Résumé

L'oscillation lente est le principal rythme du cerveau observé pendant le sommeil profond. Malgré la démonstration de son origine corticale par plusieurs études, l'étendue de la contribution thalamique demeure un sujet de discussion. En utilisant des enregistrements électrophysiologiques *in vivo* chez le chat et de la modélisation informatique, nous avons trouvé que l'inactivation local du thalamus ou l'isolation complète d'ilôts néocorticaux maintenus dans le cerveau réduisait dramatiquement les oscillations lentes et rapides dans les aires corticales affectées. L'oscillation lente commençait à récupérer 12 heures après l'inactivation thalamique. L'oscillation lente, mais non les activités rapides, avait commencé à récupérer après 30 heures et persistait pendant des semaines dans les îlots isolés. Nous avons également observé une augmentation de l'écart type des fluctuations du potentiel de membrane in vivo plusieurs heures après l'inactivation thalamique. En imitant cette amélioration dans un modèle informatique d'un cortex isolé avec une augmentation de l'activité postsynaptique des afférences intracorticales de longue portée ou par une régulation à la hausse du courant de fuite K+, mais pas avec plusieurs autres courants K+ ou Na+, a été suffisant pour récupérer l'oscillation lente. Nous concluons que dans le cerveau intact, le thalamus contribue à la génération des états actifs corticaux et assure la synchronisation à grande échelle de l'oscillation lente. Notre étude suggère aussi que des modifications de l'oscillation lente causées par la déafferentation peuvent être contrebalancées par des mécanismes compensateurs intracorticaux et que l'oscillation lente du sommeil est un état fondamental et intrinsèque du néocortex.

2.2 Abstract

Slow oscillation is the main brain rhythm observed during deep sleep in mammals.Although several studies have demonstrated its neocortical origin, the extent of the thalamic contribution is still a matter of discussion. Using electrophysiological recordings *in vivo* on cats and computational modeling, we found that the local thalamic inactivation or the complete isolation of the neocortical slabs maintained within the brain dramatically reduced the expression of slow and fast oscillations in affected cortical areas. The slow oscillation began to recover 12 hours after thalamic inactivation. The slow oscillation but not faster activities nearly recovered after 30 hours and persisted for weeks in the isolated slabs. We also observed an increase of the standard deviation of the membrane potential fluctuations recorded in vivo several hours after thalamic inactivation. Mimicking this enhancement with an increased postsynaptic activity of long-range intracortical afferents or up-regulation of K^+ leak current, but not several of other Na^+ and K^+ intrinsic currents, in a computational model of an isolated cortex was sufficient for recovering the slow oscillation. We conclude that in the intact brain the thalamus contributes to the generation of cortical active states of the slow oscillation and mediates its large-scale synchronization. Our study also suggests that the deafferentation-induced alterations of the sleep slow oscillation can be counteracted by compensatory intracortical mechanisms and that the sleep slow oscillation is a fundamental and intrinsic state of the neocortex.

2.3 Introduction

Sleep occupies roughly a third to a half of each day in the majority of mammalian species (Siegel, 2005). Thalamocortical activities during deep sleep are dominated by a slow oscillation (<1 Hz) (Blake and Gerard, 1937) that appears as an alternation of active (UP) and silent (DOWN) states of cortical neurons (Steriade et al., 1993b; Steriade et al., 2001; Timofeev et al., 2001). This synchronous neuronal activity generates the EEG slow waves (Contreras and Steriade, 1995; Chauvette et al., 2010).The slow-wave sleep is essential for memory formation and consolidation (Gais et al., 2000; Stickgold et al., 2000; Maquet, 2001; Huber et al., 2004; Marshall et al., 2006) and it has been proposed that synaptic plasticity associated with different brain rhythms contributes to memory consolidation (Timofeev et al., 2000; Steriade and Timofeev, 2003; Tononi and Cirelli, 2006; Diekelmann and Born, 2010; Timofeev, 2011; Vyazovskiy et al., 2011; Chauvette et al., 2012).

Despite recent progress, the role and the mechanisms of sleep (Steriade et al., 1993c; Destexhe and Sejnowski, 2001; Maquet, 2001; Steriade and Timofeev, 2003; Tononi and Cirelli, 2006; Diekelmann and Born, 2010) and the origin of the synchronous sleep slow oscillation remains a controversial topic. A number of studies (Timofeev and Steriade, 1996; Sanchez-Vives and McCormick, 2000; Timofeev et al., 2000; Bazhenov et al., 2002; Shu et al., 2003; Hasenstaub et al., 2005; MacLean et al., 2005; Rudolph et al., 2007; Csercsa et al., 2010) suggest that the neocortex is, in itself, sufficient to generate the slow activity characteristic of slow-wave sleep via recurrent excitatory and inhibitory intracortical interactions. Other studies, however, showed that the thalamus might actively contribute to the generation of the slow oscillation (Hughes et al., 2002; Crunelli and Hughes, 2010; David et al., 2013). These results argue for significant role of the thalamus in patterning the slow oscillation during deep sleep (Crunelli and Hughes, 2010).

The sleep slow oscillation groups other faster brain rhythms (Steriade et al., 1993a; Steriade, 2006) including fast oscillations in the beta and gamma frequency ranges (Steriade et al., 1996a; Steriade et al., 1996b; Dickson et al., 2003). Similar to the cortical slow oscillation, gamma oscillations can also be generated in isolated cortical structures in a condition of increased cortical excitability (Whittington et al., 1995; Draguhn et al., 1998).

In this study we demonstrate that thalamocortical inputs critically contribute to maintaining both the slow and the fast (beta-gamma) oscillations in the intact thalamocortical system. Full or partial cortical deafferentation

that removes thalamocortical inputs also disrupts the slow and fast rhythms in the neocortical network, although rare spontaneous active states persisted in the cortex. The slow but not the fast oscillation started to recover within hours after disruption of the thalamocortical connectivity. We found *in vivo* evidence of recovery of the slow oscillation following cortical deafferentation, and our modelling data indicate that an increase in intracortical excitatory synaptic drive may be one of the mechanisms underlying this phenomenon.

2.4 Materials and methods

2.4.1 Surgery

Experiments were carried out on cats of either sex in accordance with the guidelines published in the NIH Guide for the Care and Use of Laboratory Animals (NIH publication no. 86-23, revised 1987) and were approved by the Committee for Animal Care of Université Laval.

Acute experiments were conducted on cats anesthetized by intramuscular injection of ketamine and xylazine (respectively 10 and 2mg/kg).All recordings were obtained in the area 5 and 7 of the suprasylviangyrus. Animals were continuously supplied with lactate ringer at a rate of 10 mL/kg (i.v.). Ketamine was added to the lactate ringer to insure a supplementary dose of 20 µg kg^{-1} min^{-1}. The EEG was monitored throughout experiments, which lasted 8-36 hours and additional doses of ketamine-xylazine were administered intravenously when the EEG tended slightly toward activated pattern. Lidocaine (0.5%) was injected in all incision points. Animals were paralyzed with gallaminetriethiodide 2% and maintained under artificial ventilation. The ventilation rate and oxygenation were adjusted to keep an end-tidal CO_2 at 3-3.5%. Body temperature was maintained between 36.5 and 38°C throughout the experiment. The heart rate was continuously monitored (90-110 beats/min). The stability of intracellular recording was obtained by draining the cisterna magna, bilateral pneumothorax, hip suspension and filling the hole made in the skull with agar 4% in saline 0.9%.

For experiment consisting in inactivating the thalamus (n=10 cats), a stimulating electrode was stereotaxically inserted in the lateral posterior (LP) thalamic nucleus at the following coordinates: F8, L4.5, H4.5 (Reinoso-Suarez, 1961). Cortical response to 5 current pulses (10Hz, 1.5 mA, 0.2ms) delivered to the LP nucleus was assessed prior to the inactivation of LP nucleus (Fig. 2.1a). LP was inactivated by injection of 2µL of 20% lidocaine N-ethyl bromide (QX-314, Sigma) at five different

coordinates: F7, L3, H3; F7, L3.75, H4.3; F7, L6, H4; F9, L6, H5; F9, L6.75, H6.3. Blue coomassie (0.5%) was added to the QX-314 solution to confirm histologically sites of the injection (Fig. 2.1 a). Inactivation of LP was confirmed by the absence of cortical response to LP stimulation (Fig. 2.1a). The preparation of neocortical slabs (~6x10 mm) was described in details elsewhere (Timofeev et al., 2000).Slabs were isolated in acute cats (n=7) and in chronically implanted cats (n=2). The chronic surgery is described elsewhere (Steriade et al., 2001; Timofeev et al., 2001)

At the end of the experiment, animals were transcardiacally perfused with saline 0.9% followed by paraformaldehyde 4% glutaraldehyde 0.05% and then by sucrose 10% in PB 0.1M. Brain were removed and kept in PB 0.1M sucrose 30% until it sank and subsequently cryosectioned (80 μm).

2.4.2 Electrophysiology

To record multisite field potential, an array of 8 low impedance coaxial electrodes (Rhodes Medical Instruments) each spaced by 1.5 mm was inserted in the medial portion of the suprasylvian gyrus (bandpass filter: 0.1 Hz -10kHz).A high-impedance amplifier (low pass filter at 10kHz) with an active bridge circuitry was used to record and inject current in cells. Single, dual and triple intracellular recordings were obtained with sharp glass micropipettes filled with potassium acetate 2M (DC resistance of 30-75 MΩ). Signals were recorded with a 16-channel Vision data acquisition system (Nicolet, Madison, WI, USA) at a sampling rate of 20 KHz.

2.4.3 Data analysis

Analyses were performed off-line on a personal computer using IgorPro (WaveMetrics, Lake Oswego, OR, USA) and MatLab (MathWorks, Natick, MA,USA)software. Statistical analyses were performed in Prism 6 (GraphPad Software, Inc., La Jolla, CA). Depending on the normality of data and the equality of variances we used either parametric (Student's t-test,ANOVA with Tukey's multiple comparison) or non-parametric tests (Mann-Whitney test, Kruskall-Wallis test with post-hoc Dunn's multiple correction).

Wavelet transforms were computed for epochs of 15 seconds for frequency range of 0.1 to 70 Hz with the open source Matlab toolbox EEGlab (Schwartz Center for Computational Neuroscience, UCSD). Fast Fourier Transform was calculated for LFP recordings from the most and the least affected cortical sites.

Formal thresholds to determine the exact timing of onset of intracellular active and silent states were set as following: the average and the standard deviation of membrane potentials (V_m) were sampled in 25 ms time windows for epochs of at least 20 seconds. Values were plotted in a frequency matrix (Fig. 2.3c) and displayed two distributions corresponding to active and silent states. An initial threshold between these two distributions was chosen by visual inspection to split values in two new hyperpolarized and depolarized distributions. Average and standard deviation were computed for these distributions. The active state onset occurred when V_m crossed the average value of the depolarized distribution minus its standard deviation and stayed above this threshold for at least 50 ms. Transition to the silent state began when V_m went below the average value of the hyperpolarized distribution plus its standard deviation and stayed below this threshold for at least 50 ms. The number of active states per minute, the percentage of time spent in active states and the mean duration of silent states were averaged for each cell. To characterize the intensity of postsynaptic activity prior and after the onset of active states, we measured the standard deviation of the membrane potential in bins of 200 ms and averaged it over several cycles.

2.4.4 Computational models

Intrinsic currents – thalamus. Conductance based models of thalamocortical (TC) and thalamic reticular (RE) neurons include one compartment described by the equation:

$$C_m(dV/dt) = -g_{leak}(V - E_{leak}) - I^{int} - I^{syn} \qquad \text{(S1)}$$

where the membrane capacitance, C_m, is equal to 1 μF/cm^2, non-specific (mixed Na^+, K^+, Cl^-) leakage conductance, g_{leak}, is equal to 0.01 mS/cm^2 for TC cells and 0.05 mS/cm^2 for RE cells, and the reversal potential, E_{leak}, is equal to – 70 mV for TC cells and – 77 mV for RE cells. I^{int} is the sum of active intrinsic currents, and I^{syn} is the sum of synaptic currents. The area of a RE cell and a TC cell was 1.43×10^{-4} cm^2 and 2.9×10^{-4} cm^2, respectively (Bazhenov et al., 2002).

Both RE and TC cells include fast sodium current, I_{Na}, a fast potassium current, I_K, a low-threshold Ca^{2+} current I_T, and a potassium leak current, $I_{KL} = g_{KL}(V - E_{KL})$,where$E_{KL}$ = – 95mV. In addition, a hyperpolarization-activated cation current, I_h, was also included in TC cells. For TC cells, the maximal conductances are g_K = 10 mS/cm^2, g_{Na}= 90 mS/cm^2, g_T= 2.2 mS/cm^2, g_h = 0.017 mS/cm^2, g_{KL} = -0.03 mS/cm^2. For RE cells, the maximal conductances are g_K = 10 mS/cm^2, g_{Na} = 100 mS/cm^2, g_T=

2.3 mS/cm^2, g_{leak} = 0.005 mS/cm^2.The expressions of voltage- and Ca^{2+}- dependent transition rates for all currents are given in (Bazhenov et al., 2002).

Intrinsic currents – cortex.The cortical pyramidal cells (PY) and interneurons (IN) were represented by two-compartment models with channels simulated by Hodgkin–Huxley kinetics. Each compartment was described by Eq (S1) with the addition of the current from adjacent compartment, $I^{d,s}=g_c(V_{d,s}-V_{s,d})$, where V_d (*resp.* V_s) is the voltage of the dendritic (*resp.*axo-somatic) compartment. Based on our previous studies (Bazhenov et al., 2002; Chen et al., 2012), we assumed that the current dynamics in axosomatic compartment are fast enough to ensure that V_S is always at equilibrium state and can be defined by the equation $g(V_S - V_D)= - I_S^{int}$. The axo-somatic and dendritic compartments were coupled by an axial current with conductanceg_c.

The PY neurons and INs contained the fast Na^+ channels, I_{Na}, with a higher density in the axosomatic compartment than in dendritic compartment. In addition, a fast delayed rectifier potassium K^+ current, I_K, was present in the axosomatic compartment. A persistent sodium current, $I_{Na(p)}$, was included in both axosomatic and dendritic compartments. A slow voltage-dependent non-inactivating K^+ current, I_{Km}, a slow Ca^{2+}-dependent K^+ current, I_{Kca}, a high-threshold Ca^{2+} current, I_{HVA}, and a potassium leak current, $I_{KL} = g_{KL}(V-E_{KL})$ were included in the dendritic compartment only. The expressions of the voltage- and Ca^{2+}-dependent transition rates for all currents are given in Timofeev et al. (Timofeev et al., 2000). For axosomatic compartment, the maximal conductances and passive properties wereS_{soma}= 1.0×10 $^{-6}$ cm^2, g_{Na} = 3000 mS/cm^2 ,g_K = 200 mS/cm^2, $g_{Na(p)}$ = 0.07 mS/cm^2. For dendritic compartment: C_m=0.75 μF/cm^2 ,g_L= 0.033 mS/cm^2 , g_{KL} = 0.0025 mS/cm^2 , $S_{dend} = S_{soma}r$, g_{HVA} = 0.01 mS/cm^2 , g_{Na}= 1.5 mS/cm^2 , g_{Kca}= 0.3 mS/cm^2 , g_{Km}= 0.01 mS/cm^2 , $g_{Na(p)}$ = 0.07 mS/cm^2, E_{KL}= – 95 mV. E_{leak} was – 68 mV for PYs and – 75 mV for INs (Bazhenov et al., 2002). For interneurons, no $I_{Na(p)}$ was included. The resistance (r) between compartments was set to 10 MΩ.

The firing properties of this model depended on the coupling conductance between compartments (g_c = 1/r) and the ratio of the dendritic area to the axosomatic area R (Mainen and Sejnowski, 1996). We used a model of a regular-spiking neuron for PY cells (R =165) and a model of a fast spiking neuron for IN cells (R=50).

Synaptic currents. All synaptic currents were calculated according to:

$I_{syn} = g_{syn}[O] (V - E^{syn})$ (S2)

where$g_{syn}$is the maximal conductance, [O] is the fraction of open channels, and E^{syn} is the reversal potential. In RE and PY cells, reversal potential was 0 mV for AMPA and NMDA receptors, and –70 mV for $GABA_A$ receptors. For TC cells, the reversal potential was –80 mV for $GABA_A$ receptors, and –95 mV for $GABA_B$ receptors. A simple phenomenological model characterizing short-term depression of intracortical excitatory connections was also included to the model. According to this, a maximal synaptic conductance was multiplied to a depression variable, D, which represents the amount of available synaptic resources. Here, $D = 1 - (1 - D_i (1 - U)) \exp(-(t - t_i)/\tau)$ where $U = 0.2$ was the fraction of resources used per action potential, $\tau = 500$ msec was the time constant of recovery of the synaptic resources, D_i was the value of D immediately before the i_{th} event, and $(t - t_i)$ is the time after i_{th} event.

$GABA_A$, NMDA, and AMPA synaptic currents were modeled by the first-order activation schemes. Dependence of postsynaptic voltage for NMDA receptors was $1/(1+\exp(V_{post}-V_{th})/\sigma))$, where $V_{th}= -25$ mV, $\sigma = 12.5$ mV. $GABA_B$ receptors were modeled by a higher-order reaction scheme that considers the activation of K^+ channels by G-proteins. The equations for all synaptic currents were given in (Bazhenov et al., 1998; Timofeev et al., 2000). The values of maximal conductance for each synapse are listed in Table 1.

Spontaneous miniature EPSPs and IPSPs were also set in the current model. The arrival times of miniature EPSPs and IPSPs followed the Poisson process (Stevens, 1993), with time-dependent mean rate $\mu=(2/(1+\exp(-(t-t_0)/400))-1)/250$ where $t$was real time and t_0 was timing of the last presynaptic spike occurring.

Network geometry. The thalamocortical network model was constructed using several populations of neurons including cortical pyramidal cells (layer II-IV; layer V; layer VI), cortical interneurons (layer II-IV; layer V; layer VI), thalamocortical neurons (with matrix and core subsystems) and thalamic reticular neurons. A general connecting scheme among different populations of neurons is introduced in Fig. 2.7. In total, there were 1,500 pyramidal neurons (500 in each population), 360 interneurons (120 in each population), 250 thalamic reticular neurons, and 500 thalamocortical neurons (250 in each structure).

In addition, in this model, the neocortical network was evenly split into ten cortical columns, with a high density of short-range (within a predetermined footprint, [Table 1]) connections within each column and low-density, low-strength random connections between columns. Details of the network architecture (including the probability of connections and synaptic weights) are provided in Table 1.

In computational models, the LFP of an individual column was estimated by averaging membrane voltages of all neurons within this column.

Up-regulation of synaptic efficacy and intrinsic conductances. The increase in the standard deviation of V_m was implemented by adjusting the strength of PY-PY connection, the strength of IN-PY connection, and the amplitude and frequency of the spontaneous miniature EPSPs (Frohlich et al., 2008; Volman et al., 2011a; Volman et al., 2011b).Excitatory factors were increased (decreased) and inhibitory factors were decreased (increased) if the average PY firing rate was below (above) the target rate that was estimated by averaging the firing rate in the intact network. The adjusting parameters were set to be ±0.5% for the strength of PY-PY connections, and ±0.3% for the amplitude of miniature EPSP. The updating cycle was 2 sec.

In addition, we also tested the following five different scaling models by manipulating different biophysical variables in the model. (1) Conductance of leaking potassium current (g_{KL}) at dendritic compartment of pyramidal neuron. The adjusting scale was ±0.5%. (2) Conductance of the fast sodium current (g_{Na}) and voltage dependent potassium current (g_{Km}) simultaneously at dendritic compartment of pyramidal neuron. The adjusting scale was ±0.25% for both of them. (3) Conductance of persistent sodium current (g_{Nap}) and calcium dependent potassium current (g_{KCa}) simultaneously at dendritic compartment of pyramidal neuron. The adjusting scale was ±0.1% for both of them. (4) The strength of IN-PY connection (g_{GABA-A}) alone with adjusting scale equaling to ±2%. (5) The strength of PY-PY connection (g_{AMPA}) and minis amplitude. The adjusting scale was ±0.5% for g_{AMPA} and ±0.3% for minis amplitude.

2.5 Results

2.5.1 Thalamic inactivation disrupts cortical slow and fast activities

We chose to study the contribution of thalamic and cortical circuits to the slow oscillatory activity by inactivating the latero-posterior (LP) thalamic nucleus with the use-dependent sodium channels blocker QX-314 and recording the resulting activity in the respective cortical area (suprasylvian gyrus) in cats. In an intact preparation, local field potential recordings (LFP, array of 8 electrodes separated by 1.5 mm, Fig. 2.1a) from the suprasylvian gyrus under ketamine-xylazine anesthesia demonstrated the presence of a robust and synchronized slow oscillation (Fig. 2.1b). Electrical pulse-trains applied through an electrode located within the (LP) nucleus of the thalamus at 10 Hz elicited a cortical augmenting response (Fig. 2.1a, inset, upper trace, traces is from channel 2 in b-c). Wavelet transform analysis also pointed to the presence of a robust high frequency component in the beta-gamma frequency range during slow oscillation (Fig. 2.1d). Congruently to a previous study (Doi et al., 2007), when the LP thalamic nucleus was inactivated (Fig. 2.1a, left), the slow waves and fast rhythms in the targeted cortical regions were dramatically reduced (Fig. 2.1c, and e, see also Fig. 2.4a). Electrical stimuli applied to the inactivated thalamic site (Fig. 2.1a) did not elicit any cortical response after QX-314 injection (Fig. 2.1a, inset, middle and bottom trace), indicating that these thalamic sites were functionally inactivated. In the affected cortical regions, both slow oscillation and beta-gamma activity, which typically occurs during active cortical states, were virtually abolished (Fig. 2.1e, upper) and only slightly reduced in the periphery of the affected sites (Fig. 2.1e, lower). This suggests that thalamic inputs are required for the generation and synchronization of cortical active states during slow oscillation. To verify whether thalamic injection of QX-314 effects were not attributed to a leak of QX-314 to cortical locations, in control experiments we injected intracortically 0.1 µl, 20% of QX-314. This induced local and complete cortical inactivation with a radius of 1.5 mm (not shown).

To quantify changes in slow and fast rhythms induced by thalamic inactivation we performed power spectral analysis from 10 animals (Fig. 2.2) in which we compared activities in the most vs. least affected electrodes (based on the power spectra before and after thalamic inactivation) over time. Before thalamic inactivation the differences were restricted to frequencies 12-17 Hz, which might be explained by a particular network organization of the two cortical sites. After thalamic inactivation the

power spectra of all investigated frequencies was reduced (Mann-Whitney, $p<0.05$, Fig. 2.2, b, 1-2 and 7-8 hours).

We performed multisite intracellular recordings to investigate the source of the reduction of the LFP signal in the affected region (Figs. 2.3 and 2.4). Out of 86neurons recorded in this study, 59 neurons were located in the territory with disturbed slow oscillatory activity as estimated from the LFP recording. In the example shown in Fig. 2.3a, the intracellular pattern in the affected region (Intra 2) showed only one active state during 10 seconds epoch of recording, whereas active states co-occurred every 1-2 seconds in unaffected regions (intra 1 [anterior suprasylvian gyrus] and intra 3 [posterior suprasylvian gyrus]) separated by a distance of 11mm.

To characterize the impact of thalamocortical inputs functional removal on the occurrence of active states and percentage of time spent in this state, we detected active and silent states in each neuron according to formal thresholds (Fig. 2.3c, see method section). In the affected region (0-12 h from time of inactivation), active states occurred with a mean frequency of 16.1 ± 9.1per minute, lower than in intact regions (37.1± 12.1, $p < 0.0001$,Fig. 2.3d, Kruskal-Wallis post-hoc Dunn's multiple comparison test). Overall, active states in regions with disrupted slow oscillation occurred 11.0 ± 6.9% of the total time, while in intact regions they occupied 51.6± 26.6 % of the total time (Fig. 2.3e, $p<0.0001$, Kruskal-Wallis post-hoc Dunn's multiple comparison test). The down state duration was also longer in neurons located in the affected region (Fig. 2.3f, $p < 0.0001$, Kruskal-Wallis post-hoc Dunn's multiple comparison). These results suggest that the thalamocortical neurons contribute significantly to the generation of the cortical active states of the slow oscillation.

Dual recordings from closely located neurons (0.5-1.5mm) in affected areas demonstrate that active states can be generated in neighboring neurons either in alternation (Fig. 2.4c-d [arrowheads]) or a large number of them can be recorded in one neuron but not in another one (Fig. 2.4b [asterisks]). This contrasts to observations in intact cortical areas where alternating active and silent states occurred with a high degree of synchrony in neighboring neurons (Fig. 2.4e). Using coincidence analysis (Mukovski et al., 2007), we found that in the intact suprasylvian gyrus, neurons within a distance of < 1.5 mm (n=10 pairs) spent coincidentally 84.4 ± 13.1 % of the time in active states. By contrast, neurons within a similar interneuronal distance in the affected area displayed a lower coincidence of active states (Fig. 2.4f3, n=15 pairs, $p<0.001$, ANOVA post-hoc Tukey's multiple

comparisons test). This synchronicity was significantly lower even than for neurons recorded in intact areas separated by over 3 mm (Fig. 2.4f2, n=10 pairs, p = 0.005, ANOVA post-hoc Tukey's multiple comparisons). The lowest synchronicity of active states was observed between neurons located in intact area and those in the affected area (Fig. 4f4, n=11 pairs, p<0.0001, ANOVA post-hoc Tukey's multiple comparisons). The reduced amplitude of the slow waves in the affected region (see Fig. 2.1) can be attributed to the lack of actives states synchronicity among neurons devoid of thalamocortical inputs. In addition to its role in generating active states, these results reveal that blocking the activity of a thalamic region dramatically reduced the synchronization of cortically generated active states.

2.5.2 Time-dependent recovery of slow oscillation

Twelve-thirteen hours after thalamic inactivation the field potential activities started to recover progressively. The absence of cortical response to thalamic stimuli (Fig. 2.1a, inset, lower trace) indicated that the inactivation by QX314 was still effective. After 30 hours (n=4 cats) the activities in low frequency range of 0.5-12.0 Hz were similar in intact and affected cortical regions (Fig. 2, b). By contrast the power for the faster activities (above 12.0 Hz) were significantly depressed in the most affected by thalamic inactivation site. The remaining differences in the infraslow range (<0.5 Hz) are likely attributed to the metabolic alterations induced by prolonged anesthesia (Aladjalova, 1957).

We also recorded the intracellular activity of neurons in the affected region 12-36 hours after inactivation of the thalamus. As shown in Fig. 2.3b, 33 hours after thalamic inactivation, the simultaneously recorded intracellular activity of two cortical neurons from intact and affected areas revealed a similar pattern of the slow oscillation. For the neurons recorded in the late period in affected region (12 – 36 h) the difference in the number of active states, the time spent in active states and down state duration was not significant as compared to intact region (Fig. 2.3d-f, Kruskal-Wallis post-hoc Dunn's multiple comparisons).These results suggest that the slow oscillation gradually recovers in the absence of thalamocortical input and point to the presence of intracortical compensatory mechanisms.

We extended our investigation of the cortical recovery of the slow oscillation to fully isolated neocortical slabs (Timofeev et al., 2000)(Fig. 2.5). In the first hour after isolation, we detected in the LFP recordings of slabs of anesthetized cats an average of 1.4 ± 2.3 active states per min (Fig. 2.5a,

e and f) that was even lower than after thalamic inactivation. In total we analyzed time dependent changes in the active state generation in 7 acute and 2 chronic slabs. Within time window segments selected for analysis (Fig. 2.5, f) there was a highly significant increase in the number of active states after about 100 hour following isolation (Kruskal–Wallis test, $p<0.0001$). Dunn's multiple comparison test shows that changes were found between all investigated groups except for two pairs of data indicated in figure 2.5, f. In chronic slabs, electrographic activities were not recorded during recovery from surgery. Recordings performed a hundred and more hours from isolation revealed 35-45 active states per minute (Fig. 2.5 b-f), which is comparable to the slow oscillation in naturally sleeping cats with intact cortex (Steriade et al., 1993b).The slow oscillation in the slab did not depend on the state of vigilance. It was present during both slow-wave sleep (Fig. 2.5, b-c) and during brain activated states (Fig. 2.5b and d). These results suggest that the normal slow oscillation in the intact brain arises through interactions between thalamic and cortical circuits and that it gradually recovers in the absence of any extracortical inputs.

Concurrent to the recovery of the slow oscillation in partially deafferented cortical regions, we observed an increase in both frequency and amplitude of postsynaptic events occurring prior to the active states as a function of time from thalamic inactivation (Fig. 2.6, a-c).Because active states are associated with intense excitatory and inhibitory synaptic activities originating from a large number of interconnecting neurons, extraction and quantification of individual events might give unreliable results with a bias toward larger amplitude events. Therefore we analyzed segments of intracellular recordings that contained a silent state and its transition to an active state at different times from thalamic inactivation (Fig. 2.6) and we measured the standard deviation of the membrane potential fluctuations in bins of 100 ms near the onset of the active states (Fig 2.6, a-c, histograms). The analysis was performed on 10 neurons in control conditions (no inactivation), 29 cells in period 0-15 h and 13 cells >20 h from thalamic inactivation (Fig. 2.6, d-f).We found a progressive increase (statistically significative, $p<0.05$, F-test for linear regression). in the standard deviation of membrane potential fluctuations over time in different segments preceeding and immediately following the onset of an active state (Fig. 2.6, d-f). The Kruskal–Wallis test further showed highly significant increase in synaptic activities as a function of time from thalamic inactivation, (-200 ms to -100 ms, $p=0.0136$; -100 ms to 0 ms, $p<0.0001$ and 0 ms to 100 ms, $p<0,0001$). Dunn's multiple comparison test revealed that the values return to control level after 10-14 h since thalamic inactivation, closely matched our findings with LFP recordings (Fig. 2.2). We attribute the lower values of synaptic noise after 20 h to

the long lasting effects of ketamine-xylazine anesthesia. Overall, these results show that the progressive recovery of the neocortical slow oscillation is accompanied by an increase in neocortical postsynaptic activity.

2.5.3 Mechanisms of synchronization of slow oscillation and its recovery after thalamic inactivation

Previous models of the thalamocortical slow oscillation were based on uniform synaptic connectivity (Timofeev et al., 2000; Bazhenov et al., 2002; Compte et al., 2003). In the light of our experimental findings, we implemented in a large-scale thalamocortical network model a more realistic columnar organization (Fig. 2.7, Table 2.1, see model description in materials and methods).Specifically, we implemented a high-density local connectivity and sparse long-range connections as observed in vivo (Thomson and Bannister, 2003). The model displayed an alternation of active and silent states at a frequency of 0.62 ± 0.08 Hz. The active state initiation was driven by spontaneous transmitter release at excitatory synapses while termination was mediated by synaptic depression, activation of intrinsic hyperpolarizing conductances and synaptic inhibition (Timofeev et al., 2000; Bazhenov et al., 2002; Chen et al., 2012). This produced rhythmic activity resembling sleep slow oscillation in vivo that was synchronized across the thalamocortical network (Fig. 2.8 a-b).

Upon complete thalamic deafferentation of the first four cortical columns, the regular slow oscillation pattern was disrupted in affected cortical areas (Fig. 2.8c, d). In the intact network, both cortico-thalamo-cortical projections and long-range intracortical connectivity contributed to the synchrony of slow oscillation. However, immediately after thalamic inactivation, the remaining intracortical connections were not sufficient to drive rhythmic activity in the deafferented areas. Thus, in agreement with experimental data (Figs. 2.3a and 2.4b-d), deafferented cortical neurons were mostly silent and only displayed occasional and irregular active states that were limited to specific columns and did not propagate to the rest of the network. The simulated LFP amplitude was reduced in deafferented areas (Fig. 2.8e) as in experiments (Fig. 2.1c, e, Fig. 2.2). Occasionally, active states in the deafferented area occurred simultaneously with the intact network, however, in many cases as in experimental observations (Fig. 2.4) these events were local, explaining the low amplitude of the simulated LFP (Fig. 2.8e). In this model, the generation of the active states was driven by intracortical

mechanisms; however, active states synchronization depended on the thalamocortical projections and was severely diminished in the affected cortical areas after thalamic inactivation.

To describe more precisely the role of the thalamocortical projections in maintaining the normal pattern of the slow oscillation, we next evaluated the contribution of thalamocortical diffuse (matrix) vs specific (core) projections to the synchronization of the cortical active states. When the thalamocortical diffuse projections were fully dissected (Fig. 2.9 a), transitions between active and silent states occurred independently among columns, which is demonstrated by lower peak amplitude and longer time lag to the main peak of cross-correlation function (Fig. 2.9 c). By contrast, removing only specific projections had no impact on the synchrony among columns (p<0.001, two sample t test based on population of maximum cross correlation among columns) (Fig. 2.9 b, c). To further assess the impact of the thalamocortical input on the cortical synchronization of the slow waves, we varied the radius of thalamocortical connectivity in intact model and we found that the intracortical synchrony increased as a function of the radius (Fig. 2.9 d, e). This suggests that widespread thalamocortical projections play a critical role in the synchronization of the active cortical states across the entire cortical network.

We reproduced in the model the increase in the standard deviation of the V_m fluctuations (Fig. 2.6) by adjusting the strength of long-range intracortical excitatory synapses. When thalamic inputs were blocked, the overall firing rate of the cortical neurons decreased due to lower levels of excitability. This matched the reduction in synaptic activity levels at the onset of active states recorded in vivo (Fig. 2.6, e).Based on previous models of homeostatic changes in the neocortical network (Houweling et al., 2005; Volman et al., 2011a), the efficacy of excitatory intracortical synapses was progressively up regulated till the mean firing rate reached the target value corresponding to the slow oscillation in baseline model(Volman et al., 2011a). These processes led to a progressive recovery of the normal pattern of the sleep slow oscillation in the deafferented columns (Fig. 2.10 a). The average frequency of active states increased with time (Fig. 2.10 c) and the number of active states occurrence in affected columns was similar to the one observed in intact columns after the progressive upregulation of the intracortical excitatory drive to target value (Fig. 2.10 d). The synchronization of activity across cortical columns was also recovered (Fig. 2.10 e). When, however, long-range intracortical synaptic connectivity was excluded from the up-regulation of excitability, the frequency of active states recovered but synchronization was lost (Fig. 2.10 b).These results suggest that the scaling of the

long-range corticocortical synaptic connectivity could compensate for the loss of the thalamocortical feedback loop.

Synaptic scaling was suggested as a common mechanism of homeostatic plasticity(Turrigiano et al., 1998). However, other factors may contribute to the recovery of slow oscillation after the thalamic inactivation. This includes a homeostatic effect on neuromodulation, which can increase excitability by blocking K^+ leak currents(McCormick, 1992), and on intrinsic conductances, which can affect the expression of intracellular excitatory and inhibitory conductances (Desai et al., 1999). To test these mechanisms we implemented the up-regulation of excitability of various biophysical properties in the model. The results of these experiments for the intact and deafferented columns are shown in figure 2.11g. We first tested theregulation of the g_{KL} in dendritic compartment of all pyramidal neurons (Fig. 2.11a). We found that this mechanism was sufficient to recover the frequency and with somewhat lower synchrony of slow oscillation (Fig. 2.11b,c). In contrast, the scaling of the intrinsic persistent Na^+ and Ca^{2+}-activated K^+ currents failed to recover of normal slow oscillation (Fig. 2.11d).While activity of pyramidal neurons increased along the simulation, it did not form a regular slow oscillation pattern. Instead, it led to very long active states, which could last longer than 3 sec (Fig. 2.11e). Furthermore, synchronization level across deafferented columns was not improved along the recovery process(Fig 2.11f).Similar results were obtained with scaling of g_{Na} and g_{Km}, or $gGABA_a$ (Fig. 2.11g).

In sum, we found that the strength of excitatory connections between pyramidal neurons and the minis amplitude at these excitatory synapses (Fig. 2.10, Fig. 2.11g) were sufficient for slow oscillation recovery. Surprisingly, the passive intrinsic properties (e.g. leaking potassium current) in pyramidal neurons were also able to mediate recovery, though with lower levels of synchrony between different neurons. On the other hand, when scaling was applied to the intrinsic conductances of pyramidal neurons, the average firing rate of the network tended to increase but the normal pattern of slow oscillation failed to recover.

2.6 Discussion

Using recordings from anesthetized and behaving cats, we found that the functional removal of thalamic inputs to the neocortex dramatically reduced the occurrence of active states of the slow oscillation. The remaining active states in the affected region were infrequent and local, explaining the low amplitude LFP in that region. The slow oscillation started to recover twelve hours after thalamic inactivation. Extending our investigation of this phenomenon to completely deafferented neocortical slabs, we observed a complete recovery of the slow oscillation within two weeks. This recovery of the slow oscillation occurred in parallel with an increase in spontaneous fluctuations of the membrane potential prior to the active states several hours after deafferentation suggesting up-regulation of excitatory synaptic drive. In a large-scale thalamocortical network model analysis, we replicated the disruption of the neocortical slow oscillation induced by removing the thalamic inputs to the cortex. We tested the effect of scaling various biophysical features of the model and found that the scaling of synaptic connectivity restored the frequency and synchrony of the slow oscillation. Up regulation of g_{KL} could restore the frequency of the slow oscillation, whereas the scaling of both fast and slow intrinsic Na^+ and K^+ conductances failed to recover the cortical slow oscillation. Collectively, our experimental and modeling results show that the normal pattern of the neocortical slow oscillation requires thalamic inputs, but suggests that there are cortical compensatory mechanisms to maintain the slow oscillation if thalamic input is damaged.

2.6.1 Thalamic and neocortical contribution to the slow oscillation

The relative contribution of the neocortex and the thalamus in the expression of the slow oscillation has been debated over the last two decades. Our results confirm previous studies that demonstrated that the neocortical network was sufficient to generate the slow waves (Steriade et al., 1993b; Timofeev and Steriade, 1996; Sanchez-Vives and McCormick, 2000; Timofeev et al., 2000; MacLean et al., 2005; Hinard et al., 2012). The other line of evidences suggests that the full expression of slow oscillation requires a contribution from the thalamus (Hughes et al., 2002; Doi et al., 2007; Crunelli and Hughes, 2010; David et al., 2013).Computer models revealed that the interaction between thalamic and cortical networks may be necessary for maintaining regular transitions between active and silent states (Destexhe, 2009). The current study clearly shows that after the removal of thalamic inputs [about 6 % of excitatory synapses in the cortical network (Ahmed et al., 1994)], the slow oscillation was replaced by local active states of much shorter duration that occurred irregularly and

at a low rate. Similar results were obtained after complete isolation of a cortical area (slab), regular active states having been replaced by irregular and infrequent events. We propose that the thalamocortical neurons: 1) participate in the generation of active states, 2) contributes to the normal duration of the active states by maintaining recurrent activity and 3) plays a major role in synchronizing the slow oscillation across cortical columns.

Thalamocortical network is tightly interconnected, which makes thalamocortical oscillations synchronous. Previous experimental (Contreras et al., 1996) and computational (Destexhe et al., 1998) studies have demonstrated that the removal of the cortex leads to the desynchronization of the spindle activity in the thalamus. Here we show that thalamic inactivation desynchronizes the cortically generated slow oscillation without abolishing the generation of isolated cortical slow waves (Fig. 2.4). Importantly, after several hours following deafferentation, the cortical plasticity processes re-establish the synchronization of slow waves (Fig. 2.3). In contrast, the recovery of a synchronous spindle activity with time was not demonstrated for thalamus in decorticated animals.

It was previously demonstrated in different species that once initiated in a specific location the slow waves propagate to involve large cortical territories (Massimini et al., 2004; Volgushev et al., 2006; Mohajerani et al., 2010; Ruiz-Mejias et al., 2011). The fact that after the first hours after thalamic inactivation we observed isolated (local) cortical slow waves, which did not even propagate to neighboring regions, suggests that in intact network the thalamus plays a critical role in the generation of cortical propagation patterns. However, several hours after thalamic inactivation, the slow rhythm recovered in affected areas, indicating that after a period of reorganization the cortical network has functionally changed to promote the propagation of the slow waves.

In a large-scale model of the thalamocortical network with realistic network structure, we found that the dense local connectivity was sufficient to generate spontaneous active states but widespread cortico-thalamo-cortical projections were required to ensure the propagation of the locally generated active states to the rest of the network. These results are in agreement with previous studies suggesting the role of the wide-spread (matrix) thalamocortical projections in the synchronization of cortical sleep spindle oscillations (Bonjean et al., 2012). When this connectivity was abolished to model the thalamic inactivation, the synchrony of active states was lost in the affected cortical areas. Following a decrease in the overall level of activity, we found that the normal pattern of the slow

oscillation could not be recovered by the scaling several Na^+ and K^+ conductances. However, an up-regulation of excitatory synaptic conductances or a decrease in the potassium leak current recovered the slow oscillation, suggesting that those are the critical factors in maintenance of cortical slow oscillation.

Unlike slow rhythms, the virtual abolition of fast rhythms in the neocortex did not recover over the investigated period of 36 hours. Furthermore, the coincidence among neurons (based on fast rhythms grouped by the slow oscillation) was greatly diminished in the absence of thalamic inputs. These findings further suggest a role for the thalamus in the long-range synchrony of fast cortical activities. Although the synchronization of fast rhythms between thalamus and cortex was not investigated in details, some studies have shown a coherence of these rhythms within the thalamocortical network (Steriade et al., 1996b; Castelo-Branco et al., 1998).

2.6.2 The slow oscillation as the intrinsic property of the neocortex

In the intact brain the slow oscillation emerges as an alternation of active and silent states and it occurs exclusively during slow-wave sleep (Steriade et al., 2001; Timofeev et al., 2001; Vyazovskiy et al., 2009). However, the patterns resembling the slow oscillation appears as a common feature of isolated cortical networks that develops with different time courses from initially 'silent' cell primary cultures(Sun et al., 2010; Hinard et al., 2012), acute (Compte et al., 2008) and organotypic (Johnson and Buonomano, 2007) cortical slices, and neocortical slabs (Fig. 2.5). The main difference between the slow oscillation recorded in vivo during sleep or anesthesia and similar patterns recorded in isolated structures is the duration of silent states. Quantification of the duration of silent states in vivo demonstrate that they occupy 10%-20%of the total sleep time (Chauvette et al., 2011), while available examples of recordings in acute, organotypic slices or cultures (see above) show that the silent phase occupy over 80% of the time, which bring the overall frequency of slow oscillation to much lower values. In acute isolated neocortical slabs (Timofeev et al., 2000) (see also Fig. 2.5 a) the silent states are also long. However, field potential recordings from chronic slabs (Fig. 2.5 c) demonstrate that after a sufficient period of time the duration of silent states becomes similar to the one recorded in the intact cortex. These observations suggest that some minimal level of connectivity is needed to generate slow waves with parameters found in the intact cortex. Such minimal level of connectivity is absent in acute and organotypic slices.

We found that ongoing plastic changes in the intracortical network had begun the recovery of the slow oscillation pattern 12 hours after surgery independently of thalamic inputs, thus matching the time-course of homeostatic plasticity (Turrigiano et al., 1998; Turrigiano, 1999; Murthy et al., 2001; Desai et al., 2002). Experimental findings and a modeling approach further suggested that the homeostatic up-regulation of the intracortical excitatory synapses was sufficient to restore the normal slow oscillation pattern (Fig. 2.10); in such conditions long-range intracortical connectivity played a critical role in the synchronization of active states across the entire network.

The activities similar to the slow oscillation occur in the majority of neurons in the human brain even prior to birth (Andre et al., 2010; Moore et al., 2011).Although a role for the sleep slow oscillation in brain functions remains controversial, our results suggest that the slow oscillation is an intrinsic and a fundamental state of the thalamocortical system. This state is prominent during slow-wave sleep and we propose it is maintained by intracortical plasticity mechanisms. A reduction in critical elements of the cortical network reduces the spontaneous slow-wave activity. However it then recovers up to a normal sleep pattern after a period of time lasting from minutes to days. On the other hand, after sustained period of wakefulness the sleep pressure increases (Achermann et al., 1993), and the local populations of cortical neurons start to display local sleep-like activities even if the whole brain is in a waking state (Vyazovskiy et al., 2011). Collectively, these results demonstrate that any factor leading to a reduction of the slow oscillation triggers plastic changes that bring back this intrinsic cortical rhythm.

2.7 References

Achermann P, Dijk DJ, Brunner DP, Borbely AA (1993) A model of human sleep homeostasis based on eeg slow-wave activity: Quantitative comparison of data and simulations. Brain Res Bull 31:97-113.

Ahmed B, Anderson JC, Douglas RJ, Martin KA, Nelson JC (1994) Polyneuronal innervation of spiny stellate neurons in cat visual cortex. J Comp Neurol 341:39-49.

Aladjalova NA (1957) Infra-slow rhythmic oscillations of the steady potential of the cerebral cortex. Nature 4567:957-959.

Andre M, Lamblin MD, d'Allest AM, Curzi-Dascalova L, Moussalli-Salefranque F, T NTS, Vecchierini-Blineau MF, Wallois F, Walls-Esquivel E, Plouin P (2010) Electroencephalography in premature and full-term infants. Developmental features and glossary. Neurophysiol Clin 40:59-124.

Bazhenov M, Timofeev I, Steriade M, Sejnowski TJ (1998) Cellular and network models for intrathalamic augmenting responses during 10-hz stimulation. J Neurophysiol 79:2730-2748.

Bazhenov M, Timofeev I, Steriade M, Sejnowski TJ (2002) Model of thalamocortical slow-wave sleep oscillations and transitions to activated states. J Neurosci 22:8691-8704.

Blake H, Gerard RW (1937) Brain potentials during sleep. Am J Physiol 119:692-703.

Bonjean M, Baker T, Bazhenov M, Cash S, Halgren E, Sejnowski T (2012) Interactions between core and matrix thalamocortical projections in human sleep spindle synchronization. J Neurosci 32:5250-5263.

Castelo-Branco M, Neuenschwander S, Singer W (1998) Synchronization of visual responses between the cortex, lateral geniculate nucleus, and retina in the anesthetized cat. J Neurosci 18:6395-6410.

Chauvette S, Volgushev M, Timofeev I (2010) Origin of active states in local neocortical networks during slow sleep oscillation. Cereb Cortex 20:2660-2674.

Chauvette S, Seigneur J, Timofeev I (2012) Sleep oscillations in the thalamocortical system induce long-term neuronal plasticity. Neuron 75:1105-1113.

Chauvette S, Crochet S, Volgushev M, Timofeev I (2011) Properties of slow oscillation during slow-wave sleep and anesthesia in cats. J Neurosci 31:14998-15008.

Chen JY, Chauvette S, Skorheim S, Timofeev I, Bazhenov M (2012) Interneuron-mediated inhibition synchronizes neuronal activity during slow oscillation. J Physiol 590:3987-4010.

Compte A, Sanchez-Vives MV, McCormick DA, Wang X-J (2003) Cellular and network mechanisms of slow oscillatory activity (<1 hz) and wave propagations in a cortical network model. J Neurophysiol 89:2707-2725.

Compte A, Reig R, Descalzo VF, Harvey MA, Puccini GD, Sanchez-Vives MV (2008) Spontaneous high-frequency (10-80 hz) oscillations during up states in the cerebral cortex in vitro. J Neurosci 28:13828-13844.

Contreras D, Steriade M (1995) Cellular basis of eeg slow rhythms: A study of dynamic corticothalamic relationships. J Neurosci 15:604-622.

Contreras D, Destexhe A, Sejnowski TJ, Steriade M (1996) Control of spatiotemporal coherence of a thalamic oscillation by corticothalamic feedback. Science 274:771-774.

Crunelli V, Hughes SW (2010) The slow (<1 hz) rhythm of non-rem sleep: A dialogue between three cardinal oscillators. Nat Neurosci 13:9-17.

Csercsa R et al. (2010) Laminar analysis of slow wave activity in humans. Brain 133:2814-2829.

David F, Schmiedt JT, Taylor HL, Orban G, Di Giovanni G, Uebele VN, Renger JJ, Lambert RgC, Leresche N, Crunelli V (2013) Essential thalamic contribution to slow waves of natural sleep. J Neurosci 33:19599-19610.
Desai NS, Rutherford LC, Turrigiano GG (1999) Plasticity in the intrinsic excitability of cortical pyramidal neurons. Nat Neurosci 2:515-520.
Desai NS, Cudmore RH, Nelson SB, Turrigiano GG (2002) Critical periods for experience-dependent synaptic scaling in visual cortex. Nat Neurosci 5:783-789.
Destexhe A (2009) Self-sustained asynchronous irregular states and up-down states in thalamic, cortical and thalamocortical networks of nonlinear integrate-and-fire neurons. J Comput Neurosci 27:493-506.
Destexhe A, Sejnowski T (2001) Thalamocortical assemblies: How ion channels, single neurons and large-scale networks organize sleep oscillations. Oxford: Oxford University Press.
Destexhe A, Contreras D, Steriade M (1998) Mechanisms underlying the synchronizing action of corticothalamic feedback through inhibition of thalamic relay cells. J Neurophysiol 79:999-1016.
Dickson CT, Biella G, de Curtis M (2003) Slow periodic events and their transition to gamma oscillations in the entorhinal cortex of the isolated guinea pig brain. J Neurophysiol 90:39-46.
Diekelmann S, Born J (2010) The memory function of sleep. Nat Rev Neurosci 11:114-126.
Doi A, Mizuno M, Katafuchi T, Furue H, Koga K, Yoshimura M (2007) Slow oscillation of membrane currents mediated by glutamatergic inputs of rat somatosensory cortical neurons: In vivo patch-clamp analysis. Eur J Neurosci 26:2565-2575.
Draguhn A, Traub RD, Schmitz D, Jefferys JG (1998) Electrical coupling underlies high-frequency oscillations in the hippocampus in vitro. Nature 394:189-192.
Frohlich F, Bazhenov M, Sejnowski TJ (2008) Pathological effect of homeostatic synaptic scaling on network dynamics in diseases of the cortex. J Neurosci 28:1709-1720.
Gais S, Plihal W, Wagner U, Born J (2000) Early sleep triggers memory for early visual discrimination skills. Nat Neurosci 3:1335-1339.
Hasenstaub A, Shu Y, Haider B, Kraushaar U, Duque A, McCormick DA (2005) Inhibitory postsynaptic potentials carry synchronized frequency information in active cortical networks. Neuron 47:423-435.
Hinard V, Mikhail C, Pradervand S, Curie T, Houtkooper RH, Auwerx J, Franken P, Tafti M (2012) Key electrophysiological, molecular, and metabolic signatures of sleep and wakefulness revealed in primary cortical cultures. J Neurosci 32:12506-12517.
Houweling AR, Bazhenov M, Timofeev I, Steriade M, Sejnowski TJ (2005) Homeostatic synaptic plasticity can explain post-traumatic epileptogenesis in chronically isolated neocortex. Cereb Cortex 15:834-845.
Huber R, Ghilardi MF, Massimini M, Tononi G (2004) Local sleep and learning. Nature 430:78-81.
Hughes SW, Cope DW, Blethyn KL, Crunelli V (2002) Cellular mechanisms of the slow (<1 hz) oscillation in thalamocortical neurons in vitro. Neuron 33:947-958.
Johnson HA, Buonomano DV (2007) Development and plasticity of spontaneous activity and up states in cortical organotypic slices. J Neurosci 27:5915-5925.
MacLean JN, Watson BO, Aaron GB, Yuste R (2005) Internal dynamics determine the cortical response to thalamic stimulation. Neuron 48:811-823.
Mainen ZF, Sejnowski TJ (1996) Influence of dendritic structure on firing pattern in model neocortical neurons. Nature 382:363-366.
Maquet P (2001) The role of sleep in learning and memory. Science 294:1048-1052.

Marshall L, Helgadottir H, Molle M, Born J (2006) Boosting slow oscillations during sleep potentiates memory. Nature 444:610-613.
Massimini M, Huber R, Ferrarelli F, Hill S, Tononi G (2004) The sleep slow oscillation as a traveling wave. J Neurosci 24:6862-6870.
McCormick DA (1992) Neurotransmitter actions in the thalamus and cerebral cortex and their role in neuromodulation of thalamocortical activity. Prog Neurobiol 39:337-388.
Mohajerani MH, McVea DA, Fingas M, Murphy TH (2010) Mirrored bilateral slow-wave cortical activity within local circuits revealed by fast bihemispheric voltage-sensitive dye imaging in anesthetized and awake mice. J Neurosci 30:3745-3751.
Moore AR, Zhou W-L, Jakovcevski I, Zecevic N, Antic SD (2011) Spontaneous electrical activity in the human fetal cortex in vitro. J Neurosci 31:2391-2398.
Mukovski M, Chauvette S, Timofeev I, Volgushev M (2007) Detection of active and silent states in neocortical neurons from the field potential signal during slow-wave sleep. Cereb Cortex 17:400-414.
Murthy VN, Schikorski T, Stevens CF, Zhu Y (2001) Inactivity produces increases in neurotransmitter release and synapse size. Neuron 32:673-682.
Reinoso-Suarez F (1961) Topographischer hirnatlas der katze, fur experimental-physiologische untersuchungen. Darmstadt: E. Merck.
Rudolph M, Pospischil M, Timofeev I, Destexhe A (2007) Inhibition determines membrane potential dynamics and controls action potential generation in awake and sleeping cat cortex. J Neurosci 27:5280-5290.
Ruiz-Mejias M, Ciria-Suarez L, Mattia M, Sanchez-Vives MV (2011) Slow and fast rhythms generated in the cerebral cortex of the anesthetized mouse. J Neurophysiol 106:2910-2921.
Sanchez-Vives MV, McCormick DA (2000) Cellular and network mechanisms of rhythmic recurrent activity in neocortex. Nat Neurosci 3:1027-1034.
Shu Y, Hasenstaub A, McCormick DA (2003) Turning on and off recurrent balanced cortical activity. Nature 423:288-293.
Siegel JM (2005) Clues to the functions of mammalian sleep. Nature 437:1264-1271.
Steriade M (2006) Grouping of brain rhythms in corticothalamic systems. Neuroscience 137:1087-1106.
Steriade M, Timofeev I (2003) Neuronal plasticity in thalamocortical networks during sleep and waking oscillations. Neuron 37:563-576.
Steriade M, Nuñez A, Amzica F (1993a) Intracellular analysis of relations between the slow (<1 hz) neocortical oscillations and other sleep rhythms of electroencephalogram. J Neurosci 13:3266-3283.
Steriade M, Nuñez A, Amzica F (1993b) A novel slow (<1 hz) oscillation of neocortical neurons *in vivo* : Depolarizing and hyperpolarizing components. J Neurosci 13:3252-3265.
Steriade M, McCormick DA, Sejnowski TJ (1993c) Thalamocortical oscillations in the sleeping and aroused brain. Science 262:679-685.
Steriade M, Amzica F, Contreras D (1996a) Synchronization of fast (30-40 hz) spontaneous cortical rhythms during brain activation. J Neurosci 16:392-417.
Steriade M, Timofeev I, Grenier F (2001) Natural waking and sleep states: A view from inside neocortical neurons. J Neurophysiol 85:1969-1985.
Steriade M, Contreras D, Amzica F, Timofeev I (1996b) Synchronization of fast (30-40 hz) spontaneous oscillations in intrathalamic and thalamocortical networks. J Neurosci 16:2788-2808.

Stevens CF (1993) Quantal release of neurotransmitter and long-term potentiation. Cell 72S:55-63.
Stickgold R, James L, Hobson JA (2000) Visual discrimination learning requires sleep after training. Nat Neurosci 3:1237-1238.
Sun JJ, Kilb W, Luhmann HJ (2010) Self-organization of repetitive spike patterns in developing neuronal networks in vitro. Eur J Neurosci 32:1289-1299.
Thomson AM, Bannister AP (2003) Interlaminar connections in the neocortex. Cereb Cortex 13:5-14.
Timofeev I (2011) Neuronal plasticity and thalamocortical sleep and waking oscillations. In: Progress in brain research (Someren EJWV, Werf YDVD, Roelfsema PR, Mansvelder HD, Lopes Da Silva F, eds), pp 121-144: Elsevier.
Timofeev I, Steriade M (1996) Low-frequency rhythms in the thalamus of intact-cortex and decorticated cats. J Neurophysiol 76:4152-4168.
Timofeev I, Grenier F, Steriade M (2001) Disfacilitation and active inhibition in the neocortex during the natural sleep-wake cycle: An intracellular study. Proc Natl Acad Sci U S A 98:1924-1929.
Timofeev I, Grenier F, Bazhenov M, Sejnowski TJ, Steriade M (2000) Origin of slow cortical oscillations in deafferented cortical slabs. Cereb Cortex 10:1185-1199.
Tononi G, Cirelli C (2006) Sleep function and synaptic homeostasis. Sleep Med Rev 10:49-62.
Turrigiano GG (1999) Homeostatic plasticity in neuronal networks: The more things change, the more they stay the same. Trends Neurosci 22:221-227.
Turrigiano GG, Leslie KR, Desai NS, Rutherford LC, Nelson SB (1998) Activity-dependent scaling of quantal amplitude in neocortical neurons. Nature 391:892-896.
Volgushev M, Chauvette S, Mukovski M, Timofeev I (2006) Precise long-range synchronization of activity and silence in neocortical neurons during slow-wave sleep. J Neurosci 26:5665-5672.
Volman V, Bazhenov M, Sejnowski TJ (2011a) Pattern of trauma determines the threshold for epileptic activity in a model of cortical deafferentation. Proc Natl Acad Sci U S A 108:15402-15407.
Volman V, Sejnowski TJ, Bazhenov M (2011b) Topological basis of epileptogenesis in a model of severe cortical trauma. J Neurophysiol 106:1933-1942.
Vyazovskiy VV, Olcese U, Hanlon EC, Nir Y, Cirelli C, Tononi G (2011) Local sleep in awake rats. Nature 472:443-447.
Vyazovskiy VV, Olcese U, Lazimy YM, Faraguna U, Esser SK, Williams JC, Cirelli C, Tononi G (2009) Cortical firing and sleep homeostasis. Neuron 63:865-878.
Whittington MA, Traub RD, Jefferys JG (1995) Synchronized oscillations in interneuron networks driven by metabotropic glutamate receptor activation. Nature 373:612-615.

2.8 Figure Legends

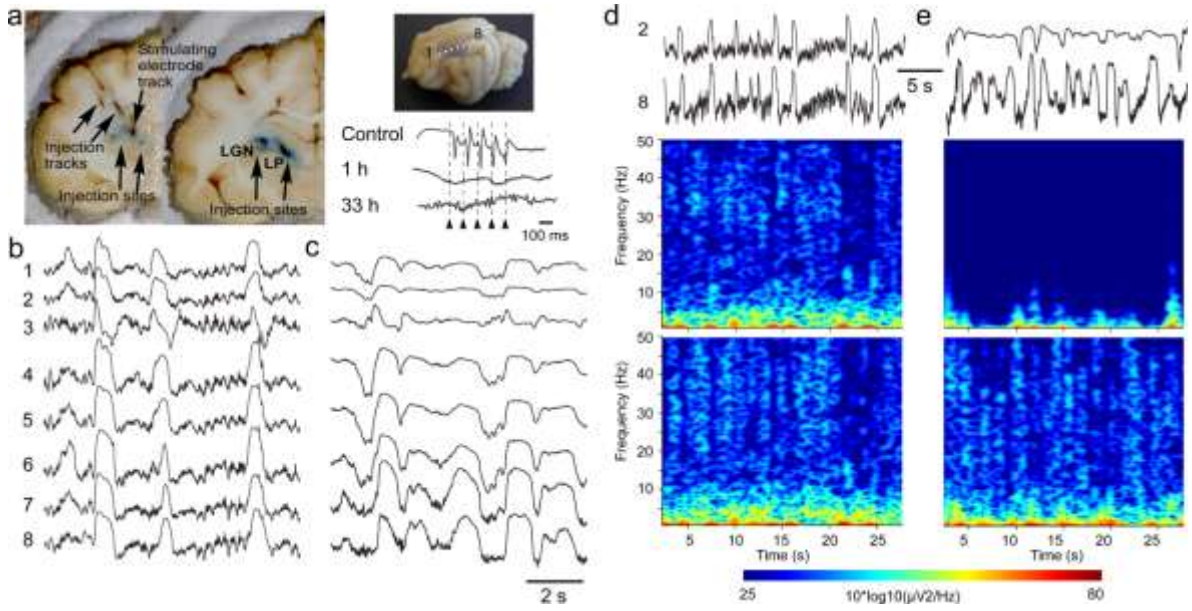

Figure 2.1 Effects of partial thalamic inactivation on the cortical slow oscillation

(a) Left, location of QX-314 injection sites (violet area) and stimulating electrode in LP nucleus.Top right, location of cortical recording electrodes 1-8. Bottom right,cortical response to LP stimulation in control and its abolition1h and 33h after inactivation. Multisite LFP recordings **(b)** before and **(c)**1 h after LP inactivation.Wavelet transform of the LFP signal from electrodes 2 and 8 **(d)**before and (**e**) after LP inactivation.

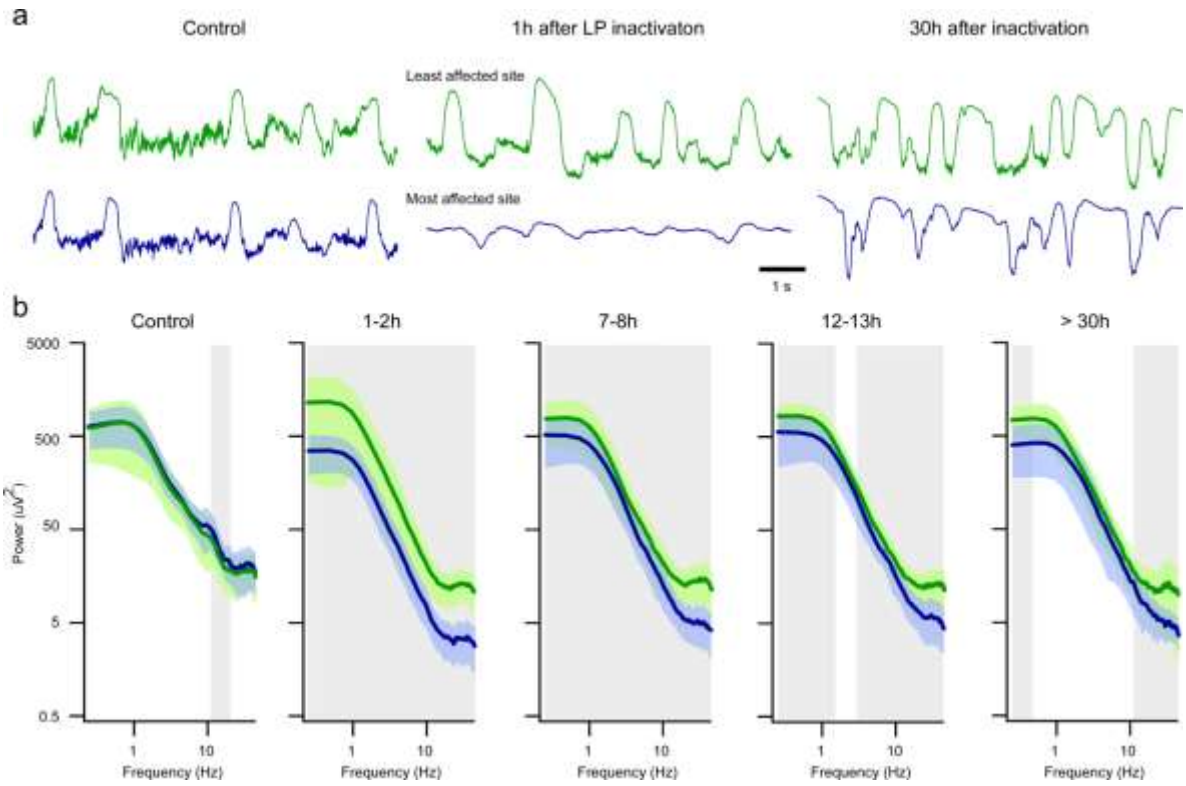

Figure 2.2 LFP power distribution in intact vs. affected by thalamic inactivation cortical regions

a) Examples of LFP recordings from suprasylvian gyrus of cats from intact (green) and affected (blue) regions. **(b)** Power spectra distribution of LFP activities recorded in intact (green) and affected (blue) regions for frequencies 0.25 to 45 Hz. Bin is 0.25 Hz. Light green and blue indicate standard deviation. Grey underlines significantly different bins (Mann-Whitney test, significance at 0.05).

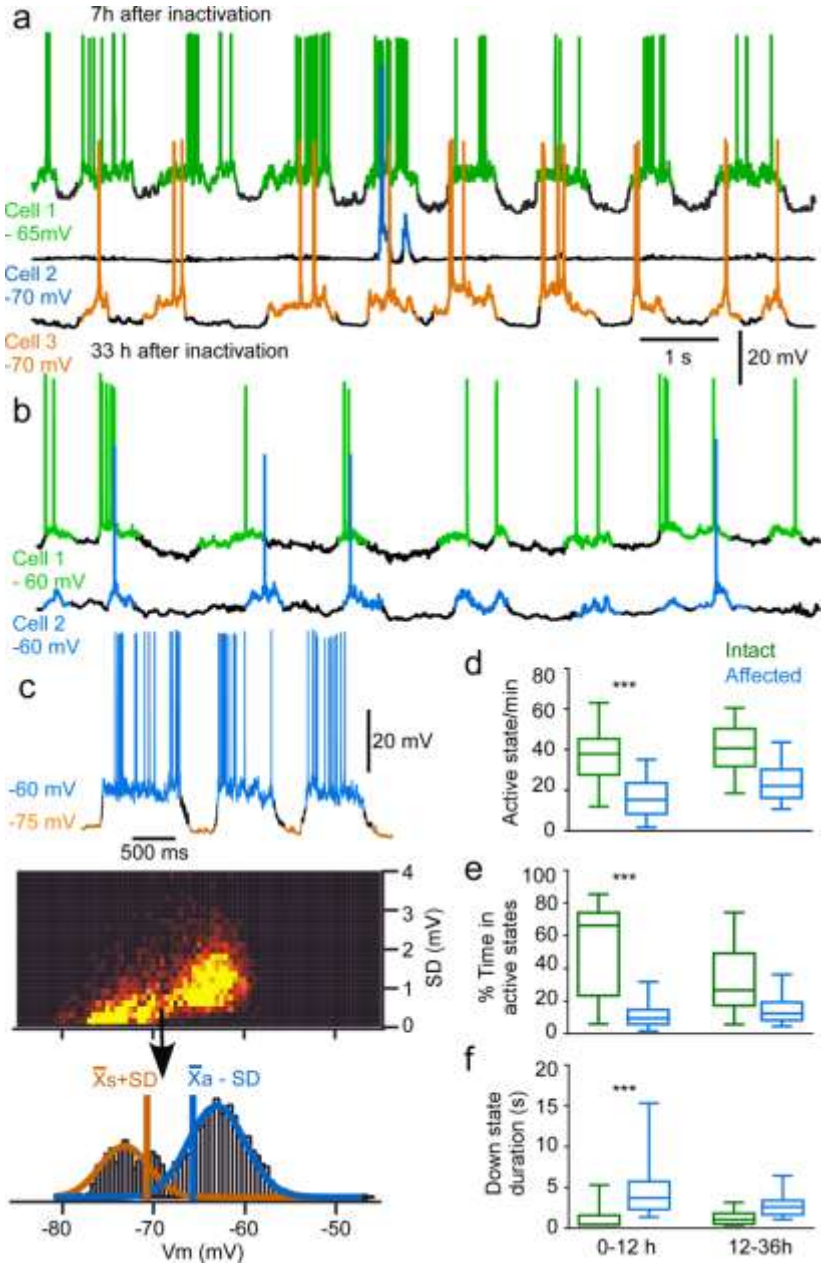

Figure 2.3 Intracellular activity in intact and partially deafferented cortical areas after inactivation of thalamic LP nucleus.

(a) Triple intracellular recordings from affected (blue) and unaffected regions (anterior - green, posterior - orange) 7h after LP inactivation.**(b)**Dual intracellular recording from unaffected (green) and recovering regions (blue) 33 h after inactivation.**(c)** Detection method for active and silent states in intracellular recordings. Vm and SD is computed in for each 25 ms window from intracellular recordings (top traces) and presented as a

color-coded frequency matrix. Active and silent states clusters are splitted according to an initial threshold (arrow) visually selected. Frequency histograms of these new Vm distributions are fitted with Gaussian curves. Silent state threshold (orange) is defined as the mean of its distribution (Xs) plus SD and active state threshold (blue) as the mean of its distribution (Xa) minus SD. Boxplots of active states occurrence **(d)**, percentage of time in active state **(e)**and silent state duration **(f)**of neurons from intact and affected (0-12h vs12-36h) regions. Statistical significance was tested with ANOVA post-hoc Dunn multiple comparison test: *** $p< 0.001$.

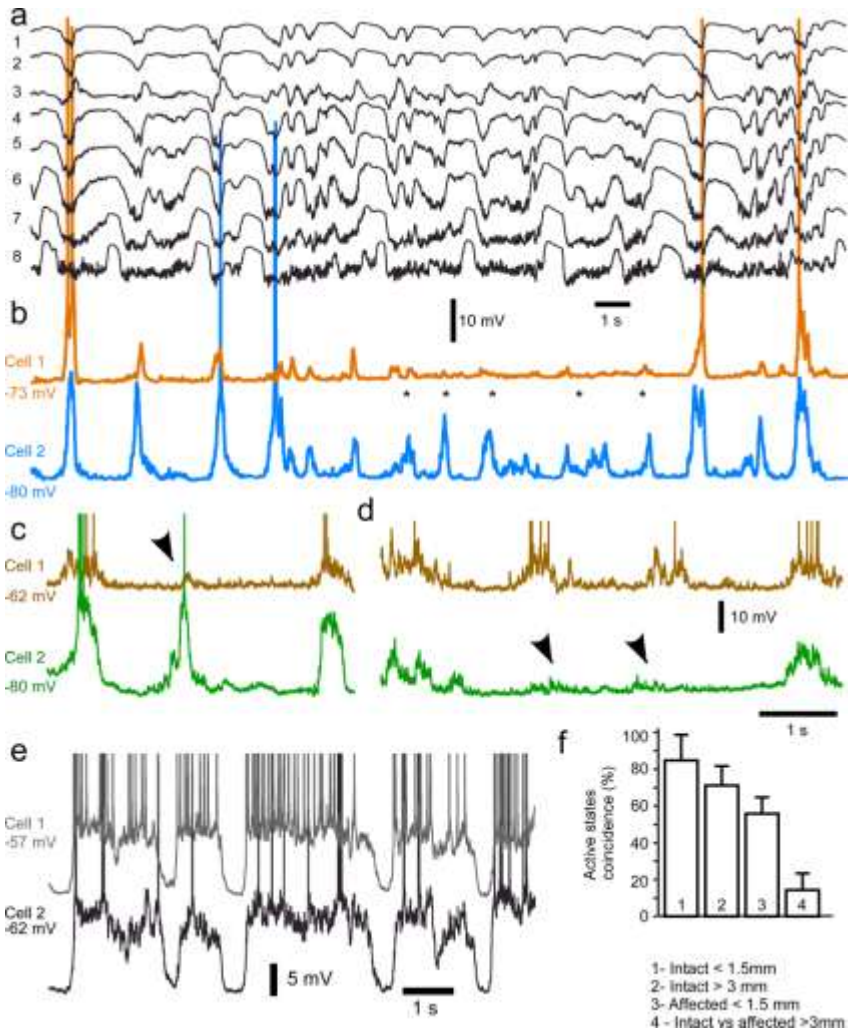

Figure 2.4 Alternating involvement in active states of closely located cortical neurons in the cortical area affected by thalamic inactivation.

(a) Multisite LFP and (b) dual intracellular recordings of closely located neurons in affected regions (between sites 1 and 2). Multiple active states (*) occurred in intra 1but not in intra 2. **(c, d)** Dual intracellular recordings from another pair of closely located neurons from affected area. Active states occurred either simultaneously or in alternation (arrows). **(e)** Dual intracellular recording of closely located neurons in the intact brain. **(f)** Mean coincidence of active states occurrence for cortical neurons in 4 conditions.

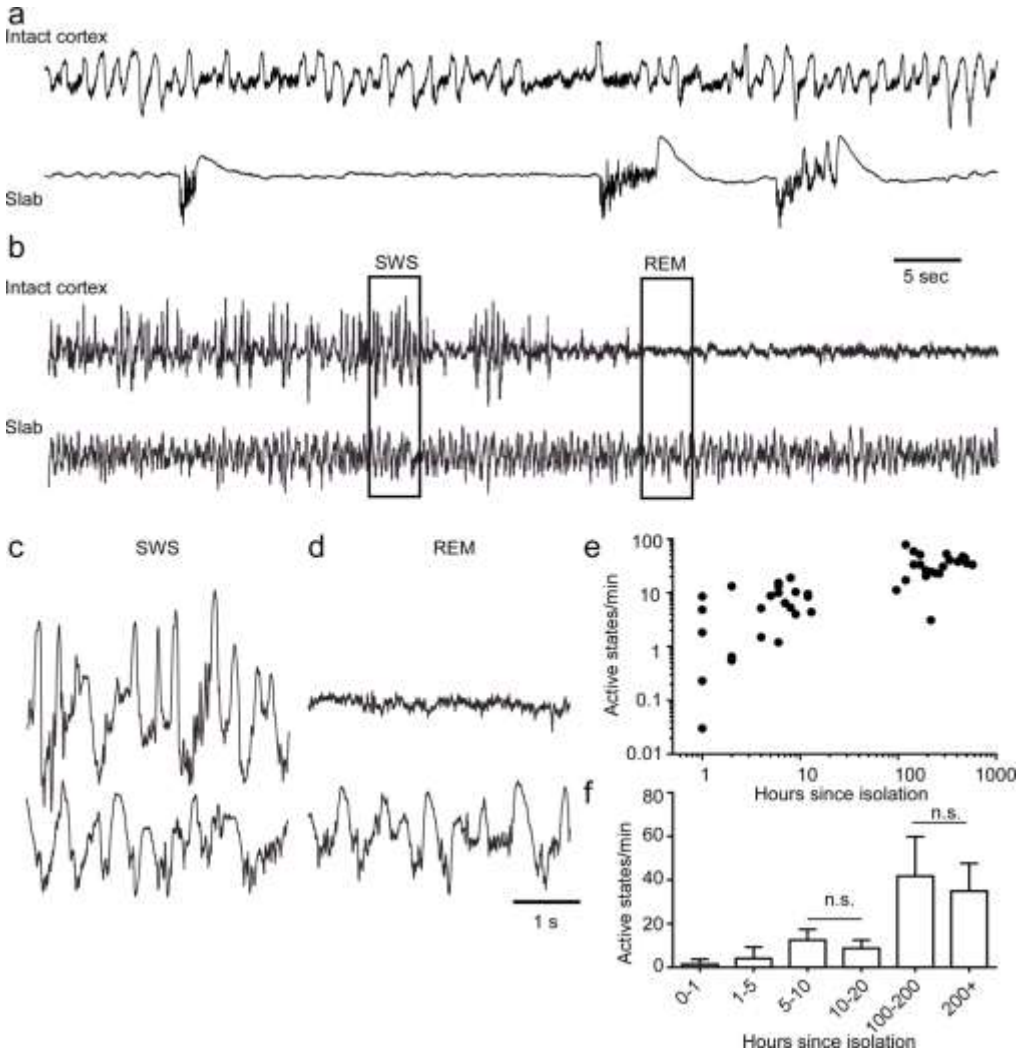

Figure 2.5 LFP activities in acute and chronically isolated neocortical slabs.

(a) Ketamine-xylazine anesthesia. LFP recorded from intact anterior suprasylvian gyrus (upper trace) and from neocortical slab (lower trace) one hour after isolation. **(b)** LFPs recorded from intact cortex (upper trace) and isolated neocortical slab in another cat (lower trace) 7 days (168 h) after isolation during a transition from SWS to REM. **(c, d)** show expanded fragments of activity shown in **b**. **(e)** Active states per minute in the slab vs. time since isolation in hours. Each point is an average for an hour and an animal. **(f)** Histogram shows active states per minute grouped in time segments used for statistical analysis.

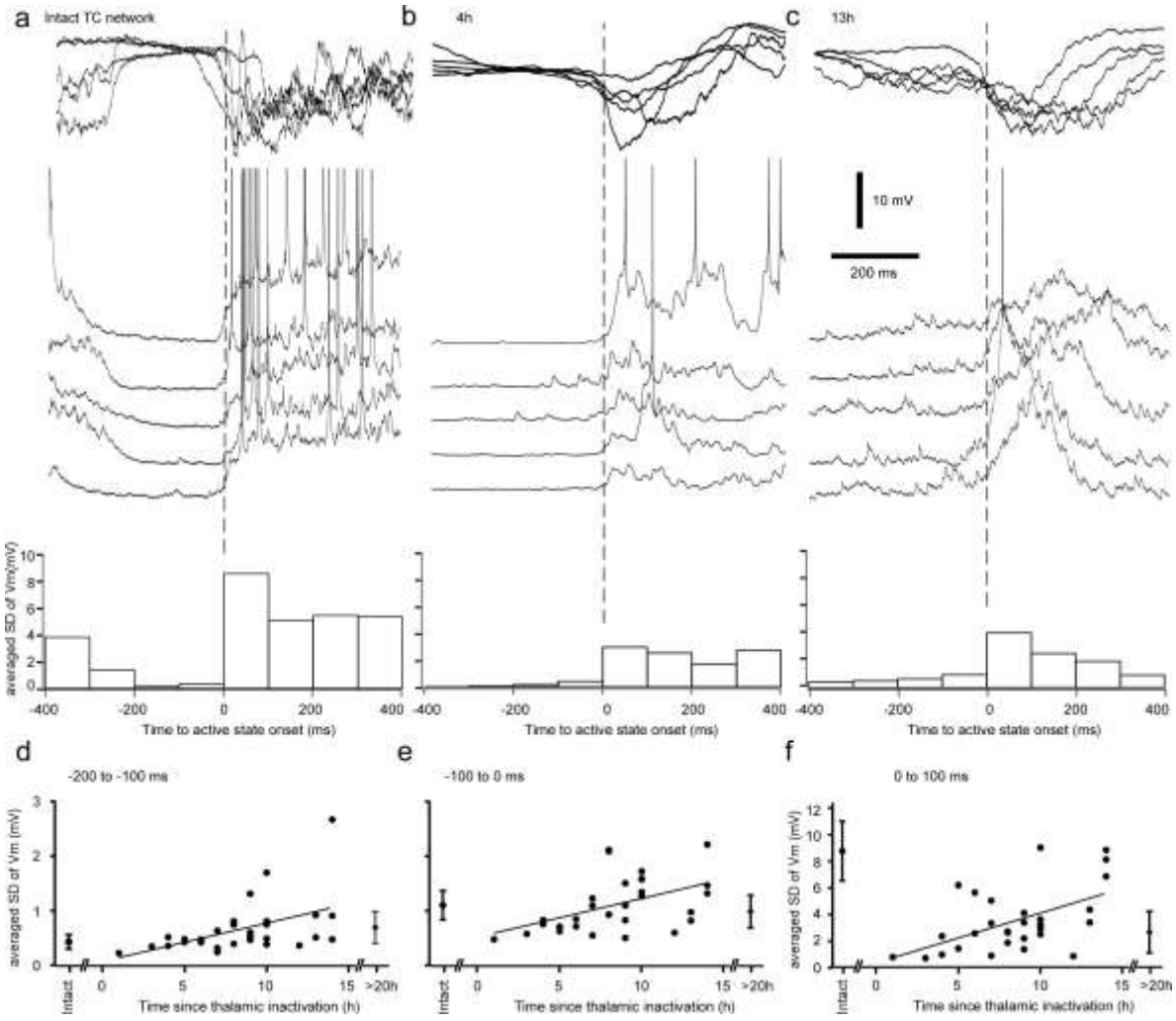

Figure 2.6 Upregulation of synaptic activites following thalamic inactivation.

Examples of LFP and intracellular recordings at the transition to the active state **(a)** before inactivation, **(b)** 4 h and **(c)** 13 h after thalamic inactivation. Below traces are the corresponding averaged standard deviation of membrane potential in bins of 100 ms **(d-f)** the averaged standard deviations are plotted against the time since the thalamic inactivation for the period -200 to -100 ms prior to active state onset **(d)**; -100 ms to active state onset **(e)**, and first 100 ms of the active states **(f)**.

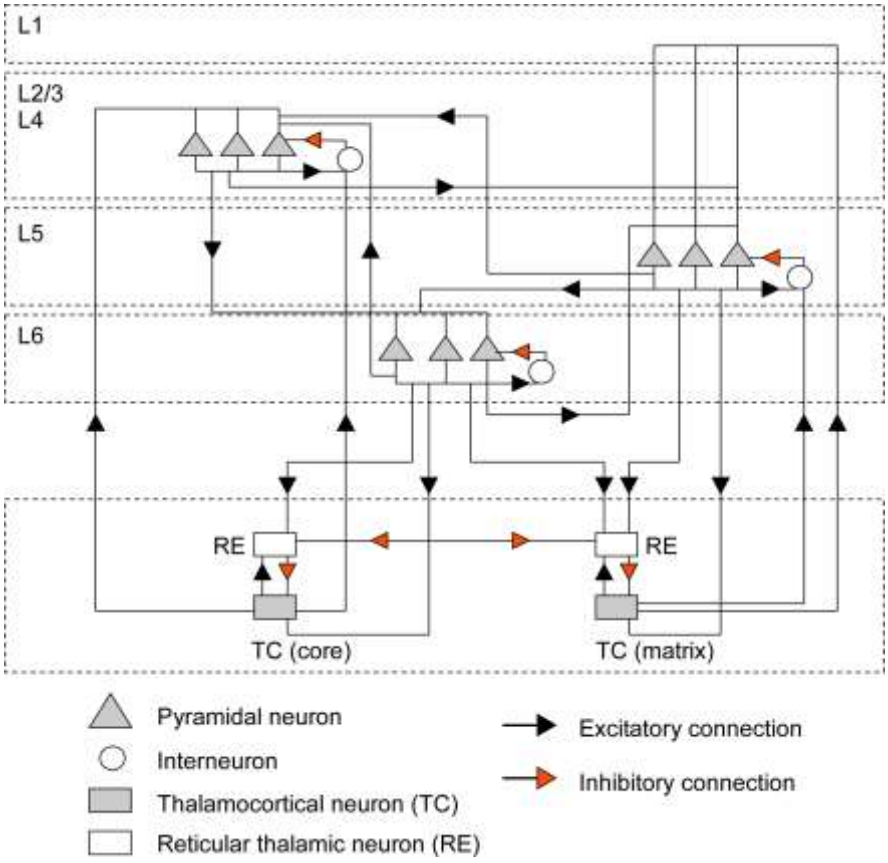

Figure 2.7 The geometry of thalamocortical network model.

The thalamortical network model includes a cortical layer II/III/IV, cortical layer V, cortical layer VI, thalamic reticular (RE), and thalamocortical (TC) neurons. In each cortical layer, there are 500 pyramidal cells (PY) and 120 interneurons (IN). They are evenly divided into ten cortical columns (50 PY and 12 IN in each column). The thalamic network includes layer of thalamic reticular neurons (250 neurons) and relay cells (500 neurons) divided into two nuclei: specific (core) and diffusive (matrix). The black arrowhead represents excitatory connections and the red arrowhead indicates inhibitory connections. The connectivity radiuses (fan-out) information is listed in Table 1.

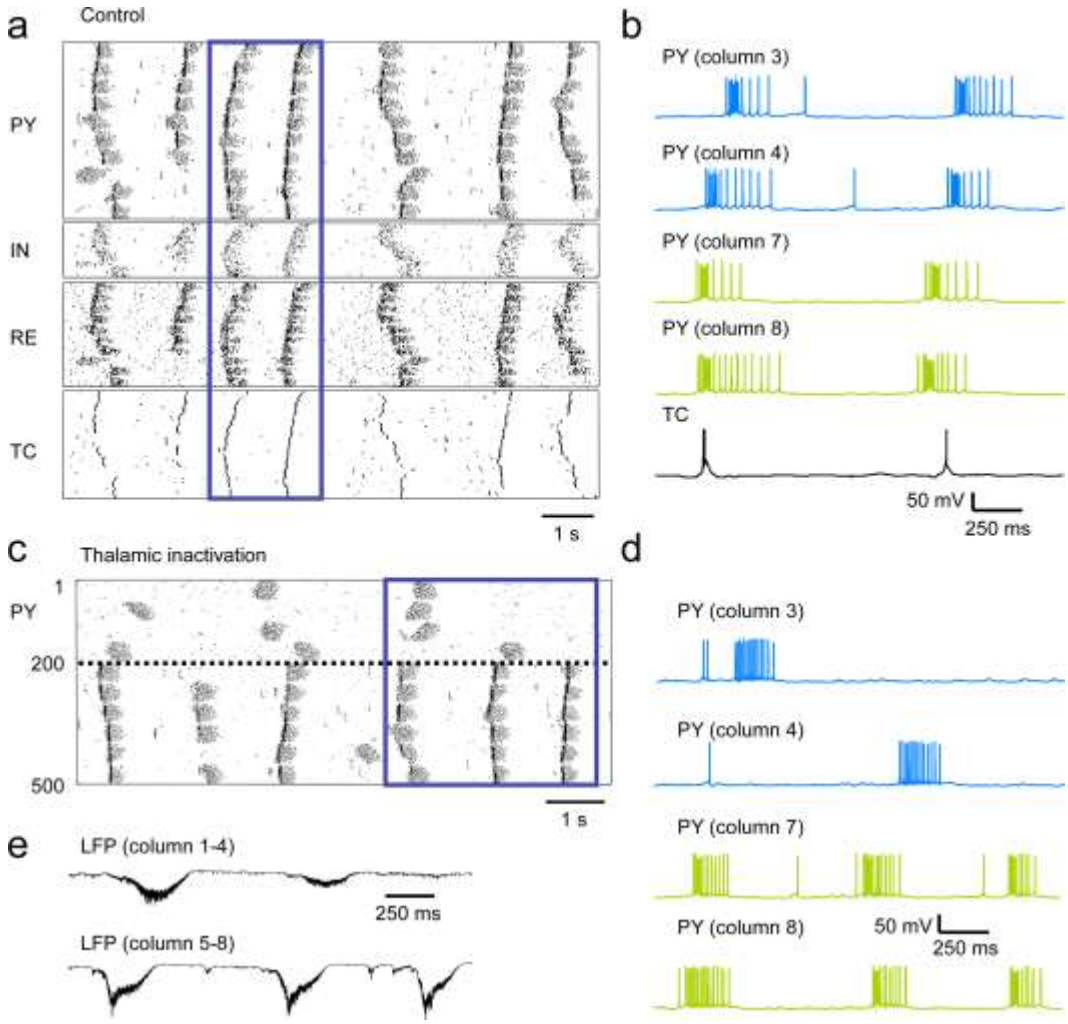

Figure 2.8 Modeling study of the effect of thalamic deafferentation on the neocortical slow oscillation.

(a) Slow oscillation in large-scale thalamocortical model. Rastergrams of pyramidal (PY), interneurons (IN), reticular thalamic (RE) and thalamocortical (TC) cells (upper panel).**(b)**Examples of membrane voltage of PY neurons from selected columns and of a TC neuron in control condition. **(c)**Removal of synaptic connectivity from TC neurons to the first four cortical columns (top) reduced active states occurrence. **(d)** Examples of membrane voltage of pyramidal neurons from selected columns after removal of thalamic inputs. **(e)**LFPs in deafferentedcolumns 1-4 were reduced in amplitude in comparison to intact columns 5-8.

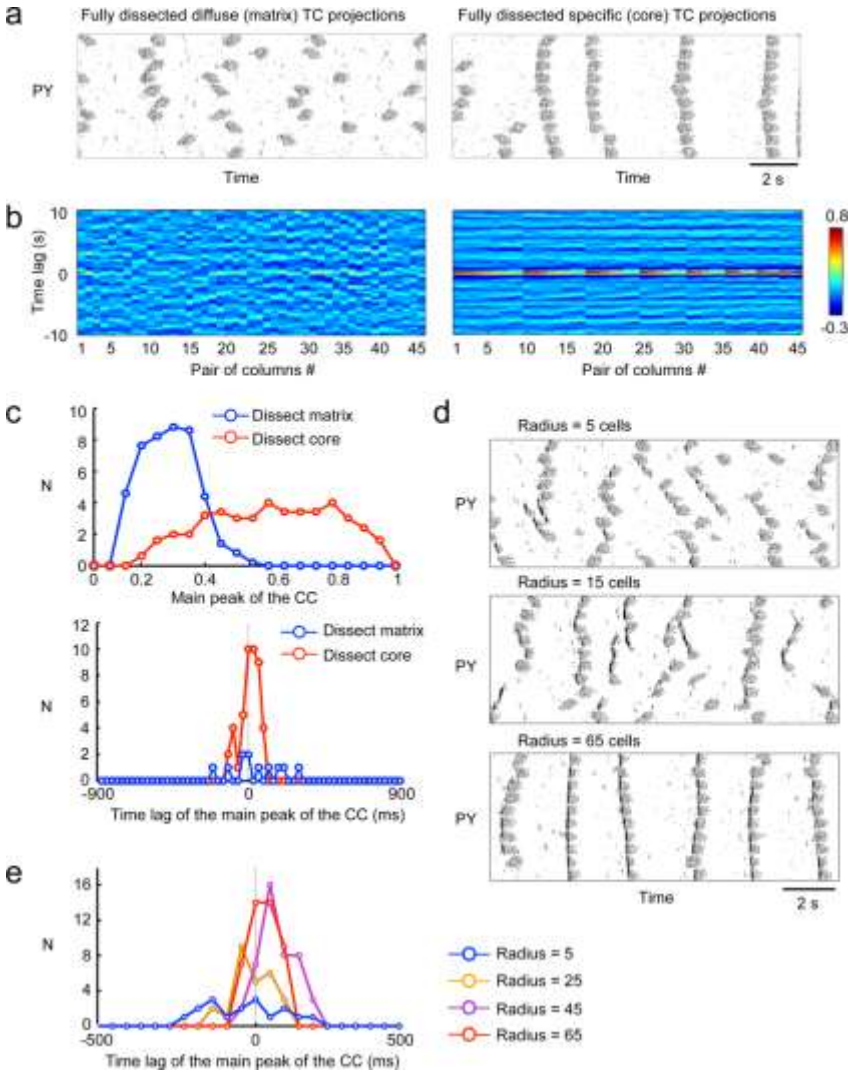

Figure 2.9 Impact of thalamocortical diffuse (matrix) vs. specific (core) projections and the target radii on the synchronization of the slow oscillation.

(a) Rastergrams of the layer IV PY neurons after full dissection of thalamocortical diffuse projections (left) or full dissection of thalamortical specific projections (right). **(b)** Cross-correlation analysis of the LFP signals between all possible LFP pairs (y-axis) from 10 columns after the full dissection of diffuse matrix (left) or specific core (right) projections. **(c)** Distributions of the peak amplitude (left) and time lag to the main peak (right) of cross-correlation function for simulations with dissected diffuse (blue) and specific (red) projections. **(d)** Raster plots obtained from three different settings of the fan-out radius from the thalamocortical matrix structure to the cortex. **(e)** Distribution of time lags to the main peak of cross-correlation function calculated for all pairs ofLFP in different spatial locations plotted for various radii of thalamocortical projections. Broader distribution indicates less synchronous spatio-temporal activity.

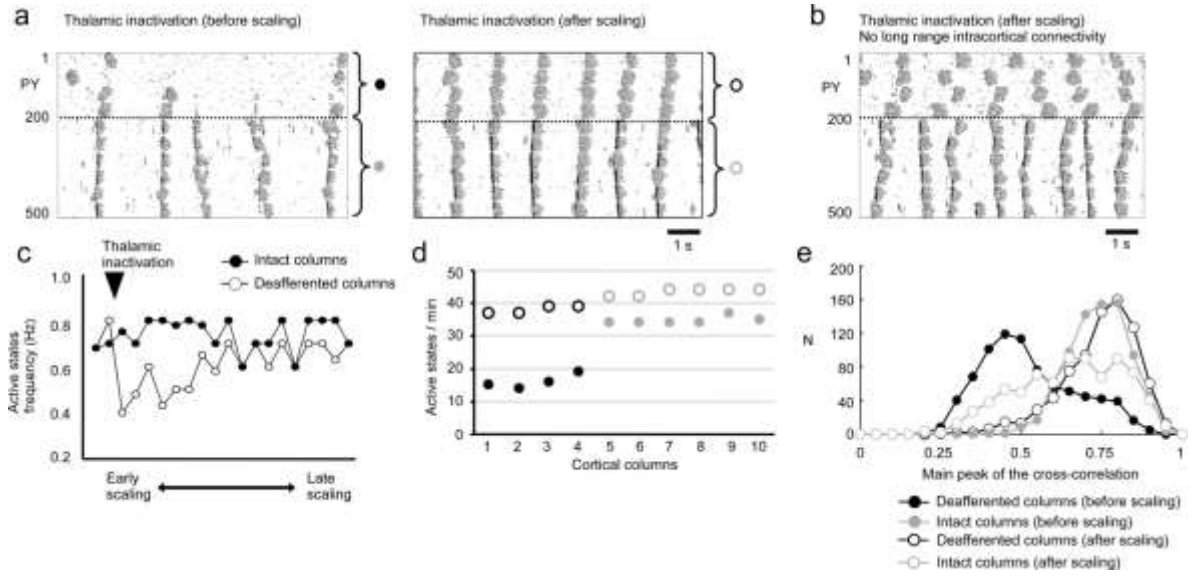

Figure 2.10 Modeling study of scaling the intracortical connectivity on the recovery of the neocortical slow oscillation.

(a) Cortical slow oscillation after thalamic inactivation. Left panel, no synaptic scaling. Right panel, pattern of cortical activity during late phase of synaptic scaling. Synaptic scaling was modeled as decrease of inhibition from IN to PY and increase of excitation and minis amplitude between PYs.**(b)** Network activity after synaptic scaling in the model without long-range intracortical connectivity. **(c)**Timecourse of active states frequency recovery in simulations with synaptic scaling. Arrowhead indicates the time of deafferentation.**(d)**Number of active states per minute after deafferentation without scaling (filled circle) or during the late phase of scaling (open circles).**(e)**Distribution of main peak of the cross-correlation function between V_m of neurons within deafferented columns (black) or intact columns (grey) without scaling (filled circles) or after scaling (open circles).

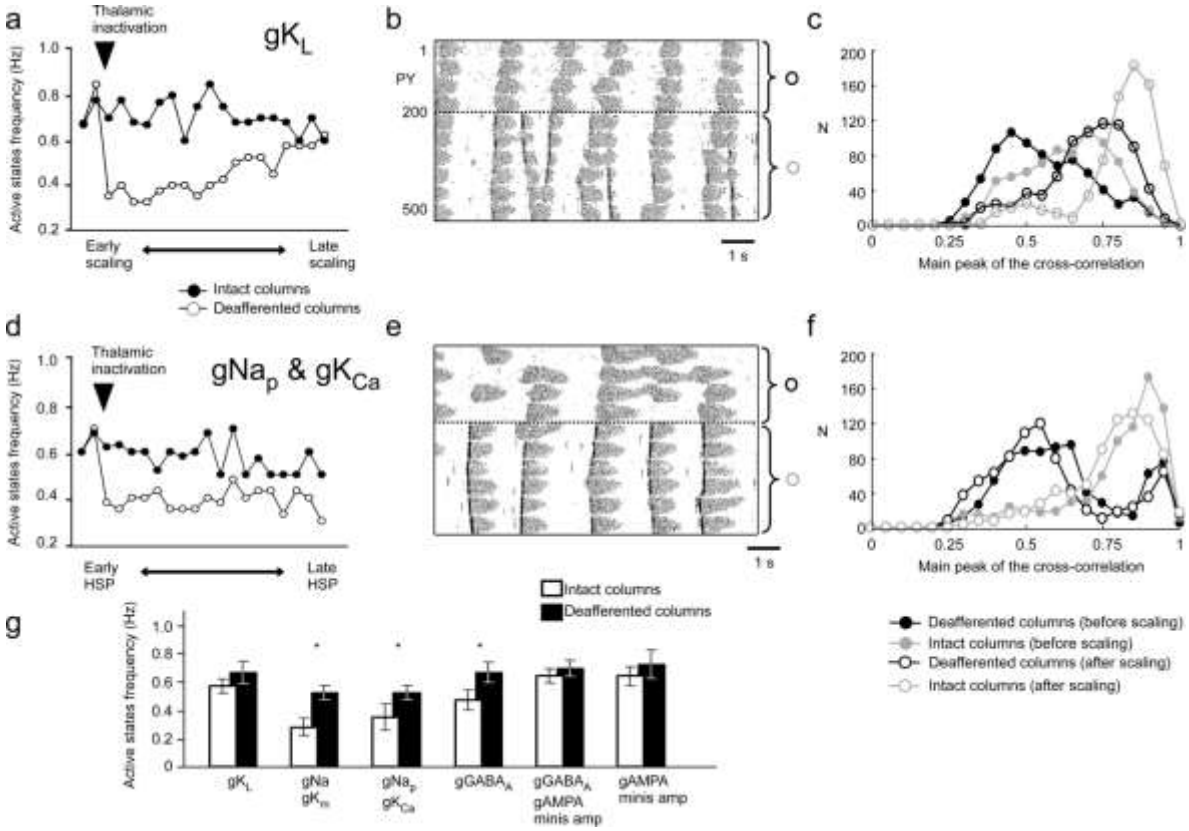

Figure 2.11 Role of different biophysical features inthe recovery of the slow oscillation

(a) Scaling was modeled by adjusting the conductance of a leak potassium current (g_{KL}) in cortical neurons. Averaged active state frequency of intact columns (filled circle) and deafferented columns (open circle) along simulation. **(b)** Representative example of the network activity during the late phase of scaling. **(c)**Distribution of the peaks of cross-correlation function between pyramidal neurons in deafferented (black) or intact (grey) columns during initial (filled circles) or late (open circles) phase of scaling. **(d-f)** Similar to (a-c), however, scaling was modeled by adjusting conductance of the slow intrinsic currents: persistent sodium current (g_{Nap}) and calcium dependent potassium current (g_{KCa}). **(g)** Frequency of active states in deafferented (open blocks) and intact (filled blocks) columns during the late phase of HSP. Six different settings of scaling are shown: (1) Potassium leak current (g_{KL}) in PYs; (2) fast intrinsic currents (g_{Na} and g_{Km}) in PYs; (3) slow intrinsic current (g_{Nap} and g_{KCa}) in PY; (4) fast synaptic inhibition ($g_{GABA\text{-}A}$) from IN to PY: (5) fast synaptic currents ($g_{GABA\text{-}A}$ from IN to PY, g_{AMPA} and minis amplitude between PYs); (6) fast synaptic excitation (g_{AMPA} and minis amplitude between PYs). * indicates experiments were no recovery was found.

2.9 Table

Table 2.1 Detailed geometry of thalamocortical network.

Pre-synaptic Cell	Post-synaptic Cell	Connection Type and Strength (mS/cm2)	Connection Radius
TC (matrix)	PY (layer V)	AMPA = 1.212	45 cells
TC (matrix)	IN (layer V)	AMPA = 0.606	10 cells
TC (matrix)	RE	AMPA = 2.424	6 cells
TC (core)	PY (II, III, IV)	AMPA = 1.212	10 cells
TC (core)	IN (II, III, IV)	AMPA = 0.606	4 cells
TC (core)	RE	AMPA = 2.424	6 cells
RE	TC (matrix)	GABAa = 0.181	6 cells
RE	TC (core)	GABAa = 0.181	6 cells
RE	RE	GABAa = 1.06	4 cells
PY (II, III, IV)	IN (II, III, IV)	AMPA = 1.212 NMDA = 0.121	1 cells
PY (II, III, IV)	PY (II, III, IV)	AMPA = 0.484 NMDA = 0.042	5 cells
PY (II, III, IV)	PY (V)	AMPA = 0.072 NMDA = 0.015	5 cells
PY (II, III, IV)	PY (VI)	AMPA= 0.072 NMDA = 0.015	5 cells
PY (V)	IN (V)	AMPA=1.212 NMDA = 0.121	1 cells
PY (V)	PY (II, III, IV)	AMPA= 0.072 NMDA = 0.015	5 cells
PY (V)	PY (V)	AMPA = 0.484 NMDA = 0.042	5 cells
PY (V)	PY (VI)	AMPA= 0.072 NMDA = 0.015	5 cells
PY (V)	RE	AMPA = 4.242	5 cells
PY (V)	TC (matrix)	AMPA = 0.606	8 cells
PY (VI)	IN (VI)	AMPA= 1.212 NMDA = 0.121	1 cell
PY (VI)	PY (II, III, IV)	AMPA= 0.072 NMDA = 0.015	5 cells
PY (VI)	PY (V)	AMPA= 0.072 NMDA =0.015	5 cells
PY (VI)	PY (VI)	AMPA= 0.484 NMDA = 0.042	5 cells
PY (VI)	RE	AMPA = 4.242	5 cells
PY (VI)	TC (core)	AMPA =0.606	8 cells
PY (II, III, IV) (across columns)	PY (II, III, IV) (across columns)	AMPA= 0.212 NMDA = 0.042	Random (300 pairs in total)
PY (V) (across columns)	PY (V) (across columns)	AMPA= 0.212 NMDA = 0.042	Random (300 pairs in total)
PY (VI) (across columns)	PY (VI) (across columns)	AMPA= 0.212 NMDA = 0.042	Random (300 pairs in total)
IN (II, III, IV)	PY (II, III, IV)	GABAa = 1.515	5 cells
IN (V)	PY (V)	GABAa = 1.515	5 cells

IN (VI)	PY (VI)	GABAa = 1.515	5 cells
IN (II, III, IV)	IN (II, III, IV)	gap junction = 0.06	1 cell
IN (V)	IN (V)	gap junction = 0.06	1 cell
IN (VI)	IN (VI)	gap junction = 0.06	1 cell

Chapter 3: Neocortical inhibitory activities and thalamocortical afferents contribute to the onset of silent states of the neocortical slow oscillation

Maxime Lemieux[1], Sylvain Chauvette[1] and Igor Timofeev[1,3†]

[1] The Centre de recherche de l'Institut Universitaire en Santé Mentale de Québec (CRIUSMQ), Université Laval, Québec, G1J 2G3, Canada

[3] Department of Psychiatry and Neuroscience, Université Laval, Québec G1V 0A6 Canada

Titre en français:
Les activités inhibitrices néocorticales et les afférences thalamocorticales contribuent à l'initiation des états silencieux de l'oscillation lente néocorticale

3.1 Résumé

Durant le sommeil à ondes lentes, les neurones du réseau thalamocortical sont engagés dans une oscillation lente (<1 Hz) qui consite en une alternance entre états actifs et silencieux. Plusieurs études ont fourni un apercu sur la transition des états silencieux, consistant essentiellement en périodes de disfacilitation, vers les états actifs. Néanmoins, les conditions qui mènent à l'initiation synchrone de l'état silencieux demeurent insaisissables. Nous avons posé l'hypothèse qu'une excitation synchrone des neurones inhibiteurs locaux contribuerait à la transition vers l'état silencieux dans le gyrus suprasylvien chez le chat durant le sommeil naturel et sous anesthésie par la kétamine-xylazine. Après la déafférentation partielle et complete du cortex, nous avons trouvé que l'initiation de l'état silencieux était plus variable entre des sites éloignés. Nous avons trouvé que la transition à l'état silencieux était précédée par une réduction des potentiels postsynaptiques excitateurs et de la probabilité de décharge chez les neurones corticaux. Nous avons testé l'impact de l'inhibition dépendante du chlore sur l'initiation des états silencieux. Nous avons découvert un barrage inhibiteur de longue durée (100-300 ms) se produisant environ 250 ms avant l'initiation de l'état silencieux chez 3-6% des neurones sous anesthésie et chez 12-15% des cas durant le sommeil naturel. Nous avons été capables d'induire des transitions à l'état silencieux avec des stimulations électriques et avons trouvé que l'efficacité était la plus élevée dans les couches corticales profondes. Les enregistrements extracellulaires dans le thalamus ont confirmé que quelques cellules thalamiques déchargeaient avant l'initiation de l'état silencieux cortical. Nous concluons que les entrées extracorticales (telles les afférences thalamocorticales) et l'inhibition dépendante du chlore jouent un rôle dans l'initiation de l'état silencieux.

3.2 Abstract

During slow-wave sleep, neurons of the thalamocortical network are engaged in a slow oscillation (<1 Hz), which consists of an alternation between the active and the silent states. Several studies have provided insights on the transition from the silent, which are essentially periods of disfacilitation, to the active states. However, the conditions leading to the synchronous onset of the silent state remain elusive. We hypothesized that a synchronous input to local inhibitory neurons could contribute to the transition to the silent state in the cat suprasylvian gyrus during natural sleep and under ketamine-xylazine anesthesia. After partial and complete deafferentation of the cortex, we found that the silent state onset was more variable among remote sites. We found that the transition to the silent state was preceded by a reduction in excitatory postsynaptic potentials and firing probability in cortical neurons. We tested the impact of chloride-mediated inhibition in the silent state onset. We uncovered a long duration (100-300 ms) inhibitory barrage occurring about 250 ms prior to the silent state onset in 3-6% of neurons during anesthesia and in 12-15% of cases during natural sleep. Electrical stimuli could trigger a network silent state with a maximal efficacy in deep cortical layers. Extracellular recordings in the thalamus revealed that some thalamic cells increase firing before the onset of the cortical silent state. We conclude that extracortical inputs (such as thalamocortical afferents) and chloride-mediated inhibition plays a role in the initiation of the silent state.

3.3 Introduction

Slow oscillation is the hallmark of the slow-wave sleep but also of several anesthetics including ketamine-xylazine (Steriade et al., 1993d; Steriade et al., 1993a; Contreras and Steriade, 1995; Steriade et al., 2001). This slow rhythm consists in an alternation of active and silent states During the active states, strong synaptic barrages contribute to the depolarization of the membrane potential of all electrophysiological types of cortical neurons close to the firing threshold (Steriade et al., 2001). During silent states, the membrane potential is hyperpolarized by 10-20 mV in cortical (Steriade et al., 2001; Chauvette et al., 2011) and thalamic neurons (Steriade et al., 1993d; Contreras and Steriade, 1995). The long-lasting hyperpolarization characterizing the silent state is attributed to disfacilitation (absence of synaptic activities) and the domination of potassium-mediated leak current(Contreras et al., 1996; Timofeev et al., 1996; Timofeev et al., 2001).Given the fact that the slow oscillation persists after thalamic lesions (Steriade et al., 1993c), cortical isolation (Sanchez-Vives and McCormick, 2000; Timofeev et al., 2000) and it was absent in the thalamus of decorticated animals (Timofeev and Steriade, 1996) it was assumed that the cortex has all the machinery to generate the slow oscillation. Later studies however point to a possible active contribution of the thalamus in the generation of the slow oscillation (Hughes et al., 2002; Crunelli and Hughes, 2010). Recent studies demonstrated that a full thalamocortical network is essential to maintain the full extent of the slow oscillation (David et al., 2013; Lemieux et al., 2014).

The silent states onset of the slow oscillation is much more synchronous than the active states onset and it was hypothesized that this high level of synchrony required network mechanisms to recruit and synchronize cortical inhibitory neurons (Volgushev et al., 2006). The ability to induce slow waves with electrical stimulations in naturally sleeping rats (Vyazovskiy et al., 2009) and by transcranial magnetic stimulation in humans (Huber et al., 2007; Massimini et al., 2009) further suggests that active mechanisms are involved in the initiation of the silent state.

The most likely candidate to initiate a silent state is the chloride inhibition provided by $GABA_A$ receptors. A large number of these receptors are located close to the soma of pyramidal neurons (Hendry et al., 1990; Gu et al., 1993) and the associated channels carries larger inhibitory conductances at the soma than those of the $GABA_B$ receptors(Connors et al., 1988).A subgroup of cortical interneurons preferentially fires at the end of active states (Puig et al., 2008). A recent modeling study has explored the impact of $GABA_A$ conductances on state transitions during the slow

oscillation and found that increasing the inhibitory connection of interneurons on pyramidal neurons enhanced the synchrony of silent state. Reducing the strength of this connection had the reverse effect on the synchrony of silent state onset (Chen et al., 2012).

A synchronizing mechanism would still be required to explain the low spatiotemporal variability of the silent state onset observed in the cortex in vivo. Because of its intricate relationship with the cortex (Sherman and Guillery, 1996) and its propensity to recruit cortical inhibition (Contreras et al., 1997), the thalamus is in an ideal position to provide a synchronizing influence on the onset of the silent state.

In this study, we hypothesized that the input that synchronizes the silent state throughout a neocortical area is provided by the thalamus. To demonstrate this hypothesis, we present data from multisite local field potential (LFP) and multiple intracellular recordings of the delays of the silent state onset in the neocortical network before and after inactivation of thalamic afferents. We also show the relative contribution of chloride-mediated inhibition in the termination of active states.

3.4 Materials and methods

3.4.1 Surgery

All experiments were conducted on cats of either sex (3-5 kg). For acute experiments, animals were anesthetized by intramuscular injection of ketamine and xylazine (respectively 10 and 2-3 mg/kg) and were subsequently intravenously supplied with ketamine (20 μg/kg*min) dissolved in saline 0.45% dextrose 5% at a rate of 10 mL kg^{-1} h^{-1}. EEG was monitored throughout experiments which lasted 8-36 hours and a supplemental dose of ketamine-xylazine was given by i.v. injection when EEG tended slightly toward activated pattern. Lidocaine (0.5%) was injected in all pressure and incision points. Animals were paralyzed with gallaminetriethiodide 2% and maintained under artificial ventilation. Ventilation rate and oxygenation were adjusted to keep an end-tidal CO_2 at 3-3.7%. Body temperature was maintained 37.5-38.5°C throughout experiment. To obtain intracellular recordings and cortical MUA during natural sleep, we chronically implanted two animals with a recording chamber above the suprasylvian gyrus as described in (Steriade et al., 2001; Timofeev et al., 2001).

3.4.2 Electrophysiological recordings

Local field potentials (LFP) and intracellular recordings were obtained from area 5 and 7 of the suprasylvian gyrus. Most LFP were obtained with low impedance coaxial electrodes (Rhodes Medical Instruments, Summerland, CA, USA). For multi-site LFP recordings, we used 8 coaxial electrodes arranged in a linear array at regular intervals of 1.5 mm. We also used tungsten electrodes (Alpha Omega, Alpharetta, GA, USA) to obtain multi-unit activity (MUA) in the lateral posterior (LP) nucleus, the ventrobasal complex (VB) of the thalamus and the medial dorsal (MD) nucleus. Thalamic firing from these nuclei was simultaneously recorded with the LFP from their respective cortical targets (suprasylvian gyrus for LP, primary somatosensory cortex for VB, and prefrontal cortex for MD). For these experiments, cortical LFPs were obtained with tungsten electrode. We also used a linear 16-channel silicon probe (100 µm interelectrode distance, NeuroNexus Technologies, Inc. Ann Arbor, MI, USA) to record the depth profile of cortical MUA around silent state transitions during natural slow-wave sleep. Signals were bandpass filtered (0.1 Hz-10 kHz) with an AC amplifier (A-M systems, Sequim, WA, USA) and digitized at a sampling rate of 20 kHz.

Dual intracellular recordings were obtained with sharp glass micropipettes (DC resistance of 30-75 MΩ)filled with potassium acetate (KAc, 2M) or with potassium chloride (KCl, 2 M). KCl was used to reverse the concentration gradient of chloride and caused a depolarization instead of a hyperpolarization when $GABA_A$ receptors were activated at resting membrane potential. Stability of intracellular recording was obtained by draining the cisterna magnum, bilateral pneumothorax, hip suspension, and filling the hole made in the skull with agar 4% in saline 0.9%. A high-impedance amplifier with active bridge circuitry (Neurodata IR-283 amplifiers, Cygnus Technology, PA, USA)was used to record and inject current in cells. For the analysis we retained neurons showing stable membrane potential below -60 mV, action potential amplitude of at least 50 mV and input resistance higher than 20 MΩ. Analyzed recordings, including dual intracellular recordings lasted more than 10 min and we analyzed at least 50 cycles of slow oscillation for each neuron or neuronal pair.

All electrophysiological data were digitized with Nicolet Vision data acquisition system (Nicolet Technologies, Madison, WI, USA) at a sampling rate 20 kHz.

3.4.3 Thalamic inactivation and neocortical slabs

To remove functional thalamocortical inputs to the recorded neocortical regions, we injected QX-314 (20% in saline) in the LP nucleus of the thalamus (5 injection sites, separated by 1.5 mm, 2 µl per injection site). Prior to inactivation, the LP nucleus was stimulated (5 pulses at 10 Hz, 0.1 ms in duration, 1.0 mA) with a coaxial stimulating electrode and we recorded the response in the neocortex. We considered the inactivation of LP inputs successful when the response was abolished by the QX-314 injection in the thalamus. To obtain fully deafferented neocortical networks, we isolated neocortical slabs (n=6) as described elsewhere (Timofeev et al., 2000).

3.4.4 Electrical laminar stimulations

Laminar microstimulations were done in the slab (Fig. 3.8) with a silicon probe made of 16 iridium electrodes at intervals of 150 µm (Neuronexus, Ann Arbor, Michigan, USA). For microstimulation of neurons in the intact cortex (see Fig. 3.9), the distance between electrodes of the silicon probe was 100 µm.

3.4.5 Data analysis and statistical tests

Data were analyzed off-line in Igor Pro version 4 (Wavemetrics, Portland, Oregon, USA).

We extracted the timing of silent state onset with the LFP recorded at each cortical site. The onset was defined as the time corresponding to the half-amplitude of the sigmoid fitting of the transition to the silent state. For each transition to the silent state, we calculated the averaged time of silent state and calculated the delay for each of the 6-8 sites to this averaged time. We represented the delay of each site to the averaged silent state onset with a boxplot. To evaluate the level of synchrony of the silent state onset for each condition (intact afferents, thalamic deafferentation, neocortical slab), we extracted the median delay to the averaged silent state onset of each site and calculated the variance of delays. Population data are presented as frequency histograms. Comparisons of variances were made with a F-test.

To determine the timing of the silent state onset in intracellular recordings, we defined it as the crossing of a threshold of the membrane potential (V_m). A frequency histogram of V_m in bins of 25 ms was built for each cell. The V_m of all neurons had a bimodal distribution that was split at the trough between the active (more depolarized V_m) and the silent (more hyperpolarized V_m) state modes. The threshold for the silent state onset was defined as the mean V_m of the active state minus one

standard deviation of this distribution (see Fig. 3.2, B, right).The minimal duration for silent state was defined as 100 ms. For dual recordings with KAc, the reference cell was randomly selected. For dual recordings with one pipette filled with KCl, the cell recorded with KAc was always selected as the reference cell. The delay of the silent state onset was calculated as the time of the onset in the test cell minus the time of onset in the reference cell.

To evaluate the rate of synaptic inputs reaching the soma of cortical neurons, we extracted depolarizing events from intracellular recordings that had low electronic noise. Traces were filtered 0-400 Hz to remove high frequency noise and derived over time to obtain the dV/dt of the V_m. An event was selected as a peak in the dV/dt trace crossing a threshold (0.25-0.4 mV/ms depending on the cell). The number of depolarizing events was calculated in bins of 5 ms for a window of ±1000 ms around the onset of the silent state. Data were normalized on the number of transition to the silent state and fitted with a sigmoidal function ±200 ms around the onset of the silent state to describe the dynamic of synaptic inputs.

With KCl-KAc simultaneous recordings, we identified synchronous inhibitory activities. We refer to these activities as long duration inhibitory events that were characterized by a hyperpolarization in the neuron recorded with KAc and a depolarization in the neuron recorded with KCl lasting more than 50 ms. To detect these events, we used a window ±100 ms with a sliding step of 10 ms. To estimate the onset and offset of detected events, we used the difference of the z-score transformation of both intracellular traces. A z-score trace from analyzed segments of several minutes was obtained by subtracting the V_m by the mean V_m of the cell (to set the mean V_m at zero) and then dividing it by the standard deviation of the V_m. The z-score difference was calculated by subtracting the z-score of the KCl trace by the z-score of the KAc trace. A hyperpolarization in the KAc and a depolarization in the KCl would give a positive difference. The threshold for the onset/offset was defined as one standard deviation of the z-score difference trace. We build frequency histogram of the delays of onset of these events to the onset of the silent state. We also estimated a window of disfacilitation that was the difference of the time of silent state onset and the time of long duration inhibitory event offset. We tested whether the proportion of these events (number of events per silent state onsets) was significantly higher than expected at chance-level with an exact binomial proportion test. This is a test based on the binomial distribution B(n, p) where n is the sample size and p is the probability of observation (5%).It verifies whether the number of events (X) is statistically different than expected by

chance (K = n * p). The proportion of events was significant when $Pr(X>K) \leq 0.025$ ($\alpha=0.05$ in a bilateral test).

We extracted MUA from thalamic recordings by filtering between 100 Hz and 10 kHz. We selected spikes with amplitude larger than 10 SD of the filtered signal during the silent state. At this threshold, we were confident to reject all events representing electronic noise. We built peri-event histograms of MUA within ±2 s of the cortical onset of silent state and transformed these histograms into z-scores. The peak firing was considered as significantly higher than baseline when the z-score was higher than 1.96 (equivalent to p=0.05). We extracted the z-score peak value and the time of this peak to the silent state onset to evaluate whether the thalamic unit was biased towards the onset of the active or the silent state.

3.5 Results

3.5.1 Level of synchrony of the transition to the silent state

Under ketamine-xylazine anesthesia, silent states occur nearly simultaneously in all recorded sites ofthe suprasylvian gyrus (Fig. 3.1, A-D). To assess the level of synchrony among these sites, we first defined the onset of the silent state as the time at half-amplitude of the sigmoidal fitting of the transition (Fig. 3.1, B). For each site, we calculated the median delay to the onset of the silent state averaged from all sites (Fig. 3.1, C).The median delays of all sites from all experiments (38 sites, 5 experiments) were centered on zero (Fig. 3.1, D). Because mean delay is at zero, the coefficient of variation cannot be used to describe the variability of the silent state onset among sites. We opted to use the variance as a measure of variability (indicative of the level of synchrony in this case) of the silent state onset. In the intact cortex, we found that the variance was 277.14 ms^2. Starting from this baseline value, we next evaluated the effect of removing inputs to the cortex on the silent state onset.

We first measured the impact of removing functional thalamocortical (TC) inputs from LP to the suprasylvian gyrus. The pharmacological inactivation of LP with QX-314 20% dramatically reduced the slow oscillation in the first 12 h. After that period, the slow oscillation power started to recover and was similar to control levels after 24 h although LP afferents were still inactivated (Lemieux et al., 2014). Below we analyzed recordings obtained more than 12 hours from the thalamic inactivation. During that late period after LP inactivation, the onset of the silent state was desynchronized among recorded sites (Fig. 3.1, E-H). The variance of the silent state onset (2104.05 ms^2, n=38 sites, 5

experiments)was significantly larger than in the intact cortex ($F=7.592$, $p<0.05$, F-test), indicating that the TC inputs contribute to the level of synchrony observed at the silent state onset in control conditions. We next tested the effect of a complete deafferentation of the neocortex on the delays of the silent state onset at different sites in an isolated neocortical slab (Fig. 3.1, I-L). The variance (3652.78 ms^2, n=31 sites in 6 experiments) was significantly larger than in the intact cortex ($F=13.177$, $p<0.05$, F-test) but similar to the effect of LP inactivation ($F=1.71$, $p>0.05$, F-test). These results suggest that TC inputs are necessary and sufficient to explain the level of synchrony of the silent state onset within an intact cortical region.

We extended our investigation of the effects of external inputs to the neocortex on the synchrony of the silent state onset at the cellular level. We first recorded simultaneously the intracellular activity of two neurons located at a distance of 4-12 mm in the intact cortex (Fig. 3.2, A). We extracted the timing of the transition to the silent state for each neuron based on the crossing of a V_m threshold and calculated the delay in the pair (see the example in Fig. 3.2, B, C). For all pairs recorded (n=23, Fig. 3.2, D), the mean delays were normally distributed around zero (D'Agostino & Pearson omnibus normality test, $p=0.6072$) and had a low variance (61.07 ms^2). Furthermore, the mean delay of the silent state onset in pairs of neurons did not depend on the distance between neurons ($p=0.136$, linear regression). The low temporal variability and the independence on the distance of the mean delay of the silent state onset suggest the presence of synchronizing mechanisms.

Because the removal of LP inputs significantly decreased the synchrony of the silent state onset at the population level in the suprasylvian gyrus (Fig. 3.1 E-H), we evaluated the impact of the thalamic deafferentation at the cellular level (Fig. 3.2 E, F, H). The transition to the silent state for neurons in the affected region with neurons in the unaffected region at a distance of ~4 mm was extensively desynchronized in comparison to neurons at a similar distance in the intact cortex (n=10 pairs after LP inactivation, n=23 pairs in the intact cortex; see an example in Fig. 3.2, E). Without LP functional afferents, the variance of all transitions to the silent state (Fig. 3.2, H) was significantly larger than for neurons at similar distance in the intact cortex (variance = 46182 ms^2, n=198 silent states after LP inactivation, variance = 2058 ms^2, n=1678 silent states in the intact cortex; $F=22.4$, $p<0.05$, F-test). For neurons recorded within the affected region at a distance <1.5 mm (Fig. 3.2, F, H), the variance of the delays to the silent state onset was also significantly higher than neurons more distantly located in the intact cortex (variance = 11990 ms^2, n=215 silent states in 10 pairs after LP

inactivation, variance = 713 ms^2, n=1782 silent states in 23 pairs in the intact cortex; F=5.82, p<0.05, F-test). Neurons recorded in neocortical slabs at distance of ~4 mm (n=9 pairs; Fig. 3.2, G, H) also showed a more variable onset of the silent state than in the intact cortex (variance = 12144 ms^2, n=124 silent states in the slab, variance = 2058 ms^2, n=1678 silent states in the intact cortex; F=5.9, p<0.05, F-test). The variances for neurons recorded within the affected region and for those recorded in the slab were similar (F=1.01, p>0.05, F-test). These results are in line with those obtained with LFP recordings and suggest that functional thalamic afferents are necessary and sufficient for the synchrony of the silent state onset.

3.5.2 Disfacilitation and inhibition prior to the onset of the silent state

We hypothesized that a reduced synaptic drive could initiate the transition to the silent state. To test this idea, we estimated the rate of synaptic inputs on neurons by extracting depolarizing events of the V_m in intracellular recordings (Fig. 3.3, A, B). For 5 cells recorded under ketamine-xylazine, we extracted an average of 109-175 events/sec. We next calculated the number of these depolarizing events in bins of 5 ms around the silent state onset and fitted the transition with a sigmoid function (Fig. 3.3, C, D). When compared to the variation of the V_m at the transition to the silent state, the sigmoidal fitting of the number of depolarizing events started to decrease before the hyperpolarization of the neuron (Fig. 3.3, D-F). The depolarizing events were triggered on the crossing of the depolarized threshold (active state) and the sigmoidal fitting of the V_m is intended for visualization purpose only. The dynamic varied from cell to cell but always preceded the variation of the V_m, both under anesthesia (Fig. 3, E) and during natural sleep (Fig. 3.3, F). These results supported our hypothesis that the transition to the silent state was initiated by a period of reduced synaptic drive. To further investigate this finding, we estimated the overall neuronal firing in the transition to silent states during slow-waves sleep in 5 separate experiments (Fig. 3.4). An overlay of cortical MUA recordings from 16 channels (Fig. 3.4, A) illustrates a tendency to decreased populational firing rates prior to the onset of silent state. A peri-event histogram of the overall firing referenced to the onset of LFP silent state (Fig. 3.4, C and D) further highlights this observation. Z-score transform shows that the firing is significantly decreased (p<0.05) 50 ms prior to the onset of silent state (Fig. 3.4,B and E). A separate analysis at different cortical depths indicate that all the recordings below the reversal potential of LFP showed a significant decrease in the neuronal firing 25-50 ms prior to the onset of silent state (Fig.

3.4, F). Due to the very sparse firing in upper cortical layers (Chauvette et al., 2010; Barth and Poulet, 2012) we did not observe a significant reduction of firing in the transition to silent states in superficial channels.

To investigate the role of chloride-mediated inhibition in the onset of the silent states, we performed dual intracellular recordings with one reference pipette filled with KAc and one test pipette filled with KCl (Fig. 3.5-3.7). Two neurons recorded at a distance < 0.5 mm display similar fluctuations of the V_m, which suggests that they receive a similar amount of synaptic activities (Timofeev et al., 2004). Loading neurons with chloride reverses the hyperpolarizing effect of chloride-mediated IPSP into a depolarizing one and if active inhibition would be involved directly at the transition to the silent state, we expected to observe a longer delay in the KCl neuron in comparison to the KAc neuron. In the example shown in figure 3.5, A-C, the mean delay of the KCl cell to the silent state onset of the reference cell was 14 ± 73.6 ms (n=87 events). In comparison, the mean delay of in a pair of control cells (KAc-KAc) at a similar distance was -1.4 ± 31.3 ms (n=70 events, Fig. 3.5, D and E).However, the cumulative density function of transitions to the silent states for each KCl-KAc recorded pair shows that such an example was rather the exception (Fig. 3.5, F). The mean delay in most KCl neurons (n=20 pairs) was still centered on zero, as was seen for control pairs (n=23 pairs, Fig. 3.5, G). We observed that the delays were more variable for KCl-KAc pairs, suggesting that reversing the gradient of chloride concentration may also, in some cases, precipitate the transition of the cell into the silent state. The mechanisms behind these events remain unknown but might have to do with voltage-dependent potassium channels.

Because we found disfacilitation preceding the onset of the silent state by 10-100 ms, we investigated if there was an increase in inhibition for this time period. We found that long duration inhibitory activities often preceded the transition to the silent state (Fig. 3.6 and 3.7) and they were occasionally observed at the beginning of the active state (Fig. 3.6, A). This phenomenon was characterized by a hyperpolarization of 3.11 ± 2.87 mV in the neuron recorded with the KAc pipette and by a depolarization of 5.40 ± 4.83 mV in the neuron recorded with the KCl pipette (n=79 inhibitory events from 20 pairs of cells). The onset of these events was 227 ± 122 ms prior the onset of the silent state (n= 79 events, Fig. 3.6, C) and lasted in average 167 ± 78 ms. Events occurring earlier were generally longer in duration ($p<0.0001$, linear regression, Fig. 3.6, D). We estimated the delay between the end of inhibitory events and the onset of silent states (window of disfacilitation) and

found there was a period of 71.2 ± 144.85 ms after the end of the identified inhibitory events and before the transition to the silent state (Fig. 3.6, E). This time window matched the time-course of reduction in depolarizing events at the end of the active states (Fig. 3.3).

These long duration inhibitory events were detected in almost every pair (18 out of 20) and in 2.6-23.0% of the silent state transitions. We evaluated that the occurrence of these inhibitory events was above the statistical chance level (alpha = 5%, exact binomial proportion test) in 35% of the pair (7 out of 20). In these 35%, such inhibitory events would occur in 14.4 ± 4.1 % of the transition to the silent state. If that proportion holds at the population level, we would expect to observe this inhibitory activity in 3.6% (0.35 x 10.3%, the lowest approximation corresponding to 14.4% – 4.1%) to 6.5% of the cortical neurons (0.35 x 18.5%, the highest approximation equal to 14.4% + 4.1%). These results suggest that under ketamine-xylazine anesthesia, inhibiting 3.6-6.5% of neurons would be sufficient to terminate the active state and initiate a transition to the silent state.

We extended our investigation of these long duration inhibitory events in relation to the onset of the silent state during natural sleep (n=6 pairs of neurons) and found they also occurred prior to the silent state onset (Fig. 3.7A, B). The hyperpolarization in the KAc neuron was 4.06 ± 3.05 mV and the depolarization in the KCl neuron was 10.19 ± 7.64 mV (n=28 events from 6 pairs of neurons). The long duration inhibition occurred296 ± 102 ms before silent state onset (n=28 events, Fig. 3.7, C) and lasted 165 ± 78 ms. As seen under anesthesia, events starting earlier lasted longer (p=0.0107, linear regression, Fig. 3.7, D). The window of disfacilitation was 140 ± 138 ms (Fig. 3.7, E). This period was two times longer than seen under anesthesia (Fig. 3.6, E) but the time-course of synaptic depression was also longer during natural sleep (Fig. 3.3, F). These events were detected in half of the pairs (3 out of 6) and seen in 19-26.8% of the silent state onset. With these numbers, we can estimate that at every silent state onset, 8-13.4% (0.5x19% for the lowest approximation and 0.5x26.8% for the highest one) of the neurons received an inhibition of long-duration and were withdrawn from the pool of active neurons contributing to recurrent activity.

3.5.3 Laminar profile of stimulation efficacy to induce a silent state

The synchronous onset of the silent state within a neocortical region requires TC afferents (Fig. 3.1 and 2) suggested that an excitatory input to the cortex could terminate the active state. We asked if an electrical stimulation could trigger a silent state and whether the efficacy was higher at cortical

depths receiving TC inputs (layer IV, 800-1200 µm in cat). We stimulated the neocortical slab with a silicon probe from the pia mater to a depth of 2250 µm (step of 150 µm). Prior to stimulation, we recorded the spontaneous activity (Fig. 3.8, A, left part of traces). The amplitude of the LFP was maximal below 1 mm and the polarity reversed between 750 and 600 µm as expected. An electrical stimulus delivered through a coaxial electrode located 1mm away from the probe triggered a silent state that was generalized throughout the cortical column (Fig. 3.8, A, right part of traces). Once the laminar position of the electrodes was assessed, we used the 16 channels silicon probe to stimulate and the coaxial electrode to record the LFP. We used two adjacent electrodes on the probe to stimulate and tested current intensity ranging from 45 to 150 µA at step of 15 µA. Electrical stimulation was delivered after at least 400 ms since the active state onset. This procedure was repeated 10 times and the efficacy was calculated as the number of success divided by 10. A successful stimulation led to a silent state within tens of milliseconds. The mapping of efficacy was done for 5 experiments and data were averaged (Fig. 3.8, B). The lowest efficacy to induce a silent state was found when stimuli were applied above 600µm and it was maximal for stimuli applied between 900 and 1500 µm. These results show that the highest efficacy of excitatory inputs (here, electrical stimuli) to trigger silent states was for depths where TC afferents make synapses with cortical neurons and just below.

The laminar stimulation in the intact cortex of a neuron whose soma was located at a depth of 1300-1400 µm showed the same tendency of higher excitability at depths below 700 µm. The intracellular recording was obtained at a distance of 200 µm from the silicon probe and stimuli were always delivered between electrodes at a regular distance of 100 µm (see schematic in Fig. 3.9, A). The average of the postsynaptic response for each site of stimulation is shown in figure 3.9, B. The lowest threshold of current intensity to obtain a response in the neuron was found when sites below 700 µm were stimulated (Fig. 3.9, C). Furthermore, these deeper sites had a shorter latency (<2 ms) to evoke a synaptic response than more superficial sites (Fig. 3.9, D). Using the same approach we investigated 13 cortical neurons. The lowest thresholds were located at depth 400-900 um (Fig. 3.9 E), which correspond to layers 3 and 4 of cats' suprasylvian gyrus (Hassler and Muhs-Clement, 1964). Therefore, the results on synaptic thresholds differ from results of field potential findings (see discussion).

3.5.4 Thalamic firing before the silent state

The thalamus was essential to synchronize the silent state onsets (Fig.3.1 and 3.2) and stimulation at cortical depths that receives TC inputs or below was more efficient to elicit silent states (Fig. 3.8).Do thalamic neurons fire before the onset of the silent state? We recorded MUA in several sites within the LP (n=24), VB (n=15), and MD (n=8) nuclei of the thalamus. We found that a subset of thalamic units fired robustly with spike bursts before the onset of the silent state in the targeted cortical region (Fig. 3.10, A-B).

Peri-event histogram triggered by silent state onset shows a progressive increase in firing density at the end of the active state (Fig. 3.10, D). When compared to the wave-triggered average of the silent state onset in the cortical LFP, the spike-triggered average showed that thalamic firing in this site was biased toward silent state onset (Fig. 3.10, C). The firing density was significantly increased toward the silent state (Fig. 3.10, E). We extracted the time and z-score values for the firing peak of each thalamic unit and found that although most units were biased toward the active state onset (40 of 47 sites), there was a subset (7 out of 47 sites) for which the peak of firing occurred before the onset of the silent state (Fig. 3.10, F). Therefore, the increase in firing of these thalamic neurons matched the increase in cortical inhibition observed prior to the onset of the silent state (Fig. 3.6, C and Fig. 3.7, C). Overall, these data suggest that thalamic afferents to the cortex could provide the excitatory input that triggers the onset of a silent state by tilting the balance of excitation and inhibition towards the silent state.

3.6 Discussion

In this study, we found that under normal conditions the transition from the active to the silent states of the slow oscillation occurs synchronously over large distance (more than 10 mm) in the cat suprasylvian gyrus. The removal of inputs to the neocortex decreases this synchrony. We identified at least 3 processes that precede the onset of the silent states: 1) a reduced density of excitatory synaptic events in a majority of investigated neurons concurrent with a decrease in firing by cortical neurons, 2) increased inhibitory activities in a subpopulation of neurons, and 3) an increased burst firing in a subset of thalamocortical neurons. We propose that the burst firing of a subset of thalamocortical neurons projecting to a given cortical area activates a subset of inhibitory

interneurons that hyperpolarize below the firing threshold a subset of cortical neurons. The lower firing of neurons reduces the excitatory drive on their targets. That triggers a chain reaction of reduced excitation underlying the synchronous onset of the silent states.

3.6.1 Balance of excitation and inhibition

A recent study showed that activation of halorhodopsin-dependent chloride-permeable channels inhibiting 14% of pyramidal neurons from infragranular (but not supragranular) layers could induce a silent state (Beltramo et al., 2013), suggesting that removing only 14% of the intracortical excitatory drive was more than sufficient to cease the recurrent activity in the neocortex. Our results suggest that under ketamine-xylazine anesthesia, removing 3-6% of the neurons is sufficient to create a period of disfacilitation (reduced EPSP barrages), which ultimately ends with a silent state. This lower proportion of inhibited neurons is lower than under natural sleep (8-13%) and may be explained by the antagonizing action of ketamine on NMDA receptors(Anis et al., 1983; MacDonald et al., 1987), which already reduced the excitatory drive in the neocortical network.

The timing of the silent state onset in each LFP was defined as the timing of the half-amplitude of a sigmoidal fitting of the transition. On the other hand, the timing of the silent state onset in intracellular recordings corresponded to the crossing of a depolarized Vm threshold (active state). Hence, results at the population level (Fig. 3.1) and those at the cellular level, especially regarding disfacilitation and the effect of chloride inhibition (Fig 3.3, 3.5-3.6) cannot be directly compared. For instance, one cannot argue that we have found such a small percentage (3-13%) of inhibited neurons prior to the silent state onset because the onset was defined as half-amplitude of the sigmoidal fitting in LFP recordings.Active states are maintained by a tight balance of excitatory and inhibitory conductances (Shu et al., 2003; Haider et al., 2006) although in the natural states of vigilance this balance is shifted toward inhibition (Rudolph et al., 2007). The inhibition controls the firing of regular-spiking neurons; inhibitory conductances are always larger than excitatory ones except prior to an action potential(Hasenstaub et al., 2005; Rudolph et al., 2007).Furthermore, $GABA_A$ conductances have been shown to be important to maintain activity within the network during the active state; the removal of this inhibition shortens the active states duration and induces epileptiform burst(Mann et al., 2009; Sanchez-Vives et al., 2010).If inhibition controls the firing of neurons, a strong and

synchronous recruitment of interneurons would have for consequence that inhibition would silence neurons and cause a disfacilitation resulting into a full silent state.

The higher efficacy of inhibition towards the end of the active state is supported by a higher frequency-dependent depression of excitatory inputs than inhibitory ones (Galarreta and Hestrin, 1998). Furthermore, the electrical coupling specifically among fast-spiking neurons (Galarreta and Hestrin, 1999) and the strong thalamocortical drive on these inhibitory neurons combined toa strong intracortical excitation of inhibitory low-threshold spiking neurons (Gibson et al., 1999) might favor inhibition over excitation and thus terminates the active state.

The canonical cortical circuit is characterized by pyramidal neurons making strong connections to other pyramidal neurons and GABAergic interneurons. These interneurons innervate somatic, initial axon segmental, and dendritic compartments on pyramidal neurons and/or interneurons (Somogyi et al., 1998). GABAergic baskets cells target essentially the soma of neocortical pyramidal neurons (Tamás et al., 1997) where GABAergic synapses dominate (Freund et al., 1983; Gu et al., 1993). Because deep layers neurons fire more than those of superficial layers (Sanchez-Vives and McCormick, 2000; Sakata and Harris, 2009; Chauvette et al., 2010; Barth and Poulet, 2012), layer V-VI are more likely to maintain the recurrent activity generating the active state. In other words, silencing these neurons directly at the soma would be the most efficient way to trigger a disfacilitation and silent state.

Results from laminar stimulations in the isolated neocortical slab reveal that stimulation of layer V exhibits the lowest threshold to trigger network silent states (Fig. 3.8). However, subthreshold neuronal responses in the intact cortex have lower threshold if the stimuli were applied around layers III-IV (Fig. 3.9).This finding is in agreement with results showing that upper cortical layers stimuli can easily induce local responses, but that deeper cortical layers stimuli can drive responses in the whole network (Beltramo et al., 2013).

Although inhibiting the soma is probably the most efficient way to induce a silent state, we cannot rule out the involvement of inhibition in other compartment, such as the one occurring at spines and dendritic shaft (Tamás et al., 1997).Also we did not investigate the potential role of $GABA_B$ receptors in the termination of active states that was shown in layers II-III of the cingulated gyrus of rats *in vitro* (Mann et al., 2009).

3.6.2 Synchronization of the cortical inhibition

The cortical synchrony of the silent state onset decreased after the pharmacological inactivation of thalamocortical inputs and was not further affected after a complete cortical deafferentation (neocortical isolated slab). This suggests that the thalamocortical inputs to the neocortex are sufficient to recruit and synchronize inhibitory interneurons. Although the elevated firing prior to the silent state onset was not a ubiquitous property of thalamic neurons (Fig. 3.10), it may be counterbalanced by the divergent nature of thalamocortical axons. There is indeed a high convergence of thalamocortical cells projections on a given suspected interneuron associated with a high divergence of a single thalamocortical cell on cortical interneurons in the neocortex (Swadlow, 1995). The threshold to induce IPSP on layer V pyramidal neurons is lower for thalamocortical inputs than for intracortical ones (Gil and Amitai, 1996), which is consistent with our finding that the threshold to induce silent state is the lowest in layer IV and V. However, we cannot rule out that long-range intracortical projections may be implicated in the silent state onset. Inhibition appears when intracortical stimulation intensity is increased and coincides with a higher firing by interneurons (Hirsch and Gilbert, 1991).The emergent inhibition due to the supralinearity of neocortical horizontal connections recruiting inhibitory networks (Tucker and Katz, 2003) could thus play a synchronizing role of inhibition during slow-wave sleep to promote the onset of the silent state.

It is expected that the removal of any elements of the thalamocortical network may alter the synchrony of the silent state onset. For instance, would removing the callosal inputs affect the synchrony of the silent state? This question remains open for further investigations but our data from slab experiments showed that the complete isolation did not caused further loss of synchronization than thalamic inactivation.

3.6.3 Electrical stimulation

Consistently with electrical stimulation in ferrets slices of frontal and occipital cortex (Shu et al., 2003), we were able to shift the current state of an isolated neocortical slab with an electrical stimulation. As the active state progresses in time, it is likely that the excitation is decreased and an input to the cortex would favor inhibition over sustained excitation. The intracellular recordings of fast-spiking neurons in neocortical slices of ferrets showed that these interneurons increased more their firing in response to stimuli triggering a silent state than to those that induced an active state onset (Shu et al., 2003). A similar ability to induce a silent state (slow wave) was obtained in naturally

sleeping rats (Vyazovskiy et al., 2009). It is of interest that transcranial magnetic stimulation in humans can non-invasively generate slow waves during the waking state (reviewed in (Massimini et al., 2009)). Although it is unknown whether electrical stimulations activated directly the synapses or the axons (or both), our data showed that layer IV and V appears as a hotspot to induce a silent state.

3.6.4 Sleep architecture, cortex and thalamus

Our results point to an active contribution of thalamocortical neurons to the termination of cortical active states during slow-wave sleep. The thalamus is also known as a site of origin of spindle, at least fast spindles (Morison and Dempsey, 1942; Steriade and Deschenes, 1984; Timofeev and Chauvette, 2013; Zheng et al., 2014). Thalamocortical neurons are hyperpolarized during slow-wave sleep, depolarized during REM sleep (Hirsch et al., 1983) and likely waking state (Steriade et al., 1993b). Upon removal of cortical inputs, thalamocortical neurons are progressively hyperpolarizing and spindle activity is progressively replaced by delta clock-like bursting (Timofeev and Steriade, 1996).At the beginning of sleep, the EEG activity is dominated by slow-delta rhythms, while toward the second half of sleep, it is dominated by spindles (Borbely et al., 1981). Based on that, we propose that thalamocortical neurons might be more hyperpolarized at the beginning of sleep and their powerful bursting triggers synchronized onset of cortical silent states. Later in the night the membrane potential of thalamocortical neurons becomes more depolarized and they contribute to spindle generation. Such changes of membrane potential of thalamocortical neurons could occur either as change in the activities of neuromodulatory systems (Steriade and McCarley, 2005)or as an up-regulation of h-current (Luthi and McCormick, 1999)which eventually leads to a reduction of T-current (Leresche et al., 2004) and low-threshold Ca^{2+} spikes. Therefore, sleep pressure expressed as enhanced slow-wave activity at the beginning of sleep or sleep deprivation might partially be mediated by the thalamus.

3.6.5 Functional implications

The present study suggests that the inhibition by the activation of $GABA_A$ receptors (chloride-mediated) in about 5% of cortical neurons under anesthesia and twice more during natural slow-wave sleep is sufficient to induce a transition from the active to the silent states of the slow oscillation. The silent state is a key signature of slow-wave sleep occupying approximately 20% of the time

(Chauvette et al., 2011) during slow oscillation. Silent states allow the replenishment of extracellular calcium (Massimini and Amzica, 2001) or may simply give the cortical and thalamic neurons a metabolic break (Vyazovskiy and Harris, 2013). The silent state also provides the ideal conditions for massive entries of calcium in neurons at the beginning of the next active states with a high synaptic efficacy (Crochet et al., 2005). This high calcium influx is essential to intracellular pathways involved in the long-term potentiation of synapses (Lamprecht and LeDoux, 2004; Chauvette et al., 2012). A possible role of the silent state could be to pave the way to memory consolidation.

3.7 References

Anis NA, Berry SC, Burton NR, Lodge D (1983) The dissociative anaesthetics, ketamine and phencyclidine, selectively reduce excitation of central mammalian neurones by n-methyl-aspartate. British journal of pharmacology 79:565-575.

Barth AL, Poulet JFA (2012) Experimental evidence for sparse firing in the neocortex. Trends in Neurosciences 35:345-355.

Beltramo R, D'Urso G, Dal Maschio M, Farisello P, Bovetti S, Clovis Y, Lassi G, Tucci V, De Pietri Tonelli D, Fellin T (2013) Layer-specific excitatory circuits differentially control recurrent network dynamics in the neocortex. Nat Neurosci 16:227-234.

Borbely AA, Baumann F, Brandeis D, Strauch I, Lehmann D (1981) Sleep deprivation: Effect on sleep stages and eeg power density in man. Electroencephalogr Clin Neurophysiol 51:483-495.

Chauvette S, Volgushev M, Timofeev I (2010) Origin of active states in local neocortical networks during slow sleep oscillation. Cereb Cortex 20:2660-2674.

Chauvette S, Seigneur J, Timofeev I (2012) Sleep oscillations in the thalamocortical system induce long-term neuronal plasticity. Neuron 75:1105-1113.

Chauvette S, Crochet S, Volgushev M, Timofeev I (2011) Properties of slow oscillation during slow-wave sleep and anesthesia in cats. J Neurosci 31:14998-15008.

Chen JY, Chauvette S, Skorheim S, Timofeev I, Bazhenov M (2012) Interneuron-mediated inhibition synchronizes neuronal activity during slow oscillation. J Physiol 590:3987-4010.

Connors BW, Malenka RC, Silva LR (1988) Two inhibitory postsynaptic potentials, and $gaba_a$and $gaba_b$ receptor-mediated responses in neocortex of rat and cat. J Physiol 406:443-468.

Contreras D, Steriade M (1995) Cellular basis of eeg slow rhythms: A study of dynamic corticothalamic relationships. J Neurosci 15:604-622.

Contreras D, Timofeev I, Steriade M (1996) Mechanisms of long-lasting hyperpolarizations underlying slow sleep oscillations in cat corticothalamic networks. J Physiol 494:251-264.

Contreras D, Destexhe A, Steriade M (1997) Intracellular and computational characterization of the intracortical inhibitory control of synchronized thalamic inputs in vivo. J Neurophysiol 78:335-350.

Crochet S, Chauvette S, Boucetta S, Timofeev I (2005) Modulation of synaptic transmission in neocortex by network activities. Eur J Neurosci 21:1030-1044.

Crunelli V, Hughes SW (2010) The slow (<1 hz) rhythm of non-rem sleep: A dialogue between three cardinal oscillators. Nat Neurosci 13:9-17.

David F, Schmiedt JT, Taylor HL, Orban G, Di Giovanni G, Uebele VN, Renger JJ, Lambert RgC, Leresche N, Crunelli V (2013) Essential thalamic contribution to slow waves of natural sleep. J Neurosci 33:19599-19610.
Freund TF, Martin KA, Smith AD, Somogyi P (1983) Glutamate decarboxylase-immunoreactive terminals of golgi-impregnated axoaxonic cells and of presumed basket cells in synaptic contact with pyramidal neurons of the cat's visual cortex. J Comp Neurol 221:263-278.
Galarreta M, Hestrin S (1998) Frequency-dependent synaptic depression and the balance of excitation and inhibition in the neocortex. Nat Neurosci 1:587-594.
Galarreta M, Hestrin S (1999) A network of fast-spiking cells in the neocortex connected by electrical synapses. Nature 402:72-75.
Gibson JR, Beierlein M, Connors BW (1999) Two networks of electrically coupled inhibitory neurons in neocortex. Nature 402:75-79.
Gil Z, Amitai Y (1996) Properties of convergent thalamocortical and intracortical synaptic potentials in single neurons of neocortex. J Neurosci 16:6567-6578.
Gu Q, Perez-Velazquez JL, Angelides KJ, Cynader MS (1993) Immunocytochemical study of gabaa receptors in the cat visual cortex. J Comp Neurol 333:94-108.
Haider B, Duque A, Hasenstaub AR, McCormick DA (2006) Neocortical network activity in vivo is generated through a dynamic balance of excitation and inhibition. J Neurosci 26:4535-4545.
Hasenstaub A, Shu Y, Haider B, Kraushaar U, Duque A, McCormick DA (2005) Inhibitory postsynaptic potentials carry synchronized frequency information in active cortical networks. Neuron 47:423-435.
Hassler R, Muhs-Clement K (1964) Architektonischer aufbau des sensomotorischen und parietalen cortex der katze. J Hirnforschung 6:377-422.
Hendry SH, Fuchs J, deBlas AL, Jones EG (1990) Distribution and plasticity of immunocytochemically localized gabaa receptors in adult monkey visual cortex. J Neurosci 10:2438-2450.
Hirsch JA, Gilbert CD (1991) Synaptic physiology of horizontal connections in the cat's visual cortex. J Neurosci 11:1800-1809.
Hirsch JC, Fourment A, Marc ME (1983) Sleep-related variations of membrane potential in the lateral geniculate body relay neurons of the cat. Brain Res 259:308-312.
Huber R, Esser SK, Ferrarelli F, Massimini M, Peterson MJ, Tononi G (2007) Tms-induced cortical potentiation during wakefulness locally increases slow wave activity during sleep. PloS one 2:e276.
Hughes SW, Cope DW, Blethyn KL, Crunelli V (2002) Cellular mechanisms of the slow (<1 hz) oscillation in thalamocortical neurons in vitro. Neuron 33:947-958.
Lamprecht R, LeDoux J (2004) Structural plasticity and memory. Nat Rev Neurosci 5:45-54.
Lemieux M, Chen J-Y, Lonjers P, Bazhenov M, Timofeev I (2014) The impact of cortical deafferentation on the neocortical slow oscillation. J Neurosci in press.
Leresche N, Hering J, Lambert RC (2004) Paradoxical potentiation of neuronal t-type ca2+ current by atp at resting membrane potential. J Neurosci 24:5592-5602.
Luthi A, McCormick DA (1999) Modulation of a pacemaker current through ca(2+)-induced stimulation of camp production. Nat Neurosci 2:634-641.
MacDonald JF, Miljkovic Z, Pennefather P (1987) Use-dependent block of excitatory amino acid currents in cultured neurons by ketamine. J Neurophysiol 58:251-266.
Mann EO, Kohl MM, Paulsen O (2009) Distinct roles of $gaba_a$ and $gaba_b$ receptors in balancing and terminating persistent cortical activity. J Neurosci 29:7513-7518.

Massimini M, Amzica F (2001) Extracellular calcium fluctuations and intracellular potentials in the cortex during the slow sleep oscillation. J Neurophysiol 85:1346-1350.
Massimini M, Tononi G, Huber R (2009) Slow waves, synaptic plasticity and information processing: Insights from transcranial magnetic stimulation and high-density eeg experiments. Eur J Neurosci 29:1761-1770.
Morison RS, Dempsey EW (1942) A study of thalamo-cortical relations. Am J Physiol 135:281-292.
Puig MV, Ushimaru M, Kawaguchi Y (2008) Two distinct activity patterns of fast-spiking interneurons during neocortical up states. Proceedings of the National Academy of Sciences 105:8428-8433.
Rudolph M, Pospischil M, Timofeev I, Destexhe A (2007) Inhibition determines membrane potential dynamics and controls action potential generation in awake and sleeping cat cortex. J Neurosci 27:5280-5290.
Sakata S, Harris KD (2009) Laminar structure of spontaneous and sensory-evoked population activity in auditory cortex. Neuron 64:404-418.
Sanchez-Vives MV, McCormick DA (2000) Cellular and network mechanisms of rhythmic recurrent activity in neocortex. Nat Neurosci 3:1027-1034.
Sanchez-Vives MV, Mattia M, Compte A, Perez-Zabalza M, Winograd M, Descalzo VF, Reig R (2010) Inhibitory modulation of cortical up states. J Neurophysiol 104:1314-1324.
Sherman SM, Guillery RW (1996) Functional organization of thalamocortical relays. J Neurophysiol 76:1367-1395.
Shu Y, Hasenstaub A, McCormick DA (2003) Turning on and off recurrent balanced cortical activity. Nature 423:288-293.
Somogyi P, Tamás G, Lujan R, Buhl EH (1998) Salient features of synaptic organisation in the cerebral cortex. Brain Res Rev 26:113-135.
Steriade M, Deschenes M (1984) The thalamus as a neuronal oscillator. Brain Res Rev 8:1-63.
Steriade M, McCarley RW (2005) Brainstem control of wakefulness and sleep. New York: Plenum.
Steriade M, Nuñez A, Amzica F (1993a) A novel slow (<1 hz) oscillation of neocortical neurons *in vivo* : Depolarizing and hyperpolarizing components. J Neurosci 13:3252-3265.
Steriade M, McCormick DA, Sejnowski TJ (1993b) Thalamocortical oscillations in the sleeping and aroused brain. Science 262:679-685.
Steriade M, Nuñez A, Amzica F (1993c) Intracellular analysis of relations between the slow (<1 hz) neocortical oscillations and other sleep rhythms of electroencephalogram. J Neurosci 13:3266-3283.
Steriade M, Timofeev I, Grenier F (2001) Natural waking and sleep states: A view from inside neocortical neurons. J Neurophysiol 85:1969-1985.
Steriade M, Contreras D, Dossi RC, Nuñez A (1993d) The slow (<1 hz) oscillation in reticular thalamic and thalamo-cortical neurons: Scenario of sleep rhythm generation in interacting thalamic and neocortical networks. J Neurosci 13:3284-3299.
Swadlow HA (1995) Influence of vpm afferents on putative inhibitory interneurons in s1 of the awake rabbit: Evidence from cross-correlation, microstimulation, and latencies to peripheral sensory stimulation. J Neurophysiol 73:1584-1599.
Tamás G, Buhl EH, Somogyi P (1997) Fast ipsps elicited via multiple synaptic release sites by different types of gabaergic neurone in the cat visual cortex. J Physiol 500:715-738.
Timofeev I, Steriade M (1996) Low-frequency rhythms in the thalamus of intact-cortex and decorticated cats. J Neurophysiol 76:4152-4168.
Timofeev I, Chauvette S (2013) The spindles: Are they still thalamic? Sleep 36:825-826.

Timofeev I, Contreras D, Steriade M (1996) Synaptic responsiveness of cortical and thalamic neurones during various phases of slow sleep oscillation in cat. J Physiol 494:265-278.
Timofeev I, Grenier F, Steriade M (2001) Disfacilitation and active inhibition in the neocortex during the natural sleep-wake cycle: An intracellular study. Proc Natl Acad Sci U S A 98:1924-1929.
Timofeev I, Grenier F, Steriade M (2004) Contribution of intrinsic neuronal factors in the generation of cortically driven electrographic seizures. J Neurophysiol 92:1133-1143.
Timofeev I, Grenier F, Bazhenov M, Sejnowski TJ, Steriade M (2000) Origin of slow cortical oscillations in deafferented cortical slabs. Cereb Cortex 10:1185-1199.
Tucker TR, Katz LC (2003) Recruitment of local inhibitory networks by horizontal connections in layer 2/3 of ferret visual cortex. J Neurophysiol 89:501-512.
Volgushev M, Chauvette S, Mukovski M, Timofeev I (2006) Precise long-range synchronization of activity and silence in neocortical neurons during slow-wave sleep. J Neurosci 26:5665-5672.
Vyazovskiy VV, Harris KD (2013) Sleep and the single neuron: The role of global slow oscillations in individual cell rest. Nat Rev Neurosci 14:443-451.
Vyazovskiy VV, Faraguna U, Cirelli C, Tononi G (2009) Triggering slow waves during nrem sleep in the rat by intracortical electrical stimulation: Effects of sleep/wake history and background activity. J Neurophysiol 101:1921-1931.
Zheng TW, O'Brien TJ, Kulikova SP, Reid CA, Morris MJ, Pinault D (2014) Acute effect of carbamazepine on corticothalamic 5–9-hz and thalamocortical spindle (10–16-hz) oscillations in the rat. European Journal of Neuroscience 39:788-799.

3.8 Figures

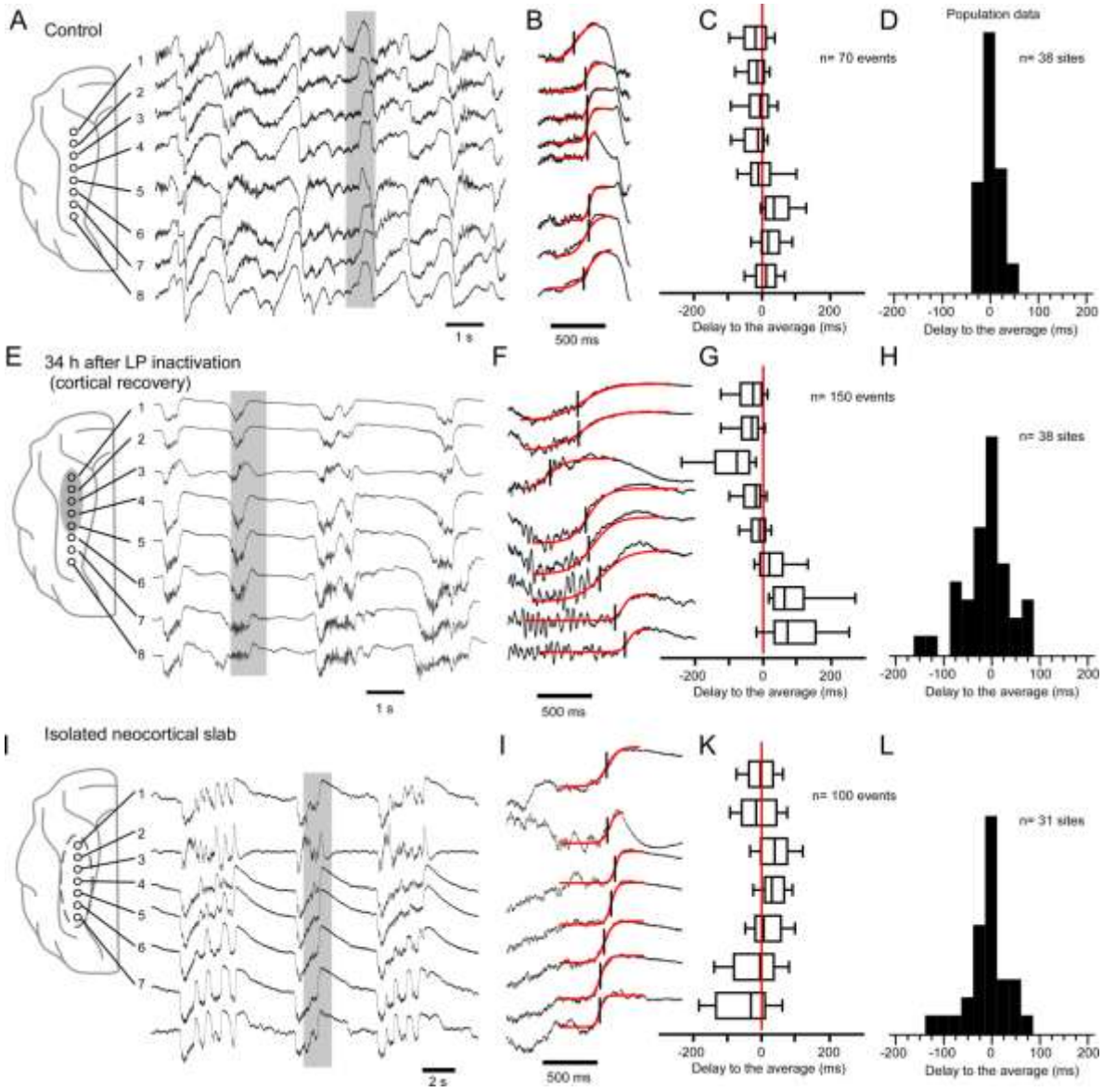

Figure 3.1 Removing inputs to the neocortex decreases the synchrony of the silent state onset.

(A) Multisite LFP recordings in the intact suprasylvian gyrus reveal a synchronous slow oscillation in the 8 cortical sites. Schema at left indicates the location of recording electrodes. Traces in the gray box are enlarged in (B) to show the simultaneous occurrence of the silent state among sites. Transitions are fitted with a sigmoid curve and the onset of the silent state is defined as the time corresponding to the half-amplitude of the curve. (C) Boxplots of the delays to the averaged silent state onset for each site. The left and right boundaries of the box are the first and third quartile respectively and the central line is the median. Horizontal lines contain percentiles 10 to 90.(D) Frequency histogram of the median delay to the averaged silent state for all sites

(n=38) from all experiment (n=5). (E) Multisite LFP recordings 34 h after pharmacological inactivation with QX-314 of thalamocortical afferents from the LP nucleus to the suprasylvian gyrus. Schema at left indicates the location of recording electrodes and the shaded region highlights the affected cortical region. Traces in the gray box are enlarged in (F) and show a reduction in the synchrony of the silent state onset. (G) Boxplots of the delays to the averaged silent state onset indicates a reduction in the synchrony of the silent state onset among sites. (H)Frequency histogram of the median delay to the averaged silent state onset after the LP nucleus inactivation for all sites (n=38) from all experiment (n=5). (I) Multisite LFP recordings in a neocortical slab. Schema at left indicates the location of the recording electrodes and the dotted line delimitates the slab. Traces in the gray box are enlarged in (J). (K) Boxplot of the delays to the averaged silent state onset for each site. (L) Frequency histograms of the median delaysto the averaged silent state for all sites (n=31) from all experiments (n=6).

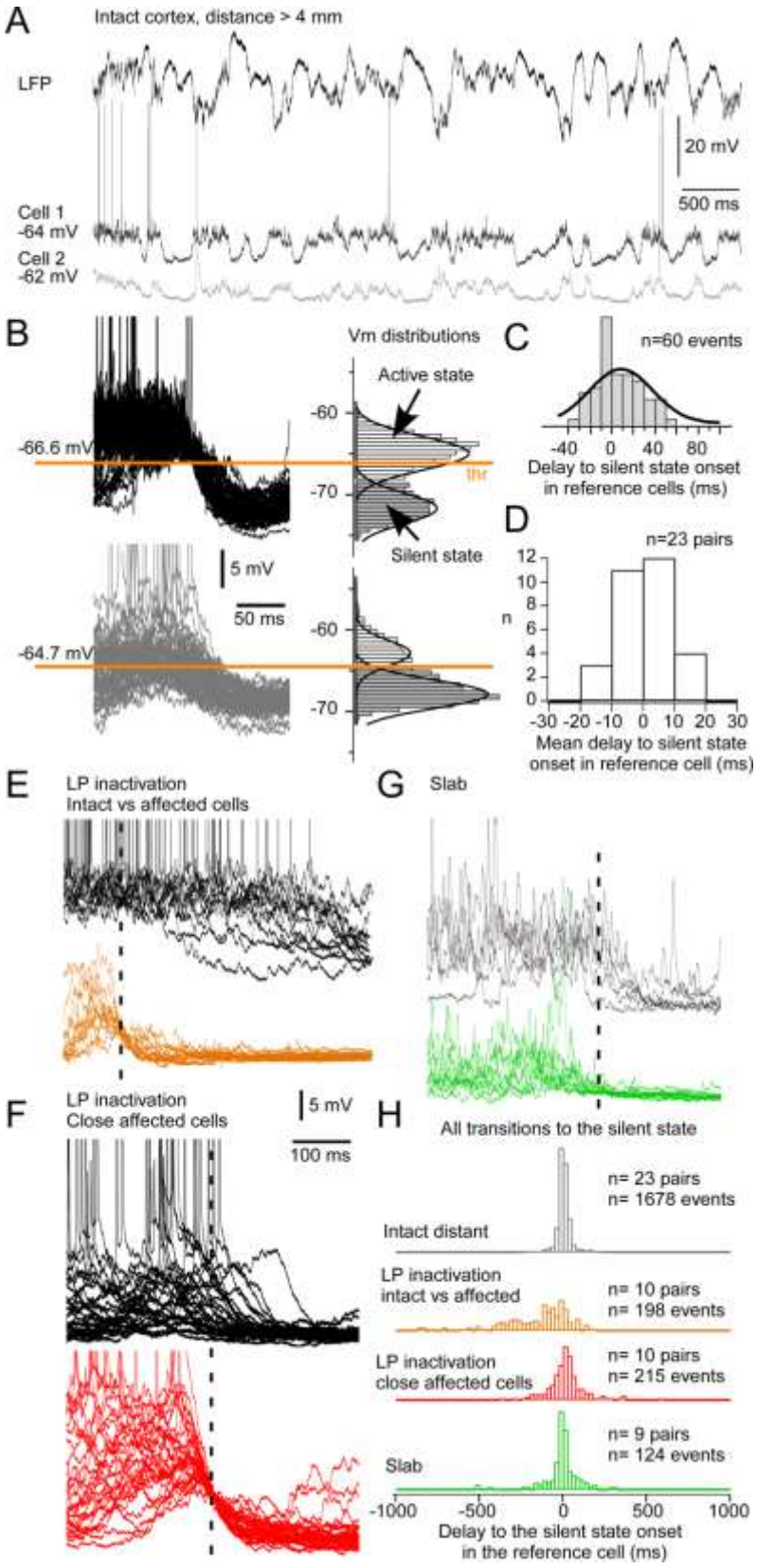

Figure 3.2 Synchrony of silent state onset at the cellular level.

(A) Example a dual intracellular recording from the suprasylvian gyrus with a lateral distance of 4 mm. The LFP was obtained simultaneously in the same region. (B) Several transitions to the silent state in both cells (left) are shown with their corresponding V_m distribution. The onset is defined when V_m crosses the active state threshold (thr). (C) Frequency histograms of the delays of the silent state onset in the gray cell to the onset in the black cell. The thick black line is the Gaussian fitting of the distribution. (D) Histograms of mean delays in each pair. Note that the distribution is centered on zero. (E) Examples of silent state onsets for a cell in the region affected by the inactivation (orange) simultaneously recorded with a cell in the intact region (black). (F) Examples of superimposed transitions to the silent state for a pair of neurons at a distance < 1.5 mm in the region affected by an LP nucleus inactivation. (G) Examples of silent state onsets for two neurons at a distance > 4 mm in the slab.(H) Frequency histograms of the delays of the silent state onset for all investigated conditions. Dashed lines in E-G indicate the crossing of the V_m threshold in cell 2.

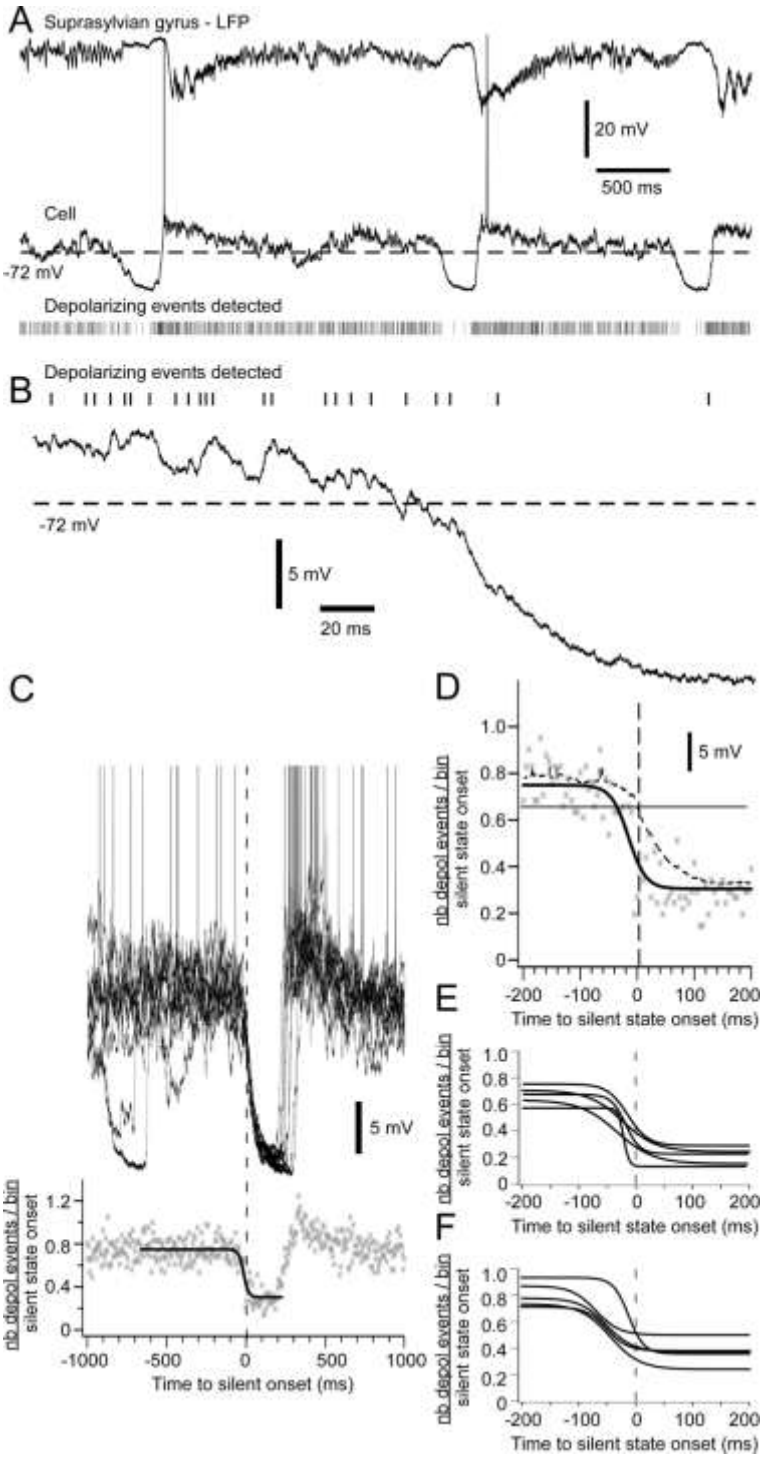

Figure 3.3 Disfacilitation prior to the silent state onset

(A) Example of LFP and intracellular recordings in the suprasylvian gyrus. Raster indicates depolarizing events detected in the intracellular trace. The dotted line is the V_m threshold used to define the onset of the silent state. (B) Examples of depolarizing events detected. (C) Ten superimposed traces aligned on the onset of the silent state are shown in the upper part. The lower part shows the number of depolarizing events per bin of 5 ms normalized to one silent state onset (n=41). Data are fitted with a sigmoidal curve (thick black line). Data are expanded ± 200 ms around the silent state onset in (D). Note that the sigmoidal fitting of the number of depolarizing events precedes variation of the V_m (dashed line). Sigmoidal fitting of 5 cells recorded (E) under ketamine-xylazine anesthesia and (F) during natural sleep.

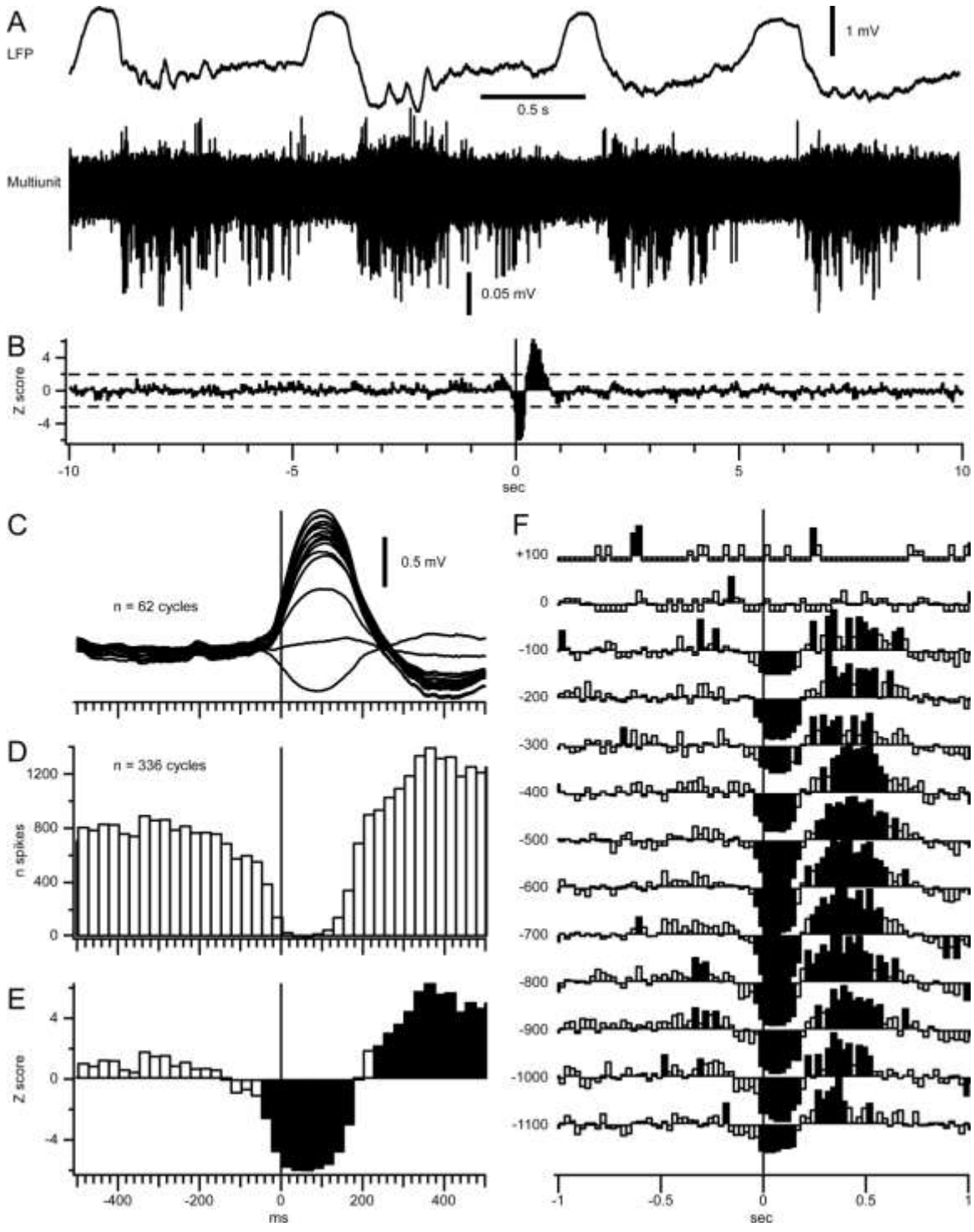

Figure 3.4 Decreased cortical firing prior to the onset of silent states.

(A) Upper trace - Deep local field potential recorded during natural sleep of a cat. Lower traces – Superimposition of 16 filtered (0.5-10 kHz) LFP recordings for multiunit activities. Recordings were performed using a linear 16-channel silicon probe with recording sites separated by 100 μm; the probe was inserted

perpendicularly to the cortical surface. Note the decreased firing towards the end of active states. (B) Z-score of multiunit firing triggered by silent state onsets (n = 336). Mean and standard deviation used for the z-score were calculated ±10 s from the silent state onset. The dotted line represent z=±1.96 (α = 0.05).(C) Wave-triggered averages of the LFPs recorded from a 16-channel silicon probe during one sleep episode. The deepest recording was used to detect the onset of silent states. (D) Peri-event histogram of cortical firing calculated from 336 cycles from 5 sleep episodes (bins = 25 ms). (E) Zoom-in of the panel B around the silent state onset. (F) Z-score of the cortical depth profile of the significant variation of firing around silent state onsets. Y-axis represents the cortical depth, depth 0 represents the depth at which the slow wave reversed and was used to align the recording depth from the 5 sleep episodes. Only depths with 5 recordings were used to calculate the depth profile z-score. For panels E and F significant values are shown as filled bins; note the significant decreased firing starting 50 ms prior the onset of silent state.

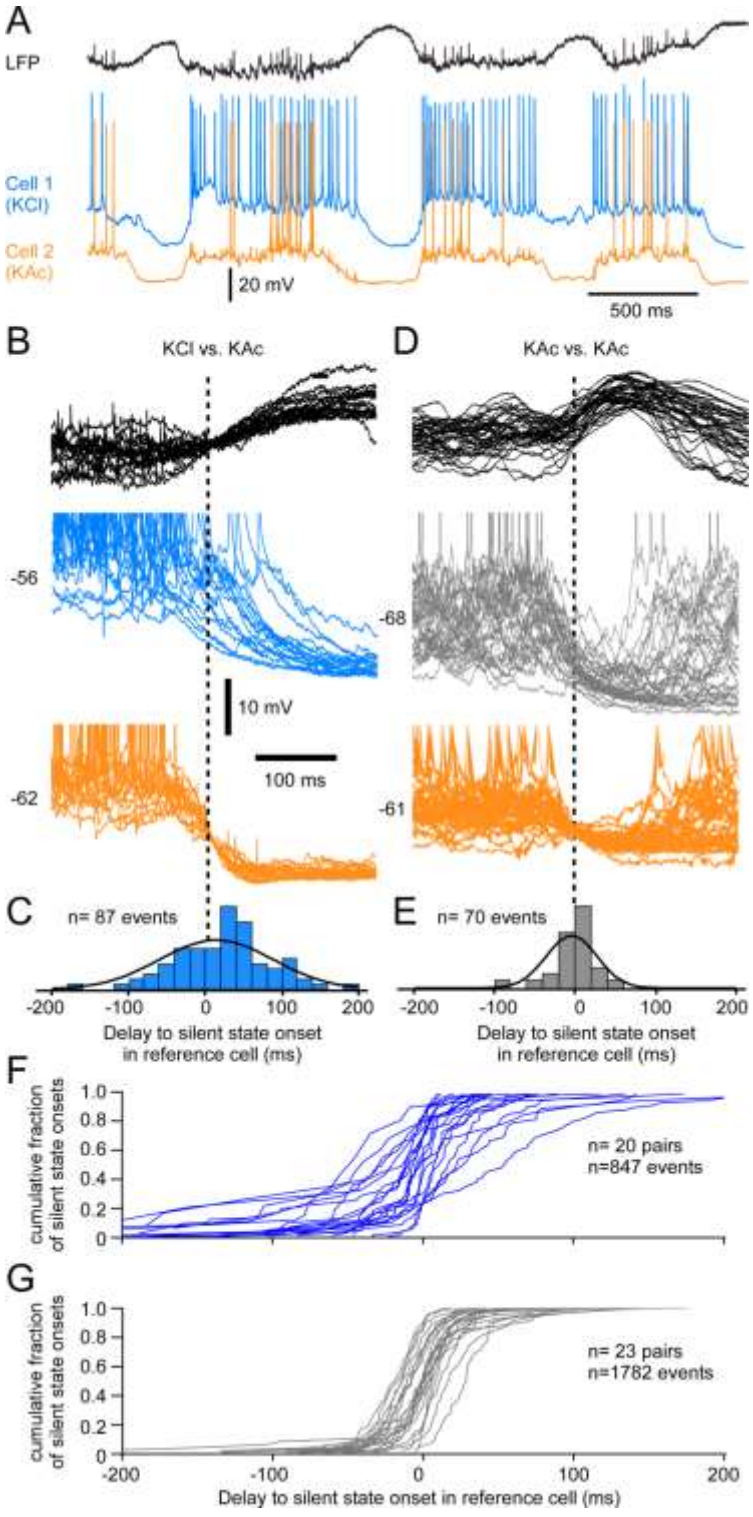

Figure 3.5 Chloride inhibition at the transition to the silent state.

(A) Example of LFP and dual intracellular recordings of closely located (<0.5 mm) neurons. Cell 1 is recorded with a pipette filled with KCl (2 M) and cell 2 (reference cell) with a pipette filled withKAc (2M). (B) Several superimposed examples of the transition to silent state triggered on the reference cell. Note the increased delay to silent state onset in cell 1. (C) Frequency histogram of delays to the silent state onset in cell 1 (KCl) in comparison to cell 2. (D) Example of two cells recorded with KAc closely located. (E) Frequency histogram of delays to the silent state. (F) Cumulative density functions for each KCl-KAc pair. (G) Cumulative density functions for each KAc-KAc pair. In panels B-E the neuron indicated by orange color was used as reference cell and the silent state onsets are indicated by a vertical dashed line.

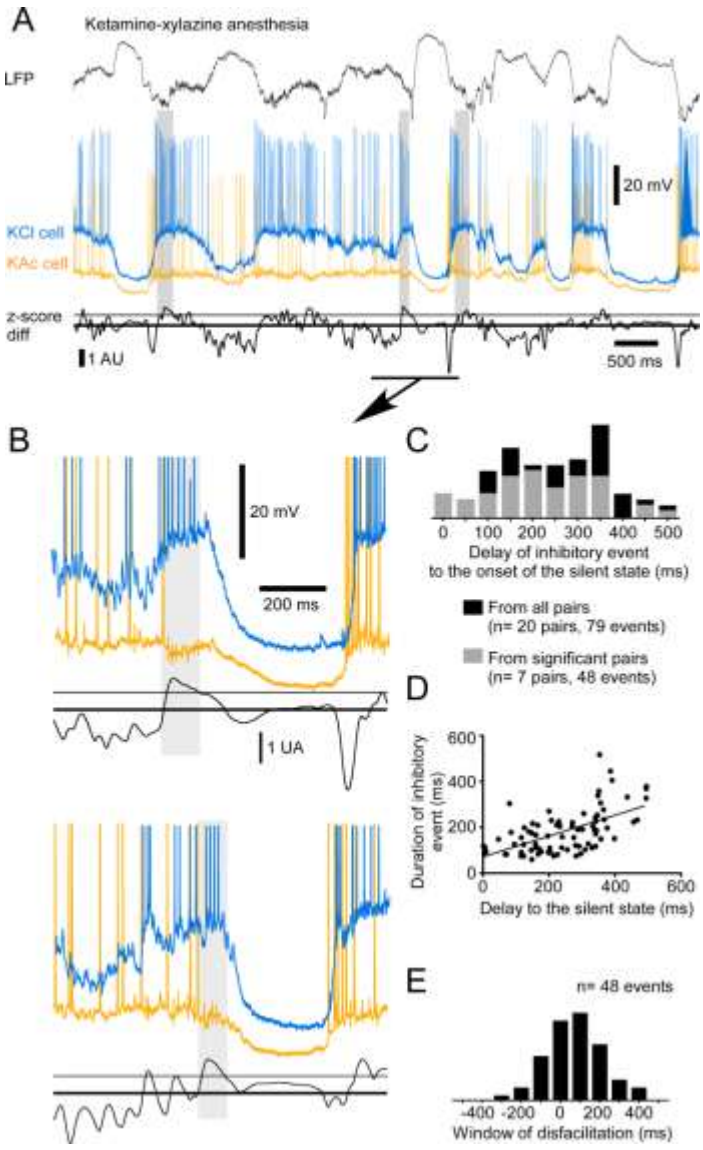

Figure 3.6 Long duration inhibition prior to the onset of the silent state under ketamine-xylazine anesthesia.

(A) Example of LFP, dual intracellular recordings and associated z-score differences. Z-score difference are presented as arbitrary unit (AU). The thick line indicates a null difference and the thin line the standard deviation of the difference (threshold for inhibitory event onset). Gray boxes indicate events of long duration inhibition. The epoch underlined is enlarged in the upper panel of (B). The lower panel is another example from the same pair of cells. (C) Frequency histogram of the delays of onset of inhibitory events to the onset of the silent state. Black bars are data from all pairs and gray bars are data for pairs with a proportion significantly higher than chance level. (D) Plot of the duration of the inhibitory event vs. the delay of onset of the event to the onset of the silent state. The slope of the linear regression is significant, $p<0.0001$. (E) Frequency histograms of the window of disfacilitation.

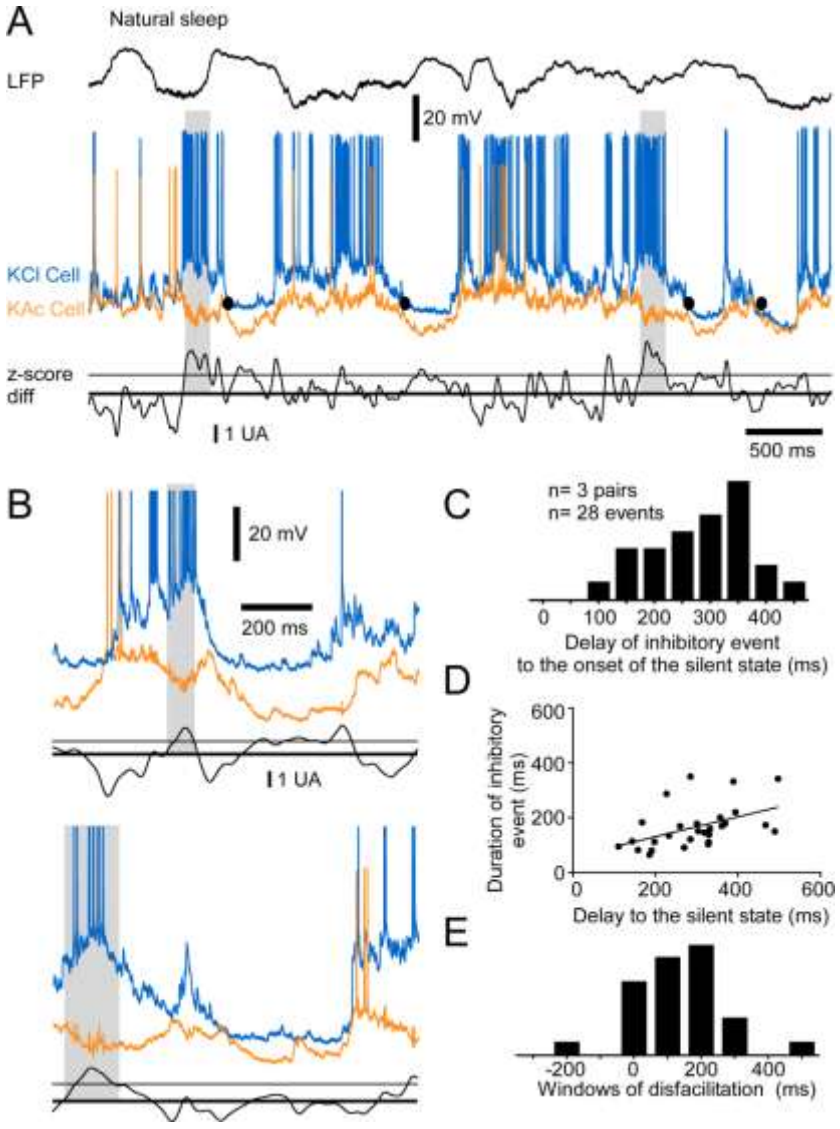

Figure 3.7 Long duration inhibition prior to the onset of silent state during natural sleep.

(A) Example of LFP, dual intracellular recordings and associated z-score difference. Gray boxes indicate events of long duration inhibition; black circles indicate the onset of silent states detected in the orange neuron. (B) Two examples from the same cells at a lower time scale. (C) Frequency histogram of the delays of onset of inhibitory events to the onset of the silent state. All data are from pairs with a proportion significantly higher than chance level. (D) Plot of the duration of the inhibitory event vs. the delay of onset of the event to the onset of the silent state. The slope of the linear regression is significant, p=0.0107. (E) Frequency histograms of the window of disfacilitation.

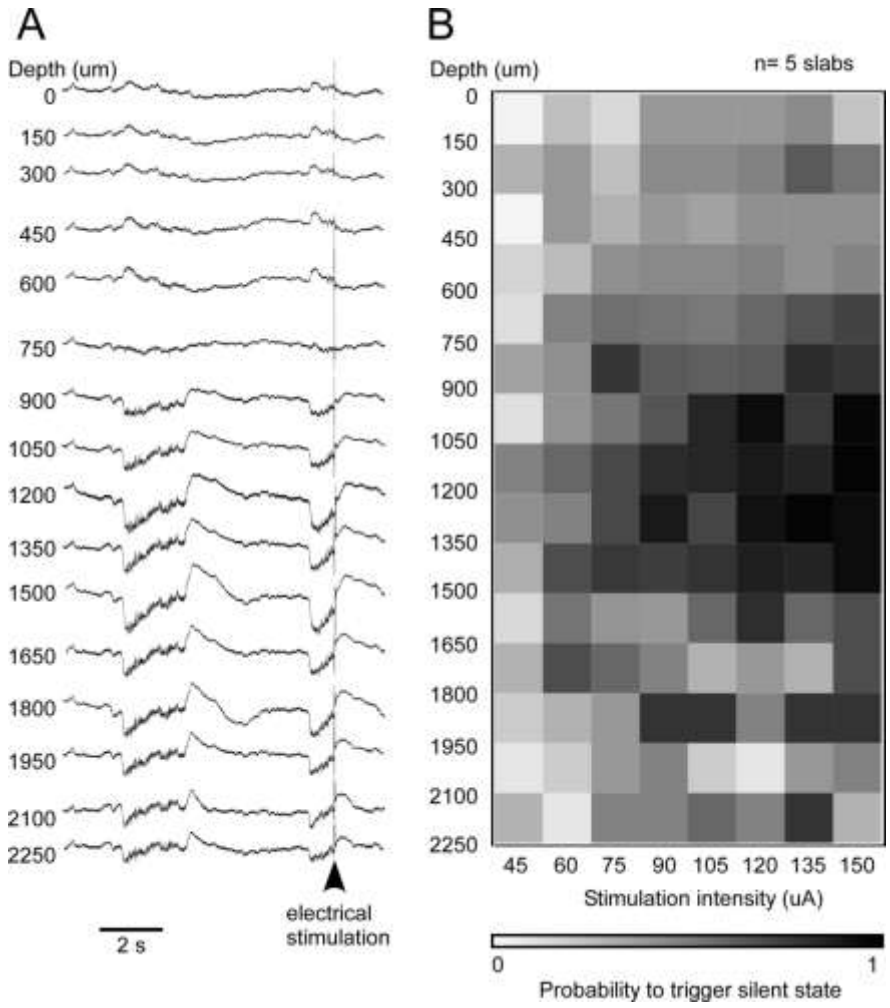

Figure 3.8 Depth profile of the efficacy to trigger a silent state.

(A)Laminar profile of LFP activity in the neocortical slab showing a spontaneous transition to the silent state and an evoked transition. (B) Depth-current intensity profile of the probability to trigger a silent state averaged from 5 experiments (at least 10 stimuli at each electrode's pair and stimulus intensity). The probability matrix is color-coded and ranges from 0% efficacy (white) to 100% efficacy (black). Note the higher efficiency between 900 and 1500 µm.

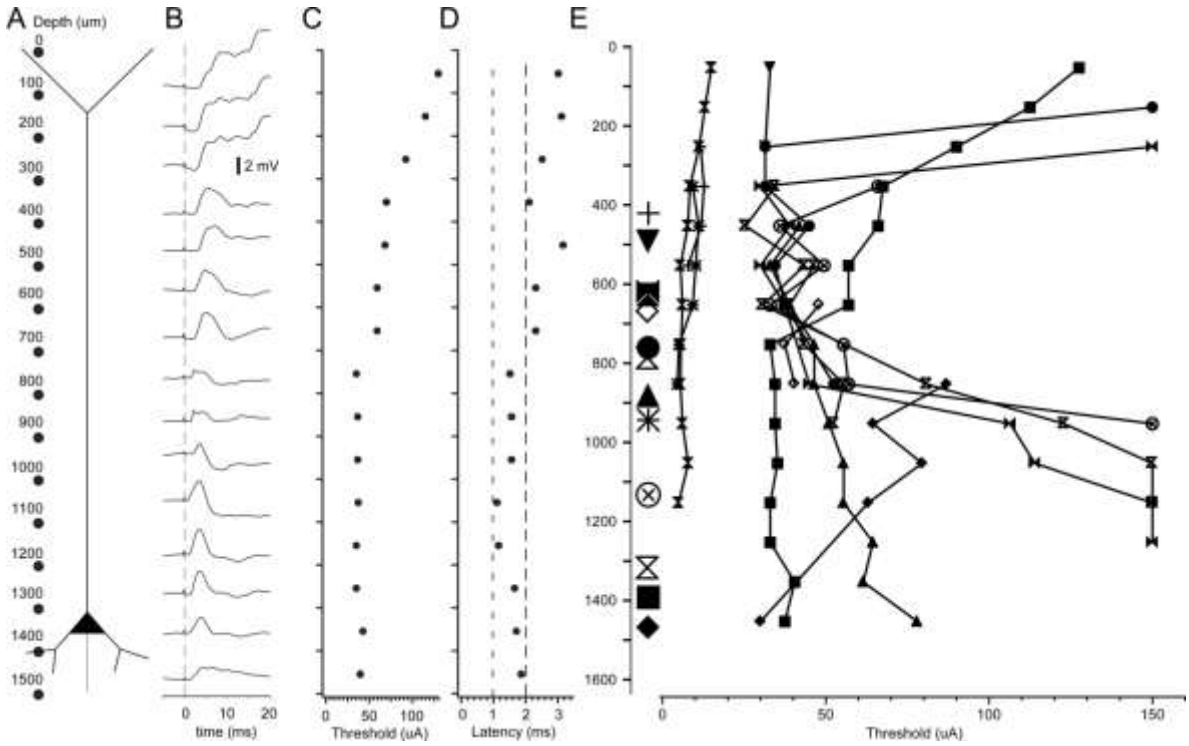

Figure 3.9 Depth profile of neuronal response to electrical stimuli.

(A) Schematic representation of the experimental approach. The 16 dots represent the 16 stimulating sites of the silicon probe at regular intervals of 100 µm. (B) Stimuli-triggered averages of responses obtained for every pair of stimulating site. The averages were obtained from at least 30 stimuli. (C) Stimulus intensity required to induce responses shown in B. (D) Latency of responses shown in B. (E) Threshold to elicit responses in 13 cortical neurons to laminar stimulation.

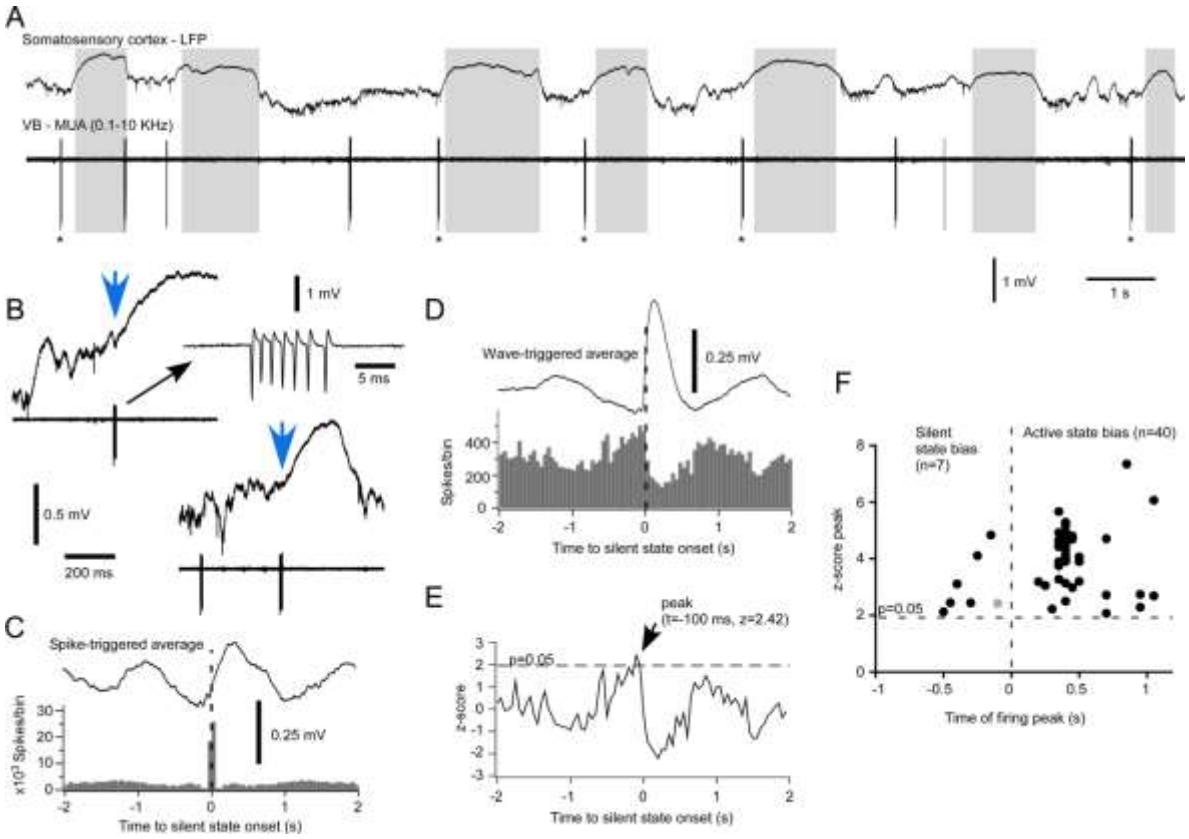

Figure 3.10 Thalamic firing in relation to cortical onset of the silent state.

(A) LFP from somatosensory cortex and MUA from the thalamic VB complex. Note the absence of firing during silent states (underlined by grey boxes). Asterisks indicate burst firing prior to the silent state onset (B) Examples of thalamic firing before the cortical silent state. The blue arrows indicate the time of silent state onset. The upper trace is enlarged to show the burst firing. (C) Average of the cortical LFP triggered on the thalamic spikes. Peri-spike frequency histograms of thalamic MUA. (D) Average of the cortical LFP triggered on the transition to silent state. Peri-event histogram of thalamic MUA (n=813 events). Note the progressive increase in firing prior to the silent state onset. (E) Z-score transform of the histograms in D. Dashed line indicate a p-value of 0.05. The time and z-value of the firing peak indicate a bias toward the onset of the silent state. (F) Population data (n=47 sites) of the z-value vs. the time of the firing peak for each unit. The example in A-E is indicated by the gray filled circle.

Chapter 4 The slow oscillation in the somatosensory and associative cortices of rabbits and cats: a comparative study of recurrent activity in the mammalian neocortex.

Maxime Lemieux[1] and Igor Timofeev[1,2]

[1] The Centre de recherche de l'Institut Universitaire en Santé Mentale de Québec (CRIUSMQ), Laval University, Québec, G1J 2G3, Canada

[2] Department of Psychiatry and Neuroscience, Laval University, Québec G1V 0A6 Canada

Titre en français:

L'oscillation lente dans les cortex somatosensoriel et associatif des lapins et des chats: une étude comparative de l'activité récurrente dans le néocortex mammalien

4.1 Résumé

Le réseau thalamocortical des mammifères génère l'oscillation lente (<1 Hz) durant le sommeil à ondes lentes et sous divers anesthésiants. Ce rythme se traduit par une alternance entre un état active et un état silencieux du réseau thalamocortical. L'état actif est l'expression de l'activité récurrente et dépend de la connectivité sous-jacente. Nous avons enregistrés le potentiel de champs local dans plusieurs sites des cortex somatosensoriel primaire et associatif chez le lapin et le chat sous anesthésie par la kétamine-xylazine. Pour étudier le niveau de synchronisation de l'oscillation lente, nous avons utilisé des analyses de coïncidence, de corrélation croisée et de propagation des états de l'oscillation lente. Nous avons trouvé que la synchronie de l'oscillation lente est plus élevée chez les chats que les lapins. Nous avons aussi trouvé que pour les deux espèces, les régions associatives démontraient une plus grande synchronisation et une plus rapide propagation que les régions somatosensorielles. Ces constatations ont été corroborées par la capacité du réseau des ilôts néocorticaux isolés à générer des états actifs de plus longues durées chez le chat que chez le lapin. Chez le lapin, l'ilôt isolé dans la région associative, mais non dans celle somatomotrice, pouvait générer de manière fiable des états actifs de courte durée en comparaison de chez le chat. Nous avons conclu que le niveau de concordance de l'oscillation lente augmente dans les cerveaux plus gros et avec plus de circonvolutions; ce niveau est également plus élevé dans les régions multimodales que dans les régions sensorielles primaires. Nous suggérons que ces conclusions reflètent le niveau de connectivité dans une espèce et une région néocorticale donnée.

4.2 Abstract

The thalamocortical network of mammals generates the slow oscillation (<1 Hz) during slow wave sleep and under several anesthetics. This rhythm translates as an alternation of an active and a silent state of the thalamocortical network. The active state is the expression of recurrent activity and depends on the underlying connectivity. We recorded LFP in multiple sites of the primary somatosensory and associative cortices in the rabbits and the cats under ketamine-xylazine anesthesia. To investigate the level of synchronization of the slow oscillation, we used coincidence, cross-correlation and propagation analysis of the states of the slow oscillation. We found that the synchrony of the slow oscillation is higher in cats than in rabbits. Also, we found for both species that the associative regions show a higher synchronization and faster propagation than in somatosensory regions. These findings were corroborated by the ability of the network of the isolated neocortical slabs to generate longer active states in the cat than in the rabbit. In the rabbit, the slab isolated in the associative region, but not in the somatomotor one, could reliably generate active states of shorter duration than in the cat. We concluded that the level of concordance of the slow oscillation increases with larger and more circonvoluted brain and is higher in multimodal than in primary sensory regions. We suggest that these findings may reflect the level of connectivity of a given species and neocortical region.

4.3 Introduction

The slow oscillation is a rhythm of the thalamocortical network during slow wave sleep (SWS) (Blake and Gerard, 1937; Achermann and Borbely, 1997; Steriade et al., 2001) and reproduced by anesthesia such as urethane and ketamine-xylazine (Steriade et al., 1993c; Steriade et al., 1993a, b; Contreras and Steriade, 1995; Sharma et al., 2010; Chauvette et al., 2011). It correlates in intracellular recordings as an alternation in the membrane potential of depolarization by synaptic barrages (the active or "UP" state) and hyperpolarization due to synaptic disfacilitation (the silent or "DOWN" state) (Contreras and Steriade, 1995; Steriade et al., 2001). The active state groups all frequency bands: delta (1-4Hz), spindles (7-15 Hz) and fast rhythms (beta rhythms, 15-30 Hz; gamma rhythms, 30-100 Hz and ripples, >100 Hz) (Steriade et al., 1993a, b; Grenier et al., 2001; Molle et al., 2002; Mukovski et al., 2007). The slow oscillation is primarily a cortical form of recurrent activity (Sanchez-Vives and McCormick, 2000; Timofeev et al., 2000) that is maintained by a balance of excitation and inhibition (Haider et al., 2006).

The presence of the slow oscillation during SWS in both mammals and birds possessing a 6-layered cortex and its absence in the 3-layer reptilian cerebral cortex (Rattenborg, 2006) suggest that this form of recurrent activity requires a certain level of connectivity. Among mammalian species, the level of intracortical connectivity between sites at a distance of 1-2 mm may differ but, to our knowledge, has not been addressed electrophysiologically. In this study, we have investigated with multisite local field potential (LFP) recordings in the rabbit and cat cerebral cortex the level of concordance and synchrony of the slow oscillation induced by ketamine-xylazine. We also compared for both species these properties in a primary sensory cortex (primary somatosensory cortex) and an associative region (in the parieto-occipital cortex). We hypothesized that the level of synchronicity should be higher in the more developed cerebral cortex of the cat and within a given species, higher in the multimodal (associative) cortex.

4.4 Methodology

4.4.1 Surgery

Cats were anesthetized with ketamine-xylazine (10 mg/kg and 2 mg/kg respectively, i.m. injection) and continuously supplied via an intravenous catheter with lactate ringer at a rate of 10 mL/kg supplemented with ketamine (20µg/kg*min). Rabbit were anesthetized with ketamine xylazine (35

mg/kg and 5 mg/kg respectively, i.m. injection). A catheter was inserted in the marginal ear vein to deliver a solution of 2.5% dextrose and 0.45% NaCl 0.45% at a rate of 5 mL/kg/h. When the EEG showed signs of activated patterns, cats were supplemented with a half of the initial dose and rabbits with a third of the initial dose. Cats and rabbits were paralyzed with gallaminetriethiodide (2%) and artificially ventilated. Oxygen and ventilating rate were adjusted to maintain an end-tidal CO_2 level of 3.3-3.7 %. Animals were put on a heating blanket to keep body temperature at 38-38.5C.

For both cats and rabbits, all incision and pressure points were injected with bupivacaine or xylocaine 0.5%. The skin and conjunctive tissue above the skull were removed and the brain exposed by craniotomy. Following euthanasia with sodium pentobarbital, brain were immersed in PFA 4% and sucrose 10% in PB 0.1 M 0.9% NaCl. Prior to cryosectioning, brains were allowed to sink in PBS sucrose 30%. Sections were processed for Nissl staining to confirm the location of isolated neocortical slab.

4.4.2 Electrophysiological recordings

To study the spatiotemporal properties of the slow oscillation in the intact cortex, an array of 8 bipolar electrodes (Rhodes Medical Instruments, Summerland, CA, USA) were inserted in the region of interest. Electrodes were at regular intervals of 1.5 mm and spanned 10.5 mm. Local field potential (LFP) signal was amplified with AC amplifier (AM300, A-M Systems, Sequim, WA, USA). Intracellular recordings were obtained with borosilicate pipettes filled with potassium acetate 2M. Intracellular activities were recorded with a DC amplifier (Neuro Data IR283, Cygnus Technology, Delaware Water Gap, PA, USA) and digitized at a sampling rate of 30 kHz on a 16-channels Vision data acquisition system (Nicolet, Madison, WI, USA).

4.4.3 Data analysis

Data (LFP and intracellular recordings) were analyzed offline with IgorPro version 4 (WaveMetrics, Lake Oswego, OR, USA).

To quantify the properties of the slow oscillation (frequency and duration of active and silent states) in each site for comparison purposes, we defined network states with a variant of a method proposed by (Mukovski et al., 2007). We opted to define states of the LFP in time binss of 50 ms. Because the bimodality associated with the two states of the slow oscillation is not always obvious in LFP recordings (in contrast to most intracellular recordings), we used in addition to the mean voltage of

the LFP the variability of fast rhythms. The approach can be described in four steps illustrated in figure 4.1. In step 1 (figure 4.1, A), LFP were filtered for fast rhythms (20-200 Hz). In step 2 (figure 4.1, B), the mean voltage of the LFP and the standard deviation of fast rhythms were extracted for each time bins. For the voltage, a positive value corresponds to the silent state (depth positivity) while a negative value is associated with the active state (depth negativity). Mean voltage and standard deviation were plotted against each other and showed that depth negativity is associated with more variability of the fast rhythms (due to network activity) while depth positivity co-occured with low variability (due to quiescence in the network during the silent state). Two clusters could be visually identified and both parameters were split according to a cut-off value of the fast rhythms. In step 3, we defined thresholds. The first threshold was for the mean voltage of the LFP and corresponded in most cases as the intersection of the active and silent state distributions (figure 4.1, B, horizontal histogram). In some cases, however, it was more accurate to use the average of the active state distribution plus the standard deviation. The second and third thresholds were used for the standard deviation of fast rhythms; the second was used for the onset of the active state (mean – standard deviation of the respective distribution) while the third was used for the onset of the silent state (mean + standard deviation). These three thresholds created 6 zones, among which one was an unequivocal active state and another one an unequivocal silent state (respectively “A” and “S” in the inset of figure 4.1, B). The four other regions (grey regions in the inset of figure 4.1, B) represented period of transition between states or aborted state in the sense of short periods of fast rhythms during the silent state or reduced fast rhythms. In any case, these events were marginal and associated with the preceding time bin in step 4. In this last step, a state binary value was assigned to each time bin (0 for silent state, 1 for active state) according to the thresholds. A sliding step of 5 ms was used for better accuracy. We used a fourth condition based on duration. A state needed to be at least 100 ms to be defined as a state. If it was shorter, the time bins were incorporated in the previous state.

State were defined with a 5 ms precision and used for coincidence analysis (Mukovski et al., 2007). Briefly, the coincidence index is the ratio of the number of time bins when sites X and Y are in a state Z and the number of time bins when site X is in state Z. This measure is sensible to permutations, that is the ratio for X-Y is different than the ratio Y-X. We calculated the coincidence for the active and the silent states for all sites and because the proportion of both states is different, we calculated a

pondered coincidence index for the slow oscillation. This pondered index is the sum of the coincidence indexes each multiplied by the fraction of time spent in active or silent state.

The propagation of state transitions was computed using two different approaches. The first one is based on the sigmoid fit of the slow wave, either from the depth-negativity to the depth-positivity (silent state onset) or the other way around (active state onset). The timing of onset was defined at half-amplitude of the sigmoid curve. This was calculated for every site. For each transition, an averaged onset was obtained from all sites and individual delays to the averaged onset were calculated. Data are presented as boxplot where the box is delimited by the first and third quartiles and the central line is the median. The whiskers limits are the minimal and maximal values. The second approach, intended to bridge propagation data to coincidence analysis, was based on the onset/offset of fast rhythms at transitions (respectively active and silent states. The timing of a transition was defined as the crossing of a threshold related to the standard deviation of fast rhythms. These thresholds were those used for the classification of states in the coincidence analysis. An averaged onset was calculated and the delay to this value was obtained for each site.

4.4.4 Statistical tests

Statistical analyses were done in Prism 6 (GraphPad Software, Inc., La Jolla, CA). For comparisons of groups, Kruskal-Wallis test were used (due to inequality of variances as tested by a Bartlett's test) with post-hoc Dunn's multiple comparisons (adjusted p-value to the number of comparisons made).

4.5 Results

For this study, we used 8 rabbits (2 with intact brain, 3 isolated slab in limbic cortex and 3 isolated slabs in somatomotor cortex) and 8 cats (4 with intact brain and 4 isolated slabs in suprasylvian gyrus). In the intact cortex, we recorded the LFP in the rabbit somatomotor region (n=9 sites), the rabbit region intercalated between the limbic and the visual regions that we presumed associative due to its location (n=7 sites), the cat suprasylvian gyrus (n=16 sites) and the cat somatosensory region (n=8 sites).

4.5.1 Composition of the power spectra

Under ketamine-xylazine anesthesia, the thalamocortical network generates different oscillations. We first assessed the percentage occupied by 3 frequency bands generated in the in the thalamocortical network of both rabbits and cats (Fig. 4.2): slow and delta rhythms (0.3-4Hz), the sigma band (7-

15Hz) and beta-gamma waves (15-45 Hz). The location of electrodes is indicated in figure 2A. Because we used a notch filter in our AC amplifier to remove the frequency generated by the electrical power line distribution, we opted not to analyze frequencies above 45Hz. A 15 seconds epoch of LFP recordings is shown for each region (Fig. 4.2, B-E) and show that the slow (<1 Hz, delta and sigma) as well as fast rhythms (beta-gamma waves) are present in all region. For the example provided, we computed the power spectral density (Fig. 4.2,F) and the proportion of each frequencies band in the 0.3-45 Hz range were extracted as the area under the curve (Fig. 4.2, G-I). Slow and delta oscillations occupied about half of the area under the power spectral function in all species-region except in the cat somatosensory region where the area occupied by slow and delta rhythma was lower. Sigma and beta-gamma waves equivalently occupied the remaining portion of the power spectra. With data from all sites, we tested for significant differences among species-regions for each of the band. The slow and delta rhythms occupied a lesser percentage of the power spectra in the cat somatosensory cortex (Kruskal-Wallis, $p<0.0001$, Fig.2, H). Although the power spectra of slow rhythms appeared smaller for the rabbit somatomotor region, it was compensated by a higher level of faster delta waves (black trace in Fig. 4.2, F, in 2-4 Hz range). Although sigma waves were similar for all species-region, fast rhythms (beta-gamma) occupied a larger part of the power spectra for this region in cats (Kruskal-Wallis, $p<0.0001$). Furthermore, the percentage of beta-gamma waves was slightly higher in the cat associative region than in the rabbit somatomotor regions (Dunn's multiple comparison, $p=0.0336$). Aside from these differences, the composition of the power spectrum was similar for the remaining species-region.

4.5.2 Properties of the slow oscillation

Our main interest was the slow oscillation. The active states is characterized by the presence of fast rhyhms whereas the silent state is a period of quiescence in the network. To quantify the properties of the slow oscillation (occurrence and percentage of time spent in active states, duration of active and silent states) in each region, we defined network states (active vs. silent) with the LFP recordings obtained in several sites of each region with an approach based on the mean voltage of the LFP and the standard deviation of the fast rhythms (Fig. 4.1). These properties for each region are summarized in table 4.1. The percentage of time spent in active states and the duration of the active and the silent state were similar for all species-regions ($p=0.8269$ and 0.4681 respectively, Kruskal-Wallis test). The only difference we observed was in the frequency of the slow oscillation that refers to the number of cycles of the slow oscillation; a cycle contains an active and a silent state. It was

only significantly higher in the rabbit somatomotor region than in the cat associative cortex (p=0.0382, Dunn's multiple comparisons test, table 4.1). The rabbit associative region and cat somatosensory cortex appears as an intermediate situation, similar to both the rabbit somatomotor and the cat associative. Although all cortical regions spent the same amount of time in the active state, the recurrent activity might be slightly less stable (shorter duration) in the rabbit somatomotor cortex.

4.5.3 Coherence and synchronization of the slow oscillation

We hypothesized that the higher number of transition in the rabbit somatomotor region was due to a weaker level of recurrent activity. Although this cannot be tested directly, we used the coherence index (Mukhovsky et al , 2007) as a mean to measure it indirectly (Fig. 4.3). Although states were defined in bins of 5 ms for all sites, a state was formally defined as an event lasting at least 100 ms. After we transformed LFP recordings into state rasters (Fig. 4.3, A-B for rabbit and D-E for cat), we computed the coincidence index for the active and silent states between each pair of sites. We used these two indexes to calculate a pondered coincidence index for the slow oscillation (Fig. 4.3, C and F). This pondered index took in consideration the fraction of time spent in each state. Population data for the different species-regions are shown in figure 4.3G. As hypothesized, the coincidence for all conditions was lower for the rabbit somatomotor regions ($p<0.001$, Kruskal-Wallis test and post-hoc Dunn's multiple comparisons). These data show that the somatomotor region in the rabbit has a lower coincidence for all conditions. The cat somatosensory region, on the contrary, displays the highest level of coincidence, or at least, in regards to the occurrence of the silent state. The associative regions of both species and the cat somatosensory cortex were similar in terms of the coincidence index of the slow oscillation.

We extended our analysis to the synchronization of the slow oscillation by measuring the cross-correlation between all sites (Fig. 4.4). Consistent with results of coincidence analysis, the cross-correlation was weaker in the rabbit neocortex (Fig. 4.4, A-C) when compared to the cat associative region (Fig. 4.4, D-F). When we pooled data (Fig. 4.1, G), we found that a weaker correlation within the somatomotor region of the rabbit when compared to associative regions of both rabbit and cat ($p<0.001$, Kruskal-Wallis test with post-hoc Dunn's multiple comparisons). Despite a strong coincidence of the silent state of the cat somatosensory region, the cross-correlation analysis showed that it was less synchronized than in both cat and rabbit associative regions ($p=0.0142$ and $p=0.0104$ respectively, Kruskal-Wallis test with post-hoc Dunn's multiple comparisons). The slow oscillation

within associative regions had a better synchrony than it did in somatosensory ones and it the latter, it was better in cat than in rabbit.

4.5.4 Propagation of the slow oscillation

We next focused on the propagation of active and silent states in the somatosensory and associative cortical regions of both rabbits and cats. In the examples shown in figure 4.5, A-D, we calculated the timing of transition with a sigmoid fit of the slow waves. For each channel, delays to the averaged state onset were calculated (see boxplots in Fig. 4.5, A-D). When compared to the cat associative region (Fig. 4.5, C and D), the propagation was much slower for both state transitions in the rabbit neocortex. Furthermore, the silent state onset was more variable than the active state onset in the rabbit, a situation that is not observed in the cat neocortex.

The approach used above is based on the LFP slow fluctuation. To have comparable grounds with the coincidence analysis (Fig. 4.3) and properties of the slow oscillation (table 4.1), we measure the states transition as the increase (active state) or decrease (silent state) of fast rhythms (Fig. 4.5, E). By using the same thresholds as those used for coincidence analysis, we calculated delays to the averaged onset of the active states and compared it to delays obtained with the sigmoid fits of the slow waves (Fig. 4.5, F). For both measures (fitting of slow waves vs. fast rhythms onset/offset), the relation of all sites to a central value (the averaged onset) remained the same ($p<0.0001$, F-test on the slope of the linear regression). We thus used the latter approach to compare the propagation of the active state (Fig. 4.5, G) and the silent state (Fig. 4.5, H) in the rabbit neocortex and the cat somatosensory and associative neocortical regions. We found that for both states, the propagation was much more variable and slower in the rabbit somatomotor region than in the rabbit associative region or in both regions studied in the cat ($p<0.05$, F-test). The active state onset was more variable in the rabbit associative region than in the cat somatosensory ($F_{7, 6, 0.025}=7.47 > 5.12$) and associative region ($F_{15, 6, 0.025}=6.46 > 3.74$). The variability of states propagation in the cat somatosensory and associative were not statistically different (active state, $F_{7, 15, 0.025}=1.16 < 4.57$; silent state, $F_{15, 7, 0.025}=1.76 < 3.29$)

4.5.5 Isolated neocortical slabs

In the intact brain, the activity within a neocortical region is influenced by other brain structures such as other cortical regions, thalamocortical inputs, the nucleus basalis and ascending projections from the brainstem. To assess the extent of intracortical recurrent activity in a given neocortical region, we isolated neocortical slabs (Kristiansen and Courtois, 1949; Timofeev et al., 2000). In cat, the configuration of circumvolutions makes it practically impossible to isolate a slab in the somatosensory region so we limited ourselves to the associative cortex. In rabbit, the lissencephalic aspect of the brain allowed us to isolate slab in the posterior (associative region) and anterior (somatomotor region) parts of the neocortex. We then recorded the spontaneous activity in these slab. For all neocortical slabs in the cat, we observed spontaneous active states at quite variable frequency (0.25-10 active states/min) and varied with the passage of time. The most significant finding was that every slab in the rabbit associative region (0.5-12 active states/min) was active whereas only one of out of three rabbit somatomotor slab was active. The silent slabs were responsive to electrical stimulation (not shown), indicating it was not a question of viability of the preparation.

We measured the duration of active states in the cat and rabbit associative slabs (Fig. 4.6). In the rabbit slab, the active states were short (330 ± 192 ms, n=318 active states, Fig. 4.6, A and C). This contrasted with the much longer active states in the cat slab (2083 ± 1860 ms, n=285 active states, Fig. 4.6, B and C; $p<0.0001$, Mann-Whitney test). Furthermore, the neocortical network within a cat slab spent more time in the active state (fourfold) than in the rabbit slab (Fig. 4.6, D). The latter measure is dependent on the duration and frequency of active states and shows that the short active states in the rabbit slab are not compensated by a higher frequency. This contrasted with the intact cortex (table 4.1) where the time spent in active states was similar for all species-regions.

We extended our investigation to the intracellular activity in the slab (Fig. 4.7) and found similar results. The intracellular active states were shorter than in cats by a factor of six (Fig. 4.7, B) rather than four for the population (LFP) active states (Fig. 4.6, D), suggesting a lower synchrony among the different neuronal elements in the rabbit slab than in the cat slab. Aside shorter active state durations ($p<0.0001$, Mann-Whitney test), the neurons in the rabbit slab also spent less time in active states ($p=0.0272$, Mann-Whitney test, figure 4.7, D) as was found for LFP recordings.

4.6 Discussion

In this study, we have compared the properties of the slow oscillation, a model of recurrent activity in the thalamocortical network (Rigas and Castro-Alamancos, 2007; Mann et al., 2009; Tahvildari et al., 2012), in the somatosensory/somatomotor and associative regions of the cerebral cortex of rabbits and cats. Using coincidence, cross-correlation and propagation analysis, we have found that the lowest concordance of the slow oscillation was in the somatosensory region of the rabbit neocortex and was maximal in the cat associative neocortical area. Isolated neocortical slab pointed out the weaker level of recurrent activity in the rabbit associative neocortex in comparison to the cat. In the rabbit, the recurrent activity was lower in the somatomotor than in the associative region. We conclude that the synchronization of the slow oscillation increases with the level of brain circumvolution and size, being maximal in the cat and smaller in the rabbit neocortex. Within a given species, it is minimal in primary sensory region and maximal in associative regions, which points to a relation between the hierarchical level of information processing and synchronization of recurrent activity.

4.6.1 Methodological consideration

In this study, we made the assumption that the more posterior sites of recording in the rabbit neocortex was homologuous to the associative region due to its location between the dorsal part of the limbic cortex and the primary visual cortex (Monnier and Gangloff, 1961). The region is lateral to the medial depression and remains, to our knowledge, uncharacterized to this day. In a study on the relation between the thalamus and the cortex in rabbits, cats and monkeys, the part of the cortex we defined as associative was described as an intercalated area between the limbic and visual cortices and was compared as homologous to the suprasylvian and marginal gyri of the cat cerebral cortex (Rose and Woolsey, 1949). In a study revising the cytoarchitectonic parcellation of the rabbit cerebral cortex by automatic scanning procedure, that region was named area occipitalis 3.2 to emphasize the similarity of that cortical region with the rest of occipital ones which are visual (Fleischhauer et al., 1980). The posterior parietal cortex of the cat is related to visual functions (Olson and Lawler, 1987) as it is in rats (Reep et al., 1994). Based on the aforementioned studies, we have considered the posterior region of the rabbit neocortex as an associative region and considered it as homologous of the cat suprasylvian gyrus.

The coincidence index informs on the fraction of time two regions spend at the same time in a given state. This fraction of time is then normalized by the amount of time spent in a state (measured in bins of 5 ms) by the site of interest. Because the network spends less time in the silent state than in the active state (about 20% vs. 80%), smaller differences in coincidence will appear more important for the silent state. This is the reason we used a pondered coincidence index (instead of an averaged index) as it takes into consideration the amount of time spent in a given state. Because the coincidence index does not inform about the synchronization of the periodicity of oscillations, we extended our investigation of the concordance among sites of the slow oscillation with a cross-correlation analysis.

4.6.2 Power spectral composition in the different species-regions

The slow and delta rhythm were combined in this study as no obvious maximum was observed although the delta rhythm tended to be higher in the rabbit somatomotor region. However, slow and delta rhythms form a continuum and there was no reason to study these rhythms separately. This higher power of the delta rhythm may relate to a lower efficacy of the network in the rabbit somatomotor cortex in maintaining longer active state, maybe due to a lower level of recurrent activity. We also observed that a stronger activity in the beta-gamma range accounted for the lower relative power of the slow rhythm in the cat somatosensory cortex. It is still uncertain why fast rhythms are stronger in the cat somatosensory cortex but interneurons within that region may have a higher activity as the activity of interneurons has been associated with the generation of fast rhythms (Bartos et al., 2007). However, to our knowledge, there is no difference reported in the literature about a different density of interneurons across neocortical regions. Finally, there was no difference in the sigma band that contains the spindles oscillation, which suggests that the thalamic contribution to both cat and rabbit is relatively the same. Despite these differences, the overall composition of the power spectrum was comparable among species and regions.

4.6.3 Associative vs. somatosensory

Synchronization of activity can be achieved in three ways: the anatomical divergence of a projecting source, co-occurrence of independent stimuli and oscillatory behavior governed by membrane properties in large ensemble of neurons such as the cerebral cortex (Usrey and Reid, 1999). In the case of network oscillation in the slow and delta range (0.1 to 4 Hz), we propose that the concordance of states (a loose form of synchrony) might also be dependent on intrinsic connectivity

to maintain the recurrent activity (active state) in the neocortex. According to this proposed scenario, a different level of connectivity would translate in a corresponding level of inter-site synchrony. It is expected that the level of connectivity varies across neocortical regions and would be higher in associative (multimodal) vs. somatosensory (unimodal).

Our data indeed revealed that the somatosensory regions generated less coincident states and a lower synchrony of the slow oscillation than associative regions. Also, at least in the rabbit, the somatomotor region could not reliably generate recurrent activity as suggested by experiments in slab. We stress here that the recurrent activity recorded simultaneously in different sites of the somatomotor displayed some coincidence and a certain level of synchronicity. After all, various cortical fields of the somatosensory and motor cortices are interconnected and receives inputs from multimodal areas in monkeys (Jones et al., 1978), cats (Schwark et al., 1992) and even in distantly related marsupials such as the short-tailed gray opossum (Dooley et al., 2013). The question is open whether this interconnectivity and divergence/convergence of afferents contributes to the observed inter-site concordance of active and silent states. It is supported by the higher concordance in the associative parietal cortex, a cortical area known to receive converging afferents from multiple cortical regions.

In the cat, the rostral part of the anterior parietal cortex (area 5a) receives mainly somesthesic and motor afferents whereas the caudal part (area 5b) receives visual inputs as well as motor inputs (Avendaño et al., 1988). The posterior parietal cortex (area 7) receives essentially inputs from visual cortices but also from motor area 6 (Olson and Lawler, 1987). Both anterior and posterior parts of the parietal cortex receive afferents from the cingulate and retrosplenial cortices (Olson and Lawler, 1987; Avendaño et al., 1988). As we could not find similar anatomical studies in the rabbit neocortex, we must rely on studies in rodents, the sister order of the lagomorphs. In the rat, the posterior parietal cortex which is located in-between the somatosensory, visual and retroplenial cortices (as in rabbits) receive afferents from somesthesic, visual, auditory, frontal and limbic regions of the cerebral cortex (Reep et al., 1994), making this region a multimodal or associative region homologous to the parietal associative region of carnivores (Olson and Lawler, 1987; Avendaño et al., 1988). Although unconfirmed, the rat posterior parietal cortex is probably homologous to the region we identified as associative in rabbits. At least, our measures of coincidence and synchrony suggest it is functionally akin to the parietal associative cortex of the cat. The associative region of the cat and the rabbit only

differ in regards of the propagation of states and the duration of recurrent activity in the isolated neocortical slab. We propose that the measure of coincidence, synchronization and propagation of the states of the slow oscillation be used as an index to characterize the level of recurrent activity in different cortical regions.

4.6.4 Rabbit vs. cat

For the intact thalamocortical system, cat shows a higher level of coincidence and synchrony than in rabbit. The propagation of state transitions was also faster in the cat. Regarding the contribution of the intracortical connectivity (isolated neocortical slab), there was a stronger recurrent activity in the cat. Cats have a convoluted brain whereas rabbits have relatively lissencephalic one with shallow depressions instead of clearly defined sulci and gyri. Such higher degree of convolution is associated with a larger cortical surface that implies more cortical neurons. Furthermore, a hypothesis regarding the driving force of gyrification suggests it may be associated with the tension generated by a larger amount of tangential corticocortical axons than radial subcortical afferents/efferents axons [reviewed by (Zilles et al., 2013)]. According to this hypothesis, it would be expected to have more intracortical connections in the more gyrified cortex of the cat and that would explain the higher concordance and synchronization of the slow oscillation as well as a stronger recurrent activity in the slab than in the almost lissencephalic cerebral cortex of the rabbit.

Behaviorally, the cat is a carnivore which relies on hunting to survive whereas the rabbit is a herbivore passively foraging for its food. It is rather intuitive that hunting requires visuomotor coordination and lesions to the parietal associative cortex has shown that this neocortical region is involved in this cognitive task (Batuev et al., 1983).Although our data cannot directly link functionally the coincidence, synchrony and speed of propagation of activity within different regions of the cerebral cortex with behavioral outcome, we propose that these measures could be used as an index of intracortical connectivity.

4.6.5 Concluding remarks

We have observed a gradient of concordance of the slow oscillation from lowest in rabbit somatomotor cortex to highest in the cat associative cortex. The cat somatosensory and rabbit associative appears as intermediate. We interpreted our data under the hypothesis that for a given species, associative regions have a more developed substrate for concordant recurrent activity than

somatosensory regions. We also propose that the development of the neocortex is accompanied by increasing intracortical connectivity evidenced by a more concordant recurrent activity within a cortical region.

The slow oscillation is a characteristic feature of the EEG in mammals and birds (Rattenborg, 2006) but the extent of its synchronization within a region differs between species and areas. We propose that cortical region with more connectivity reflects the phylogenetic development of the neocortical regions. This connectivity gives the substrate to generate a recurrent activity forming the slow oscillation. The sleep slow oscillation correlates with synaptic plasticity (Steriade and Timofeev, 2003; Chauvette et al., 2012). According to the proposed role of the slow oscillation in memory consolidation (Maquet, 2001; Diekelmann and Born, 2010; Rasch and Born, 2013), it is expected that more developed neocortex allows more learning and thus requires a more strongly correlated slow oscillation. Our use of concordance measures offer an interesting avenue to explore further the topic of the slow oscillation and the memory consolidation.

4.7 Literature cited

Achermann P, Borbely AA (1997) Low-frequency (<1 Hz) oscillations in the human sleep electroencephalogram. Neuroscience 81:213-222.

Avendaño C, Rausell E, Perez-Aguilar D, Isorna S (1988) Organization of the association cortical afferent connections of area 5: a retrograde tracer study in the cat. J Comp Neurol 278:1-33.

Batuev AS, Cherenkova LV, Yunatov YA (1983) Association brain systems and visually guided movements in the cat. Physiol Behav 31:29-38.

Blake H, Gerard RW (1937) Brain potentials during sleep. Am J Physiol 119:692-703.

Chauvette S, Seigneur J, Timofeev I (2012) Sleep oscillations in the thalamocortical system induce long-term neuronal plasticity. Neuron 75:1105-1113.

Chauvette S, Crochet S, Volgushev M, Timofeev I (2011) Properties of slow oscillation during slow-wave sleep and anesthesia in cats. J Neurosci 31:14998-15008.

Contreras D, Steriade M (1995) Cellular basis of EEG slow rhythms: a study of dynamic corticothalamic relationships. J Neurosci 15:604-622.

Diekelmann S, Born J (2010) The memory function of sleep. Nat Rev Neurosci 11:114-126.

Dooley JC, Franca JG, Seelke AMH, Cooke DF, Krubitzer LA (2013) A connection to the past: Monodelphis domestica provides insight into the organization and connectivity of the brains of early mammals. J Comp Neurol 521:3877-3897.

Fleischhauer K, Zilles K, Schleicher A (1980) A revised cytoarchitectonic map of the neocortex of the rabbit (Oryctolagus cuniculus). Anat Embryol (Berl) 161:121-143.

Grenier F, Timofeev I, Steriade M (2001) Focal synchronization of ripples (80-200 Hz) in neocortex and their neuronal correlates. J Neurophysiol 86:1884-1898.

Haider B, Duque A, Hasenstaub AR, McCormick DA (2006) Neocortical network activity in vivo is generated through a dynamic balance of excitation and inhibition. J Neurosci 26:4535-4545.
Jones EG, Coulter JD, Hendry SHC (1978) Intracortical connectivity of architectonic fields in the somatic sensory, motor and parietal cortex of monkeys. J Comp Neurol 181:291-347.
Kristiansen K, Courtois G (1949) Rhythmic electrical activity from isolated cerebral cortex. Electroencephalogr Clin Neurophysiol 1:265-272.
Mann EO, Kohl MM, Paulsen O (2009) Distinct roles of GABA(A) and GABA(B) receptors in balancing and terminating persistent cortical activity. J Neurosci 29:7513-7518.
Maquet P (2001) The role of sleep in learning and memory. Science 294:1048-1052.
Molle M, Marshall L, Gais S, Born J (2002) Grouping of spindle activity during slow oscillations in human non-rapid eye movement sleep. J Neurosci 22:10941-10947.
Monnier M, Gangloff H (1961) Rabbit brain research volume I: atlas for stereotaxic brain reseach. Amsterdam - London - New York - Princeton: Elsevier Publishing Company.
Mukovski M, Chauvette S, Timofeev I, Volgushev M (2007) Detection of active and silent states in neocortical neurons from the field potential signal during slow-wave sleep. Cereb Cortex 17:400-414.
Olson CR, Lawler K (1987) Cortical and subcortical afferent connections of a posterior division of feline area 7 (Area 7p). J Comp Neurol 259:13-30.
Rasch B, Born J (2013) About sleep's role in memory. Physiological Reviews 93:681-766.
Rattenborg NC (2006) Evolution of slow-wave sleep and palliopallial connectivity in mammals and birds: a hypothesis. Brain Res Bull 69:20-29.
Reep RL, Chandler HC, King V, Corwin JV (1994) Rat posterior parietal cortex: topography of corticocortical and thalamic connections. Exp Brain Res 100:67-84.
Rigas P, Castro-Alamancos MA (2007) Thalamocortical Up states: differential effects of intrinsic and extrinsic cortical inputs on persistent activity. J Neurosci 27:4261-4272.
Rose JE, Woolsey CN (1949) Organization of the mammalian thalamus and its relationships to the cerebral cortex. Electroencephalogr Clin Neurophysiol 1:391-404.
Sanchez-Vives MV, McCormick DA (2000) Cellular and network mechanisms of rhythmic recurrent activity in neocortex. Nat Neurosci 3:1027-1034.
Schwark HD, Esteky H, Jones EG (1992) Corticocortical connections of cat primary somatosensory cortex. Exp Brain Res 91:425-434.
Sharma AV, Wolansky T, Dickson CT (2010) A comparison of sleeplike slow oscillations in the hippocampus under ketamine and urethane anesthesia. J Neurophysiol 104:932-939.
Steriade M, Timofeev I (2003) Neuronal plasticity in thalamocortical networks during sleep and waking oscillations. Neuron 37:563-576.
Steriade M, Nunez A, Amzica F (1993a) Intracellular analysis of relations between the slow (< 1 Hz) neocortical oscillation and other sleep rhythms of the electroencephalogram. J Neurosci 13:3266-3283.
Steriade M, Nunez A, Amzica F (1993b) A novel slow (< 1 Hz) oscillation of neocortical neurons in vivo: depolarizing and hyperpolarizing components. J Neurosci 13:3252-3265.
Steriade M, Timofeev I, Grenier F (2001) Natural waking and sleep states: a view from inside neocortical neurons. J Neurophysiol 85:1969-1985.
Steriade M, Contreras D, Curro Dossi R, Nunez A (1993c) The slow (< 1 Hz) oscillation in reticular thalamic and thalamocortical neurons: scenario of sleep rhythm generation in interacting thalamic and neocortical networks. J Neurosci 13:3284-3299.

Tahvildari B, Wolfel M, Duque A, McCormick DA (2012) Selective functional interactions between excitatory and inhibitory cortical neurons and differential contribution to persistent activity of the slow oscillation. J Neurosci 32:12165-12179.
Timofeev I, Grenier F, Bazhenov M, Sejnowski TJ, Steriade M (2000) Origin of slow cortical oscillations in deafferented cortical slabs. Cereb Cortex 10:1185-1199.
Usrey WM, Reid RC (1999) Synchronous activity in the visual system. Annu Rev Physiol 61:435-456.
Zilles K, Palomero-Gallagher N, Amunts K (2013) Development of cortical folding during evolution and ontogeny. Trends Neurosci 36:275-284.

4.8 Figures

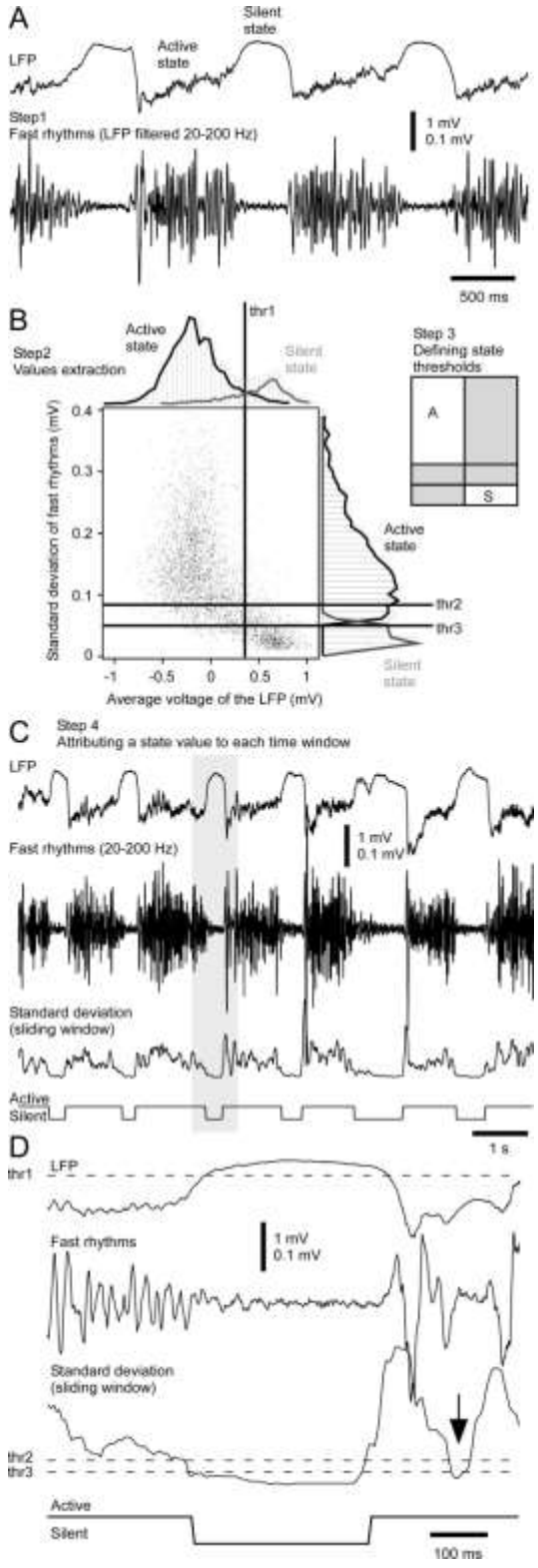

Figure 4.1 Defining state in the LFP recording.

(A) Step 1: LFP (top trace) is filtered for fast (20-200 Hz) rhythms. (B) Step 2: values for mean voltage of the LFP (x-axis and horizontal histogram) and standard deviation of fast rhythms (y-axis and vertical histogram) are extracted in time bins of 50 ms. Step 3: Values for each time bin were plotted to identify two clusters representing the active and silent states. A cutoff value for standard deviation is used to split both values into an active and a silent distribution. The first threshold (thr1) is the voltage at the intersection of both the active and silent state distributions. The second threshold (thr2) is related to the active states onset and the third threshold (thr3) to the silent state onset. The use of three threshold created six zones: A and S are unequivocal for active and silent state respectively and grey regions are transitions or aborted states belonging to the state of the previous time bin (C) Step 4: A state value is assigned to each bin according to thresholds defined in step 3. Traces from top to bottom are the LFP, the filtered trace for fast rhythms (20-200 Hz), the standard deviation of the fast rhythms (time bin of 50 ms, sliding step of 5 ms) and a binary for the bin state. Traces underlined in grey in (D) to indicate the thresholds on their respective traces. The arrow points to an example of an aborted state corresponding to a grey zone in B.

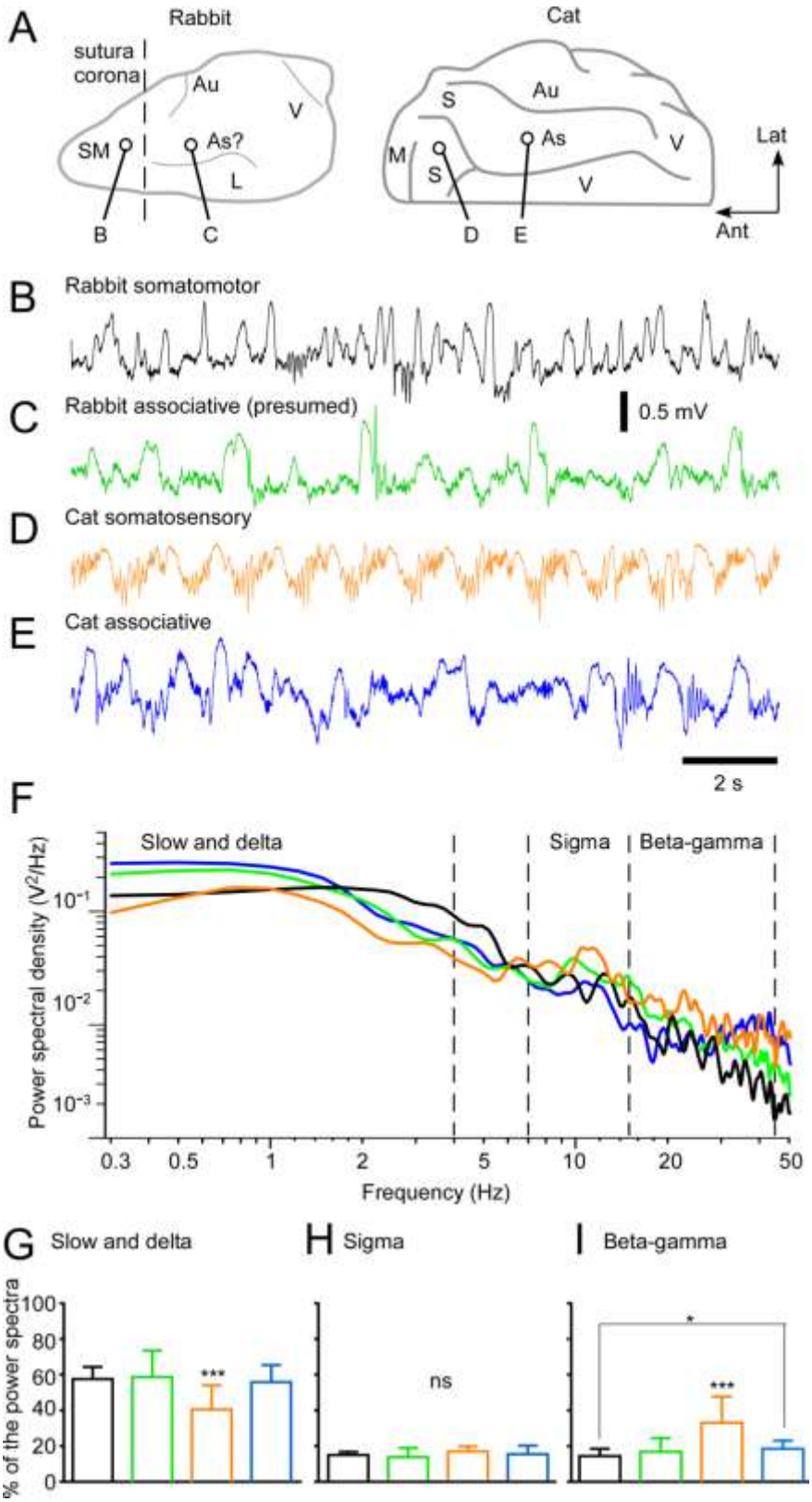

Figure 4.2 Proportion of frequency bands characteristic of ketamine-xylazine anesthesia.

(A) Schematic representation of the rabbit (left) and cat (right) cortical surface. Circles represent the approximative sites of LFP recording. Note that brains are not scaled for the sake of clarity. Segments of 15 seconds of LFP recordings showing cortical rhythms under ketamine-xylazine anesthesia in the (B) rabbit somatomotor region, (C) rabbit presumed associative region, (D) cat somatosensory region and (E) cat associative region. (F) Power spectral density of segments in B-E. Lines are color-coded to match their respective traces. Population data shown as bar plots of the percentages (average and standard deviation) occupied by (G) slow and delta (0.3-4Hz), (H) sigma (7-15 Hz) and (I) beta-gamma (15-45 Hz) rhythms. Rabbit somatomotor (n=9 sites), rabbit associative (n=7 sites), cat somatosensory (n=8 sites) and cat associative (n=16sites). Statistical significance tested with a Kruskal-Wallis test with post-hoc Dunn's multiple comparison: ***, $p<0.001$; n.s. $p>0.05$. Cortical regions: As, associative; Au, auditory; L; limbic; S, somatosensory; SM, somatomotor; V, visual.

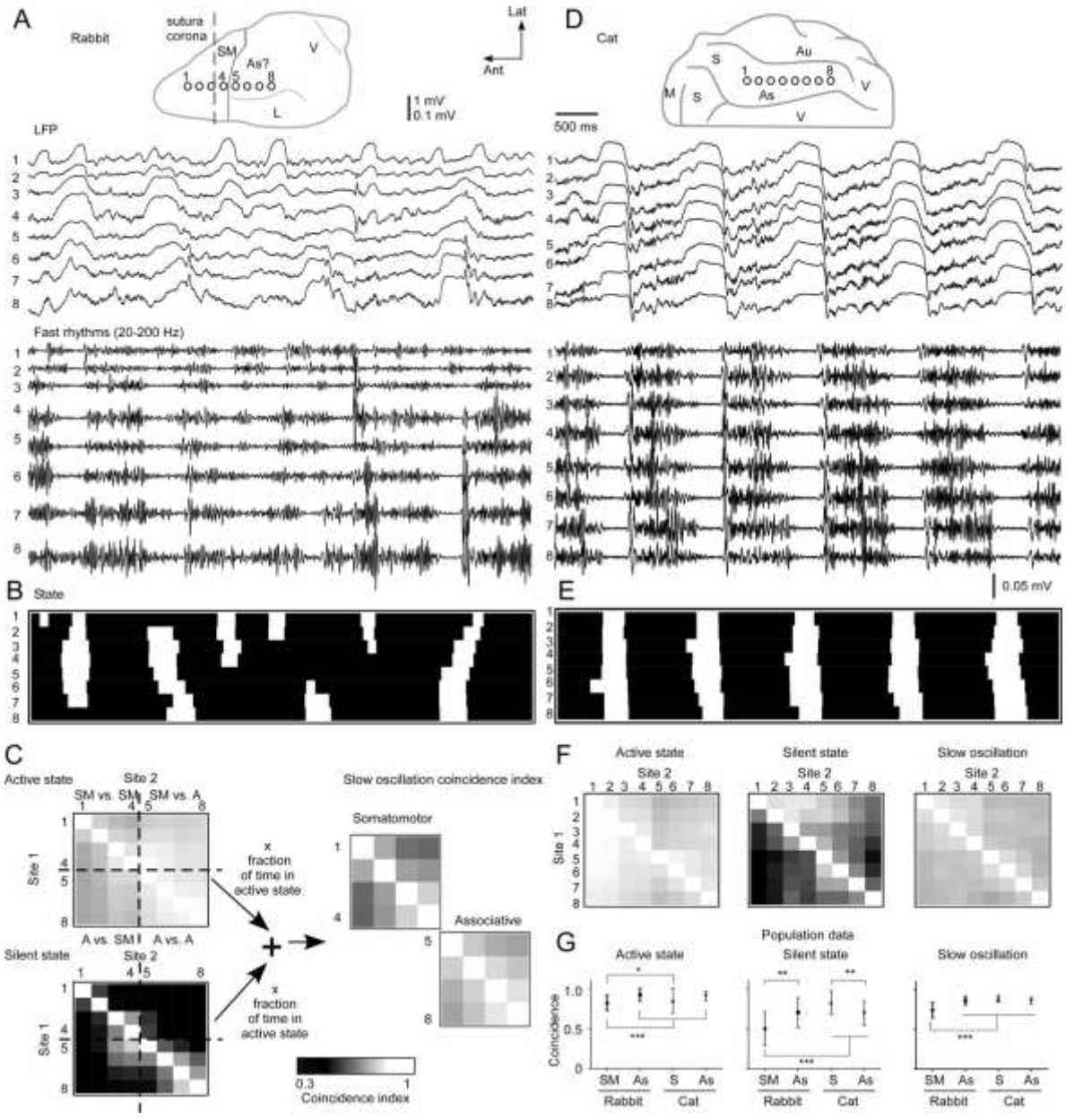

Figure 4.3 Spatiotemporal coincidence of the slow oscillation

(A) Schema at the top illustrates position of electrodes in the cerebral cortex of the rabbit. Electrodes 1-4 are in the somatomotor region and electrodes 5-8 in the presumed associative region. A six seconds segment of multisite LFP recordings at the corresponding sites are shown in the middle part. Traces filtered for fast rhythms are shown below. (B) Raster graph of the state in bins of 5 ms for all sites and corresponding to the filtered traces in (A). White denotes a silent state and black an active state. (C) Grayscale-coded matrix of coincidence index in the active and silent states for the animal shown in A and B. Dashed lines delimitate

regions of the rabbit cerebral cortex. A third matrix (left) is generated by the pondered sum of the active and silent matrices. The pondering is obtained by multiplying the coincidence values by the fraction of the time in the corresponding state. As such, a coincidence index for interareal coincidence was not calculated. (D) Top, schema of electrodes positions in the cat associative cortex. Middle, six seconds segments of multisite LFP recordings at the corresponding sites. Bottom, traces were filtered for fast rhythms. (E) Raster graph of the state of the slow oscillation in bins of 5 ms for the example shown in D. (F) Coincidence matrices for the active state, the silent state and the slow oscillation (pondered coincidence index). (G) Population data of coincidence index (mean ± standard deviation) during the active state, the silent state and the slow oscillation in different species-regions. Statistical significance tested by Kruskal-Wallis and post-hoc Dunn's multiple comparison: * $p<0.05$, ** $p<0.01$, *** $p<0.001$. Cortical regions: As, associative; Au, auditory; L; limbic; S: somatosensory; SM, somatomotor; V, visual.

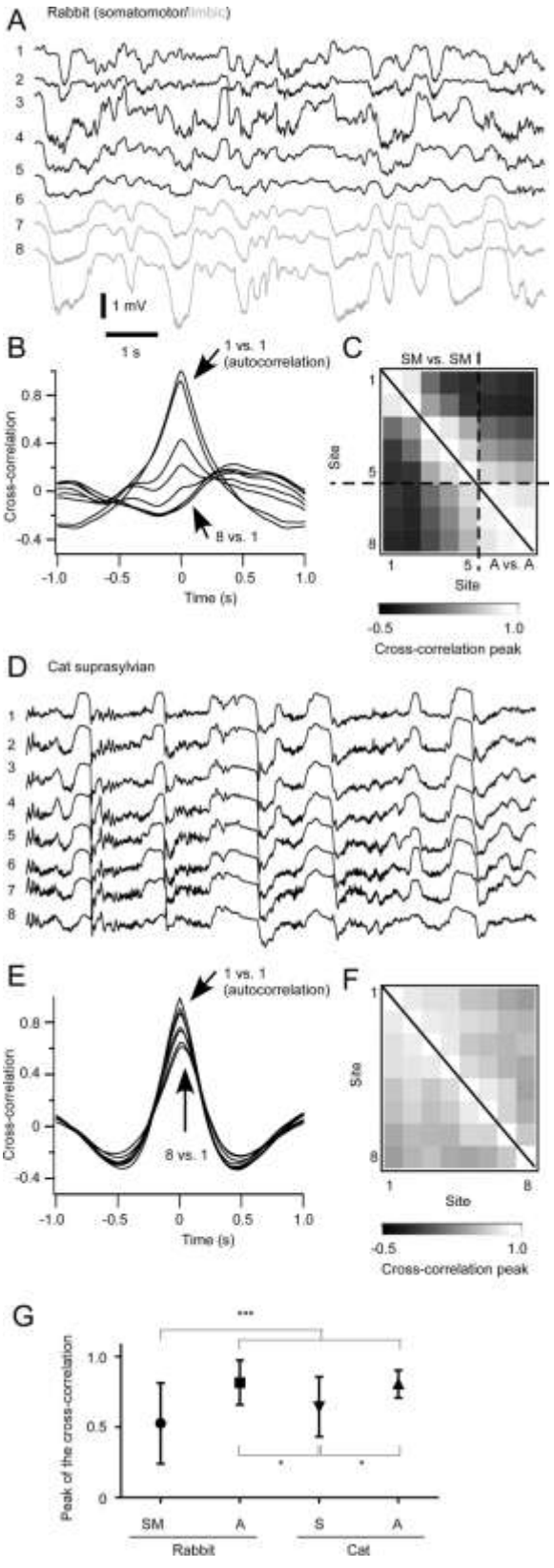

Figure 4.4 Cross-correlation of the slow oscillation

(A) A ten seconds segment of multisite LFP recordings in the somatomotor (electrode 1-5) and presumed associative (electrode 6-8) regions of the rabbit neocortex. (B) An example of cross-correlation functions between site 1 and all sites (including site 1 for autocorrelation). Note the decrease in cross-correlation with distance. (C) Grayscale-coded matrix of the cross-correlation peaks for all comparisons from the animal shown in A and B. Note that the matrix is symmetrical. Filled line indicates autocorrelation values. Dashed lines indicates intra-areal crosscorrelations. (D) A ten seconds segment of multisite LFP recordings in the associative region of the cat neocortex. (E) An example of cross-correlation functions for the example in D. (F) Grayscale-coded matrix of the cross-correlation peaks for all comparisons from the animal shown in D and E. (G) Population data of cross-correlation peaks (mean ± standard deviation). Statistical significance tested by Kruskal-Wallis and post-hoc Dunn's multiple comparison: * $p<0.05$, *** $p<0.001$. Cortical regions: A, associative; S: somatosensory; SM, somatomotor.

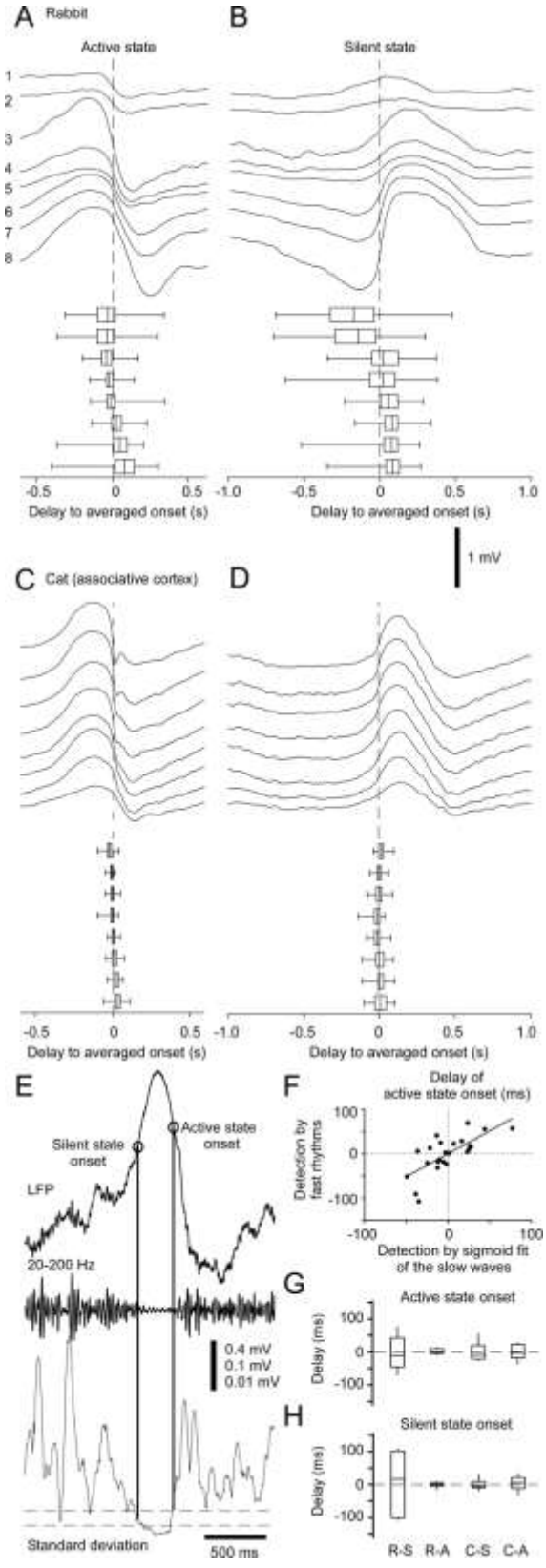

Figure 4.5 Propagation of states transitions.

(A) LFP averages of the transitions to the active state (n=122) in the rabbit neocortex. Electrodes 1-5 are in the somatomotor regions and electrodes 6-8 in the associative region. Transitions were triggered on the voltage zero-crossing of electrode 8. The timing of the active state onset was calculated by the half-amplitude of the sigmoid fit at the transition. Data are presented as boxplot (whiskers contain minimum and maximum) of the delay to the averaged onset of each transition. (B) Wave-triggered averages of the silent state onset and corresponding boxplots of delay to the averaged onset. Note that the scale is the same as in A but the range is wider. Results from the cat associative neocortex are presented in a similar way for the onset of the (C) active state and (D) the silent state. (E) Alternative approach to measure the onset of state transitions based on the onset or offset of fast rhythms (20-200 Hz). The crossing of thresholds (one for each state) of the fast rhythms standard deviation define the onset of a state. (F) Plots of the delays to the averaged onset of the active state obtained by the fast rhythms method vs. those obtained with the sigmoid fit of the slow waves. Data are from two cats and one rabbit. Significance of the regression: $p<0.0001$ ($F=23.16$ Fisher-test). Population data from the rabbit somatomotor (R-S) and associative (R-A) cortical regions and from the cat somatosensory (C-S) and associative (C-A) cortical regions for the onset of (G) the active state and (H) the silent state.

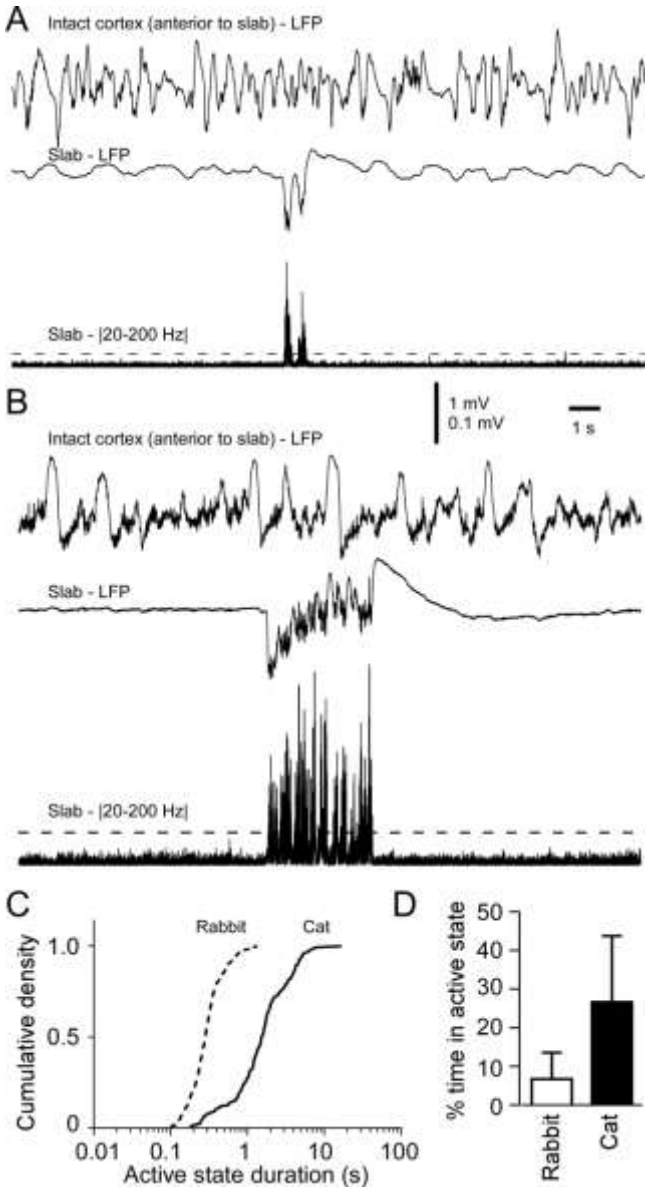

Figure 4.6 Active state duration in LFP recordings in the isolated neocortical slab.

(A) An example of LFP recordings in an isolated slab in the associative region of the rabbit neocortex. From top to bottom, LFP in the intact cortex anterior to the slab, LFP in the slab and absolute value of the trace filtered for fast rhythms (20-200 Hz). Dashed line is the threshold to define an active state. The threshold is 10x the standard deviation of the filtered trace. (B) An example of an active state in the cat isolated neocortical slab. The time and amplitude scale bars and order of traces are the same as in A. (C) Cumulative density function of the active state duration in rabbit and cat. (D) Percentage of time spent in active state in the rabbit and cat slabs.

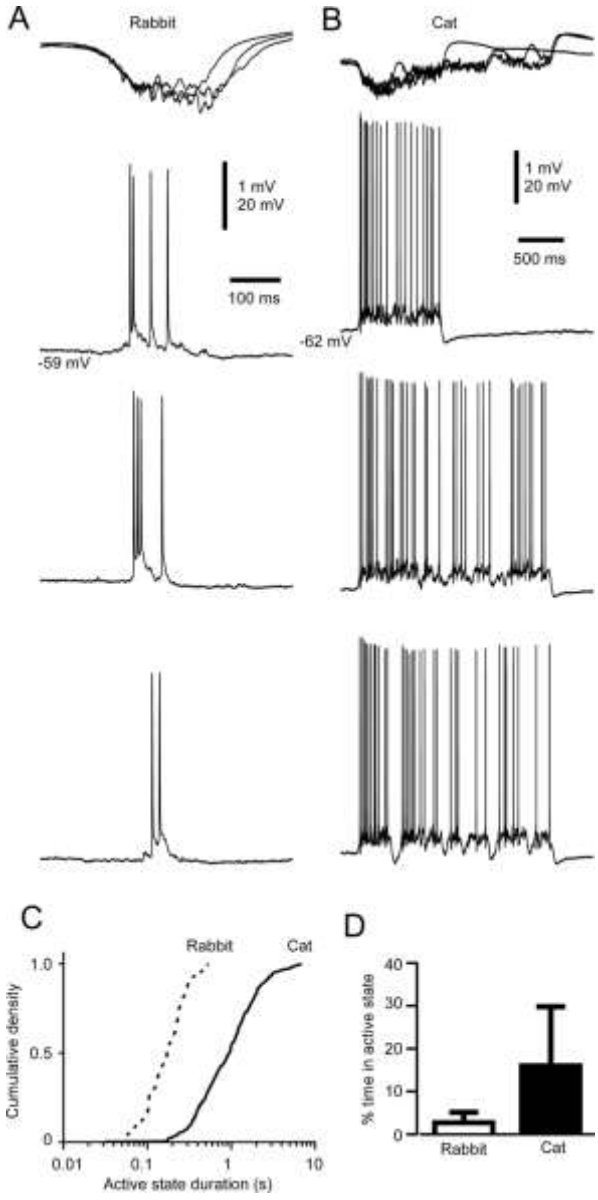

Figure 4.7 Active state duration in intracellular recordings in slabs

(A) Three examples of intracellular recordings showing representative active states in the rabbit slab. Top, superimposed LFP traces of the corresponding events. (B) Three examples of intracellular recordings showing representative active states in the cat slab. Note that the time scale bar is compressed fivefold. (C) Cumulative density functions of the active state duration in the rabbit and cat slab. (D) Percentage of time in intracellular recordings in the rabbit and the cat slab.

4.9 Table

Table 4.1 Properties of the slow oscillation in different species-regions

	Rabbit Somatomotor	Rabbit Associative	Cat Somatosensory	Cat Associative
Number of sites	9	7	8	16
Active state occurrence (min^{-1})	48.3 ± 6.7	37.2 ± 18.0	45.4 ± 9.1	37.7 ± 5.7
Active state duration (ms)	942 ± 198	1583 ± 1034	1049 ± 300	1279 ± 350
Proportion of time in active state (%)	74.1 ± 8.5	71.8 ± 22.5	75.5 ± 8.2	77.5 ± 8.3
Silent state duration (ms)	317 ± 92	393 ± 162	315 ± 59	349 ± 110

Active state occurrence, duration, proportion of time and silent state duration are presented as mean ± standard deviation. Crosscorrelation peak, active and silent states coincidences and delay to the average of the active/silent state onset are presented as ranges. Value in ( ) is the variance of delays to the averaged onset in ms^2.

Chapter 5 General discussion

5.0 Summary of the thesis

In this thesis, we studied several network properties of the slow oscillation, the major rhythm of the slow wave sleep. We have asked the question of the thalamic contribution to the normal pattern of the slow oscillation and brought forward evidences demonstrating that the thalamus is necessary to propagate the active states and synchronize the silent state onset within a neocortical area. In assessing the place of the thalamus in generating the slow oscillation, we have also found that the neocortical network could recover this slow oscillatory behavior. This suggested that slow oscillation was an intrinsic property of the neocortex and that it was homeostatically regulated.

As the active states occupied about 80% of the time during the slow oscillation (Chauvette et al., 2011), it can be inferred that the neocortical network is biased toward the active state. This raises the question of what causes the neocortical network to go silent. To address this question, we tested the possible involvement of chloride-mediated inhibition in inducing the onset of the silent state and found that only a small fraction of excitatory neurons are inhibited prior to the transition. We concluded that the active state maintained by a tight balance of excitation and inhibition.

The physical substrate of this balance of excitation and inhibition is the connectivity of the thalamocortical network. And if the level of connectivity differs from one cortical region to another and from one species to another, would we observe a difference in the concordance of states among different neocortical sites of a given region in a given species? We indeed found such evidences and propose that the slow oscillation is generated by recurrent activity and as such, could be subject to natural selection and thus evolve.

In the following sections, we discuss these findings under the hypothesis that the slow oscillation is an intrinsic property, or a default state, of the neocortex and by extension, the thalamus. We also discuss the limitations and perspectives related to our studies.

5.1 The roles of the thalamus

5.1.1 The rightful place of the thalamus

The place of the thalamus in the normal patterning of the slow oscillation has been debated over the last twenty years [reviewed in (Crunelli and Hughes, 2010)]. The survival of the slow oscillation after thalamectomy (Steriade et al., 1993a) or its absence in the thalamus after decortication (Timofeev and Steriade, 1996) suggested that the cerebral cortex was sufficient for the expression of the slow oscillation. These conclusions were further supported by the persistence of active states generation in the isolated neocortical slab (Timofeev et al., 2000b) and cortical slices bathing in physiological ionic concentrations (Sanchez-Vives and McCormick, 2000). However, the pharmacological activation of corticothalamic synapses could induce a slow oscillation in thalamic slices (Hughes et al., 2002). Thalamocortical neurons are oscillating neuron due to their intrinsic properties including the expression of I_T and I_H (McCormick and Pape, 1990). Some studies also pointed out that enhancing inhibition in the thalamus (Doi et al., 2007) or severing thalamocortical afferents to the neocortex (Rigas and Castro-Alamancos, 2007) affected the slow oscillation *in vivo*. Nevertheless, no studies addressed the extent of the thalamic impact on the cortically generated slow oscillation.

In our study of the impact of thalamic inactivation, we used multisite recording in the cortex prior and after the inactivation of thalamocortical afferents and found an unprecedentedly reported contribution of the thalamus to the cortical slow oscillation. The thalamus was essential for the propagation and synchronization of the slow oscillation across cortical sites. In its absence, few active states persisted and were of much shorter durations. The locally generated active state also lacked local synchronization. The thalamus is thus necessary for propagating and maintaining the active states and even contributes to the synchronous activity of neocortical cells. These findings are most interestingly mirrored by the role of the neocortex in the long range synchronization of the thalamically generated spindles oscillations (Contreras et al., 1996b; Destexhe et al., 1998), showing that the full expression of the slow oscillation emerges as a dialogue between the neocortex and the thalamus.

In the normal thalamocortical network, we conclude that the neocortical network and the thalamus interact to generate spatially coherent oscillations in the slow (<1 Hz) and delta (1-4 Hz) and the spindles (7-15 Hz) bands. The difference lies in the different levels of recurrent connectivity. Whereas the neocortex contained dense recurrent connections within and among layers as well as between

columns, regions and areas, the thalamus virtually lacks local excitatory connectivity. What it lacks in local connectivity, the thalamus seems to make up for with converging inputs from the neocortex and diverging outputs to the neocortex. In other words, in the intact thalamocortical network, the thalamus could be viewed as a hub that informs a cortical region about what another one is doing. During slow wave sleep or anesthesia, the cerebral cortex is partly disconnected from the outside world by the thalamic gating. Our data on QX-314 injections in the thalamus suggest that in these conditions the burst firing of thalamocortical neurons may have a deep impact on the activity within the cerebral cortex. During wakefulness, the thalamus would have less impact due to its tonic firing clashing on a background of cortical activity.

5.1.2 Technical limitations

Our only concern was that the pharmacological agents used to inactivate the thalamus (QX-314) might have leaked on the cortex even though the needle passed through another gyrus. Also, the action potentials of intracellularly recorded neurons were normal and would have been affected by QX-314 as it is a use-dependent blocker of sodium and low threshold calcium channels. We nevertheless verified that possibility by inserting a needle in the cortex while recording the LFP in multiple sites. We then injected a tiny amount of the QX-314 solution (1/20 of the volume injected in a thalamic site) to mimic a leak. We found that such a small amount had a locally restricted effect and abolished completely the activity in restricted cortical area. Although we cannot rule out a possible leak, it seems unlikely it happened during our experiment as the effect of leak would be restricted next to the trajectory of the needle, which was through another gyrus anyway.

Another question remaining unresolved is why the active states in the neocortex following thalamic inactivation are shorter in duration than those in the slab. Several hypotheses could be investigated. It is also possible that inhibition is biased after thalamic inactivation and ends rapidly the locally generated active states. It might also be found that excitation is biased and that vigorous firing at the onset of the active states depletes the extracellular calcium to a point where the failure rate would be very high. On the other hand, the slab could be a very excitable preparation that favors longer active states. The severing of the nervous tissue and blood vessels is bound to modify the ionic concentration of the extracellular space or release glutamate in the extracellular space, thus increasing neuronal excitability. The modification of the pH in the extracellular space would modify

the gap junctional coupling but the contribution of electrical coupling to the maintenance of the active state is purely speculative.

5.1.3 Future studies

Further studies should address the impact of different nuclei as our experiments were limited to the interaction of the suprasylvian gyrus (an associative area) and the lateral posterior nucleus. A preliminary experiment involving the inactivation of the ventrobasal nucleus showed it had no impact on the slow oscillation in the somatosensory cortex. The lower contribution of thalamic core nuclei in propagating and synchronizing the cortical slow oscillation was predicted by modeling experiments. However, detailed investigation *in vivo* could confirm the relative contribution of the core and matrix nuclei to the normal expression of the slow oscillation in the cerebral cortex.

5.2 Is the slow oscillation the default state of the neocortex

5.2.1 Recovery of the slow oscillation

The impairment of the slow oscillation following the thalamic inactivation led to another discovery. With the passage of time, the cortical slow oscillation can recover. It was a partial recovery in the course of the 36 hours following the inactivation of the LP nucleus and complete recovery in the isolated neocortical slab after a period of 2 weeks. Because the recovery depended on the passage of time, we hypothesized that homeostatic mechanism (s) acting on intracortical synaptic transmission were at work and we used a model to test that scenario. Homeostatic plasticity has been hypothesized as a mean to maintain a given firing rate in a network (Turrigiano et al., 1998). Too much activity would lead to downscaling of synaptic transmission whereas too little activity would trigger an up-regulation. In that sense, the slow oscillation observed during slow wave sleep and anesthesia may represent the default state of the cortical network, and by extension, of the entire thalamocortical network. In the absence of inputs to a neocortical network from the thalamus, the recurrent activity during the slow oscillation is greatly impaired but compensatory mechanisms are in place to recover.

Works done in primary culture (Murphy et al., 1992; Wagenaar et al., 2005; Hinard et al., 2012), organotypic slices (Johnson and Buonomano, 2007) as well as in the isolated neocortical slabs and in

the intact cortex partially deafferented of its thalamocortical input (this study) all points to the ability of the neocortical network to recover activity. Altogether, they also taught us that to recover activity, a certain level connectivity is essential and a system will be allowed to recover only to the extent of the preserved connectivity. Only the network contained in the slab and the cortex devoid of functional thalamic afferents can completely recover the slow oscillation with sufficient time. The organotypic slices remain largely biased towards the silent state and as for the primary cortical cultures (Johnson and Buonomano, 2007), the activity of the culture neurons is mainly disorganized with period of burst (more synchronized) occurring at the infraslow frequency (Hinard et al., 2012).

Why would there be mechanisms that maintain the slow oscillation? It may not be maintaining the slow oscillation as such than maintaining activity within the neocortical network. When disconnected from the outside world by a decrease in activity of the activating ascending reticular system or by deep anesthesia, the alternation between the active state and the silent state may be the optimal solution provided by the evolution of the neocortical connectivity. Maybe the slow oscillation is more than an optimal stable solution but well developed mechanism for the memory consolidation. As we learn, we also forget. This simple fact calls for different mechanisms which are fulfilled by long term potentiation as well as long term depression. By grouping fast rhythms in-between periods of synaptic quiescence (the silent state) recurring at a frequency <1 Hz, the slow oscillation appears as the ideal mechanism to do both. In that sense, homeostatic mechanisms may also be in place to insure the persistence of this brain rhythm.

5.2.2 Limitations and future works

Our investigations leave many unanswered question about mechanisms of the recovery. Although we have provided some evidence for an up-regulation of postsynaptic activity, its origin remains unknown. Is the postsynaptic activity due to a lower failure rate, the spontaneous release of neurotransmitters (minis) or by a higher presynaptic firing? If it is related to a higher firing, then is it because of an up regulation of intrinsic properties? It is even possible that all these factors are involved in the recovery of the slow oscillation. To answer those questions, it would be more efficient to perform dual recording in slices after different intervals of time since thalamic inactivation. That way, synaptic efficacy could be measured. Post-fixation experiments could verify if there is an up-regulation of spines density. Quantification of proteins or RNA contents could also put in evidence an increase in transcription and translation of synaptic receptors of voltage-dependent channels. In other

words, the inactivation of the thalamus and the isolation of cortical slab have a strong potential to trigger homeostatic mechanisms and might be considered as a model in the endeavor to better understand this phenomenon *in vivo*.

5.3 The silent state as a synchronous phenomenon

In the course of our experiments, we have investigated potential mechanisms underlying the synchronous onset of the silent states among different cortical sites. We tested the hypothesis of an extracortical contribution in synchronizing distant neocortical sites and we found that the thalamus was sufficient and necessary to explain the level of synchrony observed in the intact brain. These findings are in line with those obtained for the role of the thalamus in the propagation of the active states. As thalamocortical afferents are essential in propagating the active states, they are also important in the silent state onset. In the absence of these inputs, the cortical network can still generate silent states but they are desynchronized among different sites. This indicated that the mechanism(s) to generate a silent state are cortical but in the mean time, are recruited by thalamocortical afferents.

When we recorded multi-unit activity in the thalamus, it was surprising that the increase in firing prior to the silent state was quite moderate. Furthermore, in the majority of sites, we could not evidence such up-regulation. After all, the removal of thalamocortical inputs affected the inter-site synchrony and we expected a more pronounced contribution. Because the increase in firing prior to the silent state onset is not a global phenomenon in the thalamus, it suggests that only a subset of thalamocortical cells contribute to the synchronization of the silent states. The question arises whether the neurons of this subset have different properties than those that do not contribute to the onset of the silent state. Among these properties, we can imagine that the level of divergence or even the sites of termination on cortical neurons could be different. For instance, it might be biased toward inhibitory interneurons. These neurons could also receive a stronger input from corticothalamic cells. It might also be, in the end, that this is a stochastic phenomenon.

We have limited our investigation to the thalamus and we cannot exclude the contribution of another brain region. For instance, the nucleus basalis sends projection directly to the cortex and could be involved in triggering a silent state. However, the variability of the inter-site onset of the silent state was not further increased in the isolated slab which argued against another structure being involved.

5.4 The fragile balance of excitation and inhibition

5.4.1 Chloride-mediated inhibition

The second hypothesis we tested was whether chloride-mediated inhibition was involved in the transition to the silent state. We found that the phenomenon occurs in a relatively small proportion of cell. In some neurons, in was never observed. For those in which we uncovered a contribution of the chloride-mediated inhibition, in happened in less than a third of the time. Furthermore, the inhibition did not occur at the onset but preceded it by 100-300 ms. The inhibition lasted long and ended up in a period of reduction of synaptic activity. These data suggest that the active state is maintained by a tight balance of excitation and inhibition.

If inhibition is biased by transient but stronger thalamic inputs, for example, it will remove a certain proportion of excitatory cells from the pool of active neurons within the cortical network. This removal appears to create a condition where the network cannot escape the transition to the silent state. In that sense, the active and the silent states can be viewed as attractor within the network dynamic. The points of stability remains uncertain but our data suggests that removing 3-6% would be sufficient to cause the network to move into a silent state. Hence, our conclusion that the active state relies on a fragile balance of the excitation and the inhibition. A computational approach based on dynamical equations representing the excitatory and inhibitory drive will likely be the best way to identify the points of stability of this balance.

We have investigated chloride-mediated inhibition by using dual recordings. One pipette was a control (potassium acetate) while the other was the test pipette (potassium chloride). This approach is surely biased toward inhibition acting at the soma or in the proximal dendrites. We cannot rule out the effect of chloride inhibition in distal dendrites or at the spines which would prevent the propagation of local synaptic events to the soma. It is also possible that shunting inhibition plays an important role in preventing synaptic inputs to reach the soma. Finally, $GABA_B$ may also be involved. We have conducted preliminary experiment with QX-314 (which blocks G-protein pathway, a messenger downstream of $GABA_B$ receptors) and could not evidence an impact of altering $GABA_B$ effect. However, these receptors are mainly located distally and it is possible that we did not interfere with it at the soma. Their effect would then be attributable to an action in distal dendrites by preventing EPSP generated in those locations to reach the soma.

5.4.2 Laminar stimulation

In the neocortical slab, we have used electrical stimulations at regular intervals (150 µm) of the cortical depth and found that stimulations in infragranular layers were more efficient in triggering a silent state. These data are in line with a recent optogenetic study in mice where the inhibition of infragranular but not supragranular layers terminated the active states (Beltramo et al., 2013), pointing the importance of the infragranular layers in maintaining the active states. Although useful, the electrical approach we use cannot resolve how is mediated the effect of the electrical stimulation. For instance, does it activates directly the terminals of inhibitory axons or does it act at the soma of interneurons? On the other hand, it could excite pyramidal neurons who would recruit at their turn inhibitory neurons (feedback inhibition). We have indeed provided evidences that the threshold to excite a layer V pyramidal neuron was lower in infragranular layer. This latter hypothesis would suggest that the silent state onset is preceded by an increase in excitation counterbalanced by a strong inhibition. One approach to resolve this question would be to record interneurons intracellularly *in vitro* while performing laminar stimulations.

5.4.3 Future works

The identity of interneurons providing the inhibition is unknown. The most likely candidate is the basket cells innervating the soma of pyramidal neurons. A complementary role of somatostatin interneurons is also possible. These interneurons receive facilitatory inputs from pyramidal neurons which could explain the inhibition of long duration that we have observed in our intracellular recordings. The impact of neurogliaform cells is not to be neglected as they are abundant in the cortex. Finally, chandelier cells inhibit the initial segment of the axon and could prevent the recruitment of excitatory cells that would maintain the active state in the next temporal window of synaptic integration. If one or several other locations of inhibition would be found, this would show that the balance of excitation and inhibition is not as tight or fragile as we conclude in our study. Optogenetic tools to study specific types of interneurons are probably the current best options to identify the contribution of each class of interneurons.

5.5 The evolution of the slow oscillation

5.5.1 Implications of the slow oscillation concordance

One of the first questions we address in this thesis (see section 1.2.1) was whether we would observe different levels of synchrony of the slow oscillation among neocortical regions. We have provided evidences that sites within an associative region (higher-order of information processing) were more synchronous than those of a primary sensory cortex (in our case, the primary somatosensory cortex). Furthermore, we have found differences in intra-areal synchronization between the cat and the rabbit, especially in the somatosensory cortex. The cat has a large and circonvoluted brain in comparison to the relatively lissencephalic cerebral cortex of the rabbit. Among the factors of gyrification are ontogenic ones but also the number of neurons and the intracortical connectivity in the cerebral cortex [recently reviewed by (Zilles et al., 2013)] which would fit with the data we have provided. Indeed, the highest level of coincidence and synchrony in the cat somatosensory cortex and the longer active states in the isolated slab of the cat associative neocortex could be explained by more intracortical connections in the cat than in the rabbit. This hypothesis obviously requires confirmation but would suggest that the synchronization of the slow oscillation emerged and evolved with the development of the connectivity within the thalamocortical network.

5.5.2 Emergence of the slow oscillation

The slow waves in the EEG are reported in mammals and birds but not in reptiles, suggesting that the ability to generate a slow oscillation evolved independently in the these two classes of vertebrates (Rattenborg, 2006). However, it might have also disappeared in reptiles. Mammals and birds have in common a six-layered cortex (the neocortex and neopallium, respectively) in comparison to the reptiles that possess a three-layered cortex homologuous to the hippocampus. The olfactory cortex (a four-layer cortical structure) does not generate a slow oscillation per se but rather sharp waves (Manabe et al., 2011). These sharp waves resembles those seen in the EEG during sleeping behavior in crocodilians (Flanigan Jr et al., 1973) which are most reduced in amplitude and occurrence during sleep in other reptiles such as the iguana (Ayala-Guerrero and Mexicano, 2008). As crocodilians are more closely related to birds than other reptilian groups, it raises the question whether the slow oscillation emerged from the pattern of intracortical connectivity and reached its climax with the six-layered cortex?

5.5.3 Technical limitations

This study was intended as a preliminary work to evaluate the possibility to replace the cat as a model for the study of the slow oscillation with the rabbit. One weakness of this study is by consequence the small sample of rabbits and intracellular recordings. Another part missing is the isolated neocortical slab in the cat somatosensory cortex which is technically impossible given the smaller size of the post-crucian sulcus. Finally, anatomical studies comparable to those done in the rat, cat and primate brain is lacking in the rabbit.

The link between connectivity and inter-site concordance of the slow oscillation remains speculative. Also, is the coincidence and synchrony due to local connectivity or converging afferents from other areas or the thalamus? Data obtained from the isolated neocortical slab demonstrates that there is a contribution from local connectivity but the dominant quiescence of the network activity strongly suggests that long-range afferents are involved in maintaining the recurrent activity (the active state of the slow oscillation) in a neocortical site. Recordings and electrical stimulation in various sites could attempt to answer this question. A simple approach would be to use a different retrograde labeling dye or virus in two sites of a given area and quantify the proportion of similar afferents to these two sites. The anatomical data could then be correlated with electrophysiological measurements of synchronization, coincidence and propagation.

5.5.4 Future works

Future works could investigate the coincidence, synchrony and propagation in more primary sensory cortical regions (visual and auditory cortices) and associative cortical region (prefrontal cortex). Secondary sensory and limbic areas could also be investigated and it would expected that their level of concordance is intermediate with primary sensory and associative regions. Obviously, extending the current work to more mammalian species (primate, other carnivores, rodents) and even in the neopallium of birds which generate a slow oscillation would provide a wealth of information to confirm or refute our hypothesis that the slow oscillation is an intrinsic property of the neocortex/neopallium that depends on the underying connectivity of the thalamocortical network. Finally, extending these investigations to reptilian and amphibian classes could transform our proposed framework into a theory of connectivity and recurrent activity that might explain the emergence and evolution of the thalamocortical slow oscillation.

5.6 Concluding remarks

In this thesis, we have investigated the network properties of the slow oscillation, a brain rhythm of the thalamocortical network present during slow wave sleep and anesthesia. As summarized in figure 5.1, we have demonstrated by removing functional thalamocortical afferents to excitatory cells that the thalamus was essential in propagating the active states (one of the two states of the slow oscillation) in different cortical sites. We have also shown that the active states is maintained by a tight balance of excitation and inhibition and that removing a small portion of the excitatory drive is sufficient to explain the silent state onset (the other state of the slow oscillation). Because the removal of thalamocortical afferents reduced the synchrony of the silent state onset among different cortical sites, we conclude that the excitatory afferents of the thalamus recruit cortical inhibition in the generation of the silent states. These findings revealed the important place of the thalamus in shaping the normal pattern of the slow oscillation. Finally, we have provided evidences that the concordance among different sites of a neocortical region was maximal in associative regions and in large circonvoluted brain and suggested that it depends on the underlying connectivity within the thalamocortical network. We conclude that the slow oscillation is an intrinsic property of the thalamocortical network that emerged from the evolution of its underlying connections.

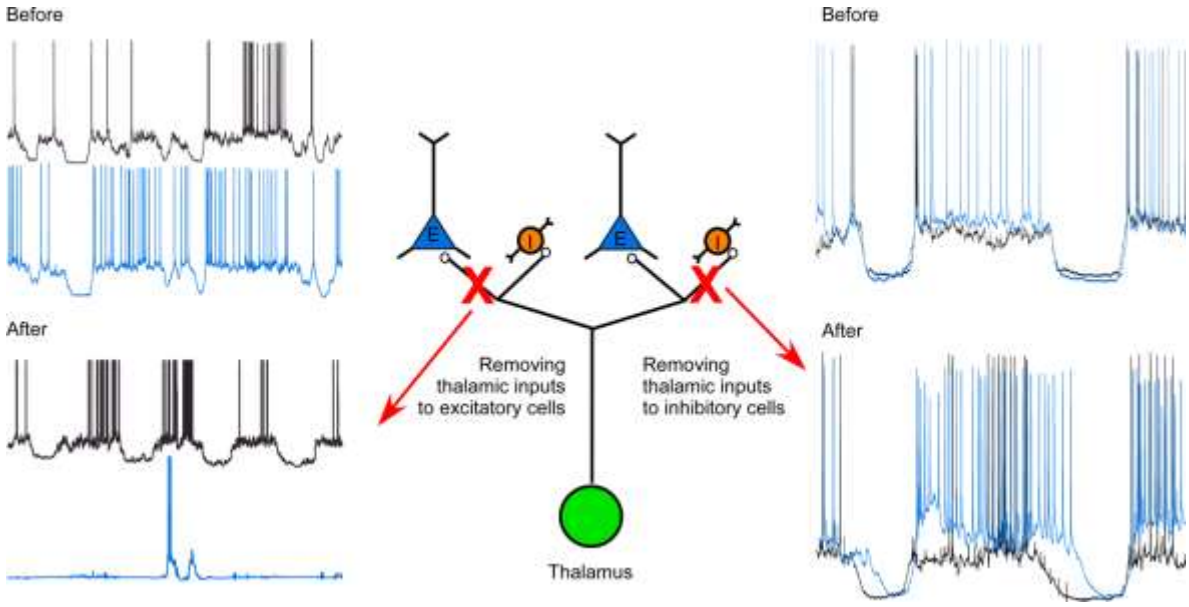

Figure 5.1 Summary of the thalamic contribution to the neocortical slow oscillation

E: excitatory cell; I: inhibitory cell

Bibliography

Abdel-Kader GA (1968) The organization of the cortico-pontine system of the rabbit. J Anat 102:165-181.

Ahmed B, Anderson JC, Douglas RJ, Martin KAC, Nelson JC (1994) Polyneuronal innervation of spiny stellate neurons in cat visual cortex. J Comp Neurol 341:39-49.

Aladjalova NA (1957) Infra-slow rhythmic oscillations of the steady potential of the cerebral cortex. Nature 179:957-959.

Albus K, Wahle P (1994) The topography of tangential inhibitory connections in the postnatally developing and mature striate cortex of the cat. Eur J Neurosci 6:779-792.

Alkire MT, Hudetz AG, Tononi G (2008) Consciousness and anesthesia. Science 322:876-880.

Amargos-Bosch M, Lopez-Gil X, Artigas F, Adell A (2006) Clozapine and olanzapine, but not haloperidol, suppress serotonin efflux in the medial prefrontal cortex elicited by phencyclidine and ketamine. Int J Neuropsychopharmacol 9:565-573.

Amzica F, Steriade M (1995) Disconnection of intracortical synaptic linkages disrupts synchronization of a slow oscillation. J Neurosci 15:4658-4677.

Amzica F, Steriade M (1998) Electrophysiological correlates of sleep delta waves. Electroencephalogr Clin Neurophysiol 107:69-83.

Andersen P, Andersson SA, Lømo T (1967a) Some factors involved in the thalamic control of spontaneous barbiturate spindles. J Physiol 192:257-281.

Andersen P, Andersson SA, Lømo T (1967b) Nature of thalamo-cortical relations during spontaneous barbiturate spindle activity. J Physiol 192:283-307.

Andersen RA, Knight PL, Merzenich MM (1980) The thalamocortical and corticothalamic conections of AI, AII, and the anterior auditory field (AFF) in the cat: Evidence ofr two largely segregated systems of connections. J Comp Neurol 194:663-701.

André M, Lamblin MD, d'Allest AM, Curzi-Dascalova L, Moussalli-Salefranque F, Nguyen The Tich S, Vecchierini-Blineau MF, Wallois F, Walls-Esquivel E, Plouin P (2010) Electroencephalography in premature and full-term infants. Developmental features and glossary. Neurophysiol Clin 40:59-124.

Artola A, Singer W (1993) Long-term depression of excitatory synaptic transmission and its relationship to long-term potentiation. Trends Neurosci 16:480-487.

Arvanitaki A (1942) Effects evoked in an axon by the activity of a contiguous one. J Neurophysiol 5:89-108.

Aston-Jones G, Bloom FE (1981) Activity of norepinephrine-containing locus coeruleus neurons in behaving rats anticipates fluctuations in the sleep-waking cycle. J Neurosci 1:876-886.

Atallah Bassam V, Bruns W, Carandini M, Scanziani M (2012) Parvalbumin-expressing interneurons linearly transform cortical responses to visual stimuli. Neuron 73:159-170.

Avendaño C, Rausell E, Perez-Aguilar D, Isorna S (1988) Organization of the association cortical afferent connections of area 5: a retrograde tracer study in the cat. J Comp Neurol 278:1-33.

Avramescu S, Timofeev I (2008) Synaptic strength modulation after cortical trauma: a role in epileptogenesis. J Neurosci 28:6760-6772.

Ayala-Guerrero F, Mexicano G (2008) Sleep and wakefulness in the green iguanid lizard (Iguana iguana). Comp Biochem Physiol A Mol Integr Physiol 151:305-312.

Bading H (2013) Nuclear calcium signalling in the regulation of brain function. Nat Rev Neurosci 14:593-608.

Bal T, von Krosigk M, McCormick DA (1995) Synaptic and membrane mechanisms underlying synchronized oscillations in the ferret lateral geniculate nucleus in vitro. J Physiol 483:641-663.

Basar E (2012) A review of alpha activity in integrative brain function: fundamental physiology, sensory coding, cognition and pathology. Int J Psychophysiol 86:1-24.

Basheer R, Strecker RE, Thakkar MM, McCarley RW (2004) Adenosine and sleep-wake regulation. Prog Neurobiol 73:379-396.

Bazhenov M, Timofeev I, Steriade M, Sejnowski TJ (1998) Computational models of thalamocortical augmenting responses. J Neurosci 18:6444-6465.

Bazhenov M, Timofeev I, Steriade M, Sejnowski TJ (1999) Self-sustained rhythmic activity in the thalamic reticular nucleus mediated by depolarizing GABAA receptor potentials. Nat Neurosci 2:168-174.
Bazhenov M, Timofeev I, Steriade M, Sejnowski T (2000) Spiking-bursting activity in the thalamic reticular nucleus initiates sequences of spindle oscillations in thalamic networks. J Neurophysiol 84:1076-1087.
Bazhenov M, Timofeev I, Steriade M, Sejnowski TJ (2002) Model of thalamocortical slow-wave sleep oscillations and transitions to activated States. J Neurosci 22:8691-8704.
Beaulieu C, Somogyi P (1990) Targets and quantitative distribution of GABAergic synapses in the visual cortex of the cat. Eur J Neurosci 2:296-303.
Beltramo R, D'Urso G, Dal Maschio M, Farisello P, Bovetti S, Clovis Y, Lassi G, Tucci V, De Pietri Tonelli D, Fellin T (2013) Layer-specific excitatory circuits differentially control recurrent network dynamics in the neocortex. Nat Neurosci 16:227-234.
Berridge CW, Foote SL (1991) Effects of locus coeruleus activation on electroencephalographic activity in neocortex and hippocampus. J Neurosci 11:3135-3145.
Bi G-q, Poo M-m (1998) Synaptic modifications in cultured hippocampal neurons: dependence on spike timing, synaptic strength, and postsynaptic cell type. J Neurosci 18:10464-10472.
Blake H, Gerard RW (1937) Brain potentials during sleep. Am J Physiol 119:692-703.
Blethyn KL, Hughes SW, Toth TI, Cope DW, Crunelli V (2006) Neuronal basis of the slow (<1 Hz) oscillation in neurons of the nucleus reticularis thalami in vitro. J Neurosci 26:2474-2486.
Boly M, Perlbarg V, Marrelec G, Schabus M, Laureys S, Doyon J, Pelegrini-Issac M, Maquet P, Benali H (2012) Hierarchical clustering of brain activity during human nonrapid eye movement sleep. Proc Natl Acad Sci USA 109:5856-5861.
Bonjean M, Baker T, Lemieux M, Timofeev I, Sejnowski T, Bazhenov M (2011) Corticothalamic feedback controls sleep spindle duration in vivo. J Neurosci 31:9124-9134.
Borbely AA (1982) A two process model of sleep regulation. Hum Neurobiol 1:195-204.
Borg-Graham LJ, Monier C, Fregnac Y (1998) Visual input evokes transient and strong shunting inhibition in visual cortical neurons. Nature 393:369-373.
Bormann J (1988) Electrophysiology of GABAA and GABAB receptor subtypes. Trends Neurosci 11:112-116.
Brumberg JC, Pinto DJ, Simons DJ (1996) Spatial gradients and inhibitory summation in the rat whisker barrel system. J Neurophysiol 76:130-140.
Burkhalter A (1989) Intrinsic connections of rat primary visual cortex: laminar organization of axonal projections. J Comp Neurol 279:171-186.
Byrne JH (2003) Learning and memory: basic mechanisms. In: Fundamental Neuroscience (Squire LR, Bloom FE, McConnell SK, Roberts JL, Spitzer NC, Zigmond MJ, eds), pp 1275-1298. San Diego: Academic Press.
Castro-Alamancos MA, Connors BW (1996) Cellular mechanisms of the augmenting response: short-term plasticity in a thalamocortical pathway. J Neurosci 16:7742-7756.
Chauvette S, Volgushev M, Timofeev I (2010) Origin of active states in local neocortical networks during slow sleep oscillation. Cereb Cortex.
Chauvette S, Seigneur J, Timofeev I (2012) Sleep oscillations in the thalamocortical system induce long-term neuronal plasticity. Neuron 75:1105-1113.
Chauvette S, Crochet S, Volgushev M, Timofeev I (2011) Properties of slow oscillation during slow-wave sleep and anesthesia in cats. J Neurosci 31:14998-15008.
Cole AE, Nicoll RA (1984) The pharmacology of cholinergic excitatory responses in hippocampal pyramidal cells. Brain Res 305:283-290.
Colonnier M (1968) Synaptic patterns on different cell types in the different laminae of the cat visual cortex. An electron microscope study. Brain Res 9:268-287.
Compte A, Sanchez-Vives MV, McCormick DA, Wang XJ (2003) Cellular and network mechanisms of slow oscillatory activity (<1 Hz) and wave propagations in a cortical network model. J Neurophysiol 89:2707-2725.

Compte A, Reig R, Descalzo VF, Harvey MA, Puccini GD, Sanchez-Vives MV (2008) Spontaneous high-frequency (10-80 Hz) oscillations during up states in the cerebral cortex in vitro. J Neurosci 28:13828-13844.
Condorelli DF, Parenti R, Spinella F, Trovato Salinaro A, Belluardo N, Cardile V, Cicirata F (1998) Cloning of a new gap junction gene (Cx36) highly expressed in mammalian brain neurons. Eur J Neurosci 10:1202-1208.
Connors BW, Prince DA (1982) Effects of local anesthetic QX-314 on the membrane properties of hippocampal pyramidal neurons. J Pharmacol Exp Ther 220:476-481.
Connors BW, Gutnick MJ (1990) Intrinsic firing patterns of diverse neocortical neurons. Trends Neurosci 13:99-104.
Connors BW, Malenka RC, Silva LR (1988) Two inhibitory postsynaptic potentials, and GABAA and GABAB receptor-mediated responses in neocortex of rat and cat. J Physiol 406:443-468.
Constantinople CM, Bruno RM (2011) Effects and mechanisms of wakefulness on local cortical networks. Neuron 69:1061-1068.
Contreras D, Steriade M (1995) Cellular basis of EEG slow rhythms: a study of dynamic corticothalamic relationships. J Neurosci 15:604-622.
Contreras D, Timofeev I, Steriade M (1996a) Mechanisms of long-lasting hyperpolarizations underlying slow sleep oscillations in cat corticothalamic networks. J Physiol 494:251-264.
Contreras D, Destexhe A, Sejnowski TJ, Steriade M (1996b) Control of spatiotemporal coherence of a thalamic oscillation by corticothalamic feedback. Science 274:771-774.
Cossart R, Aronov D, Yuste R (2003) Attractor dynamics of network UP states in the neocortex. Nature 423:283-288.
Crill WE (1996) Persistent sodium current in mammalian central neurons. Annu Rev Physiol 58:349-362.
Crochet S, Chauvette S, Boucetta S, Timofeev I (2005) Modulation of synaptic transmission in neocortex by network activities. Eur J Neurosci 21:1030-1044.
Crochet S, Fuentealba P, Cisse Y, Timofeev I, Steriade M (2006) Synaptic plasticity in local cortical network in vivo and its modulation by the level of neuronal activity. Cereb Cortex 16:618-631.
Cruikshank SJ, Lewis TJ, Connors BW (2007) Synaptic basis for intense thalamocortical activation of feedforward inhibitory cells in neocortex. Nat Neurosci 10:462-468.
Crunelli V, Hughes SW (2010) The slow (<1 Hz) rhythm of non-REM sleep: a dialogue between three cardinal oscillators. Nat Neurosci 13:9-17.
Crunelli V, Cope DW, Hughes SW (2006) Thalamic T-type Ca2+ channels and NREM sleep. Cell Calcium 40:175-190.
Csercsa R et al. (2010) Laminar analysis of slow wave activity in humans. Brain 133:2814-2829.
da Costa NM, Martin KA (2011) How thalamus connects to spiny stellate cells in the cat's visual cortex. J Neurosci 31:2925-2937.
De Gois S, Schafer MK, Defamie N, Chen C, Ricci A, Weihe E, Varoqui H, Erickson JD (2005) Homeostatic scaling of vesicular glutamate and GABA transporter expression in rat neocortical circuits. J Neurosci 25:7121-7133.
Deans MR, Gibson JR, Sellitto C, Connors BW, Paul DL (2001) Synchronous activity of inhibitory networks in neocortex requires electrical synapses containing connexin36. Neuron 31:477-485.
DeFelipe J, Farinas I (1992) The pyramidal neuron of the cerebral cortex: morphological and chemical characteristics of the synaptic inputs. Prog Neurobiol 39:563-607.
DeFelipe J et al. (2013) New insights into the classification and nomenclature of cortical GABAergic interneurons. Nat Rev Neurosci.
Del Felice A, Formaggio E, Storti SF, Fiaschi A, Manganotti P (2012) The gating role of the thalamus to protect sleep: An f-MRI report. Sleep Med 13:447-449.
Desai NS, Rutherford LC, Turrigiano GG (1999) Plasticity in the intrinsic excitability of cortical pyramidal neurons. Nat Neurosci 2:515-520.
Destexhe A, Contreras D, Steriade M (1998) Mechanisms underlying the synchronizing action of corticothalamic feedback through inhibition of thalamic relay cells. J Neurophysiol 79:999-1016.

Diekelmann S, Born J (2010) The memory function of sleep. Nat Rev Neurosci 11:114-126.
Doi A, Mizuno M, Katafuchi T, Furue H, Koga K, Yoshimura M (2007) Slow oscillation of membrane currents mediated by glutamatergic inputs of rat somatosensory cortical neurons: in vivo patch-clamp analysis. Eur J Neurosci 26:2565-2575.
Dossi RC, Nunez A, Steriade M (1992) Electrophysiology of a slow (0.5-4 Hz) intrinsic oscillation of cat thalamocortical neurones in vivo. J Physiol 447:215-234.
Durieux ME (1995) Inhibition by ketamine of muscarinic acetylcholine receptor function. Anesth Analg 81:57-62.
Eschenko O, Magri C, Panzeri S, Sara SJ (2012) Noradrenergic neurons of the locus coeruleus are phase locked to cortical up-down states during sleep. Cereb Cortex 22:426-435.
Espinosa F, Kavalali ET (2009) NMDA receptor activation by spontaneous glutamatergic neurotransmission. J Neurophysiol 101:2290-2296.
Esser SK, Hill S, Tononi G (2009) Breakdown of effective connectivity during slow wave sleep: investigating the mechanism underlying a cortical gate using large-scale modeling. J Neurophysiol 102:2096-2111.
Fabri M, Manzoni T (1996) Glutamate decarboxylase immunoreactivity in corticocortical projecting neurons of rat somatic sensory cortex. Neuroscience 72:435-448.
Fairén A, Valverde F (1980) A specialized type of neuron in the visual cortex of cat: a Golgi and electron microscope study of chandelier cells. J Comp Neurol 194:761-779.
Fanselow EE, Connors BW (2010) The roles of somatostatin-expressing (GIN) and fast-spiking inhibitory interneurons in UP-DOWN states of mouse neocortex. J Neurophysiol 104:596-606.
Fatt P, Katz B (1952) Spontaneous subthreshold activity at motor nerve endings. J Physiol 117:109-128.
Felleman DJ, Van Essen DC (1991) Distributed hierarchical processing in the primate cerebral cortex. Cereb Cortex 1:1-47.
Flanigan Jr WF, Wilcox RH, Rechtschaffen A (1973) The EEG and behavioral continuum of the crocodilian, Caiman sclerops. Electroencephalogr Clin Neurophysiol 34:521-538.
Fort P, Bassetti CL, Luppi PH (2009) Alternating vigilance states: new insights regarding neuronal networks and mechanisms. Eur J Neurosci 29:1741-1753.
Fox K, Armstrong-James M (1986) The role of the anterior intralaminar nuclei and N-methyl D-aspartate receptors in the generation of spontaneous bursts in rat neocortical neurones. Exp Brain Res 63:505-518.
Gabbott PLA, Martin KAC, Whitteridge D (1987) Connections between pyramidal neurons in layer 5 of cat visual cortex (area 17). J Comp Neurol 259:364-381.
Gais S, Plihal W, Wagner U, Born J (2000) Early sleep triggers memory for early visual discrimination skills. Nat Neurosci 3:1335-1339.
Galarreta M, Hestrin S (1998) Frequency-dependent synaptic depression and the balance of excitation and inhibition in the neocortex. Nat Neurosci 1:587-594.
Galarreta M, Hestrin S (1999) A network of fast-spiking cells in the neocortex connected by electrical synapses. Nature 402:72-75.
Gibson JR, Beierlein M, Connors BW (1999) Two networks of electrically coupled inhibitory neurons in neocortex. Nature 402:75-79.
Gil Z, Amitai Y (1996) Properties of convergent thalamocortical and intracortical synaptic potentials in single neurons of neocortex. J Neurosci 16:6567-6578.
Gilbert CD, Kelly JP (1975) The projections of cells in different layers of the cat's visual cortex. J Comp Neurol 163:81-105.
Gilbert CD, Wiesel TN (1979) Morphology and intracortical projections of functionally characterised neurones in the cat visual cortex. Nature 280:120-125.
Goldstein SA, Bockenhauer D, O'Kelly I, Zilberberg N (2001) Potassium leak channels and the KCNK family of two-P-domain subunits. Nat Rev Neurosci 2:175-184.
Gray CM, Singer W (1989) Stimulus-specific neuronal oscillations in orientation columns of cat visual cortex. Proc Natl Acad Sci U S A 86:1698-1702.

Gray CM, McCormick DA (1996) Chattering cells: superficial pyramidal neurons contributing to the generation of synchronous oscillations in the visual cortex. Science 274:109-113.
Graybiel AM (1972) Some ascending connections of the pulvinar and nucleus lateralis posterior of the thalamus in the cat. Brain Res 44:99-125.
Grenier F, Timofeev I, Steriade M (2001) Focal synchronization of ripples (80-200 Hz) in neocortex and their neuronal correlates. J Neurophysiol 86:1884-1898.
Groemer TW, Klingauf J (2007) Synaptic vesicles recycling spontaneously and during activity belong to the same vesicle pool. Nat Neurosci 10:145-147.
Gu Q, Perez-Velazquez JL, Angelides KJ, Cynader MS (1993) Immunocytochemical study of GABAA receptors in the cat visual cortex. J Comp Neurol 333:94-108.
Guillery RW (1966) A study of Golgi preparations from the dorsal lateral geniculate nucleus of the adult cat. J Comp Neurol 128:21-50.
Haider B, McCormick DA (2009) Rapid neocortical dynamics: cellular and network mechanisms. Neuron 62:171-189.
Haider B, Hausser M, Carandini M (2012) Inhibition dominates sensory responses in the awake cortex. Nature 493:97-100.
Halassa MM, Fellin T, Haydon PG (2009a) Tripartite synapses: roles for astrocytic purines in the control of synaptic physiology and behavior. Neuropharmacology 57:343-346.
Halassa MM, Florian C, Fellin T, Munoz JR, Lee SY, Abel T, Haydon PG, Frank MG (2009b) Astrocytic modulation of sleep homeostasis and cognitive consequences of sleep loss. Neuron 61:213-219.
Hasenstaub A, Sachdev RN, McCormick DA (2007) State changes rapidly modulate cortical neuronal responsiveness. J Neurosci 27:9607-9622.
Hasenstaub A, Shu Y, Haider B, Kraushaar U, Duque A, McCormick DA (2005) Inhibitory postsynaptic potentials carry synchronized frequency information in active cortical networks. Neuron 47:423-435.
Hendry SH, Hsiao SS (2003) The somatosensory system. In: Fundamental Neuroscience (Squire LR, Bloom FE, McConnell SK, Roberts JL, Spitzer NC, Zigmond MJ, eds), pp 667-697. San Diego: Academic Press.
Hendry SHC, Houser CR, Jones EG, Vaughn JE (1983) Synaptic organization of immunocytochemically identified GABA neurons in the monkey sensory-motor cortex. J Neurocytol 12:639-660.
Hill S, Tononi G (2005) Modeling sleep and wakefulness in the thalamocortical system. J Neurophysiol 93:1671-1698.
Hille B (2001) Ion Channels of Excitable Membranes, 3rd Edition. Sunderland: Sinaeur Associates, Inc.
Hinard V, Mikhail C, Pradervand S, Curie T, Houtkooper RH, Auwerx J, Franken P, Tafti M (2012) Key electrophysiological, molecular, and metabolic signatures of sleep and wakefulness revealed in primary cortical cultures. J Neurosci 32:12506-12517.
Hirsch JA, Gilbert CD (1991) Synaptic physiology of horizontal connections in the cat's visual cortex. J Neurosci 11:1800-1809.
Hirsch JA, Gallagher CA, Alonso J-M, Martinez LM (1998a) Ascending projections of simple and complex cells in layer 6 of the cat striate cortex. J Neurosci 18:8086-8094.
Hirsch JA, Alonso J-M, Reid RC, Martinez LM (1998b) Synaptic integration in striate cortical simple cells. J Neurosci 18:9517-9528.
Ho VM, Lee J-A, Martin KC (2011) The cell biology of synaptic plasticity. Science 334:623-628.
Hobson JA (2005) Sleep is of the brain, by the brain and for the brain. Nature 437:1254-1256.
Hobson JA, Pace-Schott EF (2003) Sleep, dreaming, and wakefulness. In: Fundamental Neuroscience (Squire LR, Bloom FE, McConnell SK, Roberts JL, Spitzer NC, Zigmond MJ, eds), pp 1085-1108. San Diego: Academic Press.
Holländer H (1974) On the origin of the corticotectal projections in the cat. Exp Brain Res 21:433-439.
Hormuzdi SG, Pais I, LeBeau FE, Towers SK, Rozov A, Buhl EH, Whittington MA, Monyer H (2001) Impaired electrical signaling disrupts gamma frequency oscillations in connexin 36-deficient mice. Neuron 31:487-495.

Hornung JP, Garey LJ (1981) The thalamic projection to cat visual cortex: ultrastructure of neurons identified by golgi impregnation or retrograde horseradish peroxidase transport. Neuroscience 6:1053-1068.
Houser CR, Hendry SH, Jones EG, Vaughn JE (1983) Morphological diversity of immunocytochemically identified GABA neurons in the monkey sensory-motor cortex. J Neurocytol 12:617-638.
Huber R, Ghilardi MF, Massimini M, Tononi G (2004) Local sleep and learning. Nature 430:78-81.
Hughes SW, Cope DW, Blethyn KL, Crunelli V (2002) Cellular mechanisms of the slow (<1 Hz) oscillation in thalamocortical neurons in vitro. Neuron 33:947-958.
Huguenard JR (1996) Low-threshold calcium currents in central nervous system neurons. Annu Rev Physiol 58:329-348.
Hull C, Isaacson JS, Scanziani M (2009) Postsynaptic mechanisms govern the differential excitation of cortical neurons by thalamic inputs. J Neurosci 29:9127-9136.
Iber C, Ancoli-Israel S, Chesson AL, Quan SF (2007) The AASM manual for the scoring of sleep and associated events: rules, terminology and technical specifications. Westchester: American Academy of Sleep Medicine.
Ichikawa M, Arissian K, Asanuma H (1985) Distribution of corticocortical and thalamocortical synapses on identified motor cortical neurons in the cat: Golgi, electron microscopic and degeneration study. Brain Res 345:87-101.
Ikegaya Y, Aaron G, Cossart R, Aronov D, Lampl I, Ferster D, Yuste R (2004) Synfire chains and cortical songs: temporal modules of cortical activity. Science 304:559-564.
Inoue T, Imoto K (2006) Feedforward inhibitory connections from multiple thalamic cells to multiple regular-spiking cells in layer 4 of the somatosensory cortex. J Neurophysiol 96:1746-1754.
Jacobson S, Trojanowski JQ (1974) The cells of origin of the corpus callosum in rat, cat and rhesus monkey. Brain Res 74:149-155.
Jahnsen H, Llinas R (1984) Electrophysiological properties of guinea-pig thalamic neurones: an in vitro study. J Physiol 349:205-226.
Jefferys JGR, Menendez de la Prida L, Wendling F, Bragin A, Avoli M, Timofeev I, Lopes da Silva FH (2012) Mechanisms of physiological and epileptic HFO generation. Prog Neurobiol 98:250-264.
Jenkins JG, Dallenbach KM (1924) Obliviscence during sleep and waking. Am J Psychol 35:605-612.
Johnson HA, Buonomano DV (2007) Development and plasticity of spontaneous activity and up states in cortical organotypic slices. J Neurosci 27:5915-5925.
Jones EG (1975) Varieties and distribution of non-pyramidal cells in the somatic sensory cortex of the squirrel monkey. J Comp Neurol 160:205-267.
Jones EG (1998) Viewpoint: the core and matrix of thalamic organization. Neuroscience 85:331-345.
Jones EG (2002) Thalamic organization and function after Cajal. In: Prog Brain Res (Efrain C. Azmitia JDEGJPRCER, ed), pp 333-357: Elsevier.
Jones MS, Barth DS (1999) Spatiotemporal organization of fast (>200 Hz) electrical oscillations in rat vibrissa/barrel cortex. J Neurophysiol 82:1599-1609.
Jouvet M (1967) Neurophysiology of the states of sleep. Physiol Rev 47:117-177.
Kapfer C, Glickfeld LL, Atallah BV, Scanziani M (2007) Supralinear increase of recurrent inhibition during sparse activity in the somatosensory cortex. Nat Neurosci 10:743-753.
Katzel D, Zemelman BV, Buetfering C, Wolfel M, Miesenbock G (2011) The columnar and laminar organization of inhibitory connections to neocortical excitatory cells. Nat Neurosci 14:100-107.
Kavanau JL (2006) Is sleep's 'supreme mystery' unraveling? An evolutionary analysis of sleep encounters no mystery; nor does life's earliest sleep, recently discovered in jellyfish. Med Hypotheses 66:3-9.
Kawaguchi Y, Kubota Y (1996) Physiological and morphological identification of somatostatin- or vasoactive intestinal polypeptide-containing cells among GABAergic cell subtypes in rat frontal cortex. J Neurosci 16:2701-2715.
Kawaguchi Y, Kubota Y (1997) GABAergic cell subtypes and their synaptic connections in rat frontal cortex. Cereb Cortex 7:476-486.
Kilduff TS, Cauli B, Gerashchenko D (2011) Activation of cortical interneurons during sleep: an anatomical link to homeostatic sleep regulation? Trends Neurosci 34:10-19.

Kisvarday ZF, Martin KAC, Somogyi P, Friedlander MJ (1987) Evidence for interlaminar inhibitory circuits in the striate cortex of the cat. J Comp Neurol 260:1-19.
Kisvarday ZF, Gulyas A, Beroukas D, North JB, Chubb IW, Somogyi P (1990) Synapses, axonal and dendritic patterns of GABA-immunoreactive neurons in human cerebral cortex. Brain 113:793-812.
Klemm WR (1976) Physiological and behavioral significance of hippocampal rhythmic, slow activity ("theta rhythm"). Prog Neurobiol 6:23-47.
Kristiansen K, Courtois G (1949) Rhythmic electrical activity from isolated cerebral cortex. Electroencephalogr Clin Neurophysiol 1:265-272.
Krnjevic K, Pumain R, Renaud L (1971) The mechanism of excitation by acetylcholine in the cerebral cortex. J Physiol 215:247-268.
Krueger JM, Rector DM, Roy S, Van Dongen HP, Belenky G, Panksepp J (2008) Sleep as a fundamental property of neuronal assemblies. Nat Rev Neurosci 9:910-919.
Lambo ME, Turrigiano GG (2013) Synaptic and intrinsic homeostatic mechanisms cooperate to increase L2/3 pyramidal neuron excitability during a late phase of critical period plasticity. J Neurosci 33:8810-8819.
Lamprecht R, LeDoux J (2004) Structural plasticity and memory. Nat Rev Neurosci 5:45-54.
Landisman CE, Long MA, Beierlein M, Deans MR, Paul DL, Connors BW (2002) Electrical synapses in the thalamic reticular nucleus. J Neurosci 22:1002-1009.
Larkman AU (1991) Dendritic morphology of pyramidal neurones of the visual cortex of the rat: III. spine distributions. J Comp Neurol 306:332-343.
Lazarevic V, Pothula S, Andres-Alonso M, Fejtova A (2013) Molecular mechanisms driving homeostatic plasticity of neurotransmitter release. Front Cell Neurosci 7:244.
Lee CC, Sherman SM (2009) Modulator property of the intrinsic cortical projection from layer 6 to layer 4. Front Syst Neurosci 3.
Leresche N, Lightowler S, Soltesz I, Jassik-Gerschenfeld D, Crunelli V (1991) Low-frequency oscillatory activities intrinsic to rat and cat thalamocortical cells. J Physiol 441:155-174.
Li H, Prince DA (2002) Synaptic activity in chronically injured, epileptogenic sensory-motor neocortex. J Neurophysiol 88:2-12.
Liu XB, Honda CN, Jones EG (1995) Distribution of four types of synapse on physiologically identified relay neurons in the ventral posterior thalamic nucleus of the cat. J Comp Neurol 352:69-91.
Llinas R, Yarom Y (1981) Properties and distribution of ionic conductances generating electroresponsiveness of mammalian inferior olivary neurones in vitro. J Physiol 315:569-584.
Llinas RR (1988) The intrinsic electrophysiological properties of mammalian neurons: insights into central nervous system function. Science 242:1654-1664.
Lopes da Silva FH, Witter MP, Boeijinga PH, Lohman AH (1990) Anatomic organization and physiology of the limbic cortex. Physiol Rev 70:453-511.
Lübke J (1993) Morphology of neurons in the thalamic reticular nucleus (TRN) of mammals as revealed by intracellular injections into fixed brain slices. J Comp Neurol 329:458-471.
Lund JS (1973) Organization of neurons in the visual cortex, area 17, of the monkey (Macaca mulatta). J Comp Neurol 147:455-495.
MacDonald JF, Miljkovic Z, Pennefather P (1987) Use-dependent block of excitatory amino acid currents in cultured neurons by ketamine. J Neurophysiol 58:251-266.
Mainen ZF, Sejnowski TJ (1996) Influence of dendritic structure on firing pattern in model neocortical neurons. Nature 382:363-366.
Malenka RC, Nicoll RA (1993) NMDA-receptor-dependent synaptic plasticity: multiple forms and mechanisms. Trends Neurosci 16:521-527.
Manabe H, Kusumoto-Yoshida I, Ota M, Mori K (2011) Olfactory cortex generates synchronized top-down inputs to the olfactory bulb during slow-wave sleep. J Neurosci 31:8123-8133.
Mann EO, Kohl MM, Paulsen O (2009) Distinct roles of GABA(A) and GABA(B) receptors in balancing and terminating persistent cortical activity. J Neurosci 29:7513-7518.
Maquet P (2001) The role of sleep in learning and memory. Science 294:1048-1052.

Marin-Padilla M (1969) Origin of the pericellular baskets of the pyramidal cells of the human motor cortex: A golgi study. Brain Res 14:633-646.
Markram H, Lubke J, Frotscher M, Sakmann B (1997a) Regulation of synaptic efficacy by coincidence of postsynaptic APs and EPSPs. Science 275:213-215.
Markram H, Lubke J, Frotscher M, Roth A, Sakmann B (1997b) Physiology and anatomy of synaptic connections between thick tufted pyramidal neurones in the developing rat neocortex. J Physiol 500:409-440.
Markram H, Toledo-Rodriguez M, Wang Y, Gupta A, Silberberg G, Wu C (2004) Interneurons of the neocortical inhibitory system. Nat Rev Neurosci 5:793-807.
Marshall L, Helgadottir H, Molle M, Born J (2006) Boosting slow oscillations during sleep potentiates memory. Nature 444:610-613.
Martínez-García F, González-Hernández T, Martínez-Millán L (1994) Pyramidal and nonpyramidal callosal cells in the striate cortex of the adult rat. J Comp Neurol 350:439-451.
Massimini M, Amzica F (2001) Extracellular calcium fluctuations and intracellular potentials in the cortex during the slow sleep oscillation. J Neurophysiol 85:1346-1350.
Massimini M, Tononi G, Huber R (2009) Slow waves, synaptic plasticity and information processing: insights from transcranial magnetic stimulation and high-density EEG experiments. Eur J Nurosci 29:1761-1770.
Massimini M, Huber R, Ferrarelli F, Hill S, Tononi G (2004) The sleep slow oscillation as a traveling wave. J Neurosci 24:6862-6870.
Massimini M, Ferrarelli F, Huber R, Esser SK, Singh H, Tononi G (2005) Breakdown of cortical effective connectivity during sleep. Science 309:2228-2232.
McCormick DA, Pape HC (1990) Properties of a hyperpolarization-activated cation current and its role in rhythmic oscillation in thalamic relay neurones. J Physiol 431:291-318.
McCormick DA, Bal T (1994) Sensory gating mechanisms of the thalamus. Curr Opin Neurobiol 4:550-556.
McCormick DA, Connors BW, Lighthall JW, Prince DA (1985) Comparative electrophysiology of pyramidal and sparsely spiny stellate neurons of the neocortex. J Neurophysiol 54:782-806.
McDonald C, Burkhalter A (1993) Organization of long-range inhibitory connections with rat visual cortex. J Neurosci 13:768-781.
McKinney RA, Capogna M, Durr R, Gahwiler BH, Thompson SM (1999) Miniature synaptic events maintain dendritic spines via AMPA receptor activation. Nat Neurosci 2:44-49.
Merzenich MM, Kaas JH, Wall J, Nelson RJ, Sur M, Felleman D (1983) Topographic reorganization of somatosensory cortical areas 3b and 1 in adult monkeys following restricted deafferentation. Neuroscience 8:33-55.
Merzenich MM, Nelson RJ, Stryker MP, Cynader MS, Schoppmann A, Zook JM (1984) Somatosensory cortical map changes following digit amputation in adult monkeys. J Comp Neurol 224:591-605.
Miller EK (2000) The prefrontal cortex and cognitive control. Nat Rev Neurosci 1:59-65.
Molle M, Marshall L, Gais S, Born J (2002) Grouping of spindle activity during slow oscillations in human non-rapid eye movement sleep. J Neurosci 22:10941-10947.
Moore AR, Zhou W-L, Jakovcevski I, Zecevic N, Antic SD (2011) Spontaneous electrical activity in the human fetal cortex in vitro. J Neurosci 31:2391-2398.
Morel A, Liu J, Wannier T, Jeanmonod D, Rouiller EM (2005) Divergence and convergence of thalamocortical projections to premotor and supplementary motor cortex: a multiple tracing study in the macaque monkey. Eur J Neurosci 21:1007-1029.
Moulder KL, Jiang X, Taylor AA, Olney JW, Mennerick S (2006) Physiological activity depresses synaptic function through an effect on vesicle priming. J Neurosci 26:6618-6626.
Mountcastle VB (1997) The columnar organization of the neocortex. Brain 120:701-722.
Mountcastle VB, Talbot WH, Sakata H, Hyvärinen J (1969) Cortical neuronal mechanisms in flutter-vibration studied in unanesthetized monkeys. Neuronal periodicity and frequency discrimination. J Neurophysiol 32:452-484.
Mungai JM (1967) Dendritic patterns in the somatic sensory cortex of the cat. J Anat 101:403-418.

Munglani R, Jones JG (1992) Altered consciousness: pharmacology and phenomenology BAP Summer Meeting, York, July 1991: Sleep and general anaesthesia as altered states of consciousness. J Psychopharmacol 6:399-409.
Murphy T, Blatter L, Wier W, Baraban J (1992) Spontaneous synchronous synaptic calcium transients in cultured cortical neurons. J Neurosci 12:4834-4845.
Murthy VN, Fetz EE (1992) Coherent 25- to 35-Hz oscillations in the sensorimotor cortex of awake behaving monkeys. Proc Natl Acad Sci U S A 89:5670-5674.
Murthy VN, Schikorski T, Stevens CF, Zhu Y (2001) Inactivity produces increases in neurotransmitter release and synapse size. Neuron 32:673-682.
Nakamaru-Ogiso E, Miyamoto H, Hamada K, Tsukada K, Takai K (2012) Novel biochemical manipulation of brain serotonin reveals a role of serotonin in the circadian rhythm of sleep–wake cycles. Eur J Neurosci 35:1762-1770.
Niedermeyer E (1998) Frontal lobe functions and dysfunctions. Clinical Encephalogr 29:79-90.
Nir Y, Staba RJ, Andrillon T, Vyazovskiy VV, Cirelli C, Fried I, Tononi G (2011) Regional slow waves and spindles in human sleep. Neuron 70:153-169.
Olson CR, Lawler K (1987) Cortical and subcortical afferent connections of a posterior division of feline area 7 (Area 7p). J Comp Neurol 259:13-30.
Otsuka T, Kawaguchi Y (2009) Cortical inhibitory cell types differentially form intralaminar and interlaminar subnetworks with excitatory neurons. J Neurosci 29:10533-10540.
Pare D, Lebel E, Lang EJ (1997) Differential impact of miniature synaptic potentials on the soma and dendrites of pyramidal neurons in vivo. J Neurophysiol 78:1735-1739.
Pascual O, Casper KB, Kubera C, Zhang J, Revilla-Sanchez R, Sul JY, Takano H, Moss SJ, McCarthy K, Haydon PG (2005) Astrocytic purinergic signaling coordinates synaptic networks. Science 310:113-116.
Peters A, Proskauer CC, Ribak CE (1982) Chandelier cells in rat visual cortex. J Comp Neurol 206:397-416.
Portas CM, Bjorvatn B, Fagerland S, Grønli J, Mundal V, Sørensen E, Ursin R (1998) On-line detection of extracellular levels of serotonin in dorsal raphe nucleus and frontal cortex over the sleep/wake cycle in the freely moving rat. Neuroscience 83:807-814.
Porter JT, Johnson CK, Agmon A (2001) Diverse types of interneurons generate thalamus-evoked feedforward inhibition in the mouse barrel cortex. J Neurosci 21:2699-2710.
Prince DA, Tseng GF (1993) Epileptogenesis in chronically injured cortex: in vitro studies. J Neurophysiol 69:1276-1291.
Puig MV, Gulledge A (2011) Serotonin and prefrontal cortex function: neurons, networks, and circuits. Mol Neurobiol 44:449-464.
Puig MV, Ushimaru M, Kawaguchi Y (2008) Two distinct activity patterns of fast-spiking interneurons during neocortical UP states. Proc Natl Acad Sci USA 105:8428-8433.
Puig MV, Watakabe A, Ushimaru M, Yamamori T, Kawaguchi Y (2010) Serotonin modulates fast-spiking interneuron and synchronous activity in the rat prefrontal cortex through 5-HT1A and 5-HT2A receptors. J Neurosci 30:2211-2222.
Rasch B, Born J (2013) About sleep's role in memory. Physiological Reviews 93:681-766.
Rattenborg NC (2006) Evolution of slow-wave sleep and palliopallial connectivity in mammals and birds: a hypothesis. Brain Res Bull 69:20-29.
Rausell E, Bickford L, Manger PR, Woods TM, Jones EG (1998) Extensive divergence and convergence in the thalamocortical projection to monkey somatosensory cortex. J Neurosci 18:4216-4232.
Redondo RL, Morris RG (2011) Making memories last: the synaptic tagging and capture hypothesis. Nat Rev Neurosci 12:17-30.
Reppert SM, Weaver DR (2001) Molecular analysis of mammalian circadian rhythms. Annu Rev Physiol 63:647-676.
Ribak CE (1978) Aspinous and sparsely-spinous stellate neurons in the visual cortex of rats contain glutamic acid decarboxylase. J Neurocytol 7:461-478.

Rigas P, Castro-Alamancos MA (2007) Thalamocortical Up states: differential effects of intrinsic and extrinsic cortical inputs on persistent activity. J Neurosci 27:4261-4272.
Rioult-Pedotti MS, Friedman D, Donoghue JP (2000) Learning-induced LTP in neocortex. Science 290:533-536.
Robertson RT, Cunningham TJ (1981) Organization of corticothalamic projections from parietal cortex in cat. J Comp Neurol 199:569-585.
Rouiller EM, Simm GM, Villa AEP, Ribaupierre Y, Ribaupierre F (1991) Auditory corticocortical interconnections in the cat: evidence for parallel and hierarchical arrangement of the auditory cortical areas. Exp Brain Res 86:483-505.
Rudolph M, Pospischil M, Timofeev I, Destexhe A (2007) Inhibition determines membrane potential dynamics and controls action potential generation in awake and sleeping cat cortex. J Neurosci 27:5280-5290.
Rudolph U, Antkowiak B (2004) Molecular and neuronal substrates for general anaesthetics. Nat Rev Neurosci 5:709-720.
Sakata S, Harris KD (2009) Laminar structure of spontaneous and sensory-evoked population activity in auditory cortex. Neuron 64:404-418.
Salin PA, Prince DA (1996a) Electrophysiological mapping of GABAA receptor-mediated inhibition in adult rat somatosensory cortex. J Neurophysiol 75:1589-1600.
Salin PA, Prince DA (1996b) Spontaneous $GABA_A$ receptor-mediated inhibitory currents in adult rat somatosensory cortex. J Neurophysiol 75:1573-1588.
Sanchez-Vives MV, McCormick DA (2000) Cellular and network mechanisms of rhythmic recurrent activity in neocortex. Nat Neurosci 3:1027-1034.
Sanchez-Vives MV, Mattia M, Compte A, Perez-Zabalza M, Winograd M, Descalzo VF, Reig R (2010) Inhibitory modulation of cortical up states. J Neurophysiol 104:1314-1324.
Saper CB, Chou TC, Scammell TE (2001) The sleep switch: hypothalamic control of sleep and wakefulness. Trends Neurosci 24:726-731.
Scannell JW, Burns GA, Hilgetag CC, O'Neil MA, Young MP (1999) The connectional organization of the cortico-thalamic system of the cat. Cereb Cortex 9:277-299.
Scheibel ME, Scheibel AB (1967) Structural organization of nonspecific thalamic nuclei and their projection toward cortex. Brain Res 6:60-94.
Schieber MH, Baker JF (2003) Descending Control of Movement. In: Fundamental Neuroscience (Squire LR, Bloom FE, McConnell SK, Roberts JL, Spitzer NC, Zigmond MJ, eds), pp 791-814. San Diego: Academic Press.
Shaw PJ, Cirelli C, Greenspan RJ, Tononi G (2000) Correlates of sleep and waking in Drosophila melanogaster. Science 287:1834-1837.
Sherman SM, Guillery RW (1996) Functional organization of thalamocortical relays. J Neurophysiol 76:1367-1395.
Sherman SM, Guillery RW (2002) The role of the thalamus in the flow of information to the cortex. Philos Trans R Soc Lond B Biol Sci 357:1695-1708.
Shinoda Y, Futami T, Kano M (1985) Synaptic organization of the cerebello-thalamo-cerebral pathway in the cat. II. Input-output organization of single thalamocortical neurons in the ventrolateral thalamus. Neurosci Res 2:157-180.
Shu Y, Hasenstaub A, McCormick DA (2003) Turning on and off recurrent balanced cortical activity. Nature 423:288-293.
Siegel JM (2009) Sleep viewed as a state of adaptive inactivity. Nat Rev Neurosci 10:747-753.
Silberberg G, Markram H (2007) Disynaptic inhibition between neocortical pyramidal cells mediated by Martinotti cells. Neuron 53:735-746.
Silver RA, Lubke J, Sakmann B, Feldmeyer D (2003) High-probability uniquantal transmission at excitatory synapses in barrel cortex. Science 302:1981-1984.
Simons DJ (1978) Response properties of vibrissa units in rat SI somatosensory neocortex. J Neurophysiol 41:798-820.

Sjostrom PJ, Turrigiano GG, Nelson SB (2001) Rate, timing, and cooperativity jointly determine cortical synaptic plasticity. Neuron 32:1149-1164.
Sohl G, Degen J, Teubner B, Willecke K (1998) The murine gap junction gene connexin36 is highly expressed in mouse retina and regulated during brain development. FEBS Lett 428:27-31.
Somogyi P (1977) A specific 'axo-axonal' interneuron in the visual cortex of the rat. Brain Res 136:345-350.
Somogyi P, Cowey A (1981) Combined golgi and electron microscopic study on the synapses formed by double bouquet cells in the visual cortex of the cat and monkey. J Comp Neurol 195:547-566.
Somogyi P, Kisvárday ZF, Martin KAC, Whitteridge D (1983) Synaptic connections of morphologically identified and physiologically characterized large basket cells in the striate cortex of cat. Neuroscience 10:261-294.
Somogyi P, Tamàs G, Lujan R, Buhl EH (1998) Salient features of synaptic organisation in the cerebral cortex. Brain Res Rev 26:113-135.
Stafstrom CE, Schwindt PC, Crill WE (1984) Repetitive firing in layer V neurons from cat neocortex in vitro. J Neurophysiol 52:264-277.
Steriade M, Timofeev I (2003) Neuronal plasticity in thalamocortical networks during sleep and waking oscillations. Neuron 37:563-576.
Steriade M, Nunez A, Amzica F (1993a) Intracellular analysis of relations between the slow (< 1 Hz) neocortical oscillation and other sleep rhythms of the electroencephalogram. J Neurosci 13:3266-3283.
Steriade M, Nunez A, Amzica F (1993b) A novel slow (< 1 Hz) oscillation of neocortical neurons in vivo: depolarizing and hyperpolarizing components. J Neurosci 13:3252-3265.
Steriade M, McCormick DA, Sejnowski TJ (1993c) Thalamocortical oscillations in the sleeping and aroused brain. Science 262:679-685.
Steriade M, Amzica F, Contreras D (1996a) Synchronization of fast (30-40 Hz) spontaneous cortical rhythms during brain activation. J Neurosci 16:392-417.
Steriade M, Timofeev I, Grenier F (2001) Natural waking and sleep states: a view from inside neocortical neurons. J Neurophysiol 85:1969-1985.
Steriade M, Contreras D, Curro Dossi R, Nunez A (1993d) The slow (< 1 Hz) oscillation in reticular thalamic and thalamocortical neurons: scenario of sleep rhythm generation in interacting thalamic and neocortical networks. J Neurosci 13:3284-3299.
Steriade M, Contreras D, Amzica F, Timofeev I (1996b) Synchronization of fast (30-40 Hz) spontaneous oscillations in intrathalamic and thalamocortical networks. J Neurosci 16:2788-2808.
Steriade M, Timofeev I, Durmuller N, Grenier F (1998) Dynamic properties of corticothalamic neurons and local cortical interneurons generating fast rhythmic (30-40 Hz) spike bursts. J Neurophysiol 79:483-490.
Stickgold R, James L, Hobson JA (2000) Visual discrimination learning requires sleep after training. Nat Neurosci 3:1237-1238.
Stratford KJ, Tarczy-Hornoch K, Martin KA, Bannister NJ, Jack JJ (1996) Excitatory synaptic inputs to spiny stellate cells in cat visual cortex. Nature 382:258-261.
Stroh A, Adelsberger H, Groh A, Rühlmann C, Fischer S, Schierloh A, Deisseroth K, Konnerth A (2013) Making waves: initiation and propagation of corticothalamic Ca2+ waves in vivo. Neuron 77:1136-1150.
Sun YG, Wu CS, Renger JJ, Uebele VN, Lu HC, Beierlein M (2012) GABAergic synaptic transmission triggers action potentials in thalamic reticular nucleus neurons. J Neurosci 32:7782-7790.
Sutcliffe JG, de Lecea L (2000) The hypocretins: excitatory neuromodulatory peptides for multiple homeostatic systems, including sleep and feeding. J Neurosci Res 62:161-168.
Swadlow HA (1995) Influence of VPM afferents on putative inhibitory interneurons in S1 of the awake rabbit: evidence from cross-correlation, microstimulation, and latencies to peripheral sensory stimulation. J Neurophysiol 73:1584-1599.
Tarczy-Hornoch K, Martin KAC, Stratford KJ, Jack JJB (1999) Intracortical excitation of spiny neurons in layer 4 of cat striate cortex in vitro. Cereb Cortex 9:833-843.

Thomson AM (1997) Activity-dependent properties of synaptic transmission at two classes of connections made by rat neocortical pyramidal axons in vitro. J Physiol 502:131-147.
Thomson AM (2010) Neocortical layer 6, a review. Front Neuroanat 4:13.
Thomson AM, Morris OT (2002) Selectivity in the inter-laminar connections made by neocortical neurones. J Neurocytol 31:239-246.
Thomson AM, West DC, Hahn J, Deuchars J (1996) Single axon IPSPs elicited in pyramidal cells by three classes of interneurones in slices of rat neocortex. J Physiol 496:81-102.
Thomson AM, West DC, Wang Y, Bannister AP (2002) Synaptic connections and small circuits involving excitatory and inhibitory neurons in layers 2-5 of adult rat and cat neocortex: triple intracellular recordings and biocytin labelling in vitro. Cereb Cortex 12:936-953.
Timofeev I, Steriade M (1996) Low-frequency rhythms in the thalamus of intact-cortex and decorticated cats. J Neurophysiol 76:4152-4168.
Timofeev I, Contreras D, Steriade M (1996) Synaptic responsiveness of cortical and thalamic neurones during various phases of slow sleep oscillation in cat. J Physiol 494:265-278.
Timofeev I, Grenier F, Steriade M (2000a) Impact of intrinsic properties and synaptic factors on the activity of neocortical networks in vivo. J Physiol Paris 94:343-355.
Timofeev I, Grenier F, Steriade M (2001a) Disfacilitation and active inhibition in the neocortex during the natural sleep-wake cycle: an intracellular study. Proc Natl Acad Sci USA 98:1924-1929.
Timofeev I, Bazhenov M, Sejnowski TJ, Steriade M (2001b) Contribution of intrinsic and synaptic factors in the desynchronization of thalamic oscillatory activity. Thalamus Relat Syst 1:53-69.
Timofeev I, Grenier F, Bazhenov M, Sejnowski TJ, Steriade M (2000b) Origin of slow cortical oscillations in deafferented cortical slabs. Cereb Cortex 10:1185-1199.
Timofeev I, Grenier F, Bazhenov M, Houweling AR, Sejnowski TJ, Steriade M (2002) Short- and medium-term plasticity associated with augmenting responses in cortical slabs and spindles in intact cortex of cats in vivo. J Physiol 542:583-598.
Tomioka R, Okamoto K, Furuta T, Fujiyama F, Iwasato T, Yanagawa Y, Obata K, Kaneko T, Tamamaki N (2005) Demonstration of long-range GABAergic connections distributed throughout the mouse neocortex. Eur J Neurosci 21:1587-1600.
Tononi G, Cirelli C (2006) Sleep function and synaptic homeostasis. Sleep Med Rev 10:49-62.
Trulson ME, Jacobs BL (1979) Raphe unit activity in freely moving cats: Correlation with level of behavioral arousal. Brain Res 163:135-150.
Tsien RW, Lipscombe D, Madison DV, Bley KR, Fox AP (1988) Multiple types of neuronal calcium channels and their selective modulation. Trends Neurosci 11:431-438.
Tucker TR, Katz LC (2003) Recruitment of local inhibitory networks by horizontal connections in layer 2/3 of ferret visual cortex. J Neurophysiol 89:501-512.
Turrigiano G, Abbott LF, Marder E (1994) Activity-dependent changes in the intrinsic properties of cultured neurons. Science 264:974-977.
Turrigiano G, LeMasson G, Marder E (1995) Selective regulation of current densities underlies spontaneous changes in the activity of cultured neurons. J Neurosci 15:3640-3652.
Turrigiano GG, Leslie KR, Desai NS, Rutherford LC, Nelson SB (1998) Activity-dependent scaling of quantal amplitude in neocortical neurons. Nature 391:892-896.
Vitureira N, Goda Y (2013) Cell biology in neuroscience: the interplay between Hebbian and homeostatic synaptic plasticity. J Cell Biol 203:175-186.
Volgushev M, Chauvette S, Mukovski M, Timofeev I (2006) Precise long-range synchronization of activity and silence in neocortical neurons during slow-wave oscillations. The Journal Of Neuroscience: The Official Journal Of The Society For Neuroscience 26:5665-5672.
Vyazovskiy VV, Faraguna U, Cirelli C, Tononi G (2009) Triggering slow waves during NREM sleep in the rat by intracortical electrical stimulation: effects of sleep/wake history and background activity. J Neurophysiol 101:1921-1931.
Vyazovskiy VV, Cirelli C, Pfister-Genskow M, Faraguna U, Tononi G (2008) Molecular and electrophysiological evidence for net synaptic potentiation in wake and depression in sleep. Nat Neurosci 11:200-208.

Vyazovskiy VV, Olcese U, Hanlon EC, Nir Y, Cirelli C, Tononi G (2011) Local sleep in awake rats. Nature 472:443-447.
Wagenaar DA, Madhavan R, Pine J, Potter SM (2005) Controlling bursting in cortical cultures with closed-loop multi-electrode stimulation. J Neurosci 25:680-688.
Wang G, Grone B, Colas D, Appelbaum L, Mourrain P (2011) Synaptic plasticity in sleep: learning, homeostasis and disease. Trends Neurosci 34:452-463.
White E, Hersch S (1982) A quantitative study of thalamocortical and other synapses involving the apical dendrites of corticothalamic projection cells in mouse SmI cortex. J Neurocytol 11:137-157.
Williams JA, Comisarow J, Day J, Fibiger HC, Reiner PB (1994) State-dependent release of acetylcholine in rat thalamus measured by in vivo microdialysis. J Neurosci 14:5236-5242.
Wilson CJ, Kawaguchi Y (1996) The origins of two-state spontaneous membrane potential fluctuations of neostriatal spiny neurons. J Neurosci 16:2397-2410.
Winfield DA, Brooke RNL, Sloper JJ, Powell TPS (1981) A combined golgi-electron microscopic study of the synapses made by the proximal axon and recurrent collaterals of a pyramidal cell in the somatic sensory cortex of the monkey. Neuroscience 6:1217-1230.
Wise SP, Jones EG (1976) The organization and postnatal development of the commissural projection of the rat somatic sensory cortex. J Comp Neurol 168:313-343.
Yokogawa T, Marin W, Faraco J, Pezeron G, Appelbaum L, Zhang J, Rosa F, Mourrain P, Mignot E (2007) Characterization of sleep in zebrafish and insomnia in hypocretin receptor mutants. PLoS Biol 5:e277.
Zhao Y, Sun L (2008) Antidepressants modulate the in vitro inhibitory effects of propofol and ketamine on norepinephrine and serotonin transporter function. J Clin Neurosci 15:1264-1269.
Zhu L, Blethyn KL, Cope DW, Tsomaia V, Crunelli V, Hughes SW (2006) Nucleus- and species-specific properties of the slow (<1 Hz) sleep oscillation in thalamocortical neurons. Neuroscience 141:621-636.
Zilles K, Palomero-Gallagher N, Amunts K (2013) Development of cortical folding during evolution and ontogeny. Trends Neurosci 36:275-284.
Zimmerman JE, Naidoo N, Raizen DM, Pack AI (2008) Conservation of sleep: insights from non-mammalian model systems. Trends Neurosci 31:371-376.
Zucker RS (1989) Short-term synaptic plasticity. Annu Rev Neurosci 12:13-31.